STRUCTURAL STUDIES OF TIN COMPOUNDS IN ACID MEDIA

by

VEERAGATHY MANIVANNAN, B.Sc.

A Thesis

Submitted to the Faculty of Graduate Studies

In Partial Fulfilment of the Requirements

for the Degree

Doctor of Philosophy

McMaster University

 June, 1986

STRUCTURAL STUDIES OF TIN COMPOUNDS IN ACID MEDIA

Dedicated to My Mother

and

In the Memory of My Father

DOCTOR OF PHILOSOPHY (1986)
(Chemistry)

McMaster University
Hamilton, Ontario

TITLE: Structural Studies of Tin Compounds in Acid Media

AUTHOR: Veeragathy Manivannan, B.Sc. (University of Peradeniya, SriLanka)

SUPERVISOR: Professor T. Birchall

NUMBER OF PAGES: xvi; 258

ABSTRACT

Reactions of stannane or methylstannanes $(CH_3)_{4-n}SnH_n$ (n = 1-4) in fluorosulphuric acid at low temperatures (-85°C) produce $[(CH_3)_{3-n}SnH_n]^+$ (where n = 0→3) and ^1H, ^{13}C and ^{119}Sn NMR spectroscopy have been used in their characterization. Hydrogen evolution, ^{119}Sn NMR and Mössbauer spectroscopic evidence is presented to show that at higher temperatures these species decompose to Sn^{2+}, Sn^{2+} plus $(CH_3)_2Sn^{2+}$ and $(CH_3)_2Sn^{2+}$ depending on the starting hydride. Tin-119 NMR spectra of dialkyltin cationic species in strong acid solutions are field dependent. Relaxation time measurements at three different magnetic fields have established that the dominant spin-lattice relaxation mechanism for these species at higher magnetic field is shielding anisotropy. A comparison of spin-lattice and spin-spin relaxation rates indicates that at ambient temperature a rapid chemical exchange process is occuring. In the case of the $(CH_3)_2Sn(SO_3F)_2$-HSO_3F system, variable temperature ^{119}Sn NMR spectra reveals the presence of three tin species which are involved in this exchange process.

Tin-119 NMR data for a series of tin(II) and tin(IV) acid derivatives have been determined. Tin(II) compounds exhibit a wide range of chemical shifts varying from -617 ppm to -1628 ppm, whereas tin(IV) derivatives cover a narrow range around -800 ppm. Stoichiometric mixtures of tin(II) and tin(IV) derivatives of the same acid have been analysed by ^{119}Sn NMR and Mössbauer spectroscopy. Reaction occurs only between $Sn(OCOCF_3)_2$ and $Sn(OCOCF_3)_4$ to form a mixed valence tin(II), tin(IV) compound. Partial oxidation of $Sn(OCOCF_3)_2$ results in the formation of a mixed valence tin

compound whose structure has been determined by X-ray crystallography to be $[Sn(II)_4Sn(IV)O_2(O_2CCF_3)_8]$. This structure consists of discrete noncentrosymmetric units with point group S_4, the central feature of which is a $Sn(II)_4Sn(IV)O_2$ unit containing two μ_3 oxygen atoms which each form a bridge between a Sn(IV) atom and two symmetry related Sn(II) atoms. Among the two pairs of Sn(II) atoms, each pair is bridged by two trifluoroacetates.

A systematic route has been established in the preparation of mixed valence tin compounds by the reaction of SnF_2 with tin(IV) carboxylates. These reactions have been followed by ^{19}F and ^{119}Sn NMR spectroscopy. In one case an X-ray crystal structure determination showed the compound to be $[Sn(II)_2Sn(IV)_2F_4(O_2CCF_3)_8 \cdot 2CF_3CO_2H]$. This consists of eight membered rings with alternating Sn(II) and Sn(IV) atoms bridged by fluorine and trifluoroacetate groups.

ACKNOWLEDGEMENT

I wish to express my deep appreciation and indebtedness to my research director Professor T. Birchall for his invaluable guidance, assistance and encouragement during the course of this work. I am also grateful to my supervisory committee members, Professor I. D. Brown for helpful discussions on structural analysis and Professor G. J. Schrobilgen for his resourcefullness.

Thanks are due to the technical assistance provided by Mr. B. G. Sayer and Mr. J. I. A. Thompson in the use of the NMR instruments. Special thanks are due to Mr. R. Faggiani for his valuable assistance with X-ray crystallography.

My sincere thanks to Professor C. J. L. Lock for introducing me to crystallography and for providing advice related to one of the crystal structures discussed in this thesis. Dr. R. Batchelor, Dr. J. P. Johnson and Dr. R. D. Myers are thanked for their assistance in the early stages of this work.

I very much appreciate the assistance of Dr. R. Buist in understanding NMR relaxation studies and Mr. T. R. G. Syvret in proof reading this thesis. The encouragement and friendship of these individuals will be remembered. I also wish to acknowledge Mrs. C. Dada for her speedy and accurate typing of the thesis.

Financial assistance by McMaster University in the form of a C. W. Sherman Scholarship, Departmental Scholarship and Teaching Assistantship duties is gratefully acknowledged.

Finally, I wish to thank my wife, Nirmala, for her patience, encouragement and moral support during this phase of my academic career.

TABLE OF CONTENTS

LIST OF TABLES

LIST OF FIGURES

ABBREVIATIONS

For NMR Data

δ	NMR Chemical Shift
J	Coupling Constant
$\Delta W_{\frac{1}{2}}$	Line Width at Half Height
NOE	Nuclear Overhauser Effect
η	Nuclear Overhauser Enhancement Factor
T_1	Spin-Lattice Relaxation Time

For Mössbauer Data

δ	Mössbauer Isomer Shift
Δ	Quadrupole Splitting
Γ	Line Width at Half Height

For Structural Analysis

v.u.	Valence Unit

CHAPTER 1

INTRODUCTION

The primary aim of this work was to investigate the solvolysis of tin compounds in both strong and weak acids. These solvolyses include reactions involving Sn-H, Sn-C, Sn-F, and Sn-Sn bonds. All reactions have been studied under anhydrous conditions employing the acid as the reactant as well as the solvent. It has been established that, in certain ditin compounds, cleavage of the tin-tin bond occurs to form compounds containing two different oxidation states of tin, namely tin(II) and tin(IV) within the same molecule.[1] Therefore a secondary objective of this study was to investigate other possible routes for the preparation of mixed oxidation state tin(II), tin(IV) compounds. The products from the reactions have been characterised using NMR, Mössbauer and vibrational spectroscopic techniques and in two cases by single crystal X-ray diffraction studies. In this introduction the reactions of the tin compounds which prompted these experiments are outlined. Further introductory details are given in the relevant chapters.

Birchall et al.[2] followed the reaction of tetramethyltin [$(CH_3)_4Sn$] with sulphuric acid by proton NMR spectroscopy. They showed that initially a solvated $(CH_3)_3Sn^+$ species was formed which was found to decompose to give the stable $(CH_3)_2Sn^{2+}$ species according to equations (1.1) and (1.2).

$$(CH_3)_4Sn + H_2SO_4 \longrightarrow (CH_3)_3Sn^+ + HSO_4^- + CH_4 \qquad (1.1)$$

$$(CH_3)_3Sn^+ + H_2SO_4 \longrightarrow (CH_3)_2Sn^{2+} + HSO_4^- + CH_4 \qquad (1.2)$$

It has long been known that the dialkyltin(IV) ions, R_2Sn^{2+}, occur in aqueous solution[3] and apparently this cation has a very high affinity for water molecules. This is an important factor in the high solubility of dimethyltin dihalides in water. The solution process involves a change in the hybridisation of the tin atom, and this dissolution may be described by equation (1.3).[4]

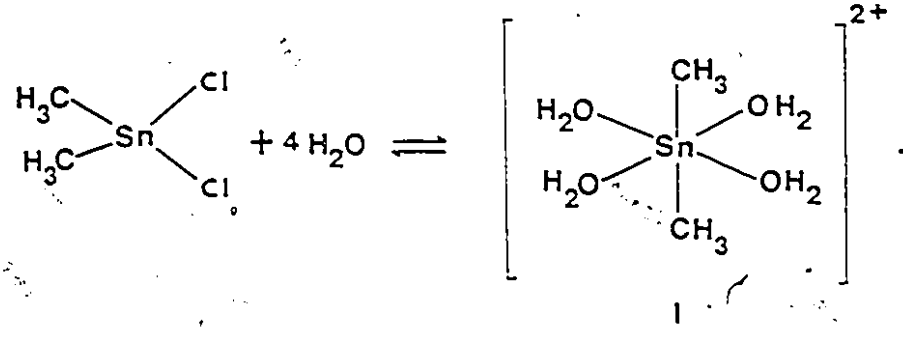

(1.3)

I

Four water molecules are coordinated in the first hydration sphere of the tin atom.[5] Raman, infrared, and NMR spectroscopic studies on aqueous solutions of dimethyltin compounds have shown that the linear CH_3-Sn-CH_3 arrangement exists in these solutions[6] and that four water oxygens are coordinated to the tin atom in a plane to give an octahedral arrangement around tin. It is convenient to picture the dimethyltin species in solution as simple aquated cations, since the tin-oxygen bonds are so polar that no Sn-O vibration was observed in the Raman spectrum.[6] However,

in strongly alkaline solutions the water molecules are replaced by hydroxo groups which are considerably better donors than water, and a Raman line due to tin-oxygen bond stretching has been observed. The species in solution can be best represented by structure (II).

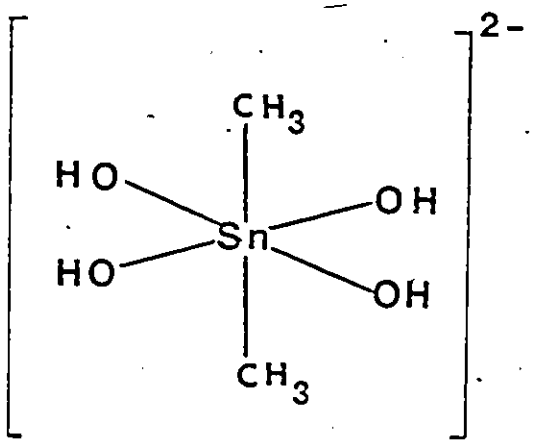

II

NMR and Mössbauer parameters of the dimethyltin(IV) cationic species in sulphuric acid are consistent with an octahedral coordination for tin, formulated as a linear $[CH_3\text{-}Sn\text{-}CH_3]^{2+}$ cation interacting with four sulphuric acid molecules in the equatorial plane. The favoured structure of the solvated ion can be written as an anionic species (III).

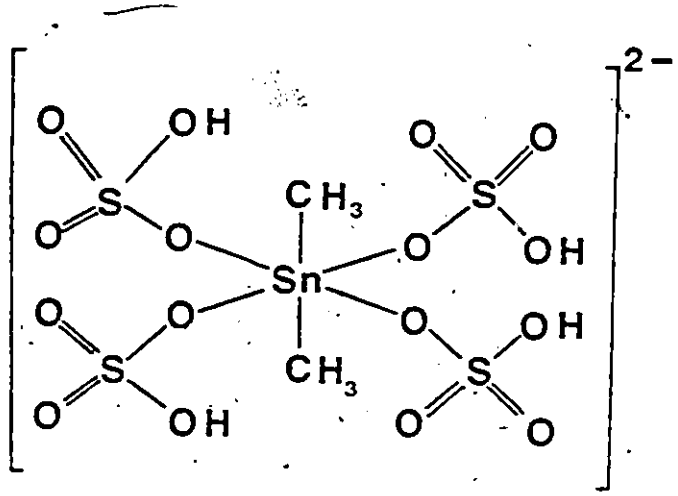

III

The solvated trimethyltin(IV) cation, $(CH_3)_3Sn^+$, has been found to exist in sulphuric acid[2] and in flurosulphuric acid solutions.[7] In the absence of strong covalent bonding from the solvent, cations of the type R_3Sn^+, would be expected to adopt a planar configuration to minimize repulsion between the bonding pairs of the metal-carbon bonds. On the basis of proton NMR and Mössbauer data, the $(CH_3)Sn^+$ is considered to be solvated in sulphuric acid and to have a trigonal bipyramidal structure with planar $(CH_3)_3Sn^+$ cations with the axial positions filled by solvent molecules. Like the dimethyltin species, the solvated trimethyltin species can be written as an anionic species (IV).

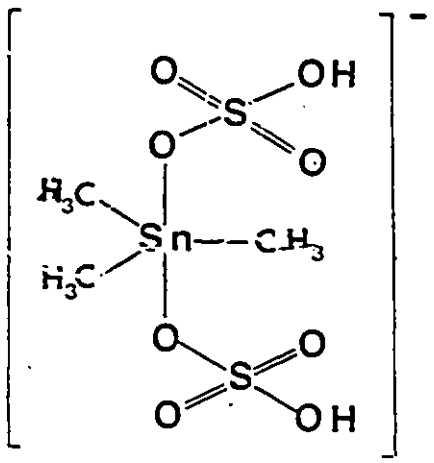

IV

Throughout this thesis the alkyltin species present in solution are, for convenience, referred to as cations. However, it is recognized that these are solvated tin species with coordination numbers of five and six for the dialkyltin species and trialkyltin species, respectively.

Webster and Jolly[8] have studied the reaction of stannane (SnH_4) in strong acid solutions. They have observed the formation of the stannonium ion (SnH_3^+) at low temperatures according to equation (1.4).

$$SnH_4 + H^+ \longrightarrow SnH_3^+ + H_2 \qquad (1.4)$$

That the existence of SnH_3^+ and $(CH_3)_3Sn^+$ in solution are well documented, suggests the possibility of cationic species with one or two methyl groups substituted for hydrogen in the stannonium cation (SnH_3^+). An obvious choice of starting materials to prepare such species would be methylstannanes [$(CH_3)_nSnH_{4-n}$; n = 1-3].

Methylstannanes are derivates of stannane (SnH_4) in which at least one hydrogen is replaced by a methyl group. Stannane (SnH_4) was

first prepared by Paneth and Fürth in trace amounts.[9] It is thermally unstable and readily decomposes to tin and hydrogen. The stability of the methyltin hydrides of the type $(CH_3)_nSnH_{4-n}$ increases as n increases. Tin hydrides are sensitive to oxygen and silicone grease, metallic tin and aluminium halides. Therefore, they have to be handled in clean glassware under an inert atmosphere or on a vacuum line and stored in sealed vessels at -196°C.

Fluorosulphuric acid is a very strong acid as well as having a low melting point (-87°C) and therefore it can be employed for low temperature solution studies. In this thesis, it was used in the preparation of cationic species of the type $[(CH_3)_nSnH_{3-n}]^+$, where n = 1-3. This acid also oxidizes alkanes to carbonium ions and a number of stable cations have been prepared in this solvent system at low temperatures.[10] The studies carried out on the methylstannane-fluorosulphuric acid system are presented in the first section of Chapter 3. NMR spectroscopy was used as the main tool to follow these reactions.

The reactions of organotin compounds (R_4Sn) with organic acids HA, have been shown to give only the mono- and disubstituted derivatives R_3SnA and R_2SnA_2 for a wide range of acids.[11] It has been reported that in the reaction with acids, vinyl groups bonded to tin are cleaved more readily from the tin than are saturated alkyl groups. In the reaction of tetravinyltin with certain carboxylic acids, all the vinyl groups were cleaved to give tin tetracarboxylates $[Sn(OCOR)_4]$ according to equation (1.5).[12]

$$Sn(CH{=}CH_2)_4 + 4\ RCOOH \longrightarrow Sn(OCOR)_4 + 4\ CH_2{=}CH_2 \qquad (1.5)$$

This study indicated that carboxylic acids of high acidity were less effective for complete cleavage. For example, although formic acid effects complete cleavage at 110°C, only two vinyl groups were removed at ordinary temperatures. Moreover, trifluoroacetic acid only removes three vinyl groups. In tetraallyltin, the high reactivity of the tin-allyl bond prevents controlled stepwise cleavage of one, two or more allylic groups.[13] The cleavage reactions of compounds $R_2Sn(CH{=}CH_2)$ (R = alkyl or phenyl groups) indicate that phenyl groups are more easily cleaved than vinyl groups. The reaction between tetraphenyltin $[(C_6H_5)_4Sn]$ and haloacetic acids (RCOOH; where R = $CHCl_2$, CH_2Cl, CCl_3, CF_3, C_3F_7) resulted in the cleavage of all phenyl groups at room temperature to yield the tetracarboxylates according to equation (1.6).[1]

$$(C_6H_5)_4Sn + 4\ RCOOH \longrightarrow Sn(OCOR)_4 + 4\ C_6H_6 \qquad (1.6)$$

Later Sawyer prepared tin(IV) acetate $[Sn(OCOCH_3)_4]$ by refluxing tetraphenyltin in acetic acid.[14]

The solvolysis of hexamethylditin $[(CH_3)_6Sn_2]$ by haloacetic acids yield tetramethylditin carboxylates $(CH_3)_4Sn_2(OCOR)_2$.[15] These compounds were shown to contain a tetramethylditin moiety with a tin-tin bond as in (V).

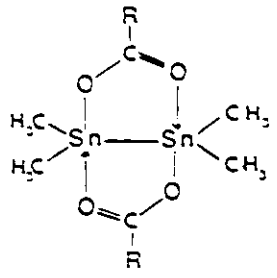

V

This result indicates that the substitution reaction predominated over the cleavage of the tin-tin bond. The reaction of hexamethylditin with fluorosulphuric acid cleaves the tin-tin bond to produce the stable dimethyltin(IV) fluorosulphate according to equation (1.7)[7]

$$(CH_3)_3Sn\text{-}Sn(CH_3)_3 + 4\ HSO_3F \longrightarrow 2\ (CH_3)_2Sn(SO_3F)_2 + 2\ CH_4 + H_2 \quad (1.7)$$

In solution, dimethyltin(IV) fluorosulphate is considered as a solvated $(CH_3)_2Sn^{2+}$ species which is in fact an anionic species represented by $[(CH_3)_2Sn(SO_3F)_4]^{2-}$ with a structure similar to (III).

The solvolysis of hexaphenylditin with a series of carboxylic acids gives compounds of empirical formula $Sn(OCOR)_3$. These were shown to be mixed valence tin compounds which have been formulated as $[Sn(II)Sn(IV)O(OCOR)_4O(OCR)_2]_2$. This reaction has been postulated by Johnson to proceed according to the following sequence.[7]

$$(C_6H_5)_6Sn_2 + RCOOH \longrightarrow \underset{(VI)}{Sn_2(OCOR)_6} + 6\ C_6H_6 \quad (1.8)$$

$$Sn_2(OCOR)_6 \longrightarrow \underset{(VII)}{Sn(IV)(OCOR)_4 \cdot Sn(II)(OCOR)_2} \quad (1.9)$$

$$Sn(OCOR)_4 \cdot Sn(OCOR)_2 \longrightarrow \underset{(VIII)}{Sn(II)Sn(IV)O(OCOR)_4O(OCR)_2} \quad (1.10)$$

$$2[Sn(II)Sn(IV)O(O_2CR)_4O(OCR)_2] \longrightarrow \underset{(IX)}{[Sn(II)Sn(IV)O(O_2CR)_4O(OCR)_2]_2} \quad (1.11)$$

Initially all tin-carbon bonds are cleaved to produce an unstable ditin species (VI). This is followed by the asymmetric cleavage of the tin-tin bond in (VI) to produce a tin(II) and a tin(IV) carboxylate (VII) which is perhaps associated via the bridging carboxylate ligands. The production of anhydride by elimination of O^{2-} would produce (VIII), the monomeric oxo-bridged tin complex. Dimerization would produce (IX), the

oxo-bridged mixed oxidation state tin compound as the final product. There is no experimental evidence for the reaction sequence proposed above. Kinetic studies carried out on the acetolysis of the analogous hexaphenyldilead shows that initial cleavage of phenyl groups occurs which is followed by rupture of the Pb-Pb bond to give Pb(II) and Pb(IV) compounds.[16] The complete reaction is given by equation (1.12).

$$(C_6H_5)_6Pb_2 + 3CH_3CO_2H \longrightarrow 3C_6H_6 + Pb(OCOCH_3)_2 + (C_6H_5)_3Pb(OCOCH_3) \quad (1.12)$$

Since the above reaction sequences (1.8) to (1.11) purport to involve the formation of tin(II) and tin(IV) carboxylates at an intermediate stage which results in the subsequent formation of a compound of empirical formula $Sn(OCOR)_3$, the reaction given by the equation (1.13) is a possible route to such compounds.

$$Sn(OCOR)_2 + Sn(OCOR)_4 \longrightarrow [Sn(OCOR)_3]_2 \quad (1.13)$$

Therefore, it would be interesting to compare the product from reaction (1.13) with that of the product (IX) isolated by the acidolysis of hexaphenylditin. With the above purpose in mind, it was decided to study the reactions between simple tin(II) and tin(IV) carboxylates. The general synthetic route for the preparation of tin(IV) carboxylate is by the cleavage of tetraphenyltin with acid according to equation (1.6) and tin(II) carboxylates are produced by the reaction of stannous oxide with the appropriate acid according to equation (1.14).[17]

$$SnO + RCOOH \longrightarrow Sn(OCOR)_2 + H_2O \quad (1.14)$$

There have been no tin-119 NMR measurements on solutions of tin(II) and tin(IV) carboxylates reported. Therefore, it was necessary to measure the tin-119 chemical shifts of these compounds before investigating the changes that occur in the solutions obtained by mixing the tin(II) and tin(IV) derivatives of the carboxylic acids. These studies are presented in Chapter 4 together with the crystal structure of a mixed valence tin compound obtained from solution of tin(II) trifluoroacetate in trifluoroacetic acid/anhydride mixture.

There are very few mixed valence tin compounds reported in the literature.[1,18-26] Most of these were obtained unexpectedly and the reaction pathways are not known. Therefore interest lies in establishing new systematic routes for the preparation of mixed valence tin compounds. It is well established that stannous fluoride (SnF_2) acts as a fluoride ion donor[27] as well as fluoride ion acceptor.[28] Reactions were carried out between SnF_2 and tin tetracarboxylates. It was found that these reactions produced compounds which were quite soluble in the parent acid. This made possible the study of their structures in solution by NMR spectroscopy and in the solid state by Mössbauer spectroscopy. The reaction between SnF_2 and $Sn(OCOCF_3)_4$ produced a crystalline material and its structure has been determined by single crystal X-ray diffraction studies. These studies are discussed in Chapter 5 of this thesis.

At this stage it is appropriate to take stock of the commonly available techniques to study the structural aspects of tin(II) and tin(IV) compounds. X-ray crystallography is the most powerful technique for providing unambiguous structural information in the solid state.

It is limited by the need to grow suitable crystals and in the handling of moisture and air sensitive crystals, since in certain instances, crystals rapidly lose their crystallinity in the absence of solvent vapour, or may decompose in the X-ray beam. A second technique, tin-119 Mössbauer spectroscopy is a powerful tool for investigating the stereochemistry of, and bonding in, tin compounds. It readily gives information about the oxidation state and coordination around the tin nucleus and crystalline materials are not required. The initial identification of mixed oxidation state compounds was established on the basis of Mössbauer effect measurements.

Solution studies have been mainly carried out by NMR spectroscopy. The compounds studied in this work contain a number of NMR active nuclei namely ^{1}H, ^{13}C, ^{19}F and ^{119}Sn. Recently, with the advent of pulsed Fourier Transform NMR techniques, high quality spectra of low natural abundant nuclei such as ^{13}C and ^{119}Sn can be recorded on a routine basis. Tin-119 NMR spectroscopy which usually exhibits resonances over a large range of chemical shifts has been widely used in this study. The tin-119 chemical shift is very sensitive to the changes in the tin environment. The spin-spin coupling constants between tin-119 and a variety of other nuclei have been measured. The most detailed studies have been carried out on couplings involving tin and hydrogen, and tin and carbon.[29,30,31] Correlations between the magnitudes of the coupling constants provide information about the stereochemistry at the tin nucleus. During the tin-119 NMR measurements of the dialkyltin cationic species in strong acids, it was realised that the linewidth of the NMR signals increased dramatically with the magnetic field being employed to observe the

resonance. This led into the measurement of NMR relaxation times at different magnetic fields. These results and their implications are discussed in the second section of Chapter 3.

CHAPTER 2

EXPERIMENTAL

2.1 Preparative Techniques and Apparatus

2.1.1 Vacuum System

Most preparative work presented in this thesis was carried out using a Pyrex vacuum system with all ground-glass high vacuum stopcocks. The volumes of hydrogen evolved in the reactions were measured with a Toepler pump. Reaction vessels and NMR tubes were connected to the vacuum line through 9 mm i.d. ball-and-socket ground-glass joints. Joints and valves were lubricated with Apiezon N high vacuum grease. The high vacuum was obtained by a Welch Duo-Seal vacuum pump and was enhanced by a mercury diffusion pump. The vacuum was monitored by a Vacustat Gauge (Edward High Vacuum Ltd.) which was accurate to 1×10^{-3} mm Hg.

2.1.2 Inert Atmosphere System

All of the samples or reagents which were sensitive to moisture or to air oxidation were handled in a dry nitrogen Labconco glove box fitted with a constant circulation liquid nitrogen cooled drying system. Materials were transferred to the glove box via an evacuable port. The atmosphere in the glove box was supplied from liquid nitrogen reservoir boil-off or from cylinders of "extra dry nitrogen" provided by Speciality Gases, and three trays of phosphorous pentoxide were maintained in the glove box to ensure a dry atmosphere.

2.1.3 Reaction Vessels

Solutions of cationic species were prepared in thick wall NMR tubes each equipped with a Rotaflo valve. Volatile organotin compounds were distilled into the tube containing strong acid which was frozen in a liquid nitrogen bath. The reaction between the two components was allowed to proceed at specific temperatures by using low temperature slush baths. Standard Dean[32] reaction vessels with NMR tubes attached were used for various other preparations requiring exclusion of air.

2.2 Purification and Preparation of Starting Materials

2.2.1 Solvents

Benzene

Benzene (J. T. Baker Chemical Co.) was dried and stored over lithium aluminium hydride. When required, it was directly condensed into the reaction vessel. Benzene-d_6 was dried over lithium aluminium hydride and distilled directly into the NMR tube.

Sulfur Dioxide

Sulfur dioxide (Matheson Co.), was dried and stored over P_4O_{10} before use. When required, it was vacuum condensed directly into the reaction vessel.

Fluorotrichloromethane

$CFCl_3$ (Canadian Liquid Air Ltd.), was dried and stored over P_4O_{10} before use. When required it was vacuum condensed directly into the reaction vessel.

2.2.2 Reagents

Tin Hydrides

Stannane, methylstannane and dimethylstannane were prepared by standard literature methods.[33-35] Their purity was checked by vapour pressure measurements at fixed temperatures, and by gas phase I.R. spectroscopy. Their NMR spectra were recorded in organic solvents by condensing the hydrides into the degassed solvent in the correct sized NMR tubes which were attached to the vacuum line. All of the hydrides were stored in sealed vessels under vacuum at -196°C and occasionally degassed.

Tetramethyltin and Tetraethyltin

Tetramethyltin and tetraethyltin (Alfa products), were used without further purification. When required, they were distilled directly into NMR tubes.

Dimethyltin- and Diethyltin Dichloride

Dimethyl- and diethyltin dichloride (Alfa Products) were used without further purification.

Tetraphenyltin

Tetraphenyltin (Aldrich Co. Ltd.) was purified by recrystallization from chloroform.

Stannous Oxide

Stannous oxide (Blue black) was freshly prepared according to the method given in reference (36).

Stannous Fluoride

Stannous fluoride (Sigma Chemical Company, St. Louis, U.S.A.) was used without further purification.

Acids and Anhydrides

The following reagents were used without further purification: trifluoroacetic acid, trifluoroacetic anhydride, dichloroacetic acid, dichloroacetic anhydride, heptafluorobutyric acid, heptafluorobutyric anhydride and trifluoromethylsulphonic acid were obtained from Aldrich Chemical Co. Inc.. Acetic acid and acetic anhydride (Certified A.C.S.) were obtained from Fisher Scientific Co.. Methanesulphonic acid and ethanesulphonic acid, obtained from Matheson, Coleman and Bell Manufacturing Chemical Company, were also used.

100 % Sulphuric acid was prepared as previously described[37] and fluorosulphuric acid was purified by double distillation.[38]

2.3 Preparations

2.3.1 Alkyltin Cations in Strong Acids

All cationic species were prepared either in sulphuric acid or in fluorosulphuric acid solutions. These fluorosulphuric acid solutions were manipulated in sealed vessels under vacuum as they are very sensitive to oxidation and hydrolysis. NMR samples of these cations were sealed under dynamic vacuum at -196°C. Sulphuric acid solutions were prepared in a dry N_2 atmosphere and deoxygenated by bubbling dry N_2 through the solutions.

(i) $(CH_3)_{3-n}SnH_n^+$ Species in Fluorosulphuric Acid

Solutions of the hydrides were prepared by condensing the hydride into the appropriate quantity of frozen degassed acid, in the correct sized NMR tube which was connected to a vacuum line. The NMR tubes were sealed and the temperature of the acid solution was maintained at -90°C

until NMR spectra could be recorded.

Hydrogen evolution experiments were carried out on the glass vacuum line equipped with a Toepler pump. The tin hydride, ~0.3 mmoles, was condensed at -196°C into a glass vessel containing 35.0 mmole HSO_3F which had been previously degassed. This solution was warmed to -78°C (Acetone-solid CO_2 bath) and the quantity of hydrogen evolved was measured. The temperature of the solution was raised to 25°C and the hydrogen that was subsequently evolved was measured. These measurements are given below:

Amount of Tin Hydride (mmoles)		Temp. (°C)	Amount of Hydrogen Evolved (mmoles)	Total Amount of Hydrogen Evolved (mmoles)
(a)	CH_3SnH_3			
(i)	0.305	-78	0.285	
		25	0.344	0.629
(ii)	0.258	-78	0.252	
		25	0.246	0.498
(b)	$(CH_3)_2SnH_2$			
	0.293	-78	0.292	
		25	0.008	0.300

All of the hydrides liberated one mole of hydrogen for every mole of hydride dissolved in fluorosulphuric acid at -78°C. Webster and Jolly[8] have already demonstrated this for solutions of stannane. On warming to room temperature no more hydrogen was evolved in the case of stannane and dimethyl stannane, whereas another mole of hydrogen was evolved from

the methylstannane solution.

(ii) Dialkyl- and Trialkyltin Species in Sulphuric and Fluorosulphuric Acids

Dimethyl and diethyltin species in sulphuric acid were prepared by the dissolution of dimethyl or diethyltin dichloride in 100% sulphuric acid at room temperature.[2] The dibutyltin species was obtained by reacting hexabutylditin with 100% sulphuric acid at room temperature. Trimethyl- or triethyltin species in fluorosulphuric acid were prepared by the reaction of tetramethyl- or tetraethyltin in fluorosulphuric acid at -30°C.

2.3.2 Tin(II) and Tin(IV) Carboxylates

(i) $Sn(CO_2CF_3)_2$

Freshly prepared blue-black tin(II) oxide (3.4 g, 0.025 moles) was placed in one side of a Dean type,[32] two bulb reaction vessel fitted with a glass frit. A mixture of 10.5 cm^3 (0.14 moles) trifluoroacetic acid and 3.5 cm^3 (0.025 moles) trifluoroacetic anhydride was distilled into it. The solid and the acid-anhydride mixture was stirred at room temperature for 18 hours. The resulting solution was filtered into the other side of the vessel to give a clear colourless solution. The remaining acid was slowly removed by distillation to give a white crystalline material. This was dried overnight on the vacuum line. A total of 3.5 g of product was obtained (Analytical data, see Table 2.1).

(ii) $Sn(CO_2C_3F_7)_2$

Freshly prepared blue-black tin(II)oxide (1.96 g, 0.014 mol) was placed in one side of a Dean type two bulb reaction vessel fitted with a

TABLE 2.1

ANALYTICAL DATA FOR THE COMPOUNDS PREPARED

Empirical Formula or Composition		%Sn	%C	%H	%Halogen	M.pt(°C)	%yield
1. $Sn(CO_2CF_3)_2$	calcd.	34.43	13.90	0.00	33.04	103	40.6
	found	34.21	14.18	0.46	33.77		
2. $Sn(CO_2C_3F_7)_2$	calcd.	21.79	17.62	0.0	48.83	72-75	45.9
	found	22.71	16.95	0.16	48.03	———	———
3. $Sn(CO_2CHCl_2)_4$	calcd.	18.83	15.23	0.63	44.42	125 - 127	65.7
	found	18.48	15.32	0.84	44.17		
4. $Sn(CO_2C_3F_7)_4$	calcd.	12.23	19.78	0.0	54.81	-	-
	found	19.29	17.81	0.30	54.46		
5. $Sn(CO_2CF_3)_3$	calcd.	25.93	15.74	0.0	37.34	181 - 184	83.3
	found	26.28	14.92	0.20	36.99		
6. $Sn_5O_2(CO_2CF_3)_8$	calcd.	38.80	12.54	0.00	29.70	-	-
	found (i)	39.87	13.98	0.20	20.62		
	(ii)	-	12.55	0.00	19.88		
7. $Sn_2F_2(CO_2CF_3)_4$- $\cdot CF_3CO_2H$	calcd.	28.25	14.28	0.12	21.48	133 - 135	67.3
	found	28.78	13.52	0.36	21.50		

glass frit. To this a mixture of 6.5 cm^3 (0.05 moles) heptafluorobutyric acid and 6.0 cm^3 (0.024 moles) heptafluorobutyric anhydride were added in the dry box and degassed on a vacuum line. The mixture was stirred at room temperature for 18 hours and the resulting solution was filtered to the other side of the bulb to give a clear colourless solution. The acid was slowly removed by distillation to give a white crystalline material. The solid was pumped to dryness overnight yielding 3.5 g of product. (Analytical data, see Table 2.1).

(iii) $Sn(CO_2CHCl_2)_4$

Tetraphenyltin (2.061 g, 4.83 mmoles) was added to one side of a two bulb reaction vessel and dry benzene (10 cm^3) was condensed into it. The vessel was taken into the drybox and to the other bulb, 10 cm^3 (121.2 mmoles) of dichloroacetic acid and 1 cm^3 (6.56 mmoles) of dichloroacetic anhydride were added. This was degassed and the acid-anhydride mixture was poured onto tetraphenyltin in benzene and stirred at room temperature for 15 hours to give a pale yellow coloured solution. When the benzene was slowly removed by distillation a crystalline material separated and the supernatant solution was decanted to the other bulb. The yellow impurities were removed by washing with small amounts of benzene to yield a white crystalline material. This was pumped to dryness to give 2.0 g of compound. (Analytical data, see Table 2.1).

(iv) $Sn(CO_2C_3F_7)_4$

1.76 g (4.12 mmoles) of tetraphenyltin was added to one side of the bulb of a two bulb reaction vessel. This vessel was taken into the drybox and an excess of heptafluorobutyric acid (12 cm^3, 92.2 mmoles) was added to the other bulb and degassed under vacuum. The acid was poured onto the tetraphenyltin and stirred at room temperature for 15 hours.

Acid and the benzene produced in the reaction were removed by distillation to give a dark red coloured syrup. $CFCl_3$ was condensed into this vessel and the syrup dissolved to give a clear solution. On cooling this solution in an ice bath, some white solid precipitated and the supernatant solution was decanted to the other bulb by keeping both bulbs cold in the ice bath in an attempt to remove the coloured impurities. The resultant white solid was pumped to dryness. The yield of this preparation was very low, but enough to characterize the compound. (Analytical data, see Table 2.1).

(v) $Sn(CO_2CF_3)_3$

1.285 g (3.70 mmoles) of tin(II) trifluoroacetate and 2.081 g (3.60 mmoles) of tin(IV) trifluoroacetate were added to one side of a Dean type two bulb reaction vessel fitted with a glass frit. A mixture of 10 cm^3 (129.8 mmoles) trifluoroacetic acid and 2 cm^3 trifluoroacetic anhydride were distilled onto the solid mixture and stirred at room temperature. Initially, all of the solid dissolved to give a clear solution. After approximately 15 minutes, a solid precipitated from the solution and this mixture was stirred for 10 hours to ensure complete precipitation. The solid was removed by filtering the supernatant to the other bulb. The acid was recondensed on to the solid and the resultant solution was filtered. This process was repeated a few times to remove the small amounts of yellow impurities. The solvent side of the vessel was sealed and the white solid was pumped to dryness overnight. A total of 2.80 g of product was obtained. (Analytical data, see Table 2.1).

(vi) $Sn_5O_2(O_2CCF_3)_8$

0.58 g of $Sn(CO_2CF_3)_2$ was dissolved in a mixture of 2.5 ml of trifluoroacetic acid and 0.5 ml of trifluoroacetic anhydride under a dry-N_2 atmosphere and placed in a tube capped with a valve via a ¼" swagelock fitting. After one month, pyramidal shaped crystals had formed. Crystals were isolated by decanting the acid solution. On pumping to dryness under high vacuum, the crystals lost their crystallinity to give a white powdered material. (Analytical data, see Table 2.1).

(vii) $SnF_2 \cdot Sn(CO_2CF_3)_4 \cdot CF_3CO_2H$

0.935 g (1.60 mmoles) of $Sn(CO_2CF_3)_4$ and 0.254 g (1.60 mmoles) of SnF_2 were placed in one side of a Dean type two bulb reaction vessel fitted with a glass frit. Into this a mixture of 7.0 cm^3 (90.86 mmoles) trifluoroacetic acid and 1.5 cm^3 (10.62 mmoles) trifluoroacetic anhydride were condensed. The resulting mixture was stirred at room temperature. After 30 minutes, most of the solid had dissolved to give a pale yellow solution. Small amounts of solid particles were still present in the solution and these were presumably the impurities from the SnF_2 used. The solution was filtered to the other side of the bulb and the acid was removed by distillation to give a white crystalline material. Small amounts of yellow coloured impurities present in this material were removed by washing with small amounts of acid. The solid was pumped to dryness yielding 0.8 g of product. (Analytical data, see Table 2.1).

2.4 Analytical Techniques and Apparatus

2.4.1 NMR Spectroscopy

(i) Proton NMR

Samples for ^{1}H NMR were prepared by sealing solutions under vacuum at -196°C in 5 mm NMR tubes. The spectra were recorded at 250.13 MHz using a Bruker WM-250 Fourier transform spectrometer without a lock substance. The spectra were accumulated in 16 K of memory at a spectral width of 10,000 Hz (1.22 Hz/data pt.) and with a pulse width of 3.0 micro sec.. Chemical shifts were measured relative to neat tetramethylsilane as an external reference.

(ii) Fluorine-19 NMR

Samples for ^{19}F NMR were prepared in the same manner as the proton NMR samples. The spectra were recorded at 235.36 MHz using the Bruker WM-250 Fourier transform spectrometer without a lock substance. The spectra were accumulated in 16 K memory at a spectral width of 25,000 Hz (3.05 Hz/-data point) and with a pulse width of 3.0 micro secs..

(iii) Carbon-13 NMR

Samples for ^{13}C NMR were prepared by sealing solutions in 10 mm o.d. NMR tubes at -196°C under dynamic vacuum. The ^{13}C NMR spectra were recorded without a lock substance, at either 62.89 or 100.62 MHz respectively on a Bruker WM-250 or WH-400 Fourier transform spectrometer. In both cases, spectra accumulated in 16 K of memory using a spectral width of 15,000 Hz (1.85 Hz/data point) and pulse width 25 micro secs. (on the WM-250) and 30 micro secs. (on the WM-400). Chemical shifts were measured relative to neat tetramethylsilane (TMS) as an external reference. In general, the spectra were broad band decoupled in the proton region.

(iv) Tin-119 NMR

Samples for ^{119}Sn NMR were prepared either in 10 mm o.d. round bottomed tubes or in 8 mm o.d. round bottomed tubes. Tin-119 NMR spectra were recorded at operating frequencies of 33.56, 93.27 and 149.21 MHz on Bruker WH-90, WM-250 and WH-400 spectrometers respectively. Samples were contained in 10 mm tubes without a lock substance on the WM-250 and WH-400 instruments. For spectra recorded on the WH-90, samples were contained in 8 mm o.d. tubes which were placed concentrically into a 10 mm o.d. tube containing D_2O or $(CD_3)_2CO$ as the lock substance. Chemical shifts were measured relative to an external reference of neat tetramethyltin. The spectra were accumulated in 8 K memory on the WH-90 and in 16 K memory on the WM-250 and WH-400 spectrometers. Initially spectra were recorded using a large sweep width (approx. 50,000-75,000 Hz.) to locate the signals and then the spectral window was narrowed down to 10,000-25,000 Hz (1.2-3.0 Hz/-data point) and the spectra were accumulated such that the signals appeared close to resonance. The pulse widths used were 15, 25 and 35 micro seconds for WH-90, WM-250 and WH-400 respectively.

Tin-119 NMR spin-lattice relaxation times (T_1) were measured using the inversion recovery technique and this operation time diagram is shown below.[39]

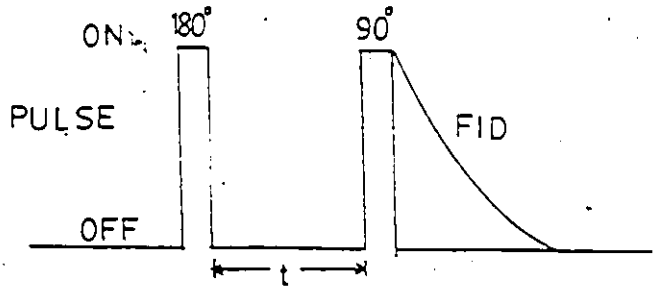

This can be described pictorally as shown below.

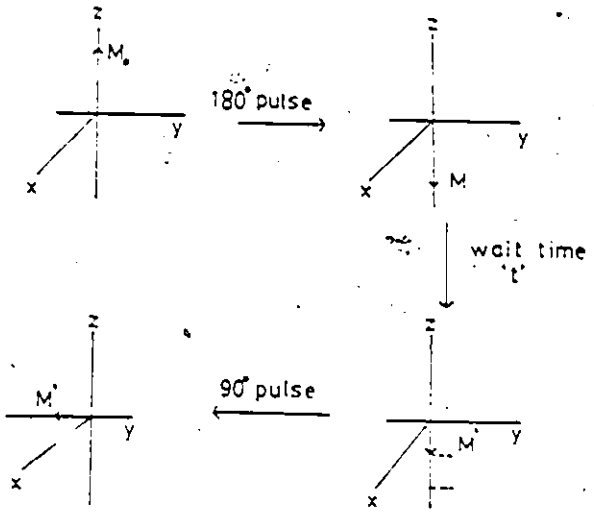

Initially, a 180° pulse is applied which inverts the magnetisation vector from $+M_o$ to $-M_o$ and is then allowed to recover for t secs.. After this period the sample is subjected to a 90° pulse and the resulting Free Induction Decay (FID) is processed. A delay time of at least $4T_1$ is left to allow the magnetisation vector to return to equilibrium before the sequence can be repeated. This experiment is repeated with a series of variable t values and the resultant spectral intensity (A_t) is measured. From this, T_1 can be calculated using the equation (2.1).

$$\ell n(A_\infty - A_t) = \ell n\ 2\ A_\infty - {}^{t}/_{T_1} \qquad (2.1)$$

A value for T_1 was obtained using a three parameter fitting procedure.[40] The lengths of 90° pulse used were 18 μs (WH-90), 28μs (WM-250), 29 μs (WH-400). The estimated errors in T_1 measurements are less than 10%.

The nuclear Overhauser enhancement (NOE) measurements were carried out in two ways by comparing the signal intensities of:

(a) Spin coupled spectra with and without NOE

(b) Spin decoupled spectra with and without NOE

Operation time diagrams for such experiments are given below.[39]

(a) Spin coupled spectra with NOE

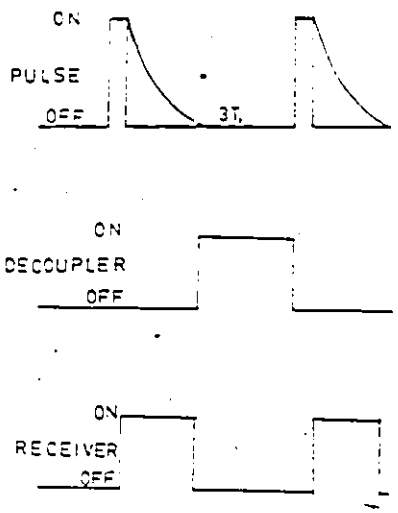

The above sequence resulted in a coupled spectrum with NOE and this can be compared with a normal coupled spectrum which was recorded by turning the decoupler off throughout the experiment.

(b) Spin decoupled spectra without NOE

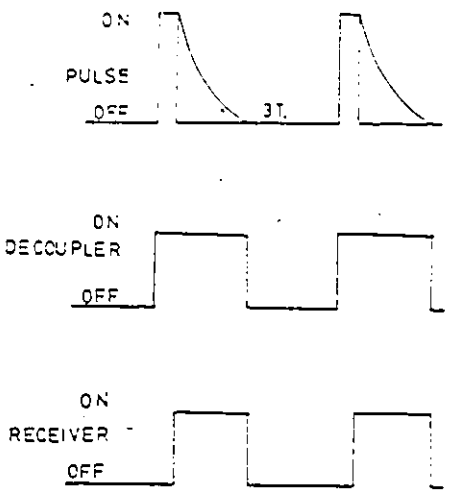

The above sequence resulted in a decoupled spectrum without NOE and its intensity is compared with that of the spectrum obtained by continuous decoupling. The intensity ratios obtained by the two methods (a) and (b) were the same within experimental errors.

Table 2.2 summarizes the NMR instruments employed and the conditions at which spectra were recorded.

TABLE 2.2

NMR instrument Manufactured by	Field strength	Ambient Temp.	Operating Frequencies (MHz)			
			^{1}H	^{13}C	^{19}F	^{119}Sn
Bruker	(T)	(°C)				
WH-90	2.114	24	-	-	-	33.56
WM-250	5.872	24	250.13	62.89	235.36	93.27
WM-400	9.395	22	-	100.62	-	149.21

The chemical shifts that are at higher frequency compared to the reference compound are considered to be positive while those at lower frequency to the reference compound are considered to be negative. The estimated errors on the chemical shifts of ^{1}H are less than 0.01 ppm, ^{13}C and ^{19}F are less than 0.1 ppm and ^{119}Sn are less than 1 ppm. The errors on coupling constants are given in the corresponding Tables.

2.4.2 Mössbauer Spectroscopy

The Mössbauer spectrometer and the details involved in obtaining ^{119}Sn gamma resonance spectra have been previously described[7], except that a Promeda multi channel analyzer was used. Samples containing approximately 15 mg of natural tin per cm^2 were prepared. The compounds used in this study

were air-sensitive and samples were prepared under a dry nitrogen atmosphere. These samples were packed in a 20 mm i.d. threaded Kel-F sample holder and sealed with teflon tape.

The source of the gamma radiation was Ca $^{119m}SnO_3$, obtained from New England Nuclear Corporation and maintained at room temperature. Samples were rigidly held either in a liquid transfer Cryotip system manufactured by Air Products and Chemical Inc. or in a cryostat manufactured by Cryo Technology Systems. Generally, samples were kept at -196°C except for variable temperature studies.

The velocity range was calibrated using a $^{57}Co/Rh$ source and a standard iron foil at room temperature. All isomer shifts were measured relative to $CaSnO_3$ as zero velocity at room temperature. Spectra were computer fitted using programmes written by either Dr. A. J. Stone[41] (modified by Dr. G. H. Grundy of McMaster University) or Dr. K. Rubenbauer.[42] The estimated error on the values quoted in the ^{119}Sn Mössbauer Tables in standard deviation units is 0.03 to 0.04 mm s^{-1}. These values are based on the statistics derived from the computer fitted spectra.

2.4.3 Infrared and Raman Spectroscopy

(i) The laser Raman spectrometer and the auxiliary instrumentation has been fully described previously.[43] Spectra were recorded at -196°C with the sample tube non-spinning. The tubes were mounted vertically with the angle between the incident radiation and the sample at 45°. The Raman scattered radiation was observed at 45° to the incident beam or 90° to the sample tube direction.

(ii) The infrared spectra were recorded using a Perkin Elmer 283 spectrometer. The powdered samples were used as nujol, or hexachlorobutadiene,

mulls with KBr windows. The gas phase i.r. spectra were obtained using a cell with KBr windows which was equipped for attachment to a vacuum line.

2.4.4 X-ray Crystallography

Since the crystals examined in this thesis were highly moisture sensitive, they were mounted in pre-dried Lindeman glass capillaries which were sealed under an atmosphere of dry nitrogen. Mounted crystals were examined under a microscope and the most suitable crystal was attached to a standard goniometer head. Alignment and full layer photographs (zero and first layer) of the crystals were taken on a Buerger precession camera when possible. The crystals were then transferred to a Nicolet P3 or a Syntex $P2_1$ diffractometer for X-ray intensity measurements. Instrumentation and data aquisition techniques for crystal structure determinations have been extensively described elsewhere[44]. Intensity measurements on the diffractometer were kindly performed by R. Faggiani of the Institute for Material Research of this university.

Intensity data from the diffractometer were stored on magnetic tapes and was transferred to computer files for further processing. Lorentz-polarization corrections were carried out using the DACTO5, DATRDN packages from the X-ray 76 system.[45] Neutral atom scattering factors[46] and anomalous dispersion correction[47] for Sn were taken from the International Tables. Specific details related to each crystal structure are discussed in the relevant sections of this thesis. All calculations were performed on a CDC-6400 or Cyber 170/730 computer using a series of programmes in the X-ray 76 system[45] and the programme SHELX.[48] Plots of atoms with thermal ellipsoids were generated using ORTEP II.[49]

2.4.5 Chemical Analysis

The tin analyses were carried out by reacting a known amount of compound, which was pre-weighed under a dry nitrogen atmosphere, with conc. sulphuric acid in a platinum crucible. This was slowly heated to dryness and then to red heat with a Meker burner. The crucible was cooled to room temperature in a desiccator and the amount of total tin was determined as SnO_2.[50]

Carbon, hydrogen and halogen analyses were carried out by Schwarzkopf Microanalytical Laboratory, New York.

CHAPTER 3

ALKYLTIN(IV) CATIONIC SPECIES IN STRONG ACIDS

3.1 Reactions of Methyltin Hydrides in Fluorosulphuric Acid

3.1.1 Introduction

Stannane and the methylstannanes have been well studied by a variety of spectroscopic techniques. Their proton magnetic resonance data have been reported by Flitcroft and Kaesz.[34] A linear relationship exists between $^{1}J_{Sn-H}$ and the tin-hydrogen stretching frequency ν(SnH).[51] Tin-119 Mössbauer spectra of stannane and some organotin hydrides have been recorded.[52] May and Spijkerman[53] have made a correlation between the Mössbauer isomer shift and $^{1}J_{Sn-H}$ for methyltin hydrides. A similar relationship has been observed for ethyltin hydrides.[54]

Sawyer and Kuivila have investigated the reaction of some organotin hydrides with acids.[55-58] They found that di-n-butyltin dihydride reacts with acetic acid to give either one of two products as shown in equations (3.1) and (3.2).[56]

$$2Bu_2SnH_2 + 2HOAc \longrightarrow \underset{\underset{AcO}{|}\quad\underset{OAc}{|}}{Bu_2Sn\text{-}SnBu_2} + 3H_2 \qquad (3.1)$$

$$Bu_2SnH_2 + 2HOAc \longrightarrow Bu_2Sn(OAc)_2 + 2H_2 \qquad (3.2)$$

1,1,2,2,-Tetra-n-butyl-1,2-diacetoxyditin is the main product when the acid-hydride ratio is 1:1 and dibutyltin diacetate is the major product

when the acid to hydride ratio is 2:1. On the other hand diphenyltin dihydride, irrespective of whether the acid-hydride ratio is 1.0 or 2.0, reacts to give as the main product 1,1,2,2-tetraphenyl-1,2-diacetoxy-ditin. Similar behaviour is observed when other carboxylic acids are allowed to react with these hydrides.[56] In addition, it was found that di-n-butyltin dihydride reacts with HCl in dioxane to produce di-n-butyl-tin chlorohydride and 1 mole of H_2 according to equation (3.3).[57]

$$Bu_2SnH_2 + HCl \longrightarrow Bu_2Sn\begin{matrix}H\\Cl\end{matrix} + H_2 \qquad (3.3)$$

This tin chlorohydride reacts further with excess acid to evolve another mole of H_2 as given by equation (3.4).

$$Bu_2Sn\begin{matrix}H\\Cl\end{matrix} + HCl \longrightarrow Bu_2SnCl_2 + H_2 \qquad (3.4)$$

It was also found that an exchange reaction (equation 3.5) between Bu_2SnH_2 and Bu_2SnCl_2 gave Bu_2SnClH.[58]

$$Bu_2SnH_2 + Bu_2SnCl_2 \longrightarrow 2Bu_2Sn\begin{matrix}H\\Cl\end{matrix} \qquad (3.5)$$

Webster and Jolly have followed the reaction of stannane (SnH_4) with strong acids.[8] Their measurements show that stannane reacts slowly with aqueous acids at low temperature to evolve 1 mole of H_2 per mole of stannane. On warming to room temperature, an additional two moles of H_2 are evolved. In fluorosulphuric acid at -78°C however, reaction occurs relatively fast with the evolution of 1 mole of hydrogen and no further hydrogen is evolved on warming to room temperature. The reaction of stannane in HSO_3F has been re-examined and the reactions

of methylstannanes in HSO_3F have been studied for the first time. These results are discussed in this chapter.

It has been shown that the reaction of excess $(CH_3)_4Sn$ with HSO_3F at -80°C forms $(CH_3)_3SnSO_3F$ with evolution of methane.[59] When excess HSO_3F is employed at 25°C the products formed are methane and $(CH_3)_2Sn(SO_3F)_2$.

$$(CH_3)_4Sn + HSO_3F \xrightarrow{-80°C} (CH_3)_3SnSO_3F + CH_4 \qquad (3.6)$$

$$(CH_3)_3SnSO_3F + HSO_3F \xrightarrow{25°C} (CH_3)_2Sn(SO_3F)_2 + CH_4 \qquad (3.7)$$

These two compounds have been isolated as pure solids and characterized by Mössbauer and vibrational spectroscopy. The nature of these species in solution prior to crystallization has been studied by ^1H NMR and frozen solution ^{119}Sn Mössbauer spectroscopy.[2] Carbon-13 NMR and ^{119}Sn NMR of these species in HSO_3F and H_2SO_4 solutions were studied in order to obtain additional information about their structures. These data are also presented in this chapter.

3.1.2 NMR Studies

The NMR data of the parent hydrides and their reaction products in fluorosulphuric acid are provided in Table 3.1. Literature data have also been included in this table. There is generally a good agreement between NMR data of this study and the literature data. Tin-119 NMR chemical shift of SnH_4 is reported here for the first time.

Firstly, the reaction of stannane with fluorosulphuric acid has been followed by ^1H NMR. This solution exhibits a single line at 7.8 ppm with tin satellites corresponding to the Sn-H coupling. Tin-119 NMR

TABLE 3.1

NMR Data for $(CH_3)_{4-n}SnH_n$ (n = 1-4) and Alkyltin(IV) Cationic Species in Strong Acids

Compound	Solvent	Temp.	Chemical Shift (ppm) $\delta_{^1H}$	$\delta_{^{13}C}$	$\delta_{^{119}Sn}$	Coupling Constant $^1J_{^{117/119}Sn-^1H}$	$^2J_{^{117/119}Sn-C-^1H}$	$^1J_{^{117/119}Sn-^{13}C}$	Ref.
		°C	ppm			Hz	Hz	Hz	
SnH_4	Neat	-50	3.85	-		1846-1931	-	-	34
	C_6H_{14}	-65	3.9	-	-493	1846, 1933	-	-	
						1929* ± 6			
CH_3SnH_3	C_5H_{12}	40	0.27, 4.14			1770/1852	62.0		34
	C_7H_8	-35			-346				a
	C_6H_{14}	-50	0.33, 4.46	-17.8	-355	1770/1850	62.0	370	
						1856* ± 10	61.0* ± 6		
$(CH_3)_2SnH_2$	C_5H_{12}	40	0.17, 4.76			1682/1758	58.0		34
	C_6H_{12}	-20			-225				b
	C_6H_{14}	-25			-226	1807* ± 5			
	C_6D_6	25	0.20, 4.63	-14.8		1705/1782	58.5	361	
$(CH_3)_3SnH$	C_6H_6				-104				c
	C_5H_{12}	40	0.16, 4.73			1664/1744	56.5		34
				-11.8				352	31
SnH_4	HSO_3F								
$[SnH_3^+]$		-78	7.5			2767, 2910			d
			7.8		-192.4	2780, 2910			
					-186	2960*			g

Continued.....

TABLE 3.1 (Continued)

N.M.R. Data for $(CH_3)_{4-n}SnH_n$ (n = 1-4) and Alkyltin(IV) Cationic Species in Strong Acids

Compound	Solvent	Temperature	Chemical Shift (ppm)			Coupling Constant			Ref.
			$\delta_{^1H}$	$\delta_{^{13}C}$	$\delta_{^{119}Sn}$	$^1J_{^{117/119}Sn-^1H}$ †	$^2J_{^{117/119}Sn-C-^1H}$ †	$^1J_{^{117/119}Sn-^{13}C}$ †	
		Temp. °C		ppm			Hz	Hz	
$[SnH_3^+]$		-30			-193.6	2775/2904			
						2913* ± 10			
$[Sn^{2+}]$		25			-1780				8
					-1601				
CH_3SnH_3	HSO_3F								
$[CH_3SnH_2^+]$		-78	0.51,8.2	-7.0	-29.3	2593/2710	73.0	463	
						2698* ± 5	73.2* ± 6		
		-60			-27.8	2690* ± 6			
$[(CH_3)_2Sn^{2+}]$			1.25				86		
$[(CH_3)_2Sn^{2+}]$		-30	1.27	10.1	-222		82		
$[(CH_3)_2Sn^{2+}]$		25	1.6	14.5	-185		88.5	600	
$[(CH_3)_2SnH^+]$	HSO_3F								
$[(CH_3)_2SnH^+]$		-85	0.57,8.4	-0.8	+156	2494/2606	68.0		
						2460* ± 150			
$[(CH_3)_2Sn^{2+}]$		25	1.66		-183		85.5		
Me_4Sn	HSO_3F								
$[(CH_3)_3Sn^+]$		-60	0.75	+6.8	+322		60,63	388	
$[(CH_3)_2Sn^{2+}]$		25	1.68	13.2	-185		88.0	600	

Continued.....

TABLE 3.1 (Continued)

Compound	Solvent	Temperature °C	$\delta(^{119}Sn)$ ppm	$^{2}J_{119Sn-C-^{1}H}$ Hz	$^{1}J_{117/119Sn-^{13}C}$ Hz	$^{3}J_{119Sn-C-C-^{1}H}$ Hz
$(CH_3)_3SnCl$	92% H_2SO_4					
$[(CH_3)_3Sn^+]$		0	+ 194	65	409	
$[(CH_3)_2Sn^{2+}]$		25	- 154	97	627	
$(C_2H_5)_4Sn$	HSO_3F					
$[(C_2H_5)_3Sn^+]$		- 20	+ 288		330	
$[(C_2H_5)_2Sn^{2+}]$		24	- 253	61	428	184
$(C_2H_5)_2SnCl_2$	100% H_2SO_4					
$[(C_2H_5)_2Sn^{2+}]$		24	- 268	68	516	188

* Measured by ^{119}Sn NMR

† Estimated error is less than 3 Hz (excluding the values whose errors are included in the Table).

‡ Estimated error is less than 5 Hz.

[a] J. D. Kennedy and W. McFarlane, Rev. Silicon, Germanium, Tin, Lead Compd., 1, 235, (1974).

[b] C. Schumann and H. Dreeshamp, J. Magn. Reson., 3, 204, (1970).

[c] A. P. Tupčiauskas, N. M. Sergeyev, and Yu. A. Ustynyuk, Org. Magn. Reson., 3, 655, (1971).

[d] T. Birchall and A. Pereira, J. Chem. Soc., Chem. Commun., 1150 (1973).

recorded at this temperature shows a quartet due to the three protons attached to tin with a coupling constant equal to that observed in the ^1H NMR (See Figure 3.1 (b)). This clearly establishes the formation of the SnH_3^+ species at this temperature. The ^1H and ^{119}Sn resonances for SnH_3^+ occur at higher frequency than those of SnH_4 indicating considerable deshielding. Upon slowly warming to -30°C, the ^1H and ^{119}Sn NMR recorded at this temperature still show the presence of the SnH_3^+ species. However, the intensity of the signals are decreased. At ambient temperature, only a weak signal was observed at 4.0 ppm in the ^1H NMR spectrum. This peak consistently appeared in every ^1H NMR spectrum recorded between -78°C and ambient temperature. The chemical shift of the signal agrees with the value for that of hydrogen gas and is presumably due to the dissolved hydrogen in HSO_3F. The ^{119}Sn NMR spectrum of the solution at room temperature shows a single line at -1601 ppm which is close to the chemical shift of $Sn(SO_3F)_2$ in HSO_3F. The ^{119}Sn Mössbauer spectrum recorded on this solution, after freezing it to 77 K, shows only one signal due to a Sn(II) species (Figure 3.2(a)). The Mössbauer parameters of this signal are very close to those of $Sn(SO_3F)_2$ (Figure 3.2, Table 3.2). The above observations establish the initial formation of SnH_3^+ species which reacts further to form $Sn(SO_3F)_2$. The Toepler pump measurement shows the evolution at -78°C of one mole of hydrogen per mole of stannane with no more hydrogen being evolved on warming to room temperature. These results can be explained by equations (3.8) and (3.9).

$$SnH_4 + HSO_3F \longrightarrow SnH_3^+ + SO_3F^- + H_2 \qquad (3.8)$$

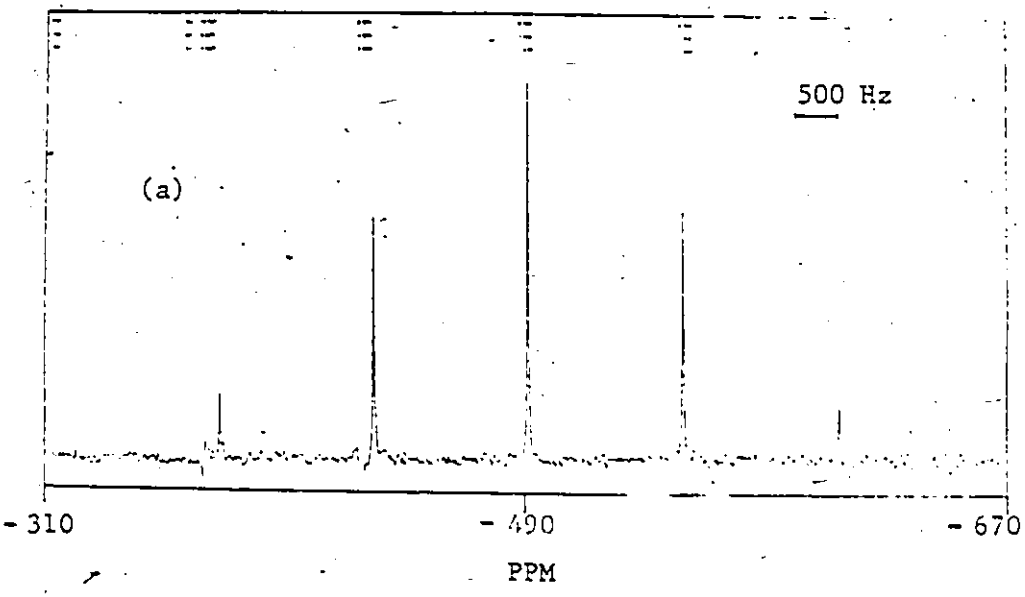

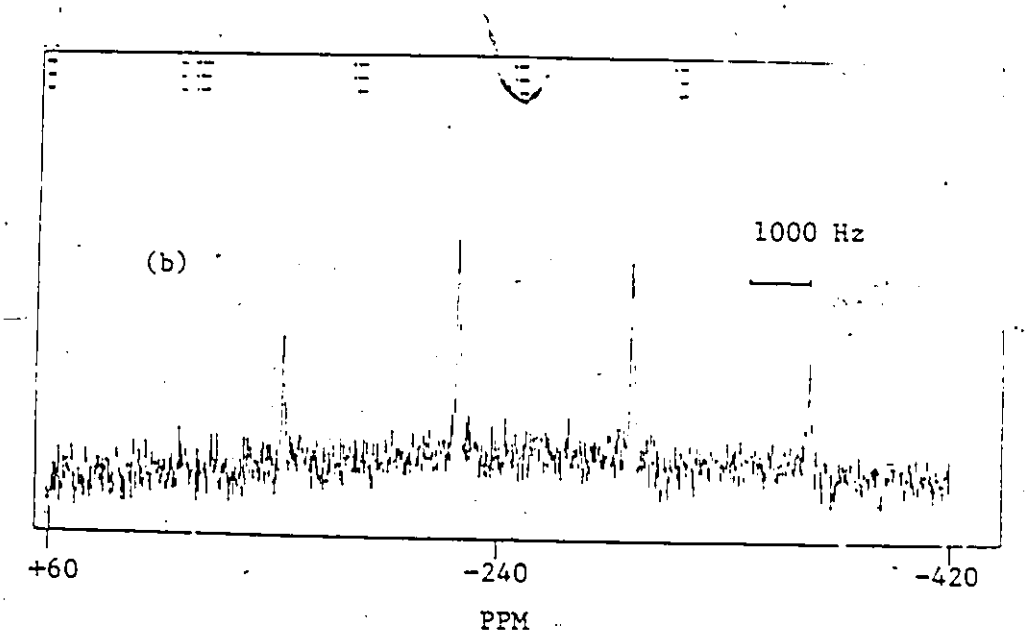

Figure 3.1: ^{119}Sn NMR spectra of (a) SnH_4 in hexane at -65°C (b) SnH_4 in fluorosulphuric acid at -78°C.

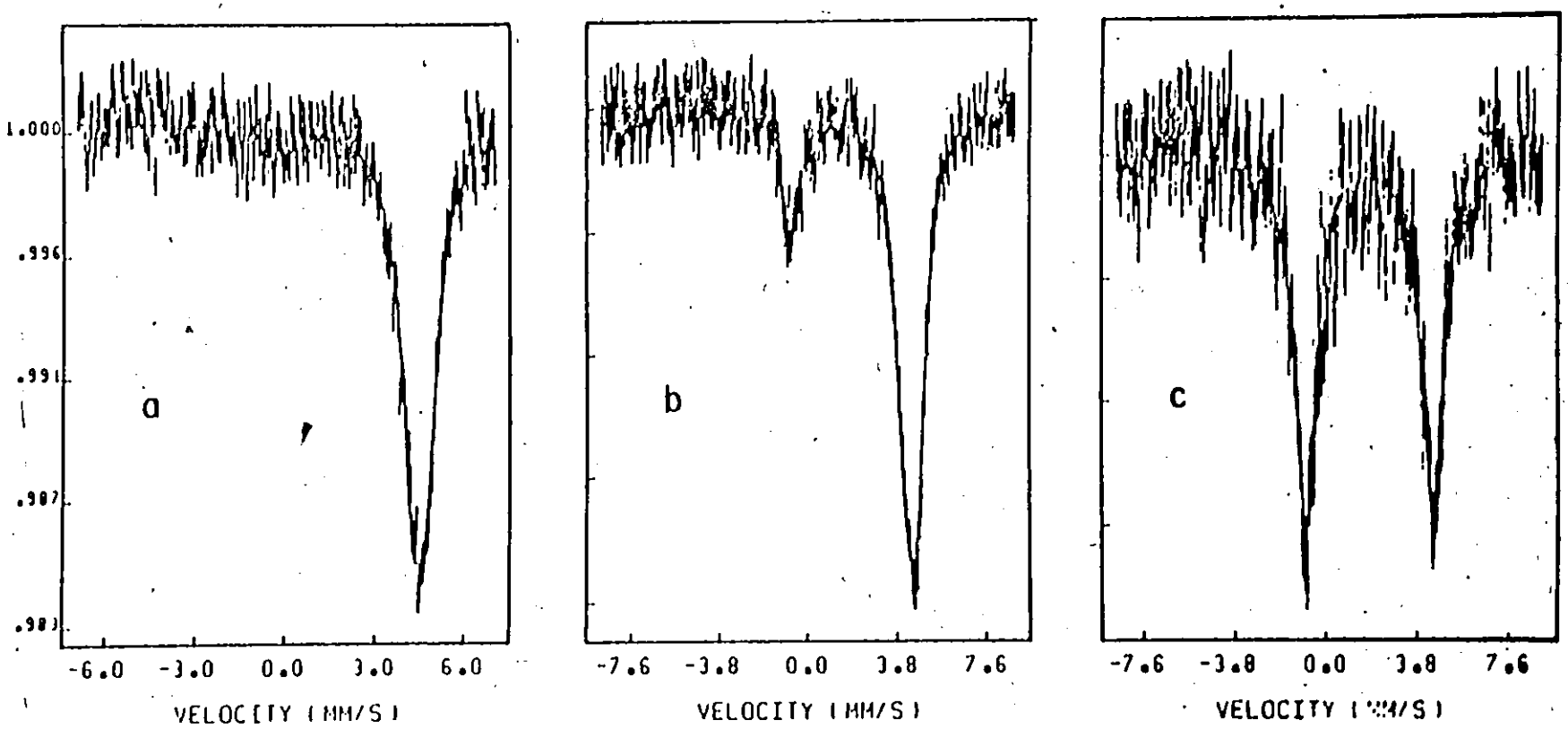

Figure 3.2: ^{119}Sn Mössbauer spectra of solutions of tin hydrides in fluorosulphuric acid after warming to room temperature, then freezing the solutions at 77 K (a) SnH_4, (b) $(CH_3)SnH_3$, (c) $(CH_3)_2SnH_2$.

TABLE 3.2

^{119}Sn Mössbauer Data for Solutions of Tin Hydrides in Fluorosulphuric Acid After Standing at Room Temperature and then Recorded at 77 K

Compound	Medium	Sn(IV)			Sn(II)		
		δ	Δ	Γ	δ	Δ	Γ
		mms^{-1}			mms^{-1}		
SnH_4	HSO_3F				4.33	0.58	0.88
CH_3SnH_3	HSO_3F	1.86	5.22	0.95	4.42	0.60	0.95
$(CH_3)_2SnH_2$	HSO_3F	1.81	5.25	1.07			
$(CH_3)_3SnH$[2]	HSO_3F	1.61	4.95				
$Sn(SO_3F)_2$[27]	SOLID				4.18	0.68	1.33
$(CH_3)_2Sn(SO_3F)_2$[2]	HSO_3F	1.89	5.41				
$(CH_3)_3SnSO_3F$[59]	SOLID	1.52	4.61	0.99, 1.04			

$$SnH_3^+ + 5HSO_3F \longrightarrow Sn^{2+} + 2H_2SO_4 + 2SO_2 + 4HF + SO_3F^- \qquad (3.9)$$

The colour of the room temperature solutions are either pale blue or green depending on the concentration. This may be indirect evidence for the formation of SO_2 since the reaction of SO_2 and HSO_3F in the presence of hydrogen produces polycations of sulphur, whose colour is similar to these solutions.[8] The evidence for the presence of HF comes from ^{19}F NMR spectroscopy. This shows a sharp single line at -160 ppm. One might have expected this to be a doublet due to H-F coupling but, in HSO_3F the protons of HSO_3F and HF exchange at a fast rate which eliminates this coupling. The ^{19}F NMR chemical shift of HF in HSO_3F has been reported to be -186 ppm.[60] The difference in the two chemical shifts is likely due to the difference in their concentrations.

The solvolysis of methylstannane ($MeSnH_3$) in HSO_3F was monitored by NMR spectroscopy and hydrogen evolution. The ^{119}Sn NMR spectrum of methylstannane in HSO_3F, at -78°C, exhibits a triplet of quartets as shown in Figure 3.3(b). The tin resonance is split into a triplet with a large Sn-H coupling constant due to the two protons directly attached to tin. This is further split into quartets by the protons of the methyl group with a smaller coupling constant. (Figure 3.3(b)). This shows that the species in solution is $CH_3SnH_2^+$. Like the SnH_3^+ cation, the tin in $CH_3SnH_2^+$ experiences a deshielding in the ^{119}Sn resonance and a large increase in coupling constant on going from the neutral hydride to the cationic species. As this solution is warmed to -60°C, the ^{119}Sn NMR shows, in addition to the $CH_3SnH_2^+$ species, another resonance at lower frequency (Figure 3.4(a)). When this solution is slowly warmed to -30°C, the signal due to $CH_3SnH_2^+$ completely

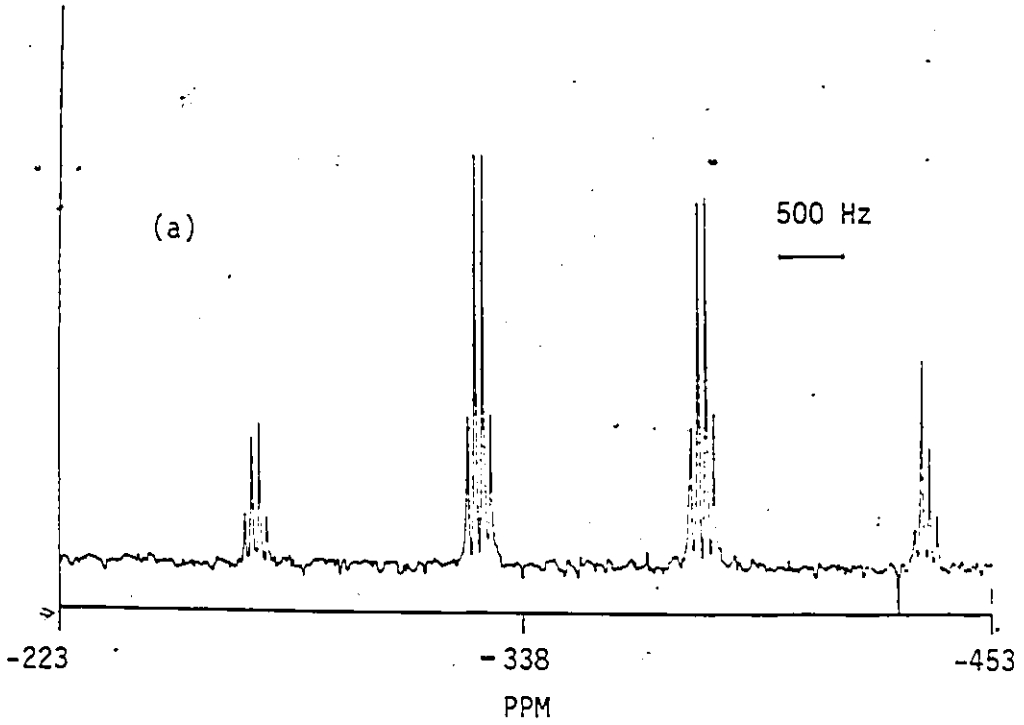

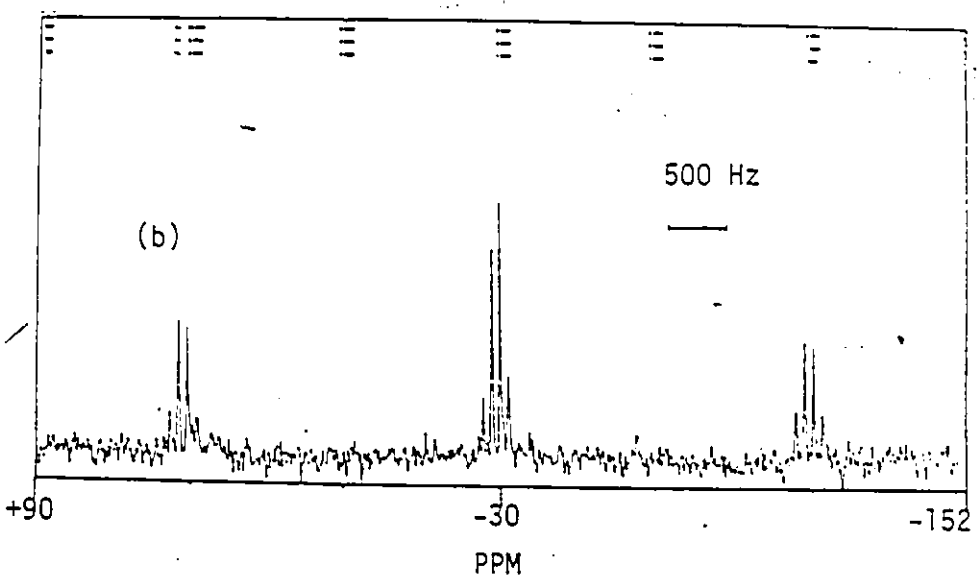

Figure 3.3: ^{119}Sn NMR spectra of (a) CH_3SnH_3 in hexane at -50°C (b) CH_3SnH_3 in fluorosulphuric acid at -78°C.

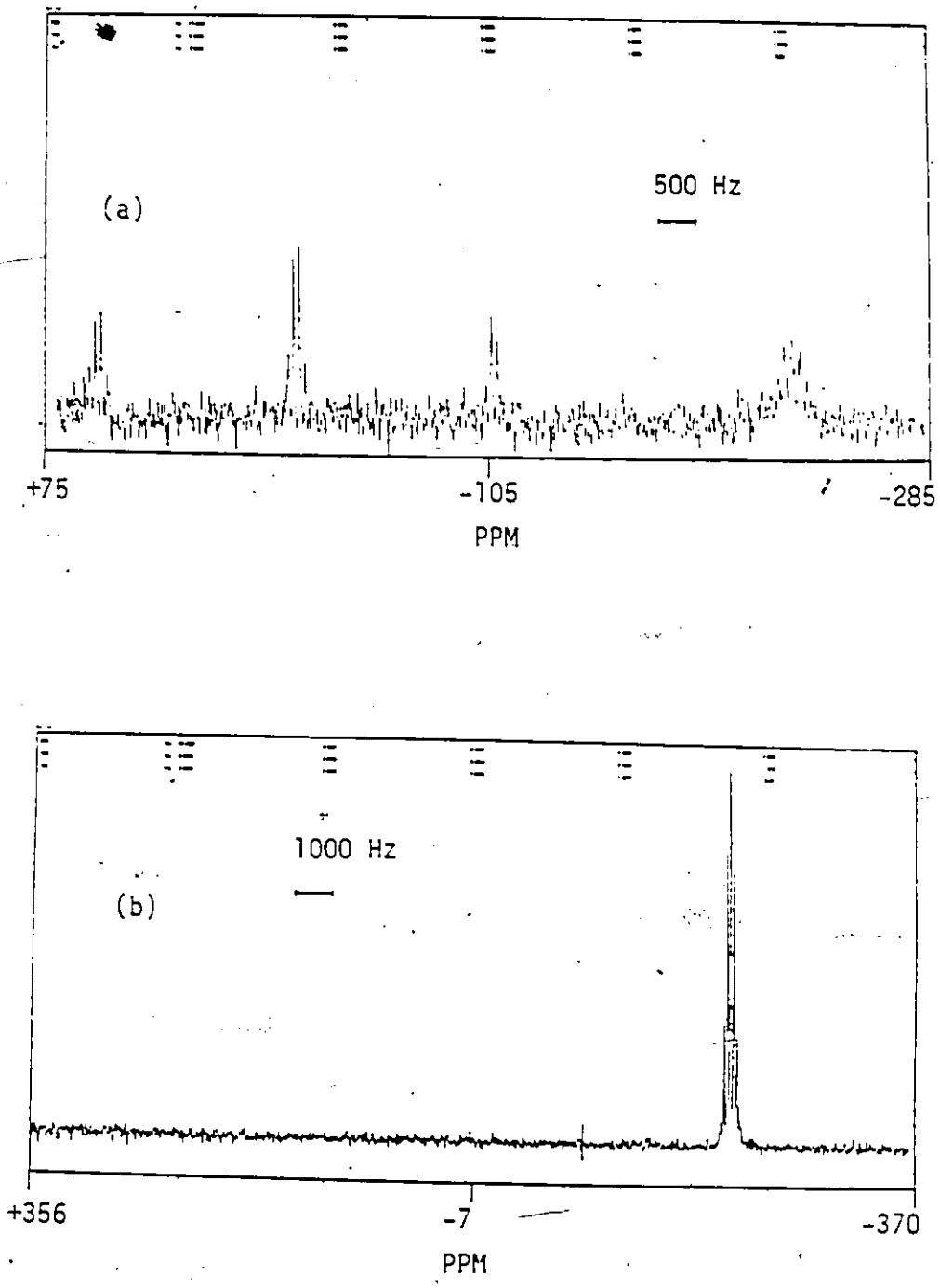

Figure 3.4: ^{119}Sn NMR spectra of CH_3SnH_3 in fluorosulphuric acid at (a) -60°C, (b) 25°C.

disappears and a clearly resolved septet is observed at -222 ppm. The ambient temperature spectrum of the resulting species (Figure 3.4(b)) is a septet having a chemical shift of -185 ppm and a coupling constant $^{2}J_{^{119}Sn-H}$ of 88 Hz. Proton spectra are consistent with the above changes and the only proton species remaining at ambient temperature shows a single line at 1.24 ppm with tin satellites separated by 86 Hz. These NMR parameters are characteristic of $(CH_3)_2Sn^{2+}$, which has been identified as the stable species when $(CH_3)_4Sn$ is reacted with HSO_3F.[2] The low frequency region of the ^{119}Sn NMR spectrum reveals a second peak at -1600 ppm which corresponds to $Sn(SO_3F)_2$ in HSO_3F. The ^{119}Sn Mössbauer spectrum recorded on this solution frozen at 77 K, is shown in Figure 3.2(b). This spectrum has been fitted to two overlapping doublets and its parameters are given in Table 3.2. These parameters agree with those for the frozen solution spectra of $(CH_3)_2Sn^{2+}$ in HSO_3F [2] and solid $Sn(SO_3F)_2$.[27] It was shown that one mole of hydrogen was produced at low temperature (-78°C) and another mole of hydrogen on warming the solution to room temperature. These observations are satisfied by equations (3.10) and (3.11).

$$CH_3SnH_3 + HSO_3F \longrightarrow CH_3SnH_2^+ + SO_3F^- + H_2 \qquad (3.10)$$

$$2CH_3SnH_2^+ + 4HSO_3F \longrightarrow (CH_3)_2Sn^{2+} + Sn^{2+} + H_2SO_4 + SO_2 + 2HF + 2H_2 + 2SO_3F^- \qquad (3.11)$$

The presence of HF in this solution is evident from its ^{19}F NMR spectrum. The mechanism of CH_3 transfer from $CH_3SnH_2^+$ to produce $(CH_3)_2Sn^{2+}$ is not clear, but presumably occurs via a ditin intermediate. Organoditin compounds are produced from organotin hydrides in acid solution.[55,56]

The solvolysis of dimethyltin dihydride in fluorosulphuric acid produces a much less stable species than the other hydrides discussed previously. The ^{119}Sn NMR spectrum of $(CH_3)_2SnH_2$ in HSO_3F at -78°C shows only one signal attributable to the final reaction product, i.e., $(CH_3)_2Sn^{2+}$. This reaction was therefore attempted at -85°C and the NMR sample was transferred to the NMR probe, also maintained at -85°C. No matter how rapidly the sample transferred, it was still not fast enough to prevent some decomposition. This ^{119}Sn NMR spectrum (Figure 3.5(b)) shows two signals. The high frequency doublet corresponds to the $(CH_3)_2SnH^+$ species with the coupling being due to one hydrogen directly bonded to tin. One would expect that each component would be split further into a septet by the methyl protons. However, in order to observe this, a better quality spectrum would be required with an improved signal to noise ratio. It was found that with longer accumulation times, at -85°C, the doublet intensity slowly decreased indicating that decomposition occured even at this temperature. The low frequency ^{119}Sn signal arises from the $(CH_3)_2Sn^{2+}$ cation. The ^1H NMR spectrum at -85°C exhibits signals due to $(CH_3)_2SnH^+$ and $(CH_3)_2Sn^{2+}$. Proton and ^{119}Sn NMR spectra of the room temperature solution exhibit well resolved signals for the $(CH_3)_2Sn^{2+}$ species. The ^{119}Sn Mössbauer spectrum of this solution frozen at 77 K, is shown in Figure 3.2(c) and the parameters are close to those for $(CH_3)_2Sn(SO_3F)_2$.[2] Dimethyltin dihydride reacts with HSO_3F to produce one mole of hydrogen gas. Again, ^{19}F NMR spectrum provides evidence for HF in this solution. The above observations can be explained by equations 3.12 and 3.13.

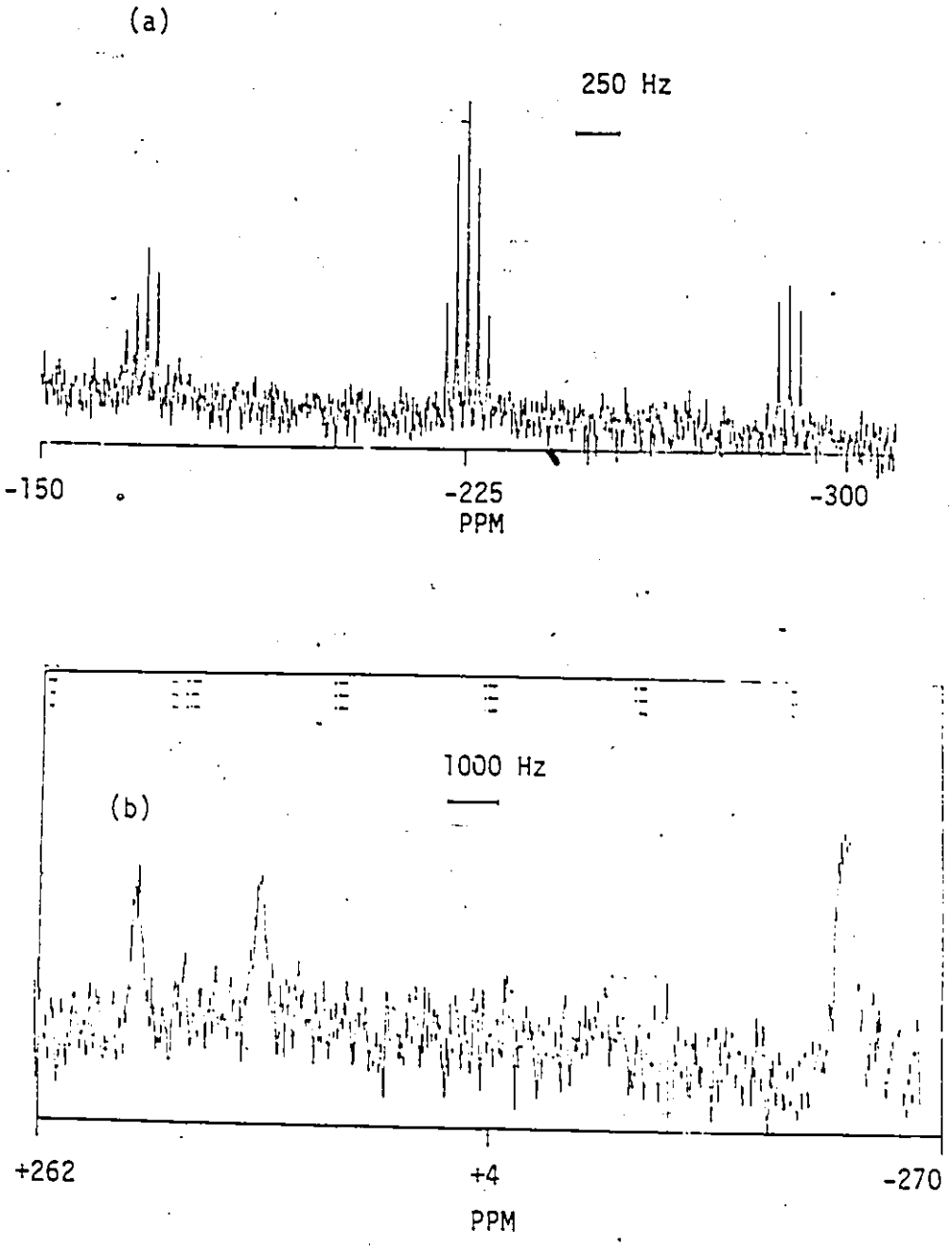

Figure 3.5: ^{119}Sn NMR spectra of (a) $(CH_3)_2SnH_2$ in C_6D_6 at 25°C, (b) $(CH_3)_2SnH_2$ in fluorosulphuric acid at -85°C.

$$(CH_3)_2SnH_2 + HSO_3F \longrightarrow (CH_3)_2SnH^+ + SO_3F^- + H_2 \qquad (3.12)$$

$$(CH_3)_2SnH^+ + 3HSO_3F \longrightarrow (CH_3)_2Sn^{2+} + SO_3F^- + H_2SO_4 + SO_2 + 2HF \qquad (3.13)$$

Trimethyltin hydride behaves in the same way as the other hydrides, producing $(CH_3)_3Sn^+$ and H_2 at low temperature followed by methane evolution at room temperature to give $(CH_3)_2Sn^{2+}$. NMR data for R_3Sn^+ and R_2Sn^{2+} (where R = CH_3, C_2H_5) in HSO_3F and H_2SO_4 are also given in Table 3.1 and were obtained by the acid solvolysis of R_4Sn and R_2SnCl_2 (where R = CH_3, C_2H_5) respectively.

In any series of main group element hydrides MH_x, replacement of hydrogen by a methyl group results in a deshielding of the M resonance. This effect has been observed in the ^{13}C, ^{15}N, ^{29}Si and ^{31}P NMR chemical shifts of their hydrides.[61-63] Methyl- and ethylstannanes[64] follow this trend and the ^{119}Sn chemical shift of stannane reported here allows completion of the correlation. The ^{119}Sn chemical shifts for $(CH_3)_{4-n}SnH_n$ are plotted against n in Figure 3.6(a). The straight line does not pass through the origin which is the value for $(CH_3)_4Sn$. This is probably because the stannane shifts were measured as dilute solutions in organic solvents whereas $(CH_3)_4Sn$ was recorded as a neat liquid. The ^{119}Sn resonances of $(CH_3)_{3-n}SnH_n^+$ (n = 0-3) in HSO_3F appear at higher frequencies than their parent hydrides and follow similar trends to those of the hydrides. This plot is also included in Figure 3.6(a). The increased shielding of the tin nucleus on substitution of a methyl group is more pronounced in the cation than in the hydrides. This reflects tighter C-Sn bonding in the cationic species which suggests that the fluorosulphate anions interact weakly with

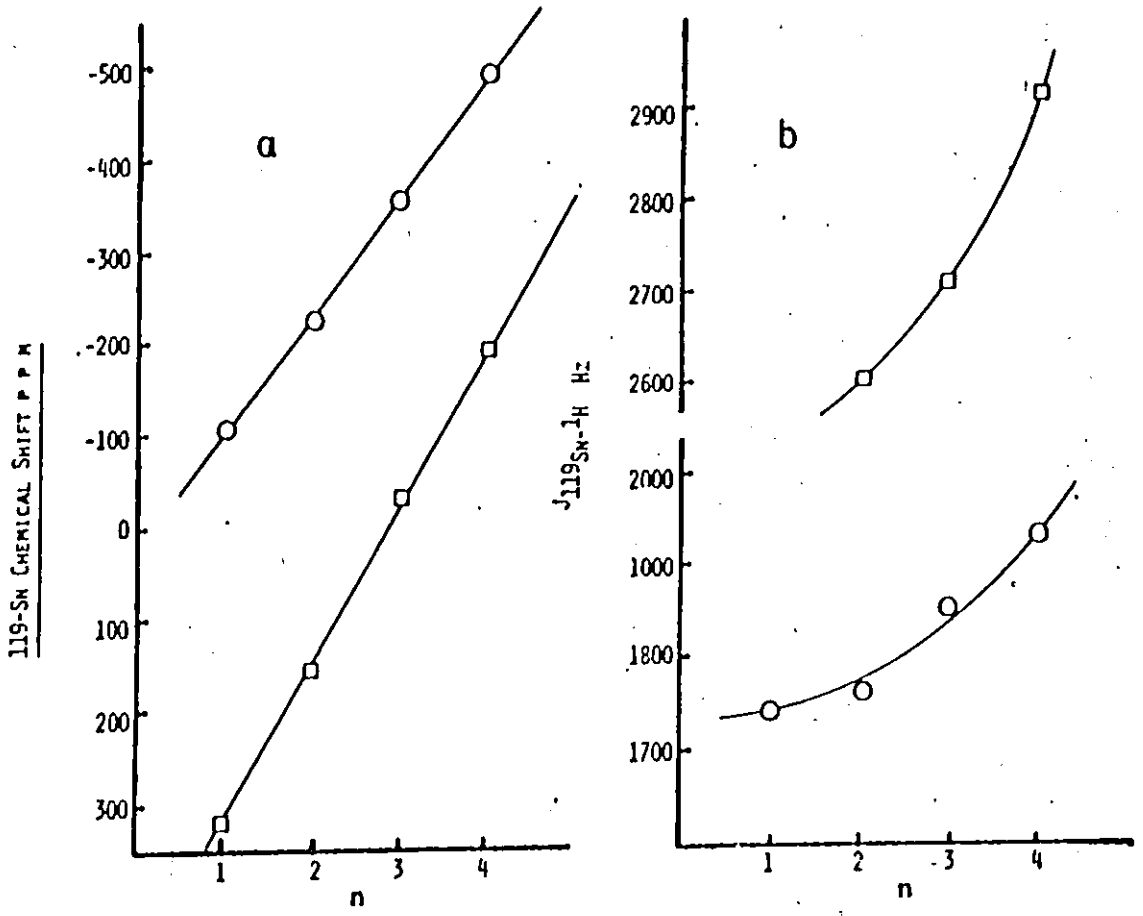

Figure 3.6: Plot of (a) ^{119}Sn NMR chemical shifts and (b) $^{1}J_{^{119}Sn-^{1}H}$ coupling constants against n in $(CH_3)_{4-n}SnH_n$: (O) parent hydride, (◊) hydride in fluorosulphuric acid

the organo-tin species in solution, although this interaction is undoubtedly present.

The direct Sn-H coupling constant is more informative and one notices a dramatic increase in the value of this coupling on going from the hydride to the corresponding cationic species. As before, the substitution of a methyl group causes a greater increase in the coupling constant of the cations compared to the hydrides. If the spin-spin coupling constant is dominated by the Fermi contact interactions,[65] the increase in the coupling constant is indicative of increased 's-character' in the bonds. If the hybridization of tin in the hydride can be considered as sp^3, one could attribute the above increase in the coupling constant to a change in hybridization at tin from sp^3 to sp^2. Mitchell[31] has observed large variations in $^1J_{^{119}Sn-^{13}C}$ for organotin compounds ranging from 240 to 1120 Hz and it is thought that one bond coupling constants should give more precise information on the hybridization at the tin atom than the coupling constants operating through two bonds. The $^1J_{^{119}Sn-^{13}C}$'s of $(CH_3)_{3-n}SnH_n^+$ fall in the range usually shown by five coordinated trialkyltin compounds.

Trimethyltin fluoride has been shown to have a five coordinate tin environment[66] and based on spectral data, $Me_3Sn(SO_3X)$ has been interpreted in terms of a five coordinate structure.[59] On the basis of frozen solution Mössbauer data, it is shown that the $(CH_3)_3Sn^+$ species in strongly acidic solutions show similar environments around tin as they do in the solid state.[2] From the coupling constants reported here, it can be seen that the $[(CH_3)_{3-n}SnH_n]^+$, (n=0→3) unit is planar

with sp^2 hybridization for the Sn-C bonds and the axial positions are presumably occupied by fluorosulphate ions to form a trigonal bipyramidal environment around the tin.

Dialkyltin cations R_2Sn^{2+} (where R = CH_3, C_2H_5) show an increase in $^1J_{^{119}Sn-^{13}C}$ and $^2J_{^{119}Sn-C-^1H}$ compared to the corresponding trialkyltin cation R_3Sn^+ (where R = CH_3, C_2H_5) in both HSO_3F and H_2SO_4 solutions. This trend is in qualitative agreement with an increasing 's-character' to the C-Sn bonds i.e., from sp^2 in $[R_3Sn^+]$, to sp in $[R_2Sn]^{2+}$ in the solvated cationic species. $Me_2Sn(SO_3X)_2$ compounds have been suggested to be six coordinate[67] and the X-ray structure of $Me_2Sn(SO_3F)_2$ showed this to be the case.[68]

Since the Mössbauer parameters of the frozen solutions of dialkyltin species in acids are similar to those of their solids, it had been concluded that these species are solvated and have trans-octahedral geometry in solution with alkyl groups occupying axial positions and the remaining coordination sites being filled by solvent molecules.[2] The ^{119}Sn NMR chemical shifts of related organotin complexes move to lower frequency as the coordination number increases from 4 to 7 encompassing a range of 600 ppm.[69] In this study, ^{119}Sn NMR chemical shifts of R_2Sn^{2+} and R_3Sn^+ species are in agreement with their assigned coordination numbers. In simple terms, six coordinated R_2Sn^{2+} species are more shielded than five coordinated R_3Sn^+ species and resonate at lower frequency.

Figure 3.7 shows a plot of $^1J_{^{119}Sn-^{13}C}$ against $^2J_{^{119}Sn-H}$ for the species listed in Table 3.1. Only the magnitude of the coupling

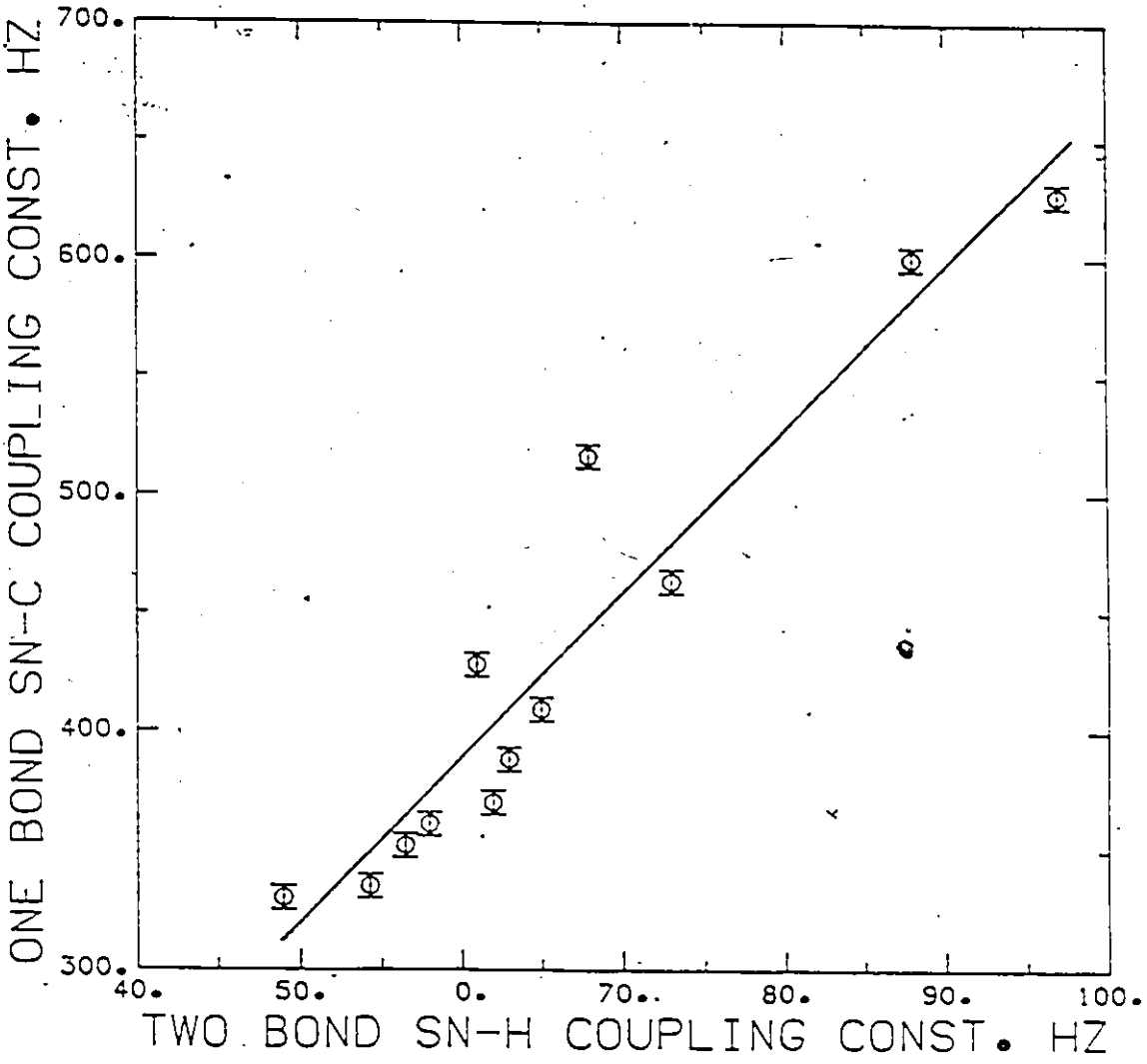

Figure 3.7: Plot of one bond Sn-C coupling constant against two bond Sn-H coupling constant for tin hydrides and alkyltin(IV) cationic species. The straight line represents the best linear fit to the data.

constant can be obtained from a simple NMR spectrum and additional experiments are required to determine its sign. For most of the dimethyl- and trimethyltin compounds, $^{1}J_{Sn-C}$ and $^{2}J_{Sn-H}$ have been determined to be negative and positive, respectively (See Tables 27 and 38 of reference (70)). However, the sign of $^{1}J_{Sn-C}$ in $(CH_3)_3SnLi$ was found to be positive.[71] In the plot shown in Figure 3.7, it is assumed that $^{1}J_{Sn-C}$ is negative and $^{2}J_{Sn-H}$ is positive. There is a reasonable correlation between these two parameters with a correlation coefficient of 0.95. A similar correlation has been observed by Kennedy and McFarlane.[71] This aids in predicting the magnitude of one coupling constant if the other one is known. Although there is an approximate linear relationship between $^{1}J_{^{119}Sn-^{13}C}$ and $^{2}J_{^{119}Sn-^{1}H}$, the line does not pass through the origin. This has been observed by the earlier workers,[71,72] and indicates that at least one of the coupling constants may involve significant contributions from terms other than the Fermi contact interaction.

3.2 NMR Relaxation Time Measurements and Chemical Exchange

3.2.1 Introduction

Frozen solution ^{119}Sn Mössbauer data and ^{1}H NMR spectroscopy of alkyltin cations in strong acids, suggests that the geometry around tin is similar to that in the solids crystallized from solution.[2] The Mössbauer isomer shift (δ) is a function of the s electron density at the tin nucleus. In the NMR experiments, the direct ^{119}Sn-^{13}C coupling constant, $^{1}J_{^{119}Sn-^{13}C}$, is sensitive to the s character in this bond if the Fermi contact term is the dominant contributor. Therefore, there should be a relationship between δ and $^{1}J_{^{119}Sn-^{13}C}$. In order to correlate these values, initially it was decided to measure $^{1}J_{^{119}Sn-^{13}C}$ from ^{119}Sn NMR spectra. In so doing, it was observed that the ^{119}Sn signal line width increased dramatically with the field of the instrument used to make the measurements. This led to a systematic study of the relaxation process involved in this system.

There have been relatively few reports concerning relaxation time measurements of the ^{119}Sn nucleus available. Puskar et al were the first to carry out a detailed spin-lattice relaxation study of organotin compounds in the liquid state.[73] The reported spin-lattice relaxation times (T_1) for ^{119}Sn varied over a range 0.5 -5secs. in the series R_4Sn (R = Me, Et, Pr). It has been found that only in the case of Me_4Sn is the relaxation behaviour due mainly to the spin-rotation mechanism. For the other two larger molecules, relaxation is dominated by spin-rotation at higher temperatures and by dipole-dipole mechanism at lower temperatures. It is established that for Me_3SnX (X = Cl, Br),

spin-rotation is the dominant relaxation mechanism and for Me_3SnI, scalar relaxation makes a significant contribution.[73] Lassigne and Wells have shown that the ^{119}Sn spin-lattice relaxation rate of liquid Me_4Sn and its deuterated modifications $Me_nSn(CD_3)_{4-n}$ (n = 0→4) are dominated by the spin-rotation interaction.[74] Sharp and Tolan have measured ^{119}Sn relaxation times for liquid state $SnCl_3I$ and SnI_3Cl and found that spin-lattice relaxation arises from competing spin-rotation and scalar interactions while spin-spin relaxation is completely dominated by scalar relaxation.[75] Recently, Blunden et al have measured ^{119}Sn spin-lattice relaxation times (T_1) and nuclear Overhauser enhancement (NOE) factors (η) for some organotin compounds.[76] A closer look at their data shows the T_1 values for $Bu_2Sn(OAc)_2$ are field dependent. This would indicate significant contribution from shielding anisotropy (SA) to the spin-lattice relaxation mechanism. However, the authors attributed this to an exchange process. The data discussed in this section shows that for dialkyltin cations in strong acids, shielding anisotropy (SA) is the dominant relaxation mechanism in ^{119}Sn NMR at high magnetic field. In addition, it has been established that chemical exchange occurs and for $(CH_3)_2Sn^{2+}$ in fluorosulphuric acid, three tin species are present which are involved in an exchange process.

3.2.2 Relaxation Studies

Tin-119 NMR spectra of dialkyltin cations in sulphuric acid solutions recorded at 33.56 MHz (2.114T) showed the expected multiplet pattern due to coupling with the protons from the alkyl group. In an attempt to improve the signal to noise ratio and to obtain higher resolution, ^{119}Sn NMR of these solutions were recorded at higher magnetic

fields (5.872T and 9.395T). Contrary to expectations, the ^{119}Sn NMR lines were broadened so that the spin-spin coupling of the protons to tin was obscured (Figure 3.8). Therefore, in order to understand this behaviour, relaxation time studies on these solutions were carried out at different field strengths.

The possible relaxation mechanisms which contribute to spin-lattice relaxation (T_1^{-1}) are:

(i) dipole-dipole , $T_{1(DD)}^{-1}$

(ii) spin-rotation , $T_{1(SR)}^{-1}$

(iii) scalar relaxation , $T_{1(SC)}^{-1}$

and (iv) shielding anisotropy , $T_{1(SA)}^{-1}$

A dipole-dipole relaxation mechanism is possible when two magnetically active nuclei are present in a molecule. Such an interaction is present between tin and the protons of the alkyl groups in the R_2Sn^{2+} species. Spin-rotation interactions arise from fluctuations of local magnetic fields produced by the rotation of a non-spherically symmetric charge cloud during collisions. This depends on the period of free rotation of the molecule and it is usually found that the larger molecules have lower spin-rotation and higher dipolar relaxation rates.[76] Since the solvated alkyltin cations are effectively large in size due to solvation and hydrogen bonding, the spin-rotation mechanism is likely to be a minor contributor. Another mechanism which contributes to spin-lattice relaxation arises when the spin-spin coupling constant between two nuclei becomes time dependent as a result of chemical

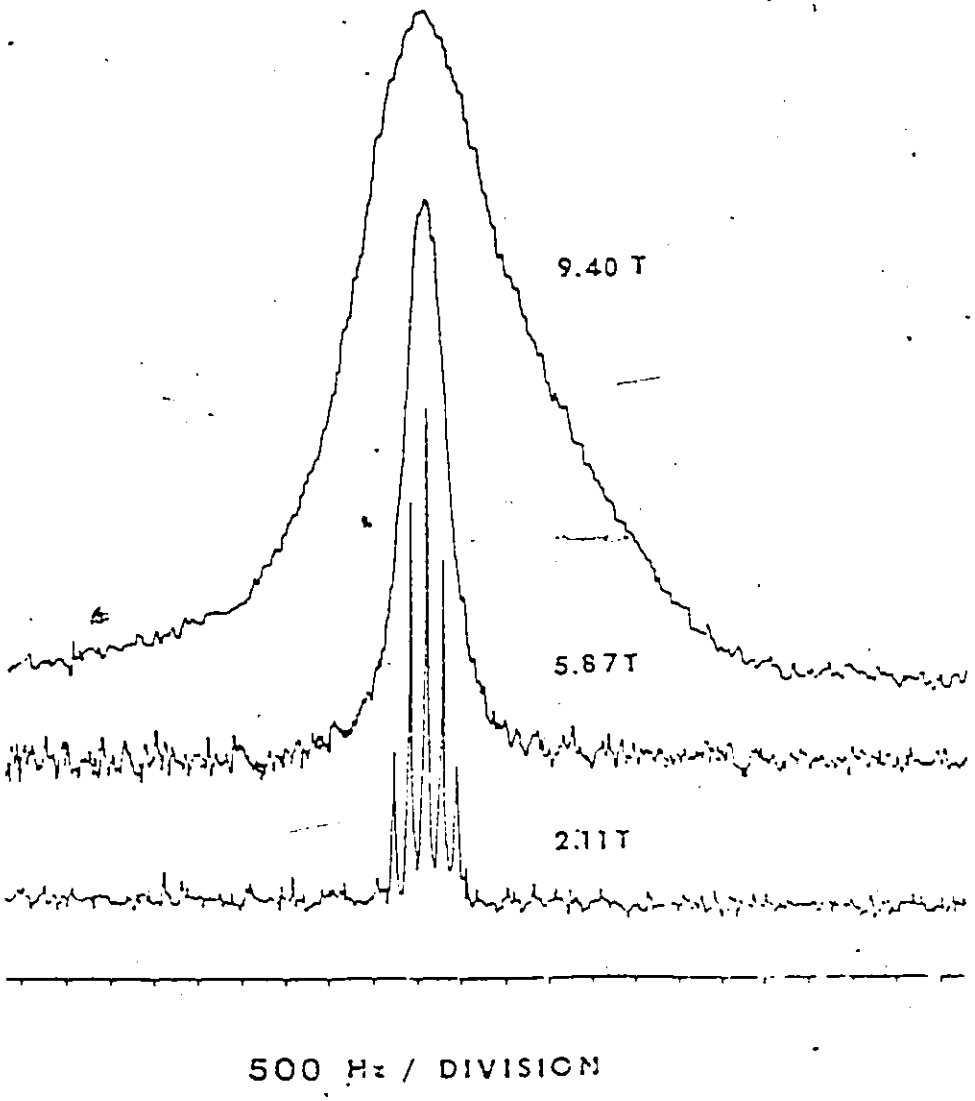

Figure 3.8: ^{119}Sn NMR spectra of 0.8 ML^{-1} $[(CH_3)_2Sn][SO_4]$ in 100% H_2SO_4 at field strengths of 2.114T, 5.872T and 9.395T.

exchange. This is referred to as scalar relaxation of the first kind.[77] In the case of alkyltin cations, an exchange process involving the cleavage of an alkyl group is unlikely. Also, this mechanism does not make significant contributions to the spin-lattice relaxation of tin because of the large difference between the resonance frequencies of the tin and proton nuclei. The scalar relaxation of the second kind usually occurs via interaction with a nucleus having a short relaxation time and is usually a quadrupolar nucleus. Therefore, this mechanism is also unlikely to contribute in the system under consideration. The shielding at a nucleus, and therefore the magnetic field acting on it, varies with the molecular orientation except for sites of very high symmetry. Molecular tumbling therefore modulates the local magnetic field, and can cause relaxation. This mechanism is known as shielding anisotropy (SA) and can be of importance at higher field strengths for heavy nuclei in molecules with symmetry lower than cubic.[77] In summary, for alkyltin cations in strong acid, the main contributors to the spin-lattice relaxation are the dipole-dipole and SA mechanisms. The spin-lattice relaxation rates due to different mechanisms, are additive, hence equation (3.14) can be written.

$$\frac{1}{T_1} = \frac{1}{T_{1(DD)}} + \frac{1}{T_{1(SA)}} \qquad (3.14)$$

The ^{119}Sn spin-lattice relaxation times (T_1) of dialkyltin cations in 100% H_2SO_4 were measured at three different magnetic fields and are provided in Table 3.3. From this data, it is clear that the T_1's for all three species are field dependent and decrease with increasing

TABLE 3.3

^{119}Sn Line Widths and Relaxation Time Measurements for

Dialkyltin Sulphates in 100% Sulphuric Acid

Compound	ν_o^2 ($\times 10^{12} s^2$)	T_1 (s)	η	T_1^{-1}	$T_{1_{DD}}^{-1}$	$T_{1_{SA}}^{-1}$	$\Delta w_{\frac{1}{2}}$	T_2^{-1}
				(s^{-1})				
$(CH_3)_2Sn(SO_4)$	1126.3[a]	0.054	-0.20(3)	18.5	2.7	15.8	85*	267
0.8 M l^{-1}	8699.3[b]	0.009		109.9	(0.2)[d]	(109.7)[d]	450*	1414
	22263.6[c]	0.0056		178.5	(0.1)[d]	(178.5)[d]	990*	3110
$(C_2H_5)_2Sn(SO_4)$	1126.3[a]	0.035	-0.29(3)	28.5	7.4	21.1	75[+]	236
1.20 M l^{-1}	8699.3[b]	0.0087		114.9	-	(114.9)[d]	670[+]	2105
	22263.6[c]	0.0063		158.7	-	(158.7)[d]	720[+]	2262
$(C_4H_9)_2Sn(SO_4)$	1126.3[a]	0.0038	-0.27(3)	26.3	-	-		
0.4 M l^{-1}	22263.6[c]	0.0064		156.2	-	-		

All measurements were made at room temperature.

* These measurements were carried out at a concentration of 1.2 M l^{-1}. Line widths are fitted using "Numarit: Iterative NMR Spectral Analysis Program" K. M. Worvill and J. S. Martin (1975), a development of NUMAR: A. R. Quirt and J. S. Martin, J. Mag. Res. 5, 318, 1971.

[+] Full width at half height.

[∓] Estimated error is less than 10%

a) Field strength of 2.1114T

b) Field strength of 5.872T

c) Field strength of 9.395T

d) Estimated values

field strength. It is interesting to note that at 2.114T, the relaxation time of the methyl species is much longer than for either the ethyl or butyl species, but as the field strength increases, the difference decreases, until at 9.395T, the ethyl and butyl groups have longer relaxation times than the methyl species.

In order to obtain an estimate of $T_{1(DD)}^{-1}$, nuclear Overhauser effect (NOE) measurements were made. In this study, the double resonance experiment was carried out by observing the ^{119}Sn resonance signal while saturating the protons. The integrated intensity of the ^{119}Sn signal will differ from its value for a single resonance spectrum. The NOE is defined as the ratio of the double resonance intensity to single resonance intensity. Since ^{119}Sn has a negative magnetogyric ratio, this results in diminution of signal intensity. The NOE operates by cross relaxation between the two spin systems and the main contributor is from dipole-dipole interactions, except when there can be scalar coupling modulated by chemical exchange.[78] Since in these systems, the alkyl groups are not directly involved in any exchange process, scalar coupling can be eliminated.

Figure 3.9 shows a plot of T_1^{-1} versus ν_o^2, where ν_o is the operating frequency of ^{119}Sn NMR at field strength B_0. The T_1^{-1} values at zero field ($\nu_o = 0$) are obtained by extrapolation. As the strength of the field apporaches zero, the SA contribution decreases and at zero field the SA mechanism is ineffective. Therefore, T_1^{-1} at $\nu_o = 0$ is mainly due to dipolar interactions since the spin rotation mechanism can be neglected due to the large size of these solvated cations. Thus, for the dimethyltin species at zero field,

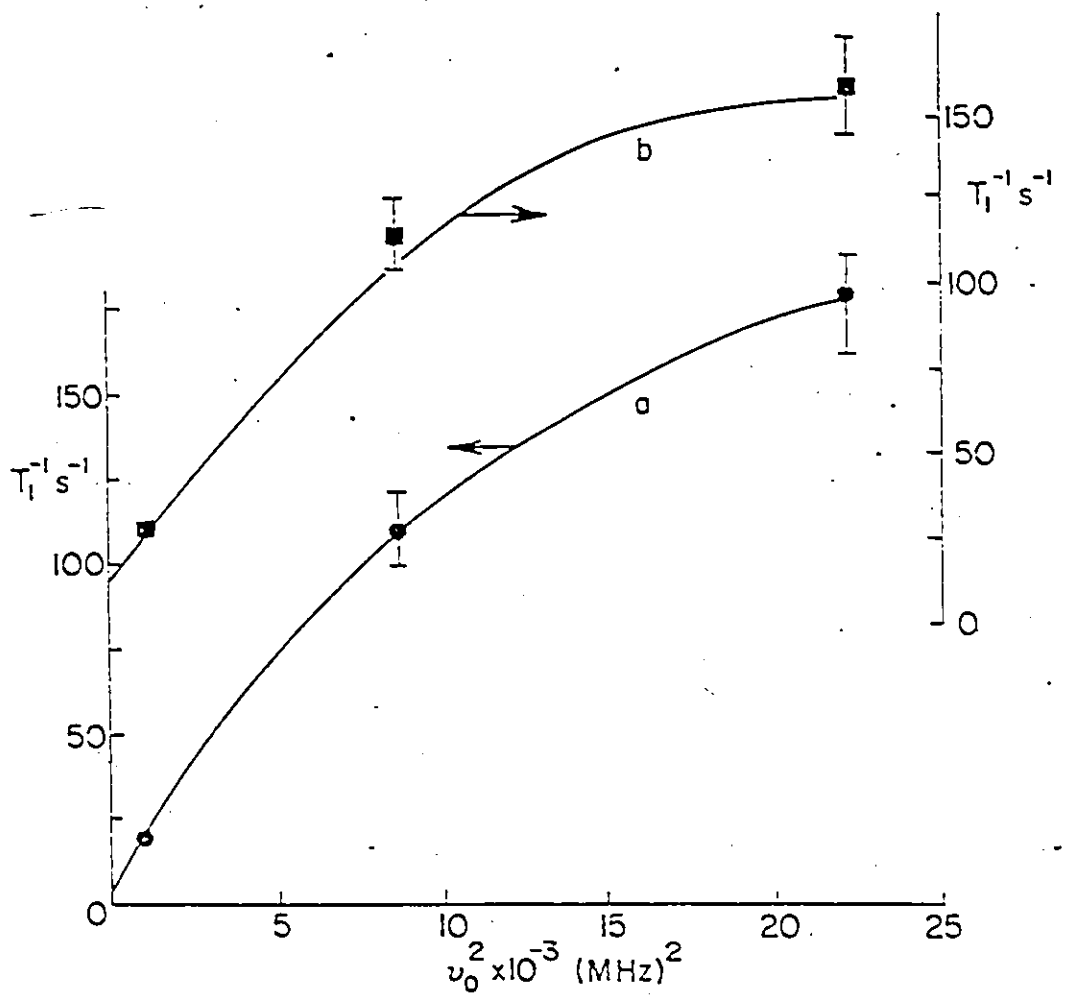

Figure 3.9: Plots of T_1^{-1} against ν_o^2 for (a) $[(CH_3)_2Sn][SO_4]$ (L.H.S.) • and (b) $[(C_2H_5)_2Sn][SO_4]$ (R.H.S.) ▪ in 100% H_2SO_4.

$T_1^{-1} = T_{1(DD)}^{-1} = 3.3\ s^{-1}$ and the corresponding value for the diethyltin species is $15.0\ s^{-1}$. If ω_o is the resonance angular frequency and τ_c is the correlation time associated with molecular tumbling, then rapid molecular motions occur when $\omega_o^2\tau_c^2 \ll 1$. This is referred to as the motional narrowing limit. Under these conditions, the relaxation rate of spin I, due to intramolecular dipole-dipole interactions with spin S, $T_{1(DD)}^{-1}$ (intra) is independent of frequency and is given by equation (3.15).

$$T_{1(DD)}^{-1}\ (\text{intra}) = \frac{\mu_o^2\gamma_I^2\gamma_S^2\hbar^2 s(s+1)}{12\pi^2\sum_i r_{IS}{}_i^6} \cdot \tau_c \qquad (3.15)$$

where μ_o is the permeability of a vacuum, h is Planks constant; γ_I, γ_S are magnetogyric ratio of nuclei with spin S and I, r_{IS_i} is the internuclear distance between nucleus of spin I and S_i, and τ_c is the molecular tumbling correlation time. If a fixed zig-zag orientation of the alkyl groups is assumed i.e.,

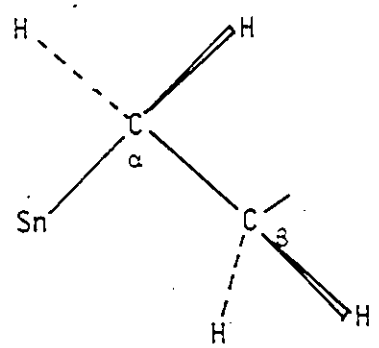

the distance from tin to the α-protons can be calculated to be 275 pm in agreement with Wallach's value,[79] and 325 pm to the β protons.

Using the $T_{1(DD)}^{-1}$ value obtained from the above plot (Figure 3.9) at zero field and equation (3.15), one can estimate τ_c to be 3.0×10^{-9} s and 1.3×10^{-8} s for the dimethyl and diethyltin species respectively. This calculation assumes isotropic motion and a rigid geometry around the tin. With these τ_c values, the magnitude of $(\omega_o\tau_c)^2$ at three different fields are calculated to be $(CH_3)_2Sn^{2+}$: 0.40, 3.09, 7.91; $(C_2H_5)_2Sn^{2+}$: 7.50, 58.04, 148.50. These values clearly show that these systems deviate from the extreme narrowing condition $(\omega_o^2\tau_c^2<<1)$ even at 2.114T. Therefore, $T_{1(DD)}^{-1}$ must be calculated using the general equations.

Recently, Werbelow[80] has derived an equation for the NOE factor (η) for coupled nuclei with magnetogyric ratios of opposite sign. Since the magnetogyric ratios of tin and proton are negative and positive respectively, this equation is the appropriate one to use in the calculations. According to his equation, if spin I is saturated and spin S is observed, the maximum fractional enhancement of the total integrated intensity of the signal is given by the expression,

$$\eta_{S-\{I\}} = - \left|\frac{\gamma_I}{\gamma_S}\right| \left[\frac{2J(\omega_I-\omega_S) - \frac{1}{3}J(\omega_I+\omega_S)}{2J(\omega_I-\omega_S) + J(\omega_S) + \frac{1}{3}J(\omega_I+\omega_S)}\right] \qquad (3.16)$$

where $J(\omega)$ is given by

$$J(\omega) = \frac{3}{10}\left[\frac{\gamma_I\gamma_S\hbar}{\gamma_{IS}^3}\right]^2 \left[\frac{\tau_c}{1+\omega^2\tau_c^2}\right]$$

Using the above equation and the estimated τ_c for the dimethyltin and diethyltin species, η_{max} can be calculated at 2.114T. From this value

and the experimentally measured NOE factors at 2.114T, $T_{1(DD)}$ can be calculated using equation (3.17).

$$NOE = 1 + \eta \; ; \; \eta = \eta_{max} \frac{T_1}{T_{1(DD)}} \qquad (3.17)$$

Note that $T_{1(DD)}$ values at zero field are different from those at 2.114T (Table 3.3). This difference is expected since these systems are outside the extreme narrowing condition.

The marked increase in the dipolar contribution on going from the dimethyl to the diethyl species is due to lower mobility, longer τ_c and the contribution from additional protons. In the case of the di-n-butyl species, its effected solvated size may not be very different from that of the diethyl species in solution and the increased number of protons will have little additional effect due to the r^{-6} dependence in equation (3.15). The dipole-dipole relaxation can also occur due to intermolecular interactions. This is possible between dipoles of identical solute and solvent molecules. Relaxation due to identical solute molecules can be reduced by keeping the sample concentration low. In order to examine the significance of dipolar effects from solvent molecules, NOE measurements were carried out on a solution of dimethyltin sulphate in D_2SO_4. If the dipolar interaction due to the solvent is important, one would expect a marked decrease in the NOE factor since the relaxation effect of deuterium (spin=1) is lower than that of the proton by a factor $\frac{8}{3}$ (γ_D^2/γ_H^2) which is equal to 0.06.[78] However, the spin-lattice relaxation time and NOE measurements, made for dimethyltin species in D_2SO_4 solution, were found to be the same as

in H_2SO_4 solution within experimental error, indicating that intermolecular dipole-dipole relaxation is not significant in this system.

At 9.395T, no NOE was detected. This indicates that the SA mechanism is the dominant one at high magnetic fields. Therefore, it is reasonable to assume at 5.872T and 9.345T, that the measured T_1^{-1} is equal to $T_{1(SA)}^{-1}$. Now, one can observe the large increase in the SA contribution as the field is increased from 2.114T through 5.872T to 9.395T.

This is the first documented case of the effect of SA for the ^{119}Sn nucleus. This mechanism is also extremely efficient for several other heavy metal nuclides such as ^{195}Pt,[81] ^{199}Hg,[82] ^{205}Tl[83] and ^{207}Pb.[84] Among the compounds studied, SA is found to be the dominant mechanism when the nucleus is in an asymmetric environment. In the case of dialkyltin species, the large asymmetry around the tin nucleus is evident from the large quadrupole splitting of its frozen solution Mössbauer spectrum. No spin-spin coupling is visible in the ^{119}Sn NMR spectrum of dialkyltin species at high magnetic fields because of broader signals. However, the effect of SA is over shadowed by the presence of chemical exchange in this system which is discussed in detail in the next section. The ^{119}Sn NMR spectra of trialkyltin cations in strong acids are expected to have smaller contributions from SA since the Mössbauer spectrum shows a smaller quadrupole splitting indicating less asymmetry around tin than in the dialkyltin species. In fact, this is evident from the ^{119}Sn NMR spectrum of triethyltin cation in fluorosulphuric acid in which coupling due to the protons of the ethyl groups are resolved at 5.872T.

For a nucleus with axial symmetry, the contribution from SA to T_1^{-1} is given by equation (3.18)

$$T_{1(SA}^{-1} = \frac{1}{15}(\gamma_I B_o)^2(\Delta\sigma)^2 \left[\frac{2\tau_c}{1 + \omega_o^2\tau_c^2}\right] \qquad (3.18)$$

where $\Delta\sigma$ is the shielding anisotropy. Using the above estimated value of τ_c (3.0×10^{-9} s for dimethyl species and 1.3×10^{-8} s for diethyl species) and the ^{119}Sn T_1 measured at 9.395T, for $(CH_3)_2Sn^{2+}$ and $(C_2H_5)_2Sn^{2+}$ in H_2SO_4, a value for $\Delta\sigma$ can be calculated. This works out to be 2005 ppm and 4478 ppm for the dimethyl and diethyl species, respectively. These values are not unreasonable compared with the range of chemical shifts observed in ^{119}Sn NMR. They may be compared with the values obtained for other cases, for example, $(CH_3)_2Hg$: $\Delta\sigma$ = 6100 ppm,[82] where one can note that ^{199}Hg NMR spectra cover a much larger chemical shift range. However, care should be taken in considering this value since the rotational correlation time may not be the same as that which modulates the SA. In addition, the presence of chemical exchange in these systems might complicate the estimation of the correlation time. It has been suggested that in some cobalt complexes this correlation time is associated with the life time of hydrogen-bonded second sphere complexes.[85] The presence of extensive hydrogen-bonding in these systems between the coordinated sulphate groups and the solvent is highly likely.

From the theory of SA effect under extreme narrowing conditions, one would have expected a linear plot of $T_{1(SA)}^{-1}$ against ν_o^2. However, our experimental data do not follow a straight line (Figure 3.9) since

these systems deviate from the extreme narrowing condition at higher magnetic fields.

3.2.3 Chemical Exchange

The observed linewidth of the signal ($\Delta\nu_{\frac{1}{2}}$) can be used to estimate the spin-spin relaxation time (T_2) using the equation, $\Delta\nu_{\frac{1}{2}} = (\pi T_2)^{-1}$, after allowance has been made for $^2J_{119}{}_{Sn-C-}{}^1{}_H$.

Thus the T_2^{-1} obtained values are given in Table 3.3 for comparison with the T_1^{-1} values. One can clearly observe a large difference between T_1^{-1} and T_2^{-1} for the dimethyltin and diethyltin sulphates in H_2SO_4 solution. This difference can arise from three possible sources which are given below.

(i) Scalar relaxation, which is unlikely to contribute for the reasons stated in the previous section.

(ii) SA, which would lead to differences between T_1^{-1} and T_2^{-1}. Since these systems are outside the extreme narrowing condition, $T_{2(SA)}^{-1}$ is estimated using the general equation given in reference (77). This leads to values of 73.1 s^{-1}, 434.8 s^{-1} and 1021.0 s^{-1} for the dimethyltin species at 2.114T, 5.872T and 9.395T respectively. The difference between T_1^{-1} and T_2^{-1} are much greater than can be accounted for by SA contribution.

This leaves,

(iii) chemical exchange as the major source of line broadening.

Tin-119 NMR spectra for the dialkyltin species in 100% H_2SO_4 solutions were recorded at two or three different concentrations. Their chemical shifts and linewidths are summarized in Table 3.4. In the case of the dimethyl and diethyl species, the chemical shift varies with concentration and their linewidths increase with dilution. However, in the dibutyltin case, there is no significant change in chemical shift or linewidth with dilution. These changes suggest the presence of chemical exchange and its rate depends on the alkyl group. The linewidth of the ^{119}Sn resonances decrease with increasing size of the alkyl group. Since only one signal is observed at ambient temperature, the linewidths indicate that the exchange rate is faster for the dibutyl species and slower for the dimethyl species.

In order to obtain further information about the exchange process, variable temperature NMR studies are required. Since H_2SO_4 freezes at 10°C, it is not a suitable solvent for low temperature work. The low freezing point of HSO_3F (-87°C) makes it the desired solvent system. Also, the slower exchange rate of the dimethyltin species makes the dimethyltin species in HSO_3F the best system to study by variable temperature NMR spectroscopy. Therefore, ^{119}Sn NMR spectra were recorded on this solution from ambient temperature to -90°C at 5.872T (Figure 3.10, Table 3.5). The ambient temperature spectrum showed a single broad signal at -106 ppm. As the temperature was lowered this signal shifted towards low frequency with increasing linewidth. At -70°C, an additional signal appeared around 8.0 ppm and the intensity of this signal increased with further cooling. By -80°C, a third broad resonance was clearly visible at around 5 ppm. During the

TABLE 3.4

Concentration and Temperature Dependence of the ^{119}Sn Chemical Shifts and Line Widths for Dialkyltinsulphonates in 100% HSO_3X (X=OH,F)

Compound	Concentration M l^{-1}	Temperature °C	δ ppm	$\Delta W_{\frac{1}{2}}$* Hz
$(CH_3)_2Sn(SO_4)$‡	1.20	24	-155	1160(990)†
	0.80	24	-156	1850
	0.40	24	-182	4100
$(C_2H_5)_2Sn(SO_4)$‡	1.20	24	-267	720
	0.80	24	-247	1160
	0.40	24	-263	700
$(C_4H_9)_2Sn(SO_4)$‡	0.40	24	-252	460
	0.20	24	-252	410
$(CH_3)_2Sn(SO_3F)_2$	1.16	24	-106	366
		-80	-218	5829
	0.40	24	-144	414
		-80	-225	2200
$(C_2H_5)_2Sn(SO_3F)_2$	1.40	24	-235	57.5
		-80	-264	1150

* Width at half height of the spectra recorded at 5.872T.

‡ Because of the high freezing point of 100% H_2SO_4 (10.657°C) it was not possible to record spectra at low temperature.

† Fitted linewidth.

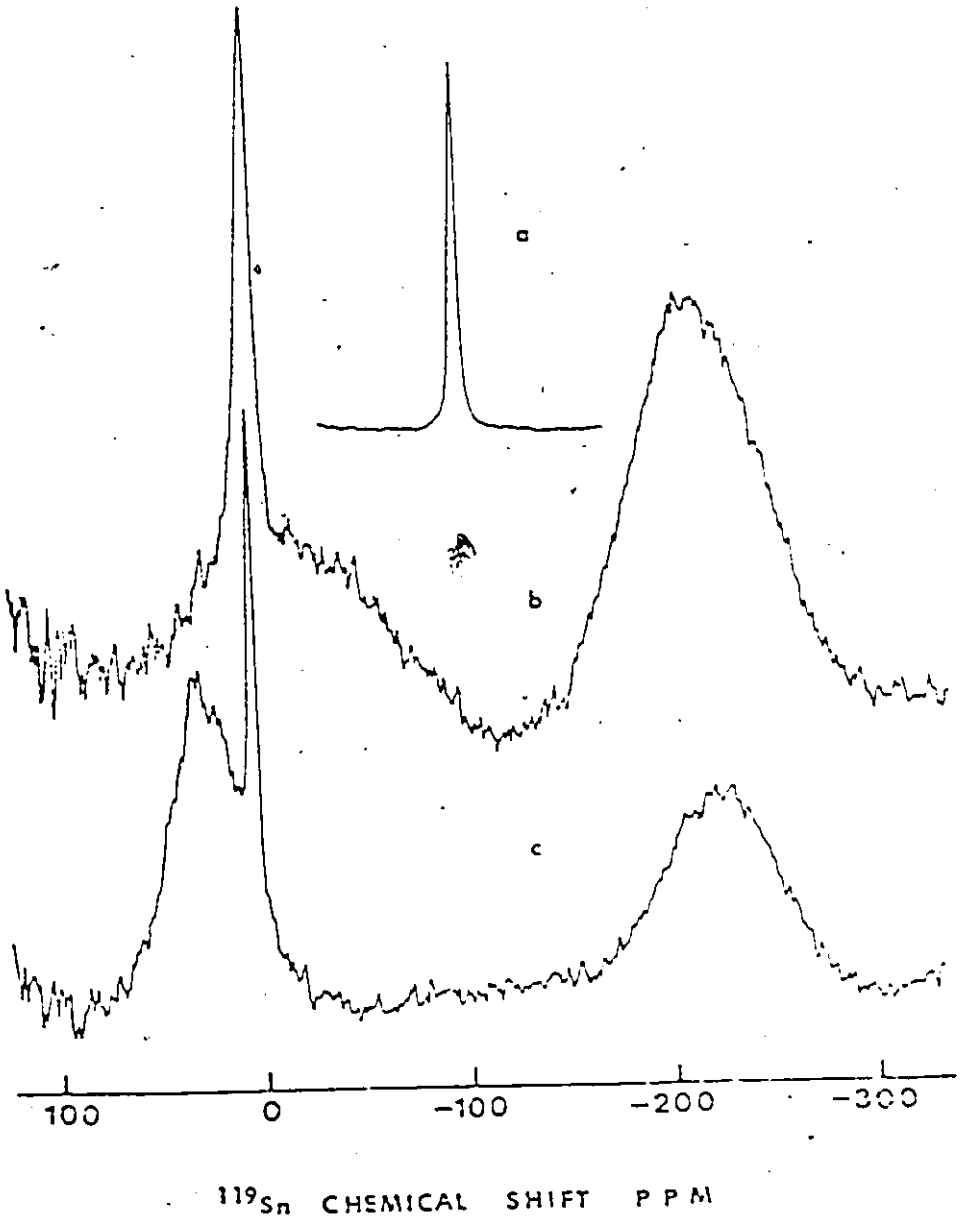

Figure 3.10: ^{119}Sn NMR spectra of 1.16 ML^{-1} solution of $(CH_3)_2Sn(SO_3F)_2$ in HSO_3F at (a) 24°C, (b) -75°C and (c) -90°C at a field strength of 5.872T.

TABLE 3.5

^{119}Sn NMR Chemical Shifts and Spin-Spin Coupling Constants for Alkyltin Fluorosulphates in Acid Solutions

Compound	Conc. / M l^{-1}	Temp. / °C	$\delta_{^{119}Sn}$ / ppm	$\pm W_{\frac{1}{2}}$ † / Hz	$^1J_{^{117}/^{119}Sn-^{13}C}$ / Hz
$(C_2H_5)_2Sn(SO_3F)_2$	1.3	Amb	-253	-	426(3)
		0	-242	-	
		-20	-248		
		-60	-259	650	
		-80	-264	1150	440(6)
		-85	-265	1625	
$(CH_3)_2Sn(SO_3F)_2$ (at 5.872T)	1.16	Amb	-106	460	568(3)
		-20	-113	846	
		-40	-119	1720	571(3)
		-60	-128	5070	573(3)
		-70	-158	8330	
			8.2	1600	
		-75	-201	6795	
			-14	9770	
			7.3	978	
		-80	-219	5830	575(5)
			5	7960	
			6.2	610	
		-90	-232	5860	566(9)
			38	353	
			32	4030	
$(CH_3)_2Sn(SO_3F)_2$ (at 9.395T)		-80	-238	7500	
			4.2	375	
			28.8	4990	
		-90	3.3	420	
			32.3	7140	

† Width measured at half height of spectra recorded at a field strength of 5.872T or 9.395T.

* Measured from the ^1H decoupled ^{13}C spectra. The ^{117}Sn and ^{119}Sn satellite peaks were not resolved and this is the average coupling.

cooling, the intensity of the low frequency signal decreased as the signals at higher frequency increased. Below -90°C, the solution was frozen and no spectrum could be obtained. The spectra recorded at 9.395T exhibited a similar behaviour except that the spectrum at -90°C showed the complete disappearance of the low frequency signal and only the two high frequency peaks were observed with increased intensity. This study confirmed that at least three different tin species were present in this solution and these are involved in exchange processes. A similar study done on the diethyltin species in HSO_3F showed only one signal whose linewidth increased as the temperature was lowered. The failure to resolve additional signals from this solution was not unexpected, since the exchange rate for the diethyltin solution was inferred earlier to be faster than in the dimethyl case and hence much lower temperatures would be required to stop the exchange.

The concentration and temperature dependence of $^1J_{^{13}C-^{119}Sn}$ was deduced by recording ^{13}C NMR spectra (see Table 3.5). Although three species can be observed in the ^{119}Sn NMR spectrum, the ^{13}C NMR spectrum exhibited only an average signal and hence the measured $^1J_{^{119}Sn-^{13}C}$ is the average value of all exchanging species. The change in this coupling is only $\sim$ 2.5% indicating that the exchanging tin species have similar geometries. It has been discussed in the previous section that the ^{119}Sn chemical shifts and $^1J_{^{119}Sn-^{13}C}$ values found for the dialkyltin species are consistent with the idea that these species are solvated and have trans-octahedral geometries in solution. Also, it was concluded earlier that the solid state geometry is preserved in

solution.[2]

Since the presence of three tin species is established by NMR, the frozen solution Mössbauer spectrum of dimethyltin species in HSO_3F was re-examined. This showed two lines with slightly different intensity and linewidth. There are several reasons possible for this. However, based on the evidence from ^{119}Sn NMR, the Mössbauer spectrum was fitted to two overlapping doublets. The parameters of the two doublets are as follows.

	I		II	$(CH_3)_2Sn(SO_3F)_2$ [67]
δ(mm s^{-1})	1.94	;	1.73	1.82
Δ(mm s^{-1})	5.51	;	5.08	5.54

These parameters are similar to those of $(CH_3)_2Sn(SO_3F)_2$ in the solid state.[67] These two overlapping spectra must arise from the two tin species which dominate the low temperature ^{119}Sn NMR spectrum (Figure 3.10) and the species corresponding to the low frequency signal which was present at higher temperature is presumably no longer present in the frozen solution. These species show large quadrupole splittings which are characteristic of trans-octahedral geometry around the tin. A comparison with the corresponding solid data suggests that the environment around tin in the lower temperature species is similar to that of the solid crystallized from these solutions. The $^1J_{^{119}Sn-^{13}C}$ values, and the Mössbauer parameters indicate that the exchanging species have a similar geometry around the tin.

Clearly there are at least three different tin species present in these strong acid solutions that are involved in equilibria which, on the NMR time scale, averages the tin environments. It has been shown

by Yeats et al.[59] that dimethyltin sulphonates in their parent acid, are not completely ionized according to equation (3.19) even in dilute solution.

$$(CH_3)_2SnSO_4 + H_2SO_4 \rightleftharpoons \underset{I}{[(CH_3)_2Sn]^{2+}} + 2\ HSO_4^- \qquad (3.19)$$

Since the NMR and Mössbauer evidence indicates six coordinate tin for these solvated species, the above equation can be rewritten as equation (3.20),

$$\underset{II}{(CH_3)_2Sn(HSO_4)_2(H_2SO_4)_2} + 2H_2SO_4 \rightleftharpoons \underset{III}{[(CH_3)_2Sn(H_2SO_4)_4]^{2+}} + 2[HSO_4^-] \qquad (3.20)$$

with the equilibrium favoured to the left.

The ambient temperature ^{119}Sn NMR signal corresponds to the average environment between (II) and (III). On cooling to low temperatures, the equilibrium is displaced towards (II) and hence the ^{119}Sn NMR signal shifts to lower frequency. This is expected since (II) has a more shielded tin atom than does (III). This would also be consistent with the increased linewidth of the ^{119}Sn signals with dilution. As the temperature is lowered further the appearance of high frequency signals indicates that the tin is becoming deshielded, however, the value of $^1J_{^{119}Sn-^{13}C}$ shows that the geometry around the tin still remains six coordinate. It is likely that (II) is an isolated species linked to its other units or solvent through hydrogen bonding with SO_3X^- or HSO_3X ligands.

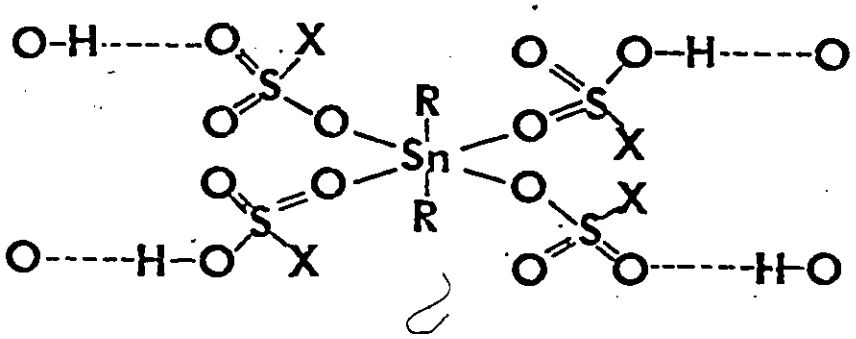

IV

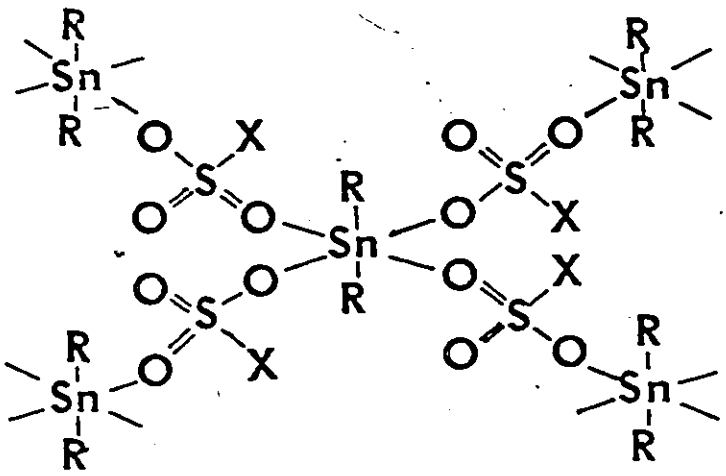

V

At lower temperatures, these weak hydrogen bonds must convert to strong linkages via sulphonate bridges. This would result in deshielding of the tin as observed. Therefore, the signal of ~ 4 ppm in the ^{119}Sn NMR at lower temperature, may correspond to a polymeric species such as IV while that at the highest frequency, ~ 29 ppm to a cross linked polymeric

unit V. This is the structure observed in the solid state for $(CH_3)_2Sn(SO_3F)_2$.[68] The ^{119}Sn Mössbauer doublets in the frozen solution of $(CH_3)_2Sn^{2+}$ in HSO_3F can be attributed to species IV and V.

CHAPTER 4

TIN(II) AND TIN(IV) CARBOXYLATES, SULPHATES AND SULPHONATES

4.1 Introduction

The early work in the area of organotin carboxylates has been reviewed by Okawara and Ohara.[86] There is a large amount of spectroscopic and diffraction data available on the structures of these compounds. Solid triorganotin(IV) carboxylates form either linear polymers involving bridging carboxylate groups and planar or near planar R_3Sn- moieties, or discrete molecules, with tin atoms occupying a distorted tetrahedral geometry. The polymeric triorganotin carboxylates, in organic solvents, usually produce oligomeric and finally monomeric species containing tetrahedral tin atoms.[87] There are so far no X-ray crystal structures of any diorganotin dicarboxylates or monoorganotin tricarboxylates available. However, the structure of dimethyltin bisfluorosulfate has been determined[68] and the structure is polymeric with intermolecularly bridging fluorosulphate groups and an octahedral trans-Me_2SnX_4 geometry around the tin atom. A similar structure is suggested for dialkyltin dicarboxylates on the basis of Mössbauer[88,89] and infrared spectroscopic[86,90] data. In solution these compounds are monomeric and probably have octahedral structures with trans alkyl groups and the six coordination at tin is achieved by solvent coordination.[86,90] Recent solution studies question the validity of regular cis or trans octahedral structures and propose a

skewed or irregular trapezoidal-bipyramidal configuration.[91] A few monoorganotin tricarboxylates were found to be monomeric in solution.[92] Among the tin tetracarboxylates, the only crystal structure determined has been tin tetraacetate[93] which contains an eight coordinate tin atom with three symmetrically chelating bidentate carboxylates and one unsymmetrically chelating bidentate carboxylate.

Many compounds of tin(II) have been investigated by Mössbauer spectroscopy. Donaldson has reported the Mössbauer parameters of a series of tin(II) carboxylates.[94] These parameters are not correlated in any obvious way. Tin(II) carboxylates exhibit relatively large quadrupole splittings when compared with other tin(II) compounds. It has been suggested that the geometry around the tin atom is that of a distorted pyramid with either inter or intramolecular carboxylate bridges. The structures of $K[Sn(O_2CH)_3]$,[95] $Ca[Sn(O_2CCH_3)_3]_2$,[96] and $K[Sn(O_2CH_2Cl)_3]_3$ [97] have been determined. These structures consist of discrete anion units in which the tin atom has three nearest neighbour oxygen atoms forming a trigonal pyramidal coordination. In addition, the environment of tin(II) is completed by the three long Sn-O bonds to form a distorted octrahedral geometry. This is viewed as the most common environment in tin(II) compounds and the longer Sn-O contacts are due to the presence of a sterically active non-bonding electron pair.[98] A similar coordination is found in the malonato complex $K_2Sn_2[CH_2(CO_2)_2]_3 \cdot H_2O$ [99] but in the oxalato complex $Na_2Sn(C_2O_4)_2$ [100] the tin(II) atom is in a distorted pyramidal environment.

The only structural information available for simple tin(II) carboxylates is for tin(II) formate which contains the tin(II) atom

in a distorted trigonal bipyramidal environment.[101] There are several examples cited in reviews of structural tin chemistry with tin(II) compounds where the tin coordination varies from three to seven, when the lone pair is included.[102,103]

There are relatively few compounds known to contain tin(II) and tin(IV) in the same molecule. The structure of mixed valence tin fluoride Sn_3F_8 has been determined.[23] This consists of an octahedrally coordinated tin(IV) atom which is bridged to two tin(II) atoms through trans fluorine atoms. This compound can be considered as $[SnF^+]_2$-$[SnF_6^{2-}]$. A mixed valence oxide of tin, Sn_2O_3 has been prepared and its Mössbauer spectrum is interpreted as due to an octrahedral Sn(IV) and a pyramidal Sn(II) environment.[19] The structure of mixed valence tin sulphide, Sn_2S_3 has also been determined.[20] An interesting compound $[Ph_3Sn][Sn(NO_3)]$ has been isolated and its structure determined.[21] This was the first example of a compound containing a tin(II)-tin(IV) bond with tin(IV) and tin(II) in four and five coordinate environments. Also the compound, $[(CH_3)_3SnC_5H_4]_2Sn$, contains organotin(II) and organotin(IV) moieties in one molecule.[22] This has been characterized on the basis of its Mössbauer parameters. Ewings et al. have determined the structure of a mixed valence tin derivative of o-nitro benzoic acid.[26] This consists of a tetra nuclear cluster molecule containing tin(II) and tin(IV) atoms. A similar structure with the trifluoroacetate group was determined by Birchall and Johnson.[18] The same authors have also reported a general synthetic procedure to obtain a series of mixed valence tin compounds by the cleavage of hexaphenylditin by carboxylic acids.[1]

There have been a large number of ^{119}Sn NMR studies carried out on organotin compounds which have been comprehensively reviewed.[30,69] There are several factors which influence ^{119}Sn chemical shifts. Coordination number, substituent and temperature are three important influences. It has been observed in various systems that five and six coordinate organotin compounds appear at lower frequencies than those of four coordinate derivatives. The variation in coordination number can arise from interactions with solvents and through the autoassociation of molecules. Polar, coordinating, solvents can produce large variations in ^{119}Sn chemical shifts as the concentration of the solute is varied. McFarlane and Wood[87] have attributed a 100 ppm chemical shift variation in trimethyltin formate in $CDCl_3$ to self-association of monomeric tetrahedral trimethyltin formate molecules. This results in oligomeric or polymeric species with five coordinated tin environments. These workers have also determined the ^{119}Sn chemical shifts of a number of triphenyl- and trineophyltin carboxylates. These shifts have been correlated with the electron withdrawing ability of the carboxylate group. In the area of tin(IV) carboxylates, there are only a few ^{119}Sn NMR studies reported for di- and triorganotin carboxylates.[87,104-106] Among these, only for the triphenyltin carboxylates has a systematic study of a series of compounds been carried out.[87,104] There have been no ^{119}Sn NMR studies reported to date on tin tetracarboxylates.

There are relatively few reports available on ^{119}Sn NMR studies of tin(II) compounds. Yeh and Geanangel have investigated the behaviours of divalent tin halides in coordinating solvents.[107] They observed

marked variation of ^{119}Sn chemical shifts with solvent, concentration and temperature. Dean has studied the ^{119}Sn NMR spectra of tin(II) complexes of phosphorus, sulphur and selenium containing ligands.[108,109] They observed a wide range of ^{119}Sn chemical shifts for these complexes. Recently, ^{119}Sn NMR measurements were reported on monomeric tin(II) amides.[110] The author compares the high ^{119}Sn resonance frequency of the tin(II) amides(+776 ppm to +100 ppm) with that of the dicyclopentadienyl tin(II) derivative[111] which appears at the other extreme, that is at low frequency (-2171 ppm).

4.2 Simple Tin(II) and Tin(IV) Carboxylates

4.2.1 Preparation

Although the preparation of tin(II) compounds derived from halogen substituted carboxylic acids has been reported[17] only a few of them have been isolated as pure compounds. The general synthetic procedure involves the reaction of tin(II) oxide with the carboxylic acid in an aqueous medium. The reaction proceeds according to equation (4.1).

$$SnO + 2RCOOH \longrightarrow Sn(O_2CR)_2 + H_2O \qquad (4.1)$$

to yield tin(II) carboxylate. In the preparation of $Sn(CO_2R)_2$; where R = $-CF_3$, $-CCl_3$, $-CBr_3$, or $-CI_3$ however, the attempted isolation of the product resulted in syrups or decomposed materials. This might be due to the use of an aqueous reaction medium which could facilitate the formation of undesired basic tin(II) compounds. Therefore, in the preparation of tin(II) trifluoroacetate the above procedure was modified,

and SnO was reacted with a mixture of CF_3CO_2H and its anhydride, $(CF_3CO_2)_2O$. The anhydride was used to remove the water produced in the reaction. This facilitated the isolation of $Sn(CO_2CF_3)_2$ as a pure crystalline material. Similarly, $Sn(CO_2C_3F_7)_2$ has been isolated as a pure compound by the reaction of SnO with a mixture of C_3F_7COOH and its anhydride. Tin(II) trifluoroacetate is a very hygroscopic compound and must be handled in an extremely dry atmosphere. It is very soluble in its parent acid. Attempts were made to grow crystals of $Sn(CO_2CF_3)_2$ for single crystal X-ray diffraction studies, but they formed long needle shaped crystals which were not suitable for such a study. On sublimation, $Sn(CO_2CF_3)_2$ gives a crystalline material whose structure has been determined to be $Sn_6O_2(O_2CF_3)_8$.[112] This was found to have a polymeric structure with six different tin(II) environments. The tin(II) atoms are connected by oxo bridges and bridging trifluoroacetate groups. It has been reported that on attempting the sublimation of tin(II) phthalate and tin(II) oxalate, both compounds decomposed, the former yielding phthalic anhydride.[113]

Tin tetracarboxylates have been prepared by the solvolysis of tetravinyltin or tetraphenyltin with acids.[1,12,14] These are also prepared from the transacylation reaction of tin tetraacetate.[114] Among the tin tetracarboxylates of halosubstituted acids, only trifluoroacetate was isolated as a pure compound whereas others were obtained as syrups or dark coloured materials.[1] The reaction of tetraphenyltin with carboxylic acids results in the cleavage of phenyl groups according to equation (1.6) to produce tin(IV) carboxylate. Tin tetraacetate has been prepared in nearly quantitative yield according to this reaction.[14]

However, this reaction (equation 1.6) with haloacetic acids usually produces coloured materials whereas the desired product is expected to be a white compound. The reason for the formation of coloured products is not clear. In the case of the trifluoroacetate, the coloured materials were removed by washing the reaction product with liquid SO_2 to yield a pure white compound.[1] The reaction between tetraphenyltin and dichloroacetic acid was carried out with a slight modification of the reported procedure.[7] Dichloroacetic acid was added to a mixture of tetraphenyltin in benzene. This reaction proceeds to give a clear pale yellow solution from which a white crystalline material separates. The direct reaction of tetraphenyltin with heptafluorobutyric acid produces a dark coloured syrup. Several solvents such as SO_2, SO_2ClF, $CFCl_3$, $C_6H_5CH_3$ and C_6H_6 were employed in attempts to remove the coloured materials. In all cases, the syrup would either dissolve completely or remain insoluble. This indicates that the impurities and the desired product have similar polarity and thus similar solubilities. In $CFCl_3$, cooling the solution to lower temperatures, results in crystallization. However, further washings to remove traces of coloured materials resulted in poor yields.

4.2.2 NMR Data

Tin-119 NMR data of tin(II) and tin(IV) carboxylates, sulphonates and fluorosulphates were recorded in the acids from which they are derived. Initially, ^{119}Sn NMR spectra were recorded on the solutions obtained from the reaction of SnO with carboxylic acids and from the reaction of tetraphenyltin with carboxylic acids. However, the ^{119}Sn NMR

chemical shifts of the above solutions were not reproducible. Therefore, it was decided to isolate pure tin(II) and tin(IV) compounds and these were then redissolved in their parent acids and their spectra were recorded.

The tin(II) acetate and tin(II) dichloroacetate are sparingly soluble in their pure acids whereas tin(II) trifluoroacetate and tin(II) heptafluorobutyrate are quite soluble. Among the tin(II) derivatives of strong acids, the sulphate and the trifluoromethanesulphonate are sparingly soluble, but the fluorosulphate is very soluble in the acid. All of the tin(IV) derivatives are reasonably soluble in their parent acids.

All of the above solutions exhibit single resonances in their ^{119}Sn NMR spectra. The ^{119}Sn NMR spectra of those compounds which are reasonably soluble, were recorded at a number of different concentrations in order to study the effect of dilution. The ^{119}Sn chemical shifts, the linewidths, and the concentrations of these solutions are summarized in Table 4.1.

The chemical shifts of $Sn(OAc)_2$ in pure acetic acid and in 2N acetic acid differ by 46 ppm and this shift is probably the result of water molecules being coordinated to tin, thus altering its environment and hence its chemical shift. The ^{119}Sn chemical shifts of these tin(II) and tin(IV) compounds are not very concentration dependent at a fixed temperature. The ^{119}Sn NMR measurements carried out over a temperature range on $Sn(O_2CCF_3)_2$ and $Sn(O_2CC_3F_7)_2$ solutions show appreciable changes in the chemical shifts and linewidths (Table 4.1). The line-

TABLE 4.1

^{119}Sn NMR Data of Tin(II) and Tin(IV) Carboxylates, Sulphates and Sulphonates

Compounds in their parent acid	Temp. °C	Conc. ML^{-1}	$\delta(^{119}Sn)$ ppm	$\Delta\nu_{\frac{1}{2}}$* Hz	
(i) Tin(II) Compounds					
$Sn(CO_2CH_3)_2$ in					
(a) pure HoAc	24	0.05	-617	95[b]	
(b) 2N HoAc	24	0.23	-663	85[b]	
$Sn(CO_2CHCl_2)_2$	24	satd. solution	-786	1000[b]	
$Sn(CO_2CF_3)_2$	24	0.6	-948	22	[a]
	- 5	0.6	-963	69	
	-18	0.6	-970	189	
	24	0.4	-948	66	
	- 5	0.4	-965	69	
	-18	0.4	-972	193	
	- 5	0.2	-965	92	
	-18	0.2	-974	96	
$Sn(CO_2C_3F_7)_2$	24	0.4	-953	493	[a]
	- 5	0.4	-969	590	
	-22	0.4	-984	577	
	24	0.2	-950	555	
	- 5	0.2	-971	516	
	-22	0.2	-987	480	
$Sn(SO_4)$	24	0.06	-1584	20[b]	
$Sn(SO_3CF_3)_2$	22	satd. solution ~0.03	-1576	160[c]	
$Sn(SO_3F)_2$	22	0.34	-1628	125[c]	

Continued.....

TABLE (4.1) Continued

(ii) Tin(IV) Compounds	Temp °C	Concentration ML^{-1}	$\delta(^{119}Sn)$ ppm	$\Delta\nu_{\frac{1}{2}}$* Hz	
$Sn(CO_2CH_3)_4$	24	0.11	-857	29	
	24	0.05	-857	25	
$Sn(CO_2CHCl_2)_4$	24	0.16	-855	48	
	24	0.08	-854	76	
$Sn(CO_2CF_3)_4$	24	0.20	-821	50	b
	24	0.10	-821	52	
	24	0.05	-820	48	
$Sn(CO_2C_3F_7)_4$	24	0.03	-727	85	
$Sn(SO_3CF_3)_4$	24	0.03	-880	55	
	24	0.01	-880	55	

* Width measured at half height of peaks recorded at a field strength of a) 2.118T

b) 5.872T

C) 9.395T

width of the ^{119}Sn NMR signals of tin(II) and tin(IV) compounds are broad and in the case of $Sn(CO_2CF_3)_2$ and $Sn(CO_2C_3F_7)_2$ the linewidths increase as the temperature is lowered together with changes in their chemical shifts. This suggests the presence of fast exchange between different tin environments on the NMR time scale. The tin atoms can have different coordination numbers with carboxylate groups acting as either mono- or bidentate ligands. However, the concentration ranges employed did not have any significant effect in shifting the equilibrium processes. The chemical shifts of a series of triphenyltin(IV) carboxylates have been reported over a concentration range 0.1 - 0.5 mol/l, and they show only a very small concentration dependence.[104] Recently, tri-n-butyl- and di-n-butyltin(IV) carboxylates in solutions of non-coordinating solvents were studied by ^{17}O NMR.[115] These workers, observed only one ^{17}O NMR signal and this effect was interpreted as being due to fast exchange of the oxygen atoms of the carboxylate groups bonded to the central tin atom.

It is interesting to note the wide range of ^{119}Sn chemical shifts of the tin(II) compounds compared to the narrow range shown by tin(IV) compounds listed in Table 4.1. Tin(II) chemical shifts cover a range of approximately 1000 ppm on going from the acetate to the fluorosulphate. As the acidity of the parent acid increases, the ^{119}Sn chemical shift of tin(II) compounds move to lower frequency. The chemical shifts of tin(IV) compounds change by approximately 130 ppm and there is no apparent trend with acidity of the ligand. For triphenyltin(IV) carboxylates, a linear relationship between ^{119}Sn chemical shifts and the pk_a of the corresponding carboxylic acid has been observed.[57,104]

4.2.3 Mössbauer Data

Mössbauer parameters of the newly isolated tin(II) carboxylates, $Sn(CO_2CF_3)_2$ and $Sn(CO_2C_3F_7)_2$ are provided in Table 4.2. The parameters for $Sn(CO_2CF_3)_2$, isolated as a pure material, are different from the reported values of the yellow syrup.[94] Donaldson recorded the spectra of some tin(II) carboxylates which were obtained as solids and also recorded the spectra of their frozen solution.[94] Since the parameters of the solid and the frozen solution were the same, he concluded that the parameters of the frozen tin(II) carboxylates were the same as those of the solid salt. However, the present study shows, in the case of $Sn(CO_2CF_3)_2$, the frozen solution Mössbauer parameters to be different from those of the isolated solid (Table 4.2, Figure 4.1). In fact, the frozen solution has a higher isomer shift and a smaller quadrupole splitting than that of the solid. This indicates that the tin environment is relatively more symmetrical in the frozen solution than in the solid state. This might have been expected since, in solution, trifluoroacetate ligands can easily coordinate the tin atom. The solid state and frozen solution Mössbauer spectra of $Sn(CO_2C_3F_7)_2$ were also recorded. These show two lines in the tin(II) region with unequal linewidths. This is fitted to two overlapping doublets. The fitted parameters are included in Table 4.2. The frozen solution parameters are marginally different from those of the solid. This indicates that there is no dramatic change in the coordination of tin between the solid and solution state in this case. The solution ^{119}Sn NMR spectrum however, shows only a single line. This is possible if a fast exchange process occurs on the NMR time scale between the two different tin sites observed in the frozen solution Mössbauer

TABLE 4.2

^{119}Sn Mössbauer Data for Some Tin Carboxylates

Compound	Temp K	Δ [a] mm s^{-1}	Γ [a] mm s^{-1}	Γ [a] mm s^{-1}	Relative area [b] A2/A1
A. Tin(II) Compounds					
$Sn(OAc)_2$ [94]	77	3.31	1.77		
$Sn(O_2CCF_3)_2$	77	3.53	2.29	1.01	1.09
$Sn(O_2CCF_3)_2$ (Frozen Solution)	77	3.64	1.59	0.94	
$Sn(O_2CCF_3)_2$ [94]	77	3.16	1.76		
$Sn(O_2CC_3F_7)_2$	77	3.62 4.06	1.68 1.30	1.03 1.03	
$Sn(O_2CC_3F_7)_2$ (Frozen Solution)	77	3.75 4.24	1.61 1.30	0.86 0.86	
$Sn(O_2CCHCl_2)_2$	77	3.60	1.66	1.18	1.24
$Sn(O_2CCHCl_2)_2$ [94]	77	3.48	1.64		
$Sn(SO_3CF_3)_2$ [25]	77	4.15	0.84	0.98	
B. Tin(IV) Compounds					
$Sn(OAc)_4$	77	0.16	0.59	1.11	
$Sn(O_2CCF_3)_4$ [1]	77	- 0.04	1.56	0.95	
$Sn(O_2CCHCl_2)_4$	77	0.22	0.58	1.21	
$Sn(O_2CCHCl_2)_4$ [1]	77	- 0.01	0.79	1.04	
$Sn(O_2CC_3F_7)_4$	77	0.03	0.68	1.08	
$Sn(O_2CC_3F_7)_4$ [1]	77	0.03	1.27	0.97	

Continued.....

TABLE 4.2 (Continued)

Compound	Temp K	δ	Δ	Γ^a	Relative Area Sn(IV)/Sn(II)
		mm s^{-1}			
C. Tin(II), Tin(IV) Compounds					
$Sn(O_2CCF_3)_2$	77	0.00	0.33	0.90	1.35(2)
$Sn(O_2CCF_3)_4$		3.94	1.16	0.97	
	77	0.00	0.52	0.98	1.29(2)
		3.94	1.06	0.99	
	4	0.11	0.53	1.01	1.00(2)
		3.90	1.08	1.03	
$Sn(O_2CCF_3)_3$[1,c]	77	- 0.03	0.52	0.81	1.16
		3.94	1.11	0.85	
	4	- 0.02	0.52		0.91
		3.93	1.20		
$Sn(SO_3CF_3)_2$[d]	77	4.28	0.58	0.93	
$Sn(SO_3CF_3)_4$[d]					
$Sn(SO_3CF_3)_3$[7,e]	77	- 0.22	-	0.97	1.22
		4.39	0.41	1.01	

a) Full width at half height.

b) Relative area under the resonance curves of the higher velocity signal to the lower velocity signal of the asymmetric doublet.

c) Compound isolated by the solvolysis of $(C_6H_5)_6Sn_2$ by CF_3CO_2H. It is formulated as $[Sn(II)Sn(IV)O(O_2CCF_3)_4O(OCCF_3)_2]_2$.

d) Solid isolated after washing the mixture with CF_3SO_3H.

e) Compound isolated by the solvolysis of $(C_6H_5)_6Sn_2$ by CF_3SO_3H.

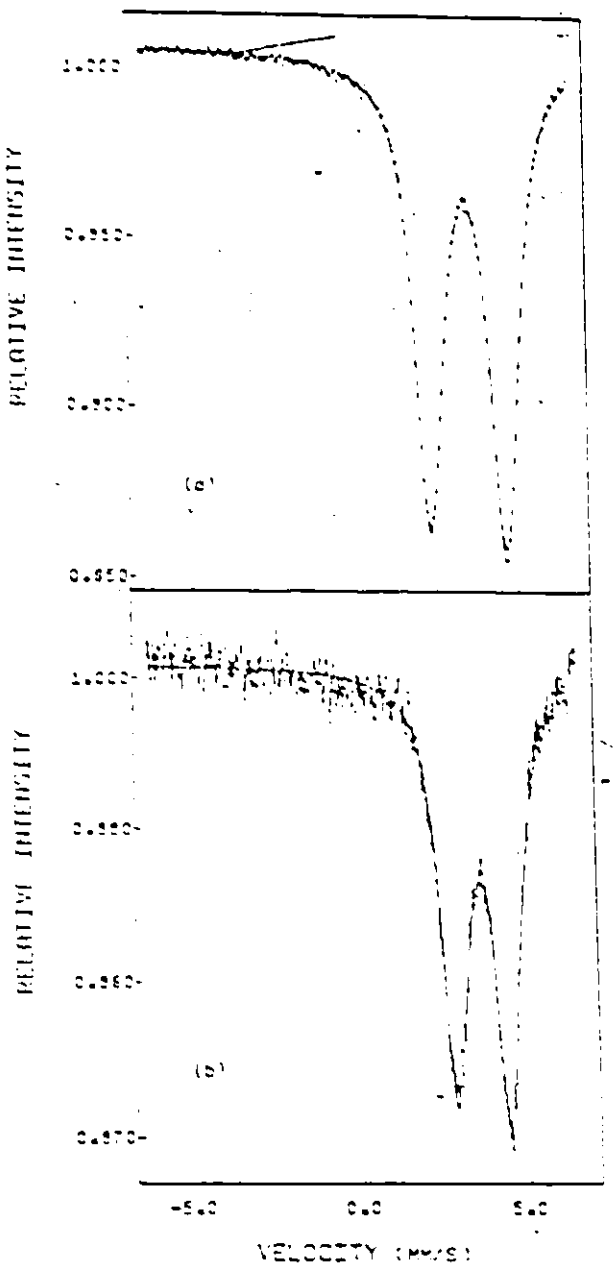

Figure 4.1: ^{119}Sn Mössbauer spectra of (a) solid $Sn(CO_2CF_3)_2$ and (b) frozen solution of $Sn(CO_2CF_3)_2$ in CF_3CO_2H at 77 K.

spectrum.

The tin(IV) carboxylates which were isolated as pure solids in this study are tin(IV) dichloroacetate and, in small amounts, tin(IV) heptafluorobutyrate. The Mössbauer parameters of these solids are provided in Table 4.2 together with the previously reported values which were obtained from coloured syrups.[1] The quadrupole splittings in the two solids are smaller than those of the syrups. Tin tetraacetate exhibits a single line and has been fitted assuming a small quadrupole splitting. This is consistent with its structure which contains an eight coordinate dodecahedral tin atom.[93] A similar non-polmeric dodecahedral structure has been observed for $Sn(NO_3)_4$.[116] Tin(IV) dichloroacetate and tin(IV) heptafluorobutyrate both show small quadrupole splittings indicating lower than cubic symmetry at the tin nucleus. These compounds could have a distorted four coordinated tin environment with four monodentate carboxylate groups, six coordination at tin achieved by some carboxylates being bridged, or an eight coordinated tin with four bidentate carboxylate groups as in the acetate case.[93] Tin(IV) trifluoromethylsulphonate was isolated as a pure compound and its Mössbauer spectrum exhibits a single line with no quadrupole splitting.[25] The tin environment appears to be cubic within the limits of resolution of the Mössbauer technique.

4.3 Stoichiometric Mixtures of Sn(II) and Sn(IV) Compounds

The ^{119}Sn NMR data of tin(II) and tin(IV) compounds can be used as a guide to interpret ^{119}Sn NMR spectra of solutions containing the two oxidation states of tin. Since ^{119}Sn solution NMR and Mössbauer parameters of the simple solid tin(II) and tin(IV) carboxylates and

sulphonates are well established (Table 4.1, 4.2), the reactions between tin(II) and tin(IV) compounds derived from the same acid can be monitored by variations in their spectroscopic parameters. These reactions were carried out in order to explore possible synthetic routes to prepare new mixed oxidation state tin compounds. This study shows that no mixed oxidation state tin compound is formed in the case of either the acetate or the trifluoromethylsulphonate. However, the reaction between $Sn(CO_2CF_3)_2$ and $Sn(CO_2CF_3)_4$ appears to result in compound formation. These data are discussed below.

Tin(II) acetate and tin(IV) acetate were mixed together in equimolar amounts in $HOAc/Ac_2O$ and refluxed to give a clear solution. On cooling to room temperature the solution stayed clear for a few days. The ^{119}Sn NMR spectrum of this clear solution was recorded at ambient temperature and showed two single lines of approximately equal intensity (Table 4.3). One signal appeared at -625 ppm, shifted about 8 ppm from that of $Sn(OAc)_2$ and the other signal appeared at the same position as that of $Sn(OAc)_4$. The difference of 8 ppm may not be significant when the wide range of chemical shifts shown by tin(II) compounds is considered. It is concluded that the tin environments in this solution are similar to the environments of the tin atoms in $Sn(OAc)_2$ and $Sn(OAc)_4$ in their acid solutions. Some solid did precipitate from the above solution after standing at room temperature for a few days. This solid is presumably $Sn(OAc)_2$, since it is sparingly soluble in HOAc at room temperature. The solid isolated from the filtrate by removing the acid by distillation was shown by Mössbauer and solution NMR spectroscopy to be $Sn(OAc)_4$. Therefore, it is concluded that there is no reaction between the two

TABLE 4.3

^{119}Sn NMR Data of Mixtures of Tin(II) and Tin(IV) Acid Derivatives

And Reaction Products of Hexaphenylditin With Acids

1. Mixtures of tin(II) and Tin(IV) acid derivatives in their parent acid	Temp (°C)	$\delta(^{119}Sn)$ ppm	$\Delta\nu_{\frac{1}{2}}$* (Hz)
a) $Sn(CO_2CH_3)_2/Sn(CO_2CH_3)_4$[b]	24	- 625	20
		- 855	15
b) $Sn(CO_2CF_3)_2/Sn(CO_2CF_3)_4$[a]	24	- 746	43
		-1173	934
c) $Sn(SO_3CF_3)_2/Sn(SO_3CF_3)_4$[c]	24	- 879	70
		-1626	315
2. $(C_6H_5)_6Sn_2$ in Acids HA			
where A =			
a) $-O_2CCH_3$[c]	24	- 628	56
		-1404	5000
b) $-O_2CCF_3$[a]	24	- 746	50
		-1173	800
c) $-O_4SH$[b]	24	- 885	46
		-1103	46
d) $-O_3SC_2H_5$[b]	24	- 869	75
		-1248	600
e) $-O_3SCH_3$[b]	24	- 873	74
		-1408	156
f) $-O_3SCF_3$[a]	24	- 879	75
		-1712	500
g) $-O_3SF$[a]	24	- 890	90
		-1860	50

* Width measured at half height. All samples were recorded at 5.872T except sample 1(a) which was recorded at 2.114T.

a Solid isolated from the reaction and then redisolved in the parent acid

b Reaction gives a clear solution

c Solid separated from the reaction and NMR was recorded of the supernatant solution.

components.

The attempted reaction between $Sn(SO_3CF_3)_2$ and $Sn(SO_3CF_3)_4$ was carried out by adding an equimolar amount of $Sn(SO_3CF_3)_2$ to a solution of $Sn(SO_3CF_3)_4$ in CF_3SO_3H. Solid was present in the reaction medium even after it was refluxed on a water bath. Since $Sn(SO_3CF_3)_2$ is sparingly soluble in the acid, it was difficult to say whether any reaction had occured. Tin-119 NMR spectroscopy of the supernatant solution was recorded which exhibited two single lines (Table 4.3). The frequency of one signal appeared at the same chemical shift as that of $Sn(CO_2CF_3)_4$ and the other signal was shifted by 50 ppm to lower frequency from the position of $Sn(SO_3CF_3)_2$. A solid separated from this NMR solution and this was washed with CF_3SO_3H and its ^{119}Sn Mössbauer spectrum showed it to contain only a single absorption with non-resolvable quadrupole splitting in the tin(II) region (Table 4.2). The parameters of this signal agreed with those for $Sn(SO_3CF_3)_2$. It is concluded that no mixed oxidation state compound is formed on mixing Sn(II) and Sn(IV) trifluoromethylsulphonates.

The reaction between $Sn(CO_2CF_3)_2$ and $Sn(CO_2CF_3)_4$ was carried out by mixing equimolar amounts of the reactants in CF_3CO_2H. It should be noted that both $Sn(CO_2CF_3)_2$ and $Sn(CO_2CF_3)_4$ are soluble in the parent acid. The above mixture was stirred at room temperature. On stirring, initially both components dissolved to give a clear solution and after a few minutes solid precipitated from the solution. This solid was isolated by filtration and then washed a few times with the acid. This solid was redissolved in CF_3CO_2H and its ^{119}Sn NMR spectrum was recorded. This exhibited two single lines (Table 4.3). The chemical shifts of these

signals were different from those of the parent components. The high frequency signal (-746 ppm) was shifted about 70 ppm to higher frequency from the position of $Sn(CO_2CF_3)_4$. The low frequency signal (-1173 ppm) was shifted about 225 ppm to lower frequency from the position of $Sn(CO_2CF_3)_2$. The ^{119}Sn NMR chemical shifts were found to change only by a few ppm with concentration and the large shifts observed for the above solution showed that an interaction had occurred between these two components. The ^{119}Sn Mössbauer spectrum of the isolated solid from the reaction of $Sn(CO_2CF_3)_2$ and $Sn(CO_2CF_3)_4$ showed a single absorption, with a non-resolvable quadrupole splitting, near zero velocity and a doublet in the tin(II) region (Figure 4.2, Table 4.2). This indicates that the tin(IV) site of the product is in a near cubic environment in contrast to the tin environment in $Sn(CO_2CF_3)_4$ which shows a large quadrupole splitting. The absorption due to the tin(II) species of the product shows a higher isomer shift and smaller quadrupole splitting than that of $Sn(CO_2CF_3)_2$. Therefore, it is clear from the Mössbauer parameters that the reaction product cannot be a simple mixture of $Sn(CO_2CF_3)_2$ and $Sn(CO_2CF_3)_4$. The ratio of the areas of the tin(IV) signal to the tin(II) signal was 1.32(3) at 77 K and the spectrum recorded at 4 K showed that their areas are equal. The magnitude of the Mössbauer resonance absorption is related to the recoil free fraction which depends on how strongly the tin nucleus is held in the lattice. The above observation indicates that at higher temperatures, tin(II) is held loosely compared to tin(IV) and at 4 K one would expect both sets of nuclei to be held tightly in the lattice, hence the area ratio at this temperature gives a true measure of the relative amounts of the two oxidation states. Since

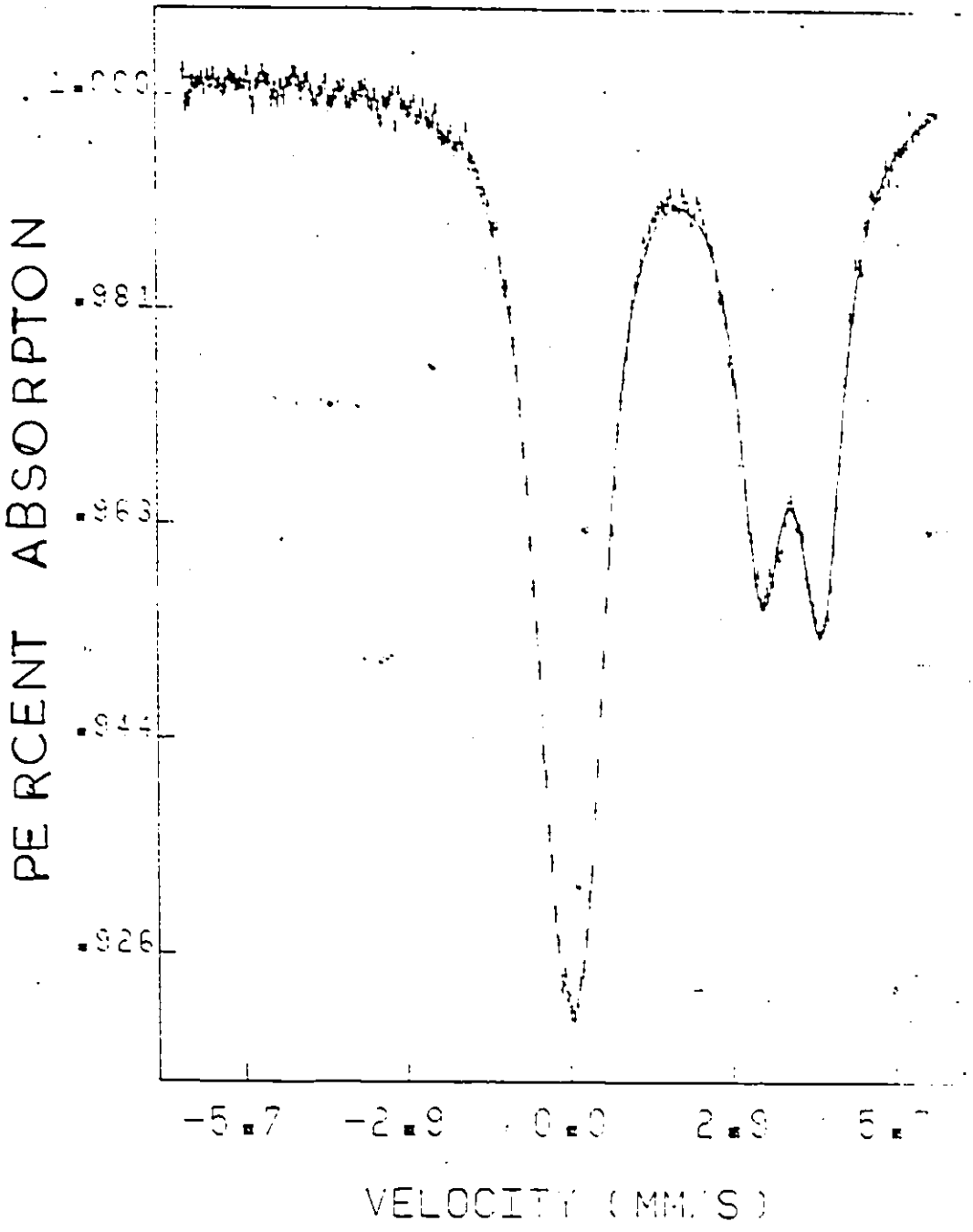

Figure 4.2: ^{119}Sn Mössbauer spectrum of the solid isolated from the reaction between $Sn(CO_2CF_3)_2$ and $Sn(CO_2CF_3)_4$ at 77°K.

this value is close to one, the implication is that the compound contains tin(II) and tin(IV) in equal amounts.

The spectroscopic data of the above product, (I), can be compared with that of the compound obtained by the cleavage of hexaphenylditin with CF_3CO_2H (II). These two compounds have the same empirical formula $Sn(CO_2CF_3)_3$. Tin-119 NMR signals of (I) and (II) dissolved in CF_3CO_2H have very similar NMR parameters (Table 4.3). The ^{119}Sn Mössbauer isomer shift and quadrupole splitting of the two solids are the same within experimental error. This shows that (I) and (II) have very similar local tin environments in the solid and solution states. However, the ratio of the area under the Mössbauer resonance absorption of Sn(II) to Sn(IV) in the two compounds are marginally different at 77 K and at 4 K (Table 4.2). This indicates that the recoil free fraction of the Sn(II) and the Sn(IV) are slightly different in the two compounds. In order to obtain further information about how tightly Sn(II) and Sn(IV) atoms are bound in the lattice, Mössbauer measurements at several intermediate temperatures between 77 K and 4 K are required. The IR spectral data for the two compounds (I) and (II) are given in Table 4.4 for comparison; they are very similar. Solid (II) contains all of the bands shown by the solid (I). In addition solid (II) shows a few extra bands in the $\nu_{sym}(CO_2)$, $\nu_{asym}(CO_2)$ regions and in the region 400 cm^{-1} - 700 cm^{-1}, where vibrations associated with oxygen atoms bridging two or more tin atoms occur. The structure of the crystals obtained by the recrystallization of (II) from benzene has been determined to be $[Sn(II)Sn(IV)O(O_2CCF_3)_4]_2 \cdot C_6H_6$.[18] This contains centrosymmetric $[Sn(II)Sn(IV)O(OCOCF_3)_4]$ units in which Sn(II) and Sn(IV) atoms are bridged by μ_3 oxygen atoms and bridging trifluoroacetate

TABLE 4.4

Infrared Spectroscopic Data[a]

I[b]	II[c]	Assignment
1770(m)	1765(s)	
	1720(m,sh)	
1680(s)	1680(s)	$\nu_{asym}(CO_2)$
1650(s)	1650(s)	
1615(s)	1615(s)	
	1575(s)	
	1480(m)	
	1463(s)	
1450(m)	1450(s)	$\nu_{sym}(CO_2)$
1435(m)	1433(s)	
1365(w)	1370(s)	
1220(s)	1220(s)	
1190(s)	1190(s)	
1150(s)	1150(s)	$\nu_{asym}(CF_3)$, $\nu_s(CF_3)$
1130(s)	1130(s)	
	869(w)	
855(m)	855(m)	$\delta(CO_2)$, ν(C-C)
850(sh)	850(m)	
	840(m)	
789(m)	789(m)	
	785(m)	
	778(m)	$\nu(CO_2)$, ν(Sn-O-Sn)
730(s)	729(s)	
	629(m)	
620(m)	619(m)	
580(m)	585(m)	ν(Sn-O)
545(m)		
520(m)	525(m)	CF_3 bend

a) Abbreviations: s = strong, m = medium, w = weak, sh = shoulder.

b) Solid isolated from the reaction of $Sn(CO_2CF_3)_2$ with $Sn(CO_2CF_3)_4$.

c) Solid isolated from the solvolysis of $(C_6H_5)_6Sn_2$ by CF_3CO_2H-from reference (1).

groups. On the basis of the vibrational data, it is tentatively suggested that compound (I) might not have oxo bridges and that the arrangement of trifluoroacetates might be slightly different from the arrangement in (II). A crystal structure determination of compound (I) would verify this if suitable crystals could be obtained.

The solvolysis of hexaphenylditin by a variety of inorganic acids (HSO_3X; where X = F, CF_3, OH, CH_3, C_2H_5) leads to compound formation according to the equation (4.2).[7]

$$(C_6H_5)_6Sn_2 + 6HSO_3X \longrightarrow Sn_2(SO_3X)_6 + 6\ C_6H_6 \qquad (4.2)$$

It was shown by ^{119}Sn Mössbauer spectroscopy that these compounds can be formulated as $Sn(II)Sn(IV)(SO_3X)_6$.[7] Solid products, free of excess acids, were obtained with HSO_3X, where X = CF_3 or F. When X = OH, CH_3, or C_2H_5, compounds completely free of acid were not isolated even when the reaction was carried out almost stoichiometrically. In all cases, Mössbauer spectra were recorded as frozen solutions. The solid isolated from the reaction when X = SO_3F, was tentatively given the formula $Sn(II)Sn(IV)O(SO_4)(SO_3F)_2$ based on the analysis, yield and vibrational data. The product obtained when X = CF_3, however, agreed with the expected formulation $Sn(SO_3CF_3)_3$. In this thesis, the above compounds in their parent acids have been examined by ^{119}Sn NMR spectroscopy. All of these solutions showed two resonances with no apparent spin-spin coupling between the nuclei (Table 4.3). One signal was due to tin(IV) and the other signal was due to tin(II). It is difficult to differentiate immediately which signal corresponds to which tin environment. Previous data (Table 4.1) showed that the chemical shifts of tin(IV) derivatives

of acids cover a small range at about -850 ppm, whereas tin(II) acid derivatives cover a much wider range. The signals due to strong acid derivatives of tin(II) appeared at much lower frequency. On this basis, the signals exhibited from the solutions obtained by the reaction of hexaphenylditin with strong acids can be assigned as follows: the high frequency signal is due to tin(IV) and the lower frequency signal due to tin(II). This assignment is also consistent with the assumption that the tin(II), having a '5s' electron pair, will be more shielded and hence will resonate at lower frequency. The linewidths of these tin signals are much broader than are usually obtained and furthermore the linewidths of the two signals in each spectrum are quite different. When comparing the series, the tin(II) signals are consistently broader than those from the tin(IV) and the linewidths of the tin(II) signals vary considerably with the acid systems. There are several factors which affect the linewidths. The contributors to the line broadening in this case are likely to be shielding anisotropy (SA) and chemical exchange. Shielding anisotropy can make significant contributions to the line width of the tin(II) signals at higher magnetic fields because of the possible large asymmetry in the environments. Also, chemical exchange is likely to broaden the signals. The effect of various acid ligands on the exchange rates is significant for the tin(II) signals whereas the tin(IV) signals appear to be unaffected.

Tetraorganodistannoxanes form a ladder structure, in which three tin atoms are bridged by an oxygen. A ^{119}Sn NMR study on these systems shows that the coupling between any two tin atoms, through oxygen, varies in the range 60 - 200 Hz.[117] Similarly, if the hexaphenylditin-acid

reaction products contain tin(II) and tin(IV) atoms connected by oxo bridges, and acid groups, as in the structure of $[Sn(II)Sn(IV)O(O_2CCF_3)_4]_2 \cdot C_6H_6$,[18] then one would expect tin(II)-tin(IV) coupling to be in the above range. If the coupling is at the lower end of this range, it might be difficult to observe the satellites due to tin(II)-tin(IV) coupling, because of the broadness of the signals. No couplings were detected.

4.4 Comparison of Tin-119 NMR and Mössbauer Data

The measured NMR chemical shift gives information about the electron cloud surrounding the nucleus through the consideration of shielding. There are several factors which may contribute to the shielding of a nucleus in a molecular environment and generally expressed as,

$$\sigma = \sigma_p + \sigma_d + \sigma_n$$

Here, σ_p and σ_d are the diamagnetic and paramagnetic contributions to the shielding respectively. These arise from the local electron cloud and are comprised of all contributions from remote sources including other atoms in the molecules, solvent molecules and ring currents. The chemical shifts of the heavier nuclei such as tin, are generally assumed to be dominated by the paramagnetic contribution which may be written approximately as:

$$\sigma_p \propto - \frac{1}{\Delta E} \left[\langle r^{-3} \rangle_{5p} P + \langle r^{-3} \rangle_{5d} D \right]$$

where, ΔE is the mean electronic excitation term, the $\langle r^{-3} \rangle$ terms are the mean inverse cubes of the 5p and 5d electron-nuclear radii, and the P and

D terms reflect the imbalance of the 5p- and 5d orbitals. Within a closely related series of compounds, the ΔE terms may be taken as comparable and, if the D term may be neglected, then the chemical shifts should show a dependence on the P term. There are many factors which influence ^{119}Sn NMR chemical shifts, and therefore the above simplification is limited to a qualitative explanation for the observed trends.

Tin-119 Mössbauer quadrupole splitting is related to the tensor of the electric field gradient (eq) created at the nucleus. The p-electron imbalance has an influence on the electric field gradient but the origin of this can only be assessed if a determination of the sign of e^2qQ is made. Since the NMR chemical shift (δ_{NMR}) and the Mössbauer quadrupole splitting ($\Delta_{Möss}$) are both related to the imbalance in the p-electrons, one would expect a correlation between these parameters. Such a correlation can only be anticipated within a series of compounds of similar structure and where the tin environment is similar throughout the series in both the solid state and solution. Jones has observed a linear correlation for the series of compounds $(Ph_3Sn)_2E$ and $(Me_3Sn)_2E$ where E = S, Se or Te.[118]

A plot of ^{119}Sn NMR solution chemical shifts (δ_{NMR}) and the corresponding Mössbauer quadrupole splittings ($\Delta_{Möss}$) of the solids for the tin(II) compounds listed in Table 4.1 is shown in Figure 4.3. It should be noted that both the solid and frozen solution Mössbauer spectra were recorded for $Sn(CO_2CF_3)_2$. The parameters in the two cases were found to be different and their quadrupole splittings are plotted against the solution NMR chemical shifts. In this case, the frozen solution value clearly fits the correlation better than the value for the solid. The

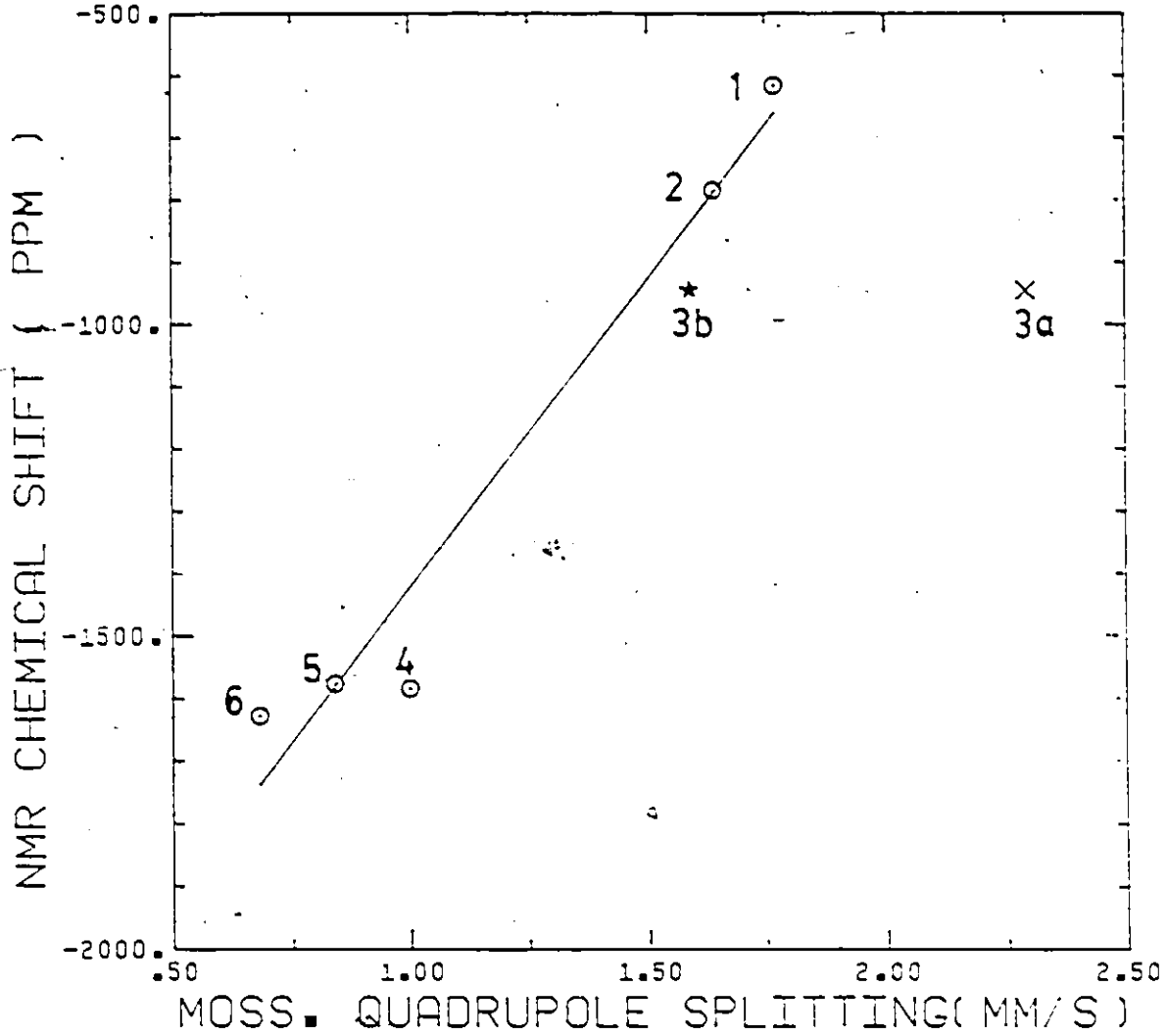

Figure 4.3: Plot of solution ^{119}Sn NMR chemical shift against solid ^{119}Sn Mössbauer isomer shift for tin(II) acid derivatives, SnX_2, where X= (1) $CH_3CO_2^-$ (2) $CHCl_2CO_2^-$ (3a) $CF_3CO_2^-$, solid (3b) $CF_3CO_2^-$, frozen solution (4) HSO_4^- (5) $CF_3SO_3^-$ (6) SO_3F^-. The straight line represents the best linear fit to the data (excluding points 3a and 3b).

assumption that the other tin(II) compounds have similar tin environments both in the solid and solution might not be valid. Most of the tin(II) compounds listed here are sparingly soluble in their parent acids. This makes it difficult to get the required amounts of tin into solution in order to record a spectrum and furthermore, while freezing the saturated solutions, precipitation of crystalline material may occur. This would defeat the purpose of the experiment, which is to obtain the solution parameters.

4.5 Mixed Valence Tin(II), Tin(IV) Compound Derived From $Sn(CO_2CF_3)_2$

4.5.1 Crystal Structure of Di-$\mu_3$oxo-octakis-μ-(trifluoroacetato)-tetratin(II)tin(IV)

Crystals were formed from a solution of tin(II) trifluoroacetate [$Sn(CO_2CF_3)_2$] in trifluoroacetic acid as described in the experimental section. A suitable crystal of size 0.35x0.35x0.45 mm was sealed in a Lindemann glass capillary tube and precession photographs were obtained. Zero and first layer photographs showed diffraction patterns consistent with the tetragonal system and systematic absences were consistent with space groups either $I\bar{4}2d$ or $I4_1md$. The same crystal was mounted on the diffractometer and the cell previously found was accurately determined from a least squares refinement of 15 well centred reflections. A full set of intensities were measured on this unit cell on a Nicolet P3 diffractometer. The crystal data and other parameters associated with the structure determination of this compound are summarized in Table 4.5. The structure was solved in the space group $I\bar{4}2d$ as described below.

An empirical absorption correction was carried out on the intensities (total of 7126 reflections) using the PSI programme, provided by the diffractometer manufacturer and modified locally for the CDC computer by Z. Tun and J. F. Britten. Equivalent reflections were then averaged to give 2999 unique reflections of which 206 reflections with intensities less than or equal to zero were removed. The remaining 2793 reflections were used in the structure determination. The positional parameters of the two tin atoms in the asymmetric unit were obtained from a three-dimensional Patterson synthesis, and were used to phase the initial structure factor calculations. The position of fluorine, oxygen,

TABLE 4.5

Crystal Data Table

Compound	$Sn_5O_2(O_2CCF_3)_8$
Formula weight	1529.19
Crystal shape and size	pyramidal, 0.35 x 0.35 x 0.45 mm
Systematic absences	hk0; h+k = 2n+1 h00; h = 2n+1
	0kl; k+l = 2n+1 0k0; k = 2n+1
	h0l; h+l = 2n+1 00l; l = 4n+1
	hhl; 2h+l = 4n+1
Space group	$I\bar{4}2d$
Unit cell parameters	a = b = 12.448(3)Å
	c = 33.300(5)Å
Volume	5161(2) $Å^3$
Z	4
d_{calcd}	1.968 g cm^{-3}
Linear abs. coeff.	25.44 cm^{-1}
PSI scan 2theta Max/Min	43.76, 4.88
Chi Max/Min	114.79, 65.21
No of refl. used	11
Psi increment/range	10
Min. corr. factor	0.707
No. of refl. to determine cell	15
Limits in 2θ	$18.3° \leq 2\theta \leq 27.6°$
Reflections measured	$0 \leq h,k \leq 16, -43 \leq \ell \leq +43$

Continued.....

TABLE 4.5 (Continued)

Max. 2θ, reflections	55.1°
Standard reflections (e.s.d)	4 4 0 (1.09%); - 2 3 9 (1.05%)
Temp.	23°C
No. of reflections collected	7126
No. of unique reflections	2999
No. with I > 0	2793
No. with I < 0	206
Final R_1[a], R_2[b]	0.1509, 0.0987
Final shift/error max (av)	0.017(.004)
x (secondary extinction)	0.00015
Final difference map	
highest peak ($e \cdot Å^{-3}$);location	4.8; 0.10, 0.38, 0.16
lowest valley ($e \cdot Å^{-3}$);location	-3.1; 0.12, 0.08, 0.60
weighting scheme	$1/\sigma(F_o)^2$
s[c], error in an observation	
of unit weight	5.98
No. of variables	60

[a] $R_1 = \dfrac{\Sigma||F_o|-|F_c||}{\Sigma|F_o|}$

[b] $R_2 = \left[\dfrac{\Sigma w(|F_o|-|F_c|)^2}{\Sigma w|F_o|^2}\right]^{\frac{1}{2}}$

where $w = \dfrac{1}{\sigma(F_o)^2}$, $\sigma(F_o)$ being the error derived from the counting statistics.

Continued.....

TABLE 4.5 (Continued)

$$c\ s = \left[\frac{\Sigma w(|F_o|-|F_c|)^2}{N_R - N_V}\right]^{\frac{1}{2}}$$, where N_R = number of reflections and

N_V = number of parameters varied during the refinement.

and carbon were located from a different Fourier synthesis and a least squares refinement was carried out using SHELX.[48] Some difficulties were encountered in the refinement because the $-CF_3$ groups were rotationally disordered. The final solution reported here, replaces each $-CF_3$ group with two partially occupied $-CF_3$ groups of fixed geometry related by a rotation about the C-C bond. Thus only the fluorine atoms are disordered. The scale factor and all variable positional and thermal parameters were refined using SHELX[48] with weights $\omega=1/\sigma^2(F_o)$ (where $\sigma(F_o)$ is the error derived from counting statistics). Refinements were terminated when the maximum shift/error was less than 0.05. Finally refinement was converged at R_1 = 0.151 and R_2 = 0.099 (see Table 4.5 for the definition of R_1 and R_2). The final positional coordinates and the temperature factors of the atoms in the asymmetric unit are given in Table 4.6. The relevant bond distance and bond angles are given in Table 4.7.

The structure of the molecule is shown in Figure 4.4 and the stereoscopic view of molecular packing in the cell is shown in Figure 4.5. It consists of noncentrosymmetric $[Sn(II)_4Sn(IV)O_2(O_2CCF_3)_8]$ molecules which belong to the point group S_4. The central feature of the molecule is shown below.

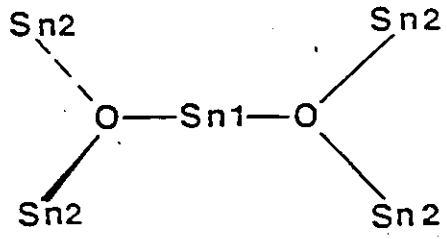

TABLE 4.6

Atomic Positional Parameters ($x10^4$) and Temperature Factors ($Å^2 x10^3$) for $[Sn(II)_4Sn(IV)O_2(O_2CCF_3)_8]$ (F atoms are disordered with F1, F2, F3 site occupied by 65.0% of an atom; F4, F5, F6 site occupied by 35.0% of an atom; F7, F8, F9 site occupied by 55.5% of an atom and F10, F11, F12 site occupied by 44.5% of an atom).

Atom	x/a	y/b	z/c	U_{iso} or U^*_{eq}
Sn(1)	0	0	0	48(2)*
Sn(2)	1058(2)	1099(2)	898(1)	70(2)*
O(1)	0	0	582(5)	54(5)
O(2)	604(11)	1512(11)	38(4)	53(4)
O(3)	2357(13)	- 72(16)	443(4)	79(5)
O(4)	-279(13)	1294(14)	1410(4)	75(5)
O(5)	1628(12)	- 261(15)	1317(4)	86(6)
C(1)	2303(19)	- 557(18)	145(6)	49(6)
C(2)	3402(8)	-1011(10)	56(3)	64(7)
C(3)	1182(10)	-1134(8)	1477(3)	79(7)
C(4)	1757(11)	-1633(11)	1809(3)	123(11)
F(1)	1104(10)	4027(8)	-339(3)	107(5)
F(2)	590(10)	3822(8)	240(3)	107(5)
F(3)	1933(10)	3021(8)	39(3)	107(5)
F(4)	1202(10)	3413(8)	316(3)	95(9)
F(5)	390(10)	4124(8)	-152(3)	95(9)
F(6)	1882(10)	3457(8)	-247(3)	95(9)
F(7)	-1470(11)	2598(11)	1853(3)	122(8)
F(8)	-1636(11)	1129(11)	2139(3)	122(8)
F(9)	-2742(11)	1603(11)	1711(3)	122(8)
F(10)	-2466(11)	2174(11)	1626(3)	152(13)
F(11)	-1274(11)	2246(11)	2054(3)	152(13)
F(12)	-2199(11)	873(11)	2001(3)	152(13)

	U_{11}	U_{22}	U_{33}	U_{12}	U_{13}	U_{23}
*Sn(1)	50(1)	50(1)	43(2)	-	-	-
*Sn(2)	81(2)	71(2)	56(1)	14(1)	10(1)	1(1)

TABLE 4.7

Selected Bond Distances (Å) and Bond Angles (°) for

$[Sn(II)_4Sn(IV)O_2(O_2CCF_3)_8]^{+}$

(i) Tin Co-ordination

(a) Lengths

Sn(1)-O(1)	1.937(16)	Sn(2)-O(1)	2.172(8)
Sn(1)-O(2)	2.030(14)	Sn(2)-O(2)	2.964(14)
		Sn(2)-O(3)	2.653(17)
		Sn(2)-O(4)	2.395(14)
		Sn(2)-O(5)	2.306(17)

(b) Angles

O(1)-Sn(1)-O(2)	86.4(4)	O(1)-Sn(2)-O(2)	61.6(5)
O(1)-Sn(1)-O(2")	93.6(4)	O(1)-Sn(2)-O(3)	75.3(4)
O(2')-Sn(1)-O(2")	90.2(6)	O(1)-Sn(2)-O(4)	89.3(5)
O(2)-Sn(1)-O(2')	172.9(5)	O(1)-Sn(2)-O(5)	91.0(5)
		O(2)-Sn(2)-O(3)	70.1(4)
		O(2)-Sn(2)-O(4)	122.6(5)
		O(2)-Sn(2)-O(5)	140.4(5)
		O(3)-Sn(2)-O(4)	152.4(6)
Sn(2)-O(1)-Sn(2')	121.9(7)	O(3)-Sn(2)-O(5)	75.8(5)
Sn(2)-O(1)-Sn(1)	119.0(4)	O(4)-Sn(1)-O(5)	81.8(5)

ii) Trifluoroacetate Groups

(a) Lengths

C(1)-O(2)	1.159(26)	C(3)-O(4)	1.163(20)
C(1)-O(3)	1.164(26)	C(3)-O(5)	1.332(21)
C(1)-C(2)	1.510(25)	C(3)-C(4)	1.457(17)

(b) Angles

O(2)-C(1)-O(3)	121.6(22)	O(4)-C(3)-O(5)	117.7(14)
O(2)-C(1)-C(2)	130.4(18)	O(4)-C(3)-C(4)	123.2(12)
O(3)-C(1)-C(2)	108.0(18)	O(5)-C(3)-C(4)	116.6(12)

+ (') denotes symmetry equivalent position (-x,-y,z) and

(") denotes symmetry equivalent position (-y,x,-z).

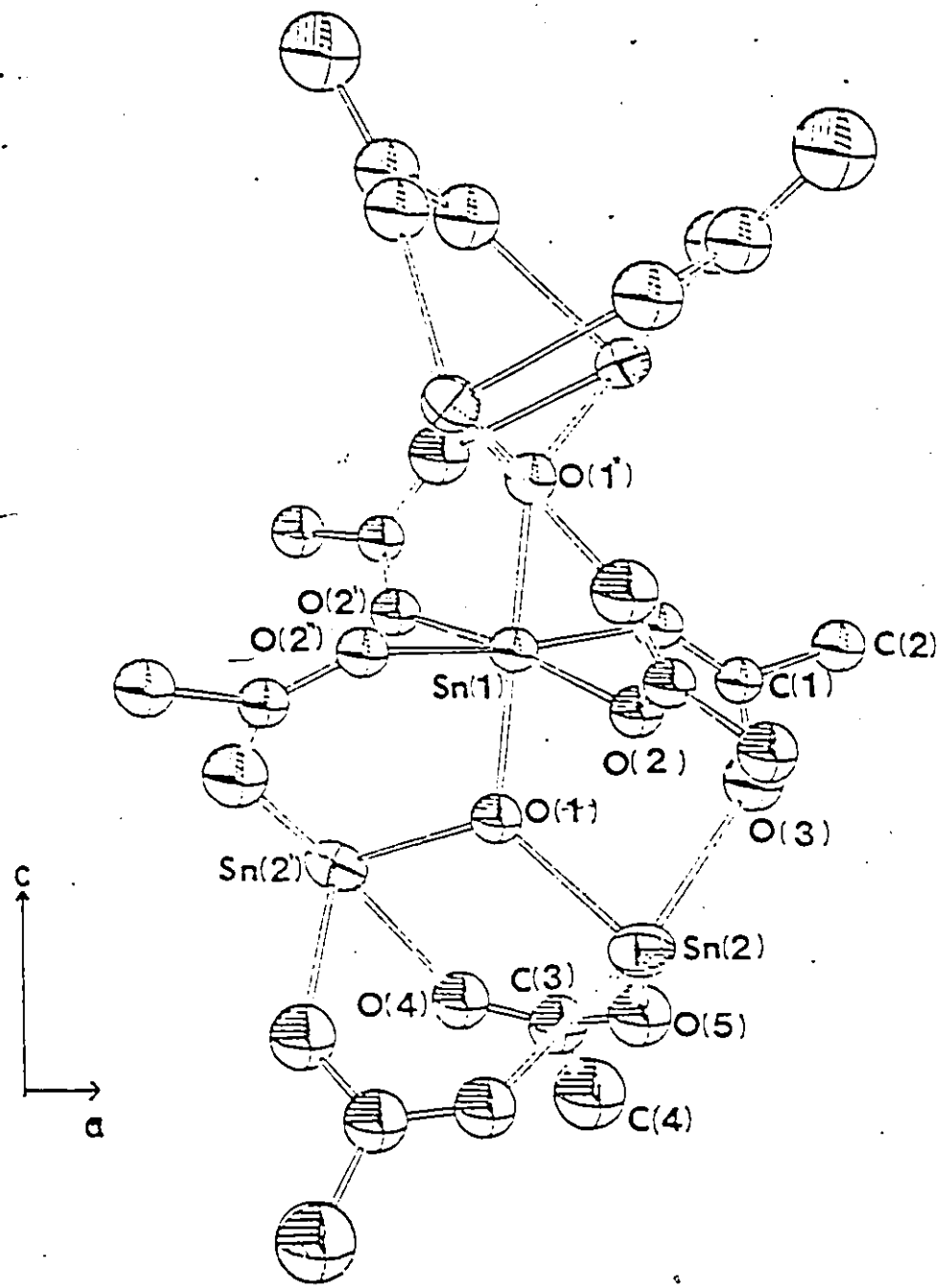

Figure 4.4: Molecular structure of Di-μ_3-oxo-octakis-μ-(trifluoroacetato)-tetratin(II)tin(IV) viewed down the b axis. The labelling of atoms as in Table 4.6. Fluorine atoms are omitted for clarity.

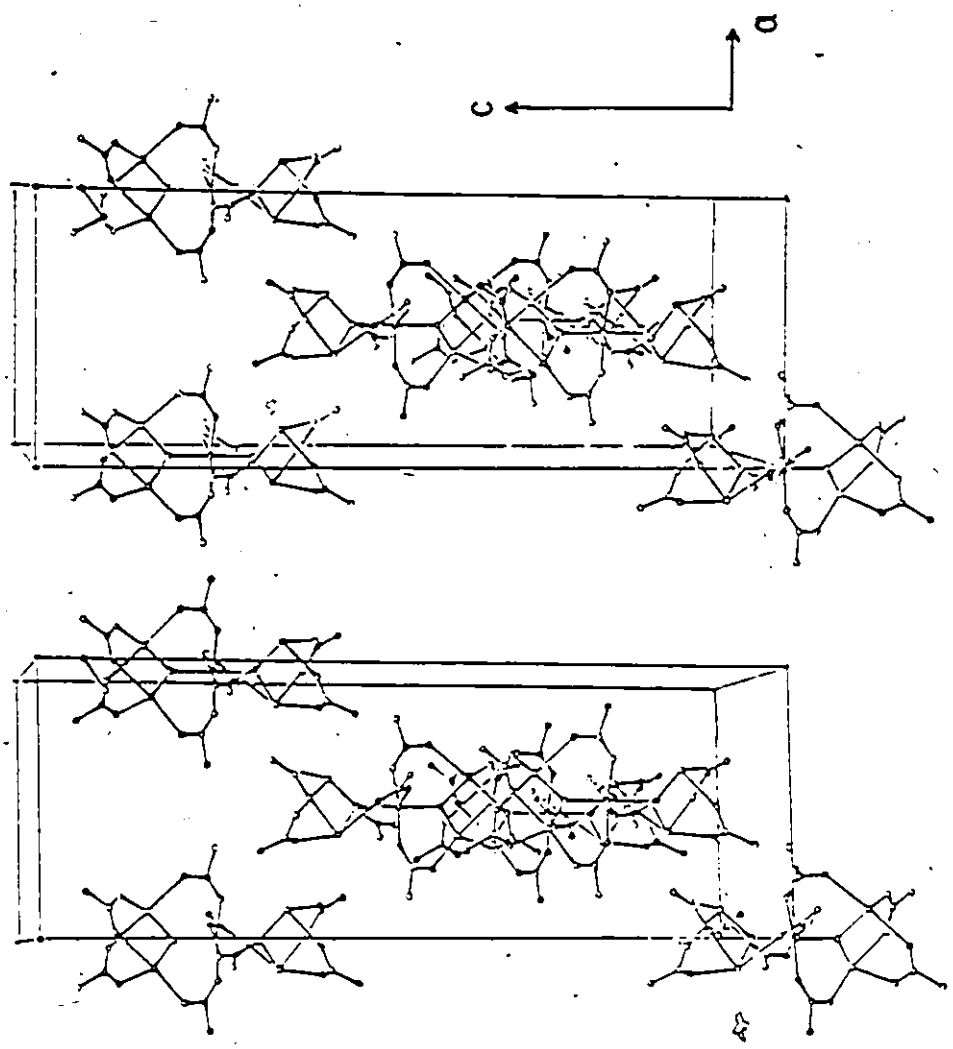

Figure 4.5: Stereoscopic diagram of the packing of molecules of $[Sn(II)_4Sn(IV)O_2(O_2CCF_3)_8]$. The view is down the b axis. Of the molecules having their centres at the corners of the cell only one is shown.

It consists of oxygen atoms which are bonded to a Sn(IV) and two Sn(II) atoms in a planar three coordinate arrangement. Such planar units are a common feature in oxoorganotin compounds.[18,26,119-121] The Sn(II) atoms at the ends of the group are bridged by two trifluoroacetate groups. In addition, four trifluoroacetate groups bridge between the central Sn(IV) atom and the Sn(II) atoms.

The Sn(IV) atom (referred to as Sn(1) in Figure 4.4) is in a slightly distorted octahedral environment with the axial Sn-O bond distances to the bridging oxygen atoms [1.94(2)Å] being shorter than the equatorial Sn-O distance [2.03(1)Å]. Similar six coordination was shown by the tin(IV) atoms in the other mixed valence tin compounds, whose structures have been reported,[18,26] although in those cases, the bond lengths were more nearly equal. One pair of O(2) atoms [O(2), O(2')] are 0.90Å below the plane perpendicular to the S_4 axis which passes through Sn(1). The other pair of O(2) atoms are 0.90Å above this plane.

The Sn(II) atoms (referred to as Sn(2) in Figure 4.4) show a range of Sn-O bond distances from 2.17Å to 2.96Å. The strength of these bonds can be analysed using Brown's bond valence approach.[122] This is based on the fact that the length of a bond is inversely related to its bond valence and that the sum of the bond valences around each atom must equal the atom valence.[123] The bond valence (s) can be calculated in valence units (v.u.) from the observed bond length (R) using the empirical relationship:

$$S = \exp[R_o - R)/0.37]$$

with only one fitted parameter R_o.[124] This value has been estimated by considering the bond lengths observed between Sn-O atoms in a number of

structures. The bond valences for Sn(II)-oxygen bonds are calculated using a R_o value of 1.990 .[125] The geometry of the Sn(2) atom is shown in Figure 4.6 with its bond valencies. The strength of these bonds can be classified as follows.

The shortest Sn(2)-O bond (0.61 v.u.) is that to oxygen O(1), which bridges the three tin atoms. There are two other Sn-O bonds of intermediate strength [Sn(2)-O(4), 0.34 v.u.; Sn(2)-O(5), 0.42 v.u.] formed by the trifluoroacetates bridging the two Sn(2) atoms. Another slightly weaker Sn-O bond [Sn(2)-O(3), 0.17 v.u.] is formed by those trifluoroacetates bridging Sn(1) and Sn(2). An additional weaker interaction between Sn(2) and O(2) is considered to be significant [Sn(2)-O(2), 0.07 v.u.] and could account for the distortion of the Sn(2)-$[O(2)]_4$ unit from planarity.

Since the ratios of ionic radii (r^+/r^-) for oxides and fluorides of Sn(II), Sb(III), Te(IV), I(IV) and Xe(VI) lie in the range 0.5-0.7, they should all be six coordinate. Therefore, Brown considers the environment of the central atom to be octahedral which has been distorted by the lone pair.[126] Gillespie has discussed in detail the irregularity of coordination around atoms with stereoactive lone pairs.[127] The lone pair blocks bonding on one side and forces the other bonds closer together. It was shown by comparing the molecular volume per anion between different Sn^{2+} and Sn^{4+} containing structures for tin oxides, fluorides and oxyfluorides that a lone pair requires a volume comparable with that of an oxygen or fluoride anion.[128,129]

The effect of the lone pair on the coordination of Sn(II) is clearly seen by the presence of a vacant space and the distortion of

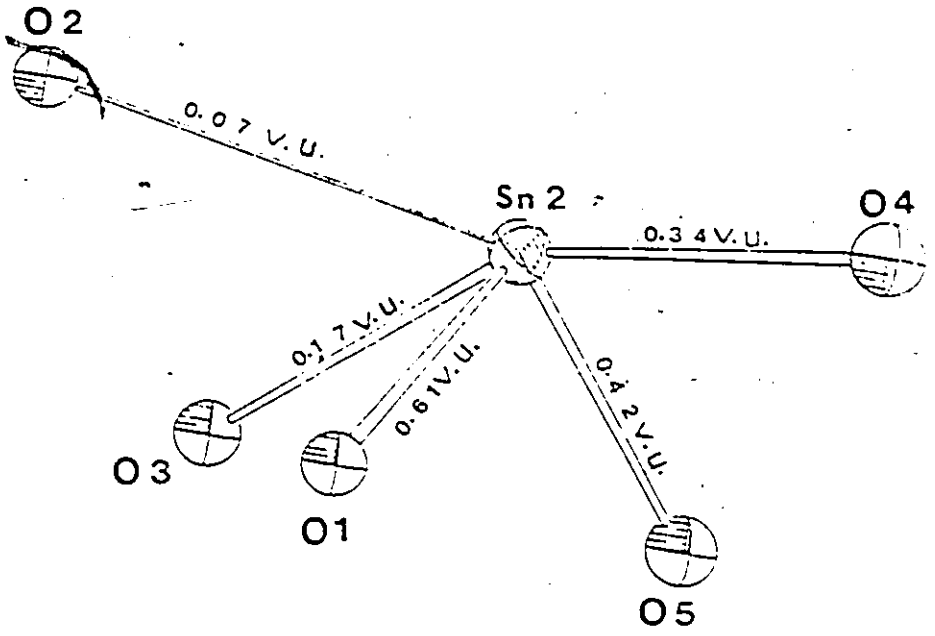

Figure 4.6: Geometry of Sn(2) atom. Bond valencies are given along the bonds in valence unit (v.u.).

the angles between the Sn(2)-oxygen bonds. In the structure discussed here, the environment of Sn(2) can be considered to be six coordinated based on an octahedron with the lone pair occupying one of the axial positions opposite to the short Sn(2)-O(1) bond. This can be described as SnX_5E coordination, where E represents the lone pair. Very few five coordinate (pseudo-six coordinate) examples of tin(II) are known. They are α-SnF_2,[130] $BaSnF_4$ [131] and the mixed valence tin trifluoroacetate reported by Birchall and Johnson.[18] More usually, Sn is considered to adopt an SnX_3E or SnX_4E coordination.[98]

The asymmetry of the C-O distances [C(3)-O(4), 1.16(2); C(3)-O(5), 1.33(2)Å], observed for the trifluoroacetates bridging the two Sn(II) atoms indicates bonding of the type Sn(II)-O-$\overset{|}{C}$=O→Sn(II). This pattern has been observed for the carboxylates which bridge two tin(IV) atoms[132] or tin(II) and tin(IV) atoms.[18,26] The differences in the C-O bond lengths causes a distortion in the C-C-O angles. The short C-O bond is expected to have more double bond character and bond repulsion results in an increase in one C-C-O angle at the expense of the other [O(4)-C(3)-C(4), 123.2(12); O(5)-C(3)-C(4), 116.6(12)]. Although the C-O bond distances in the other carboxylate group [C(1)-O(2), 1.16(3); C(1)-O(3), 1.16(3)Å] appear to be equal, large errors are associated with them. However, previous structural studies[18,26] indicate that the carboxylates bridging tin(II) and tin(IV) atoms show bonding of the type Sn(IV)-O-$\overset{|}{C}$=O→Sn(II).

4.5.2 Mössbauer Data

The Mössbauer parameters of the crystal whose structure was described in the preceeding section are summarized in Table 4.8 and the spectrum of the powdered sample recorded at 77 K is shown in Figure 4.7. This clearly shows the presence of two non-cubic environments, one due to Sn(IV) and the other, more intense, due to Sn(II). The data are consistent with the X-ray crystallographic results discussed in the above section. The tin(IV) site exhibits a well resolved quadrupole doublet (Δ = 1.12 mm/s) which is in agreement with the distorted environment found i.e., Sn(IV)-O(1) = 1.937(16)Å and Sn(IV)-O(2) = 2.030(14)Å, with the plane of the four Sn(IV)-O(2) being buckled (see Figure 4.4) as described earlier. This distortion is more severe than in the two previously reported X-ray crystal structures of mixed oxidation state tin carboxylates.[18,26] In both of the previous cases, no quadrupole splitting was observed for the Sn(IV) atom.

The parameters of the doublet arising from the tin(II) nuclei is typical for tin(II) carboxylates.[94] X-ray crystallography shows that the Sn(II) is in a distorted SnX_5E environment, the short Sn(II)-O(1) bond (0.61 v.u.) being opposite the space presumably occupied by the lone pair (Figure 4.6). The bond strengths range from 0.42 v.u. to 0.34 v.u. for the short bonds, to 0.07 v.u. for the longest. The isomer shift and the quadrupole splitting observed for these Sn(II) atoms is similar to the values obtained for the simple tin(II) trifluoroacetate (δ = 3.53, Δ = 2.29 mm/s). Therefore, it could be inferred that the $Sn(CO_2CF_3)_2$ has a similar tin environment to that of the Sn(II) atoms in the crystal structure described above.

TABLE 4.8

Mössbauer Data for $[Sn_4(II)Sn(IV)O_2(O_2CCF_3)_8]$

Compound	Temp(^{0}K)	δ (mms^{-1})	Δ (mms^{-1})	Γ (mms^{-1})	Δ (mms^{-1})	Δ (mms^{-1})	Γ (mms^{-1})	$\frac{ASn(II)}{ASn(IV)}$
$Sn_5O_2(CO_2CF_3)_8$	4	0.10	1.11	1.01	3.66	1.85	1.09	2.75
	4*	0.17	0.97	1.15	3.36	1.86	1.12	2.98
	20	0.10	1.07	1.07	3.65	1.84	1.08	2.77
	34	0.09	1.04	1.25	3.60	1.82	1.11	2.73
	55	0.09	1.03	1.19	3.52	1.78	1.08	2.77
	77	0.09	1.12	0.84	3.59	1.78	0.92	2.82
	125+	0.06	1.14	1.00	3.58	1.78	1.00	2.58
	150+	0.12	1.13	1.00	3.57	1.76	1.00	2.32
$[Sn_2O_2(O_2C_6H_4NO_2$-ortho$)_4(THF)]_2$[26]	77	0.068	0.00	1.18	3.597	1.823	0.829	
$[Sn_2O(O_2CR)_4O$-$(OCR)_2]_2$[1]	77	-0.03	0.52	0.81	3.94	1.11	0.85	0.86

* Amount of tin used in this measurement was 2 mg/cm^2 and both source and absorber were at 4K; in all other measurements the amount of tin used was 15 mg/cm^2.

\+ Linewidths were fixed to be 1.00 mms^{-1} in order to obtain realistic fits because of the poor statistics.

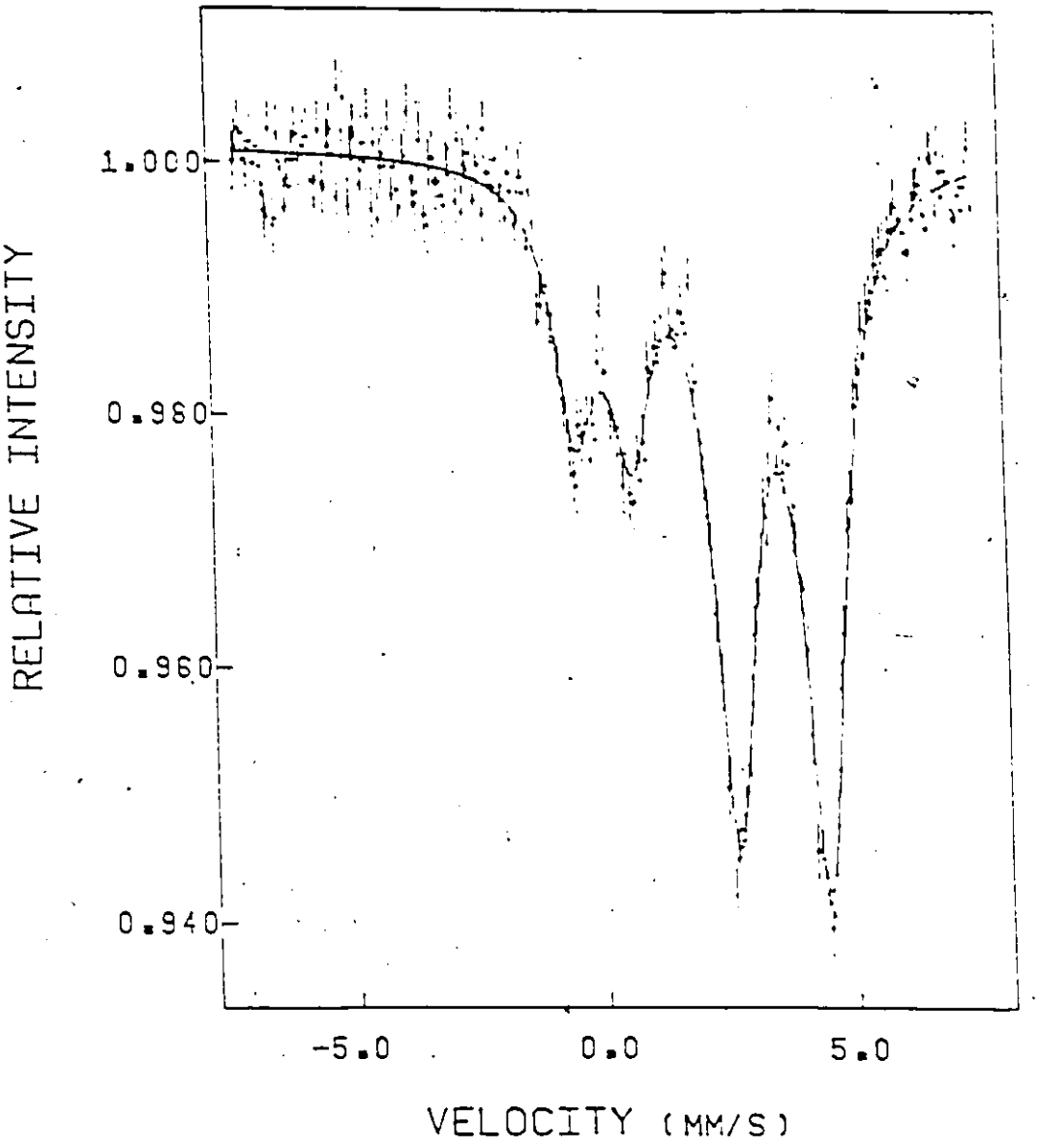

Figure 4.7: ^{119}Sn Mössbauer spectrum of $[Sn(II)_4Sn(IV)O_2(O_2CCF_3)_8]$ at 77 K.

The variable temperature Mössbauer data provides additional information about the lattice structure. The recoil-free fraction (f) is related to the mean square vibrational amplitude of the Mössbauer atom. Since the vibrational amplitude is temperature dependent, the recoil-free fraction itself is temperature dependent and through this, chemical information can be extracted. Since for a thin absorber, f is directly related to the area [A(T)] under the resonance curve of a Mössbauer spectrum, the temperature variation of f may be followed by experimentally evaluating the parameter A(T). Semi-logarithmic plots of resonance areas (normalized to 77 K) against temperature for the tin(II) and tin(IV) sites of the above mixed valence tin compound are shown in Figure 4.8. These are found to be linear in the temperature range $4 \leq T \leq 150$ K with correlation coefficients 0.994 [Sn(II)] and 0.986 [Sn(IV)].

The Debye model of solids can be expressed in the high temperature limit, as in equation (4.2).[133]

$$\ln f = - \frac{3E_\gamma^2}{Mc^2 k_B \theta_D^2} T, \text{ when } T > \theta_{D/2}. \qquad (4.2)$$

Here, E_γ is the Mössbauer γ-ray energy, M is the nuclear mass and θ_D is the 'Debye temperature' of the lattice. In the low temperature limit, $(T \rightarrow 0)$ $\ln f$ becomes independent of temperature with all atoms in the zeroth vibrational state. Under these conditions, the recoil-free fraction is given by (4.3) and this reflects the zero point motion of the atom in its potential energy well.[133]

$$\ln f = - \frac{3E_\gamma^2}{Mk_B \theta_D} \qquad (4.3)$$

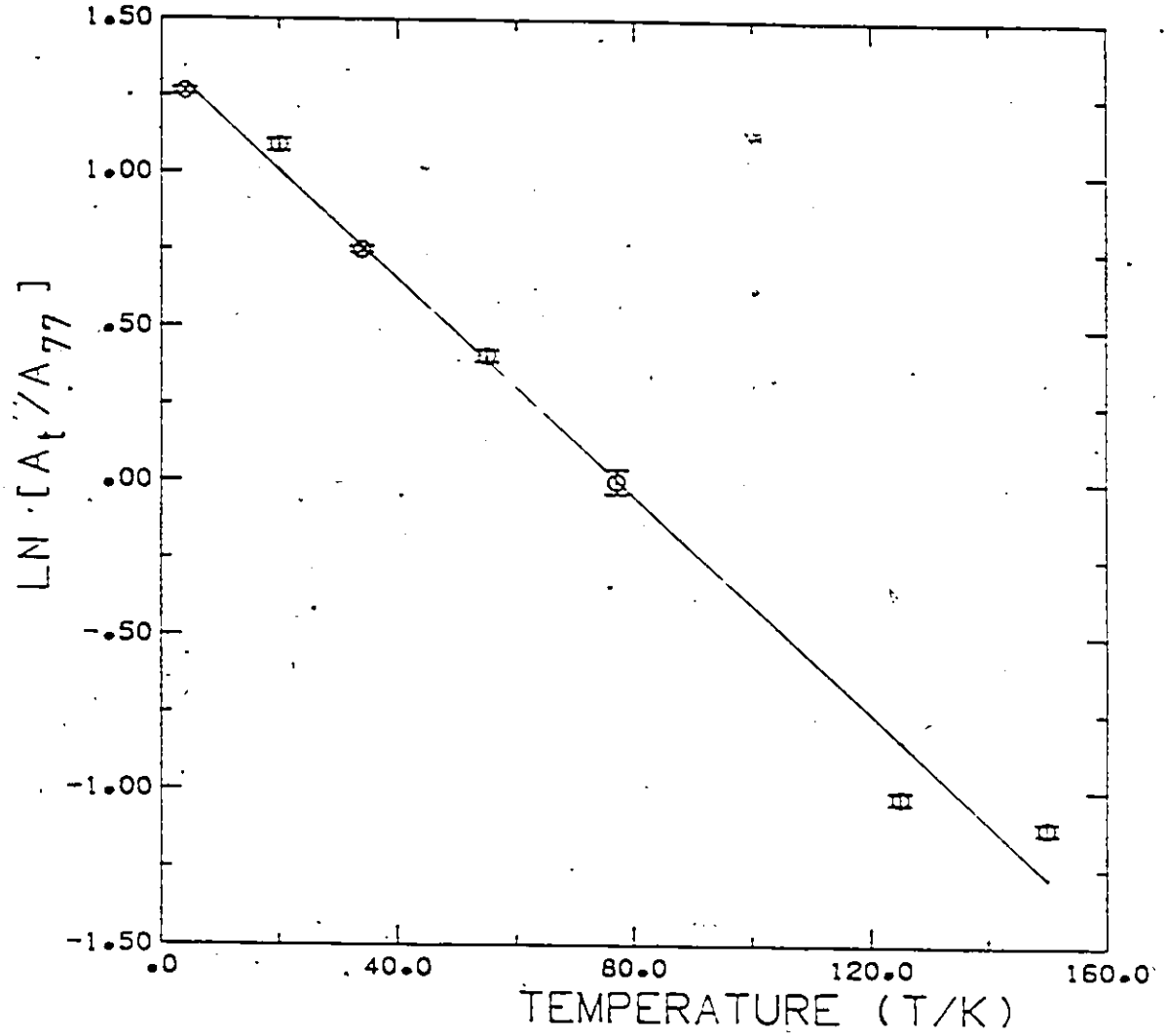

Figure 4.8(a): Plot of the logarithim of the area under the Mössbauer resonance curve (normalised to 77 K datum) against temperature for the Sn(II) site of $[Sn(II)_4Sn(IV)O_2(O_2CCF_3)_8]$. The straight line represents the best linear fit to the data.

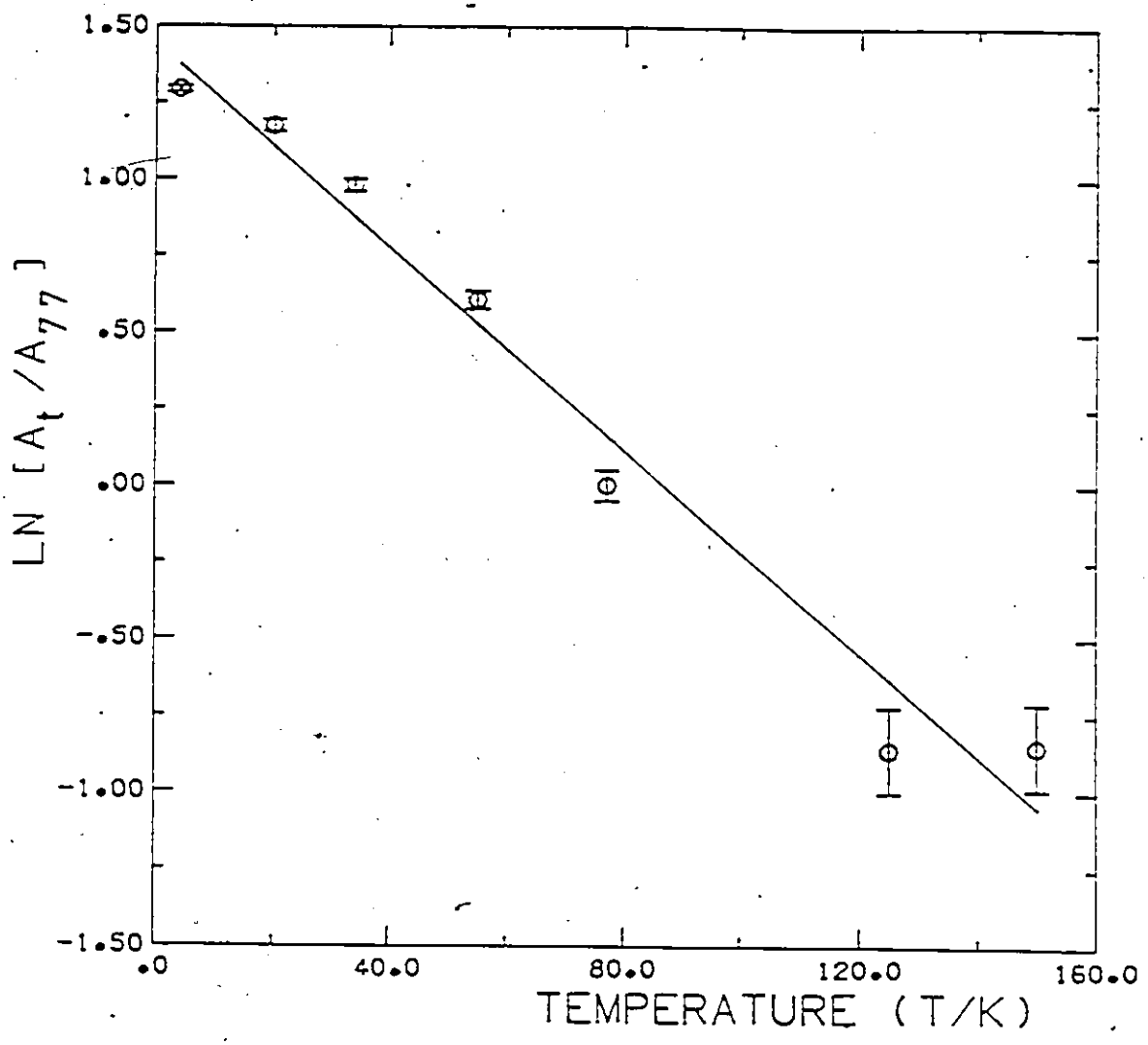

Figure 4.8(b): Plot of the logarithim of the area under the Mössbuaer resonance curve (normalised to 77 K datum) against temperature for the Sn(IV) site of $[Sn(II)_4Sn(IV)O_2(O_2CCF_3)_8]$. The straight line represents the best linear fit to the data.

Herber et al.[134] in their variable temperature study ($4 \leq T \leq 175K$) of cyclic dibutyldistannoxane have observed a linear function in the high temperature limit ($60 \leq T \leq 175$ K) and then departure from linearity at lower temperatures which reflects the zero point motion. The plot shown in Figure 4.8(a) is linear in the range $4 \leq T \leq 150$ K and no deviation is observed. In Figure 4.8(b), although a least square fitted line is drawn, there appears to be a deviation from linearity at temperatures lower than 20 K reflecting the zero point motion of Sn(IV) atoms. Hence, the lattice vibrations of the tin(II) atoms in the temperature range, $4K \leq T \leq 150$ K and tin(IV) atoms in the range, $20K \leq T \leq 150$ K are in agreement with the Debye model of solids at higher temperatures. The gradient of this plot is a useful guide to the lattice structure. The more tightly bound are the tin atoms, the more gentle the slope. The temperature coefficients (gradients) of the Sn(II) and Sn(IV) atoms are 1.76×10^{-2} and 1.66×10^{-2} K^{-1} respectively. These values can be compared with those reported for a number of organotin compounds of known structures.[135] The compounds which have lattices consisting of non-interacting monomeric molecules have temperature coefficients of $\sim 1.8 \times 10^{-2}$ K^{-1} irrespective of coordination number. Strongly hydrogen bonded lattices exhibit temperature coefficients of $\sim 1.0 \times 10^{-2}$ and tightly packed ionic lattices such as tin(II) oxide, exhibit values as low as 0.23×10^{-2} K^{-1}. The values for the two types of tin atoms in the mixed valence o-nitrobenzoate prepared by Harrison et al.[26] are 1.71×10^{-2} for the Sn(II) atoms and 1.30×10^{-2} K^{-1} for the Sn(IV) atoms. The values obtained for the compound under discussion in this thesis are consistent with the monomeric nature of the structure with the Sn(IV) atoms being slightly more tightly

bound than the Sn(II) atoms in the lattice.

The relative areas of the Sn(II) and Sn(IV) resonances should reflect the relative numbers of such nuclei. It is clear that the relative areas are not the 4:1 expected from the crystallographic results. The temperature dependent study shows that the ratio varies from 2.32 at 150 K to 2.98 at 4 K (Table 4.8). The ratio never reaches the expected value of 4 even by 4 K, indicating that even at this temperature the tin sites are still "rather soft". This is clear from Figure 4.8(a) which demonstrates that the Sn(II) atoms are far from their zero point vibrational state even at 4 K.

4.5.3 Vibrational Data

Table 4.9 contains a summary of the I.R. and Raman data for both $Sn(CO_2CF_3)_2$ and $Sn(IV)Sn(II)_4O_2(CO_2CF_3)_8$. No vibrational bands were detected at frequencies higher than $\sim$ 1780 cm^{-1} confirming that free trifluoroacetic acid is not present in either of these materials. There is little difference in the spectra of the two compounds in the range 1780 - 1100 cm^{-1} with the bands at $\sim$ 1700 cm^{-1} to $\sim$ 1400 cm^{-1} being associated with $\nu_{sym}(OCO)$ and $\nu_{asym}(OCO)$ while in the range 1200-1100 cm^{-1} bands arising from vibrations due to $-CF_3$ groups were found. In the regions below 1100 cm^{-1}, the spectra from the mixed oxidation state compound are more complex than those for the tin(II) trifluoroacetate. Tentative assignments have been made in Table 4.9.

Decon et al.[136] have pointed out the difficulties in deciding between the presence of unidentate, bridging or chelating carboxylates. They conclude that when $\nu_{asym}(OCO)$ is at higher frequency and when $\nu_{sym}(OCO)$ is at a lower frequency than in the ionic carboxylates, one can infer the

TABLE 4.9

Vibrational Spectroscopic Data of $Sn(II)(O_2CCF_3)_2$ and $[Sn(IV)Sn_4(II)O_2(O_2CCF_3)_8]$

$Sn(II)(O_2CCF_3)_2$		$Sn(IV)Sn_4(II)O_2(O_2CCF_3)_8$		
IR*	Raman+	IR*	Raman+	Assignment
		1776(w)		
1710(s)		1700(m)		
1690(s)	1696(22)	1660(m)	1660(43)	$\nu_{asym}(CO_2)$
1645(s)		1610(s)	1625(55)	
1465(m)	1456(23)	1450(w)	1450(100)	$\nu_{sym}(CO_2)$
1410(m)	1418(43)	1430(m)	1430(29)	
1225(s,b)		1224(m)	1200(12)	
1200(s,b)		1189(s)	1182(15)	$\nu(CF_3,CF_2)$
1170(s,b)		1154(m)	1118(3)	
1039(w)				
970(w)				
850(m)	853(100)	854(w)	850(34)	$\delta(CO_2),\nu(C-C)$
	816(24)	794(m)	845(63)	
	814(18)			
780(m)				
720(s)	730(2)	724(s)	728(2)	$\nu(Sn-O-Sn)$
680(m)			718(2)	
620(sh)	636(13)		610(4)	$\nu(CO_2)$
600(m)		604(m)	600(4)	$\pi(OCO)$
590(sh)				
	236(19)		290(32)	
	204(76)		271(12)	$\nu(Sn-O)$
	170(2)		205(11)	
	160(5)		150(13)	$\delta(OSnO)$

* Abbreviations:- s = strong, sh = shoulder, m = medium, w = weak, b = broad.

\+ Relative intensities are given in parentheses.

presence of unidentate carboxylate. In the case of the mixed valence compound, more than one strong band is observed for the symmetric and antisymmetric stretches of the -OCO group. This is in agreement with the structural analysis (Figure 4.4) which clearly shows two kinds of carboxylates. The difference (Δ) between the values of $\nu_{asym}(OCO)$ and $\nu_{sym}(OCO)$ for $Sn(II)_4Sn(IV)O_2(O_2CCF_3)_8$ in fact are mostly lower than the corresponding values for the alkali metal trifluoroacetates (for NaO_2CCF_3; $\nu_{asym}(OCO)$ 1680, $\nu_{sym}(OCO)$ 1457 cm^{-1}, Δ(ionic)= 223 cm^{-1}). Also, more than one C-C vibration is observed in the region 800-950 cm^{-1} indicating the presence of more than one carboxylate ligand. This band can be assigned confidently since the ν(C-C) stretch occurs as an intense band in the Raman spectrum.

For $Sn(CO_2CF_3)_2$, the difference (Δ) between $\nu_{asym}(OCO)$ and $\nu_{sym}(OCO)$ is mostly lower than Δ(ionic). This indicates the presence of bridging and/or chelating carboxylate groups. Note that tin(II)formate has symmetrical as well as asymmetrically bridging formate ligands showing multiplicity in its ν_{asym} and ν_{sym} bands.[101]

CHAPTER 5

REACTIONS OF STANNOUS FLUORIDE WITH TIN(IV) CARBOXYLATES

5.1 Introduction

It is known that tin(II) fluoride exists in three different phases. The common stable phase is α-SnF_2. It is known that the α form transforms into the β and γ phases at higher temperatures. A variety of methods have been used to study these phases and the transformations they undergo. For example, Mössbauer spectroscopic studies have been carried out on all three phases.[137] In addition, crystallographic data are available for all three phases.[129,138] It was shown that the most stable phase, α-SnF_2, exists in the form of cyclic tetramers Sn_4F_8, which contain two different tin(II) atoms having coordination of the type SnF_3E and SnF_5E respectively, where E represents the lone pair.[130] It is well established that tin(II) fluoride can accept as well donate fluoride ions. For example, SnF_2 accepts fluoride ions to form trifluorostannate(II) SnF_3^-, and pentafluorodistannate(II) $Sn_2F_5^-$, ions in aqueous solution.[28] The crystal structure of $NaSn_2F_5$ has been determined and it consists of an infinite chain of $[Sn_2F_5]$ units where each unit may be considered as two SnF_3 units sharing a fluorine atom.[139] The i.r. and Mössbauer studies on the SnF_2-MF_2 systems (where, M = Mg, Ca, Sr, Ba, Pb) are consistent with the presence of SnF_3^- ions.[140] The X-ray crystal structure of $[NH_4][SnF_3]$[142] consists of infinite chains of $(SnF_4)^{2-}$ pyramids connected at the corners. Solutions of SnF_2-MF-H_2O systems have been recently studied by ^{19}F, ^{119}Sn NMR and frozen solution Mössbauer spectroscopy.[143] These results

indicate that a rapid exchange of F^- ions occurs between hydrated SnF_2 and the dominant species present, SnF_3^-.

It has been shown by Birchall et al.[27] that SnF_2 can also act as a fluoride ion donor similar to lead difluoride in the adduct $PbF_2 \cdot SnF_2$, which was thought to have the ionic structure $(PbF)^+(SnF_3)^-$.[140] The reaction between SnF_2 and strong Lewis acids such as BF_3, AsF_5, and SbF_5 gave $SnF_2 \cdot BF_3$, $SnF_2 \cdot AsF_5$, $SnF_2 \cdot SbF_5$ and $SnF_2 \cdot 2SbF_5$. On the basis of their vibrational and ^{119}Sn Mössbauer spectra, the 1:1 adducts were formulated as salts of the fluorine bridged $[(Sn-F)_n]^{n+}$ cation with the appropriate counter anion BF_4^-, SbF_6^- or AsF_6^-. The 1:2 adduct was reported as $Sn(SbF_6)_2$.[27] Later, a crystal structure of the adduct $SnF_2 \cdot AsF_5$ was shown to be $[(SnF)_3^{3+}(AsF_6)_3^{3-}]$ and consists of discrete cations having a six membered ring consisting of alternating tin and fluorine atoms.[144] The very high Mössbauer isomer shift and non-resolvable quadrupole splitting of $Sn(SbF_6)_2$ indicates a stereochemically inactive non-bonding electron pair and a symmetric tin environment.[27] Recently, Edwards et al.[145] have synthesized and X-ray crystallographically determined the structure of $Sn(SbF_6)_2 \cdot 2AsF_3$ which exhibits the highest ^{119}Sn Mössbauer isomer shift yet recorded. It was found that the decomposition of $SnF_2 \cdot AsF_5$ and the direct reaction of two moles of SnF_2 with one mole of AsF_5 produces the white compound $2SnF_2 \cdot AsF_5$. This was formulated as $[Sn_2F_3]^+[AsF_6]^-$.[146] The crystal structure determination of $(Sn_2F_3)(BF_4)$ shows the presence of the $[Sn_2F_3]^+$ cation as the base unit of a polymeric chain.[147] In addition, the structure of Sn_2ClF_3 consists of an infinite three dimensional cationic network $(Sn_2F_3)_n^{n+}$ with the chlorine atoms occupying holes in the structure.[148]

Yeh and Geanangel[107] have reported ^{119}Sn NMR data for tin(II) halides in donor solvents. They observed single lines with no coupling patterns. Their chemical shifts were markedly dependent on solvent, concentration and temperature. Recently, ^{19}F and ^{119}Sn NMR spectroscopy has been used to study the SnF_2-MF-H_2O ($M = Li^+, Na^+, K^+, Cs^+, NH_4^+$) system.[143]

Earlier, ^{19}F NMR had been used to characterize cis and trans isomers of tin(IV) fluoro compounds in solution. Dean and Evans[149] have reported ^{19}F NMR spectra for about 100 species of the type $[SnF_{6-n}X_n]^{2-}$ in solution, where X is a unidentate ligand. In addition, ^{19}F NMR of polymeric fluoroanions $(Sn_2F_{11})^{3-}$ and $(Sn_2F_{10})^{2-}$ have been reported.[150] Tin-119 NMR spectra of fifteen compounds of the type $SnCl_xBr_yI_z$ ($x+y+Z = 4$) and ten isomers of the type $[SnCl_xBr_{6-x}]^{2-}$ were observed.[151] In addition, several chlorofluorostannates $[SnCl_nF_{6-n}]^{2-}$ have been identified in solution by means of ^{119}Sn NMR spectroscopy.[152] The Sn-F coupling constants in these compounds were found to be in the range 1500-2400 Hz.

The oxidation of stannous fluoride in HF yields a mixed valence tin fluoride Sn_3F_8. The crystal structure of this compound shows it to contain trans fluorine bridged $Sn(IV)F_6$ units linked to polymeric Sn(II)F chains.[23] The solvolysis of hexaphenylditin by CF_3SO_3H produced a mixed valence tin compound with empirical formula $Sn(SO_3CF_3)_3$.[7] The analytical data and Mössbauer parameters of this compound agree with that of the compound isolated from the solvolysis of tetravinyltin by CF_3SO_3H.[25] Since the tin(II) site of this compound exhibits a high Mössbauer isomer shift with a small quadrupole splitting, it has been formulated as $[Sn]^{2+}$-

$[Sn(SO_3CF_3)_6]^{2-}$. This compound was reacted with stannous fluoride. Since strong Lewis acids such as SbF_5 abstract both fluorines from SnF_2, it was expected that in the reaction of SnF_2 with $[Sn]^{2+}[Sn(SO_3CF_3)_6]^{2-}$ at least one fluorine would be transferred from SnF_2 to the tin(II) site of $Sn_2(SO_3CF_3)_6$ to give $[Sn(II)F]_2^{2+}[Sn(SO_3CF_3)_6]^{2-}$. On the basis of the Mössbauer spectrum this clearly did not happen, but the two fluorines were transferred to tin(IV) rather than to tin(II). This indicates that tin(IV) has a higher affinity for fluorines compared to tin(II). Therefore, this led to an investigation of the reaction of SnF_2 with tin tetracarboxylates in order to explore the possibility of preparing new mixed valence tin compounds. By analogy to the above reaction one might expect the fluorines to be transferred to the tin(IV) atom to form an adduct of the type $[Sn^{2+}][F_2Sn(OCOR)_4^{2-}]$.

5.2 NMR Data

5.2.1 NMR Data of SnF_2 with $Sn(CO_2R)_4$

An equimolar mixture of SnF_2 and $Sn(CO_2CF_3)_4$ gives a clear solution in CF_3CO_2H. It should be noted that while $Sn(CO_2CF_3)_4$ is soluble in CF_3CO_2H, SnF_2 is insoluble. The formation of a clear solution therefore suggests that a reaction between these two compounds might have occured. The solution was filtered to remove small impurity particles and then the acid was removed under vacuum to leave a white crystalline material. Some of this solid was dissolved in CF_3CO_2H for NMR studies which were carried out over a temperature range from ambient to -20°C. Since CF_3CO_2H freezes at -17°C, studies at temperatures much lower than this could not be carried out using the above solution. Therefore, into the above

solution, an equal volume of liquid SO_2 was distilled and the resultant solution was then used to obtain NMR spectra at temperatures as low as -50°C. Tin-119 and ^{19}F NMR data from these solutions are given in Table 5.1. The ambient temperature ^{119}Sn NMR spectrum exhibited a triplet centred around -805 ppm. When the lower frequency region was scanned, a broad signal was observed at -1374 ppm (Figure 5.1). The CF_3CO_2H/SO_2 solution was cooled to -48°C and the ^{119}Sn NMR spectrum showed a triplet similar to the one obtained at ambient temperature but resonating 5 ppm to higher frequency (Figure 5.2). In addition, satellite peaks were observed about each line of the triplet. The broad signal observed at ambient temperature was now shifted to lower frequency by 75 ppm and in addition was split into a triplet (Figure 5.2). Satellite peaks were also observed about each line of this triplet with a separation of 265 Hz. These satellites are attributed to tin-tin coupling.

Tin-119 spectra recorded on the above solutions after a few weeks had passed, showed a large reduction in the intensity of the triplet at ~ -800 ppm which had been replaced by an intense doublet. At the same time in the low frequency region at low temperature, a triplet was observed with relatively low intensity and a broad line in the same region of the spectrum (Figure 5.3). It is apparent from the above observation that the species initially formed undergoes decomposition with time at room temperature.

A ^{19}F NMR spectrum was recorded only on the solution obtained by dissolving the product in CF_3CO_2H. This spectrum was recorded after a few weeks and it exhibited two single lines at -99.0 and -91.9 ppm with satellite peaks due to fluorine coupled to ^{117}Sn and ^{119}Sn isotopes

TABLE 5.1

NMR Data for Mixtures of SnF_2 and $Sn(CO_2R)_4$

1. $SnF_2/Sn(CO_2CF_3)_4$ in CF_3COOH/SO_2

	Temp.(°C)	$\delta(^{119}Sn)$† ppm	$\Delta W_{\frac{1}{2}}$ (Hz)	$^1J_{(^{119}SnF)}$ (Hz)	$^2J_{(^{119}Sn\text{-}F\text{-}^{117/119}Sn)}$ (Hz)
After 24 hrs.	Amb.	- 805(t)	75	2106(5)	
		-1374(b)	930		
	- 48°C	- 800(t)	90	2118(6)	262(2)^{S1}
		-1428(t)	90	1128(4)	265(5)^{S2}
After 2 months	- 53°C	- 799(t)	120	2100(10)	
		-1425(t)		1150(10)	
		- 792(d)	80	2210(10)	
		-1351(b)	560		

2. $SnF_2/Sn(CO_2CF_3)_4$ in CF_3COOH

	Temp.	$\delta(^{119}Sn)$†	$\Delta W_{\frac{1}{2}}$	$\delta(^{19}F)$	$\Delta W_{\frac{1}{2}}$	$^1J_{(^{117}SnF)}$	$^1J_{(^{119}SnF)}$
After 2 weeks	Amb.	- 805(t)	112				2124(5)
		-1339(b)	5250	- 99.0	92		2100(5)
		- 799(d)	100	- 91.9	123	2111(3)	2207(3)
		?					
	- 20°C	- 780(t)	100				2138(4)
		-1317(b)	440	- 99.2	248		2069(10)
		- 773(d)	65				
		?		- 93.8	42	2135(3)	2227(3)

3. $SnF_2/Sn(CO_2C_3F_7)_4$

	Temp.	$\delta(^{119}Sn)$†	$\Delta W_{\frac{1}{2}}$	$^1J_{(^{119}SnF)}$	$^2J_{(^{119}Sn\text{-}F\text{-}^{117.119}Sn)}$
(i) After 2 months	Amb.	- 811(t)	138	2160(10)	
		-1453(b)	2150		
	- 23°C	- 809(t)	71	2170(7)	331(5)^{S3}
		-1461(t)	195	635(5)	326(10)^{S4}
(ii) After 5 months	Amb.	- 811(t)	66	2154(10)	
		?			
		- 803(d)	98	2284(5)	
		?			

Continued.....

TABLE 5.1 (Continued)

4.	$SnF_2/Sn(CO_2CHCl_2)_4$ in $CHCl_2COOH$	Amb.	- 808(t) ? v. broad	430	2155(5)
	$SnF_2/Sn(CO_2CHCl_2)_4$ in $CHCl_2COOH/SO_2$	-30°C.	- 801(t) - 1363(b)	67 2950	2158(5)

* Width measured at half height of signals recorded at a field strength of 5.872T.

† Signals due to decomposition product

‡ Abbreviations in parentheses: b = broad, d = doublet, s = singlet, t = triplet.

§ Intensity ratio of the satellite signal to the main signal is (1) 0.21 (2) 0.26 (3) 0.25 (4) 0.30

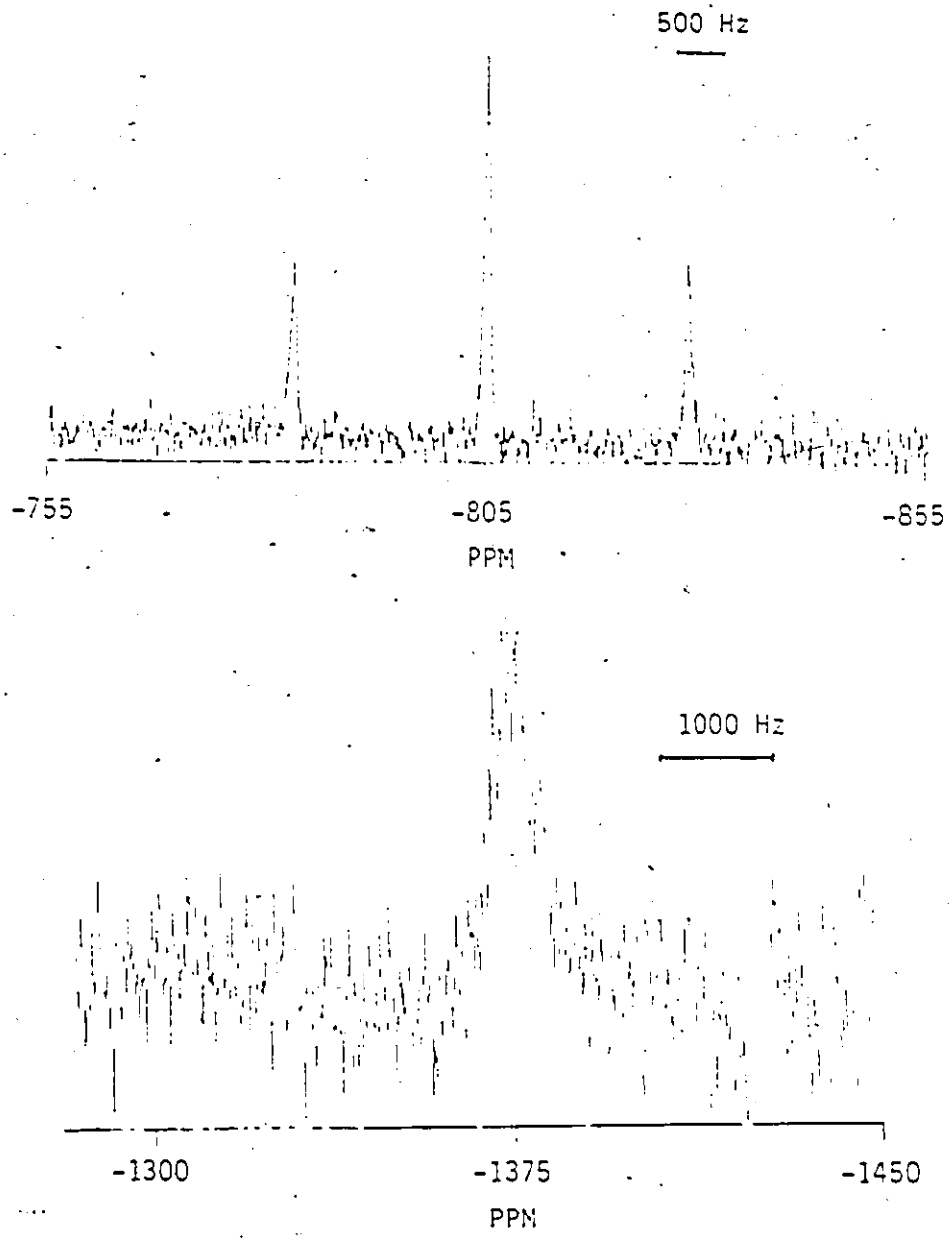

Figure 5.1: ^{119}Sn NMR spectra of $SnF_2/Sn(CO_2CF_3)_4$ mixture in a mixture of solvents CF_3CO_2H and SO_2 at 24°C. The above spectra were recorded at two different chemical shift ranges.

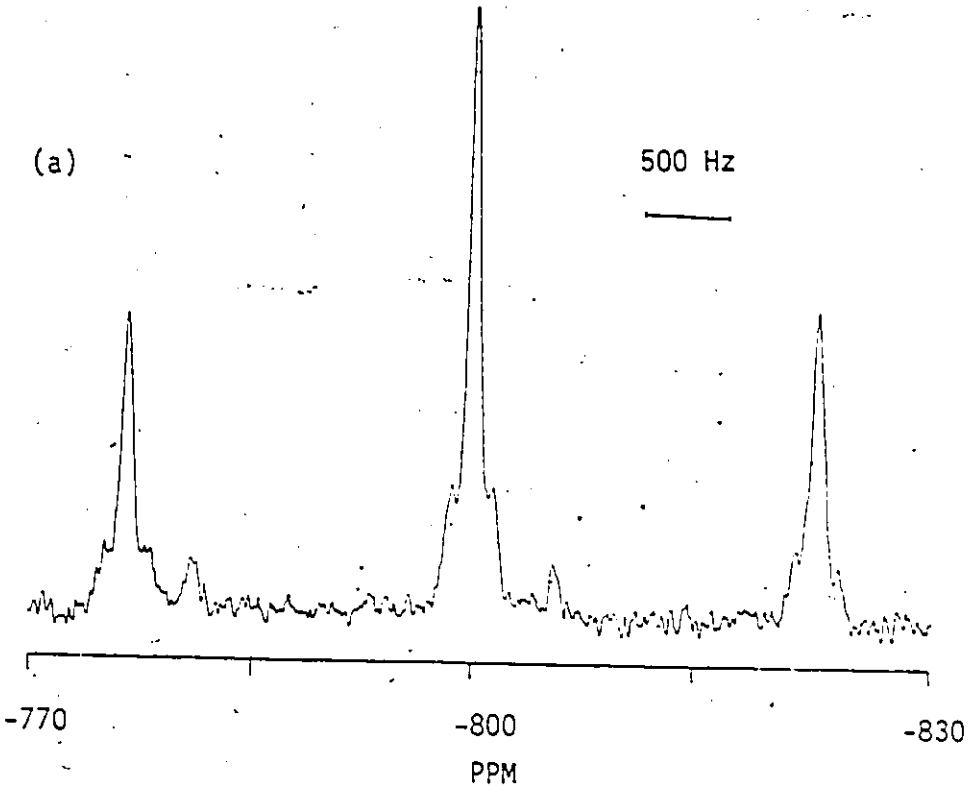

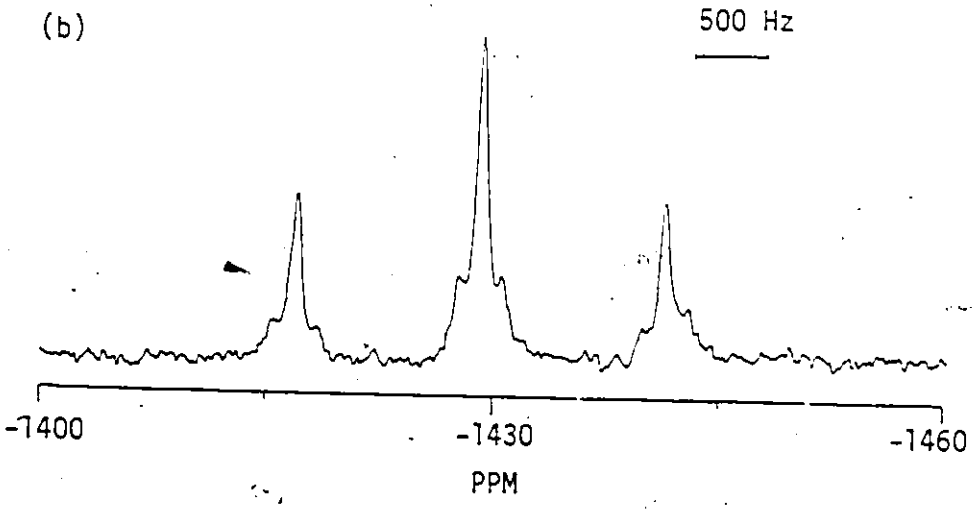

Figure 5.2: ^{119}Sn NMR spectra of $SnF_2/Sn(CO_2CF_3)_4$ mixture in CF_3CO_2H/SO_2 at -48°C. The above spectra were recorded at two different chemical shift ranges.

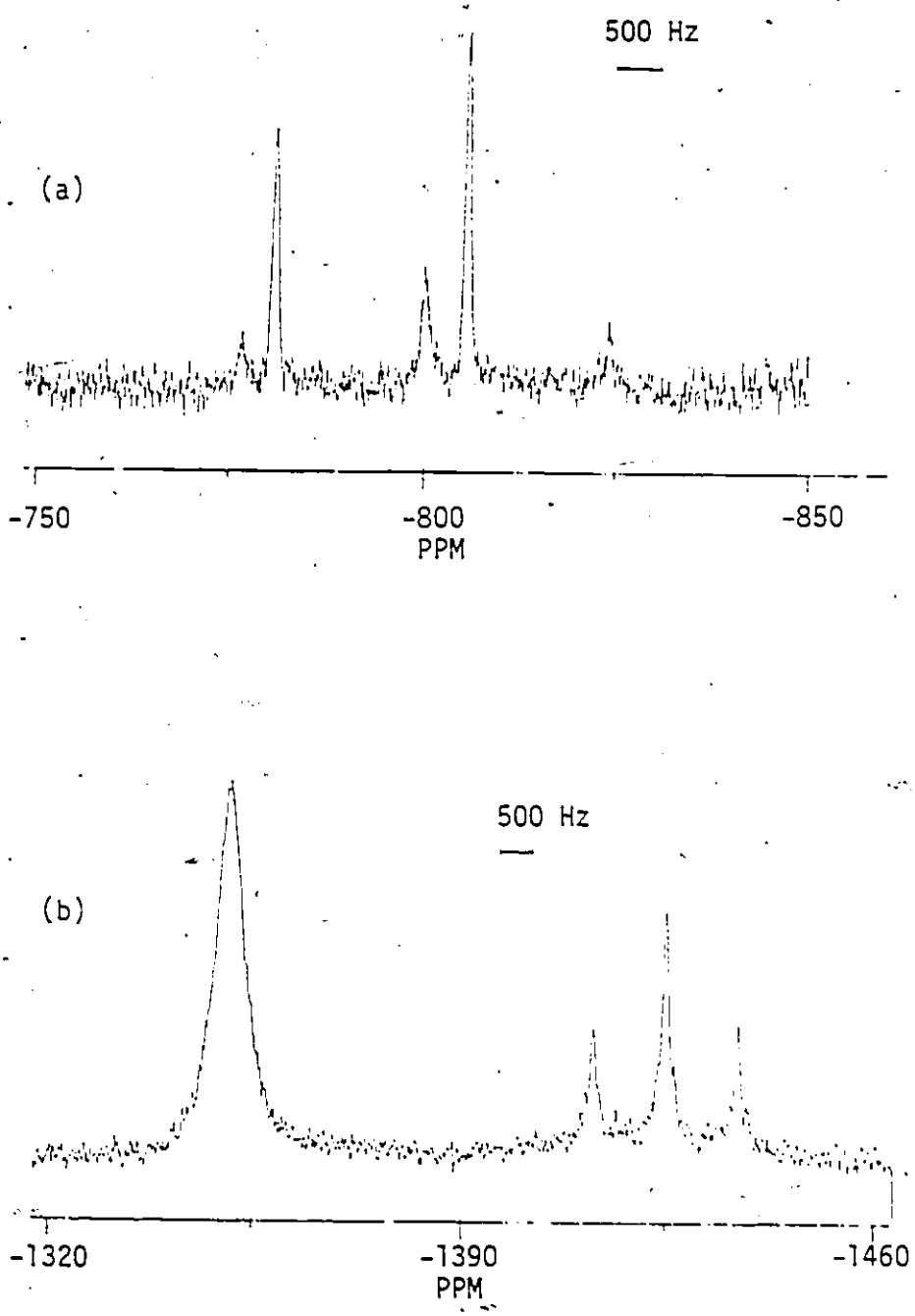

Figure 5.3: ^{119}Sn NMR spectra of $SnF_2/Sn(CO_2CF_3)_4$ mixture in CF_3CO_2H/SO_2 after 2 months at -53°C. The above spectra were recorded at two different chemical shift ranges.

(Figure 5.4(a)). The separation of the satellite peaks associated with signals at -99.0 ppm is equal to the coupling observed in the triplet signal in the ^{119}Sn spectrum at -805 ppm. The satellites of the signal at -91.0 ppm correspond to the doublet observed in the ^{119}Sn spectrum at -799 ppm due to the decomposition. On cooling this solution to -15°C, one signal broadened whereas the other signal became sharper (Figure 5.4(b)).

The reaction between SnF_2 and $Sn(CO_2C_3F_7)_4$ in $C_3F_7CO_2H$ yields a dark red coloured solution. Since it was not possible to isolate $Sn(CO_2C_3F_7)_4$ as a pure compound in reasonable amounts, this reaction was carried out by the addition of SnF_2 to $Sn(CO_2C_3F_7)_4$ in $C_3F_7CO_2H$. The ^{119}Sn NMR spectrum of the above solution gave a triplet centred at -811 ppm. In the low frequency region a broad signal was observed around -1453 ppm (Figure 5.5). On cooling at -23°C, the ^{119}Sn spectrum showed the same triplet, which was shifted by only 2 ppm. In addition, satellite peaks were observed due to the tin-tin coupling which were equally spaced around the peaks of the triplet. The low frequency signal was not split into a triplet and the satellite peaks were barely seen on the shoulders of this triplet. The separation of the satellites in the two triplets are the same within experimental error (Figure 5.6). The ^{119}Sn NMR spectrum recorded on this solution after five months showed a small amount of a doublet at -803 ppm with the triplet at -811 ppm. It is apparent that the decomposition of the species giving rise to the triplet signal is much slower in the case of heptafluorobutyrate (Figure 5.7).

The reaction between SnF_2 and $Sn(CO_2CHCl_2)_4$ was carried out by mixing equimolar amounts of reactants in $CHCl_2CO_2H$. $Sn(CO_2CHCl_2)_4$ is

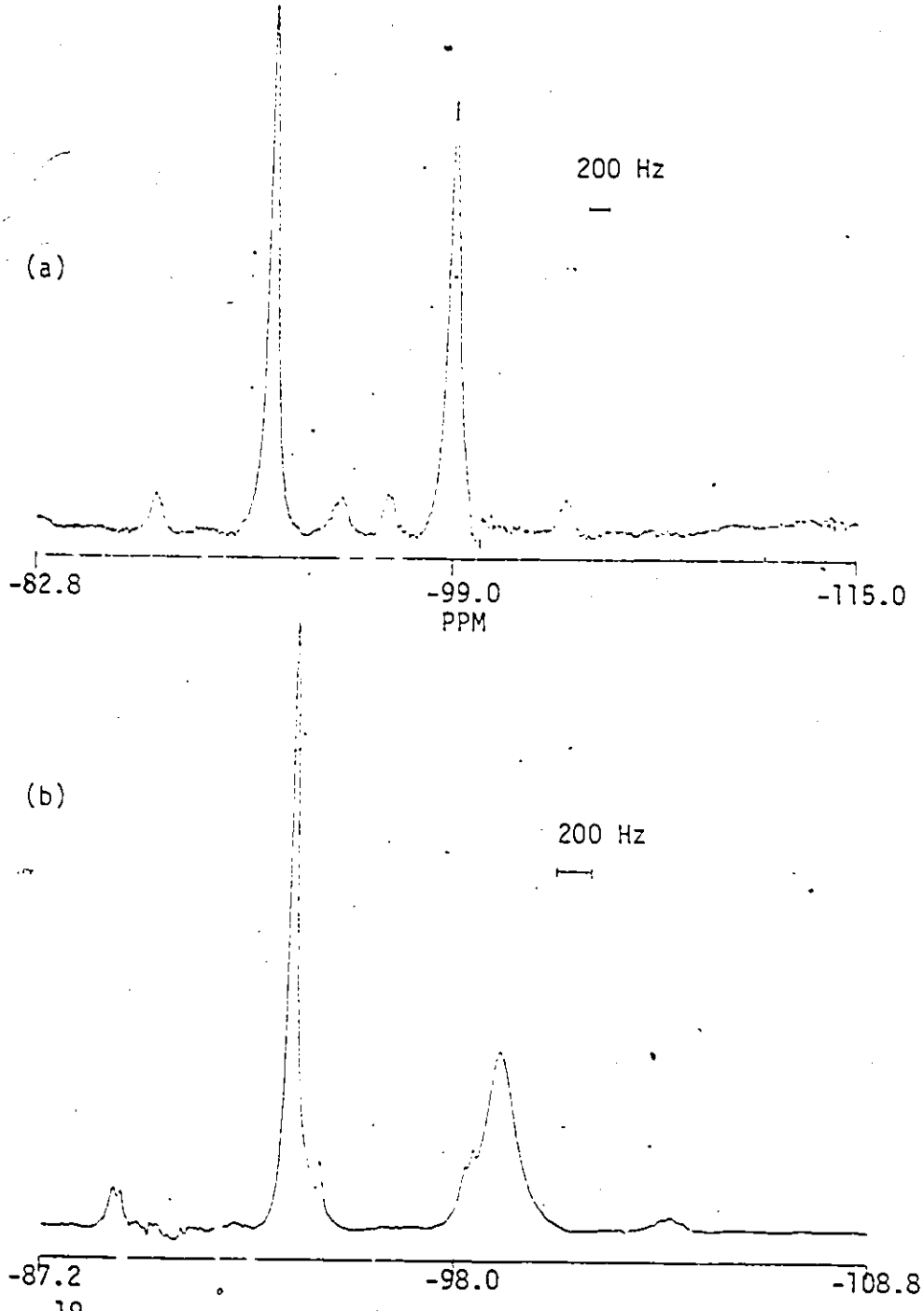

Figure 5.4: ^{19}F NMR spectra of $SnF_2/Sn(CO_2CF_3)_4$ mixture in CF_3CO_2H after two weeks at (a) 24°C (b) -20°C.

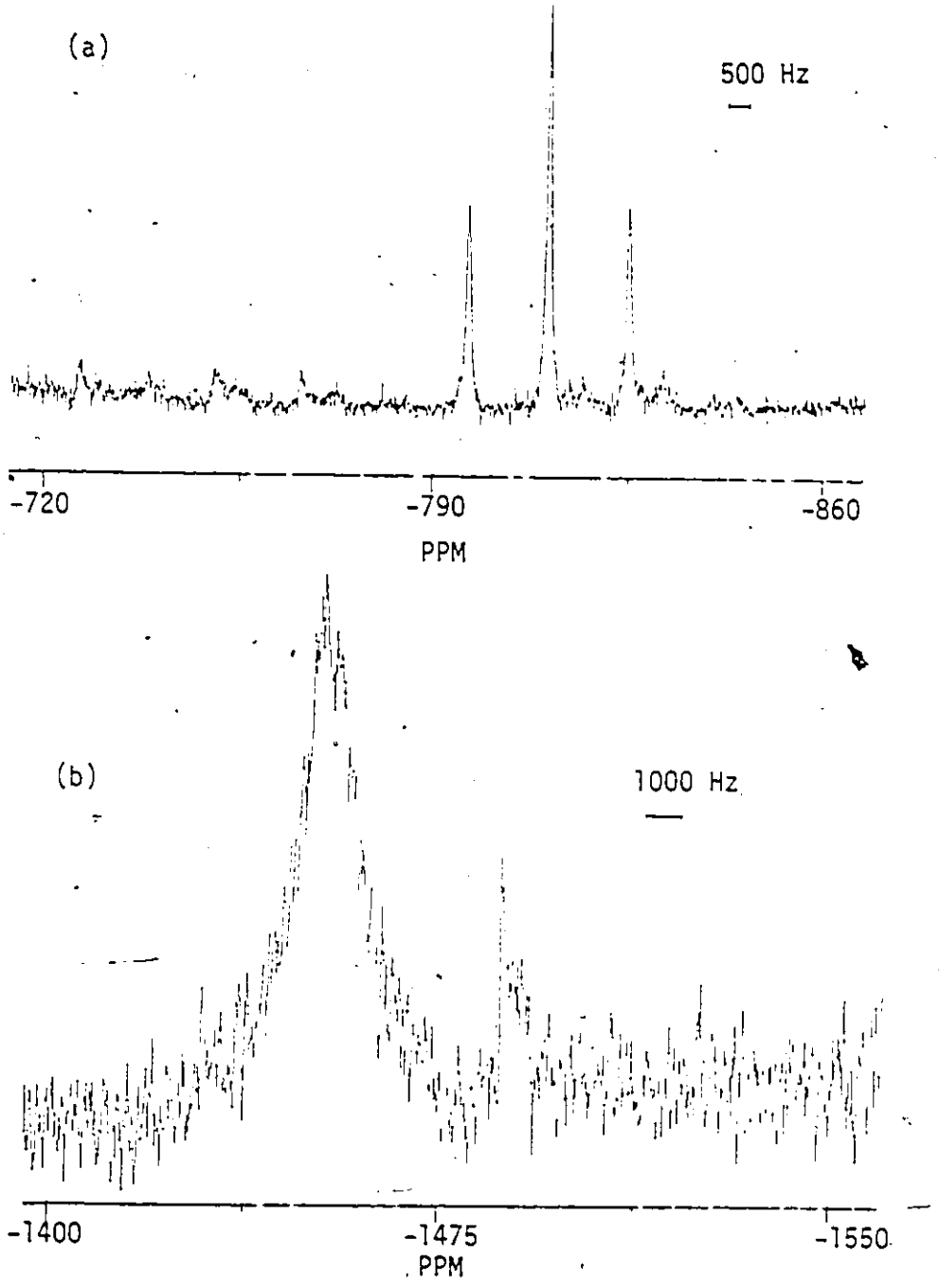

Figure 5.5: ^{119}Sn NMR spectra of $SnF_2/Sn(CO_2C_3F_7)_4$ mixture in C_3F_7COOH at 24°C. The above spectra were recorded at two different chemical shift ranges.

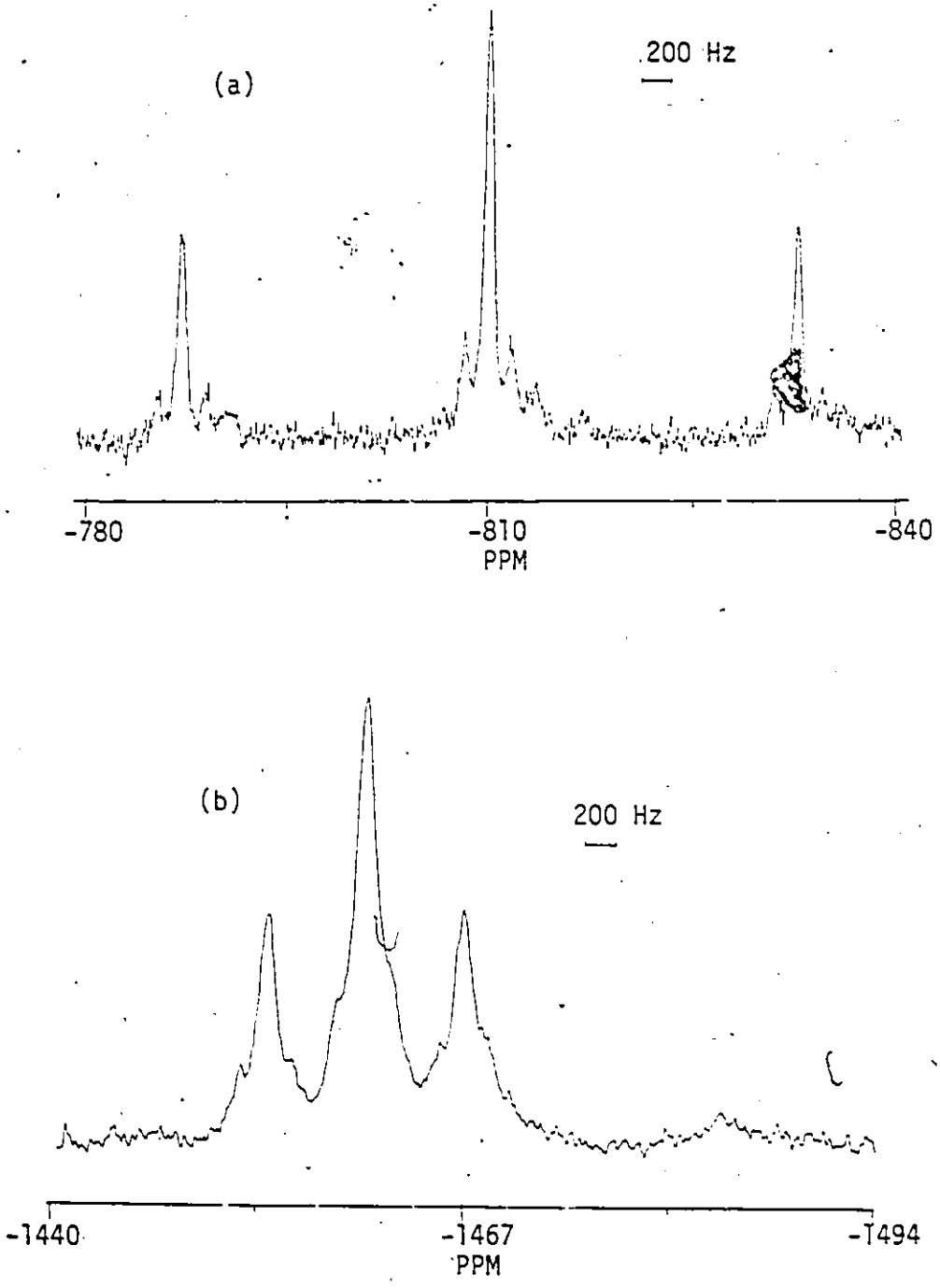

Figure 5.6: ^{119}Sn NMR spectra of $SnF_2/Sn(CO_2C_3F_7)_4$ mixture in C_3F_7COOH at -23°C. The above spectra were recorded at two different chemical shift ranges.

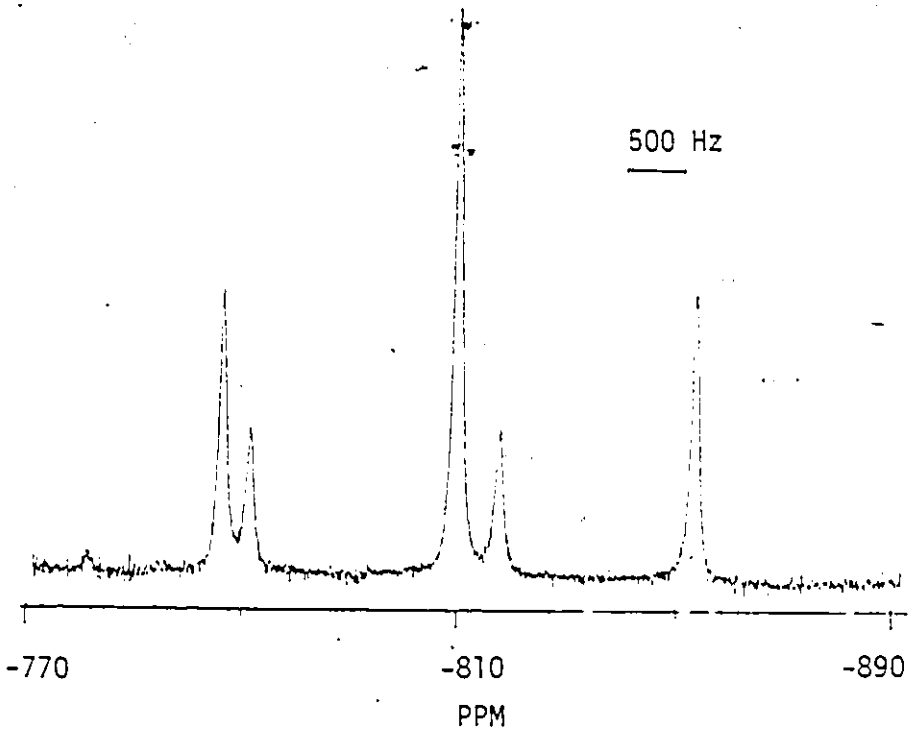

Figure 5.7: ^{119}Sn NMR spectrum of $SnF_2/Sn(CO_2C_3F_7)_4$ mixture in C_3F_7COOH after 5 months at 24°C.

soluble in this acid whereas SnF_2 is insoluble. On stirring the mixture at room temperature, more solid separated out from the reaction medium. The solution was filtered into an NMR tube and used for ambient temperature NMR studies. Tin-119 NMR spectroscopy of this solution showed only a triplet at -808 ppm. When the low frequency region was scanned, no additional signals were apparent. For low temperature work, an equal volume of liquid SO_2 was distilled into the mixture and the resultant solution was reexamined. The ^{119}Sn NMR spectra recorded at -30°C exhibited the same triplet, but with a narrower line width, at -801 ppm. At this temperature in the lower frequency region, a broad signal was now observed around -1363 ppm. Since this solution freezes at temperatures lower than -30°C, it was impossible to record spectra below this temperature.

Solutions of $SnF_2/Sn(CO_2R)_4$ (where R = CF_3, C_3F_7, $CHCl_2$) basically exhibited two sets of signals in the ^{119}Sn NMR spectra (Table 5.1). One appeared around -800 ppm and did not change significantly when the acids were varied. The other set of signals was observed in the range of -1300 ppm to -1460 ppm. The position of this signal varied with the acid ligand as well as with temperature. At this stage, it is worth comparing the previous ^{119}Sn NMR data of tin(II) and tin(IV) carboxylates given in Table 4.1. This shows that tin(IV) compounds appear in a narrow range -800 to -850 ppm, whereas tin(II) compounds cover a wide range and mostly appear in the lower frequency region. On this basis, the signals observed in this experiment can be assigned. The peaks around -800 ppm are most likely due to tin(IV) species and the lower frequency signals are probably due to tin(II) species.

Tin-119 NMR chemical shifts of a series of chlorofluorostannate(IV) $[SnCl_nF_{6-n}]^{2-}$ have been reported.[152] These values range from -810 ppm for SnF_6^{2-} and steadily become less negative on substitution of Cl by F atoms. The tin(IV) resonances of the solutions studied here occur in the same range. The one bond Sn-F coupling constants $[^1J_{Sn-F}]$ for the series $[SnCl_nF_{6-n}]^{2-}$ range from 1580 Hz to 2430 Hz. When comparing $^1J_{Sn-F}$ for the cis and trans isomers of $[SnCl_4F_2]^{2-}$, the trans isomer shows a larger coupling and, from the intensity of the ^{119}Sn NMR signals, it was suggested that the cis configuration might be more stable than the trans arrangement. Dean[149] has reported the ^{19}F NMR spectra of a number of tin(IV) fluoro compounds. This includes a series of anions of general formula $[Sn(CO_2R)_2F_4]^{2-}$ and $[Sn(CO_2R)F_5]^{2-}$ with a variety of R- groups. The $^1J_{Sn-F}$ of these anions are in the range 1700 Hz to 1870 Hz. The coupling constants of the tin(IV) signals in the $SnF_2/Sn(CO_2R)_4$ solutions reported in Table 5.1 fall in the range 2100 - 2300 Hz. This clearly shows that the observed splitting arises through direct tin(IV)-fluorine coupling.

There are only a few reports available on ^{119}Sn NMR studies of tin(II) fluoro compounds. The ^{119}Sn NMR chemical shifts of SnF_2 in donor solvents such as HMPA and DMSO varies between -600 ppm and -650 ppm.[107] The ^{119}Sn NMR spectrum of SnF_2-MF-H_2O system exhibit broad lines over a range -700 to -800 ppm.[143] No coupling of fluorine to tin was observed in the above systems. The tin(II) signals of the $SnF_2/Sn(CO_2R)_4$ systems appear at lower frequency than those of SnF_2 and $Sn(CO_2R)_2$ (where R = CF_3, C_3F_7, $CHCl_2$). There are no tin(II)-fluorine coupling constant values reported yet in the literature. The tin(II) resonances in the $SnF_2/Sn(CO_2R)_4$ solutions are also spin coupled to two fluorines. The

magnitudes of these Sn(II)-F couplings are quite different and appear to depend on the nature of R- group (1150 Hz for R = CF_3; 635 Hz for R = C_3F_7). These may not be the limiting spectra and the couplings could change if spectra could be obtained at lower temperatures.

The low temperature ^{119}Sn spectra of the two solutions $SnF_2/Sn(CO_2R)_4$ (where R = CF_3, C_3F_7) show satellite peaks due to tin-tin coupling in both the tin(II) and tin(IV) resonances. Since the separation of satellites in the tin(II) and tin(IV) signals are equal, it can be said that tin(II) and tin(IV) are coupled together. There are a number of direct tin-tin couplings reported for organoditin compounds. These values range from ~ 4000 Hz (for R_6Sn_2)[153] to 15,000 Hz [for $Me_4Sn_2(OAc)_2$].[154] There are quite a few two bond tin-tin couplings reported through different elements. For example, $^2J_{Sn-C-Sn}$ is in the range 275 Hz to 325 Hz for the compounds $(Me_2Sn)_2CRR'$ (where R,R' are alkyl groups).[155] In compounds of the type $R_6Sn_3X_n$ (X = S, Se, Te; n = 2,3) where Sn atoms are part of the ring system, $^2J_{Sn-X-Sn}$ is in the range 155-250 Hz,[156] while in hexaorganodistannoxanes $[(R_3Sn)_2O]$, $^2J_{Sn-O-Sn}$ is in the range 400 to 600 Hz.[157] When comparing the above literature values with the magnitude of the tin-tin couplings observed in the $SnF_2/Sn(CO_2R)_4$ systems (265 Hz when R = CF_3; 330 Hz when R = C_3F_7), it is clearly seen that these values fall into the second category. Thus the observed satellites are due to two bond tin-tin coupling and it is interesting to note that this coupling is between two different oxidation states of tin. This is the first example of tin-tin coupling observed between two different oxidation states of tin. Furthermore, the intensity of the satellite peaks are approximately 0.23 times the intensity of the main signal. This is consistent with the fact that

a tin(II) or a tin(IV) is magnetically coupled to two tin(IV) or tin(II) respectively as discussed below.

Let us consider that one Sn(IV) nucleus is coupled to two Sn(II) nuclei.

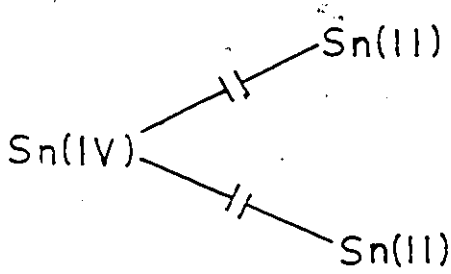

Then, the coupling of the Sn(IV) nucleus with Sn(II) nuclei is controlled only by the Sn(II) isotopomers. Since the difference in ^{119}Sn-^{117}Sn and ^{119}Sn-^{119}Sn coupling constants are small, they were not resolved in the above spectra. Therefore, in this calculation, the intensity of the satellites due to ^{119}Sn-^{117}Sn and ^{119}Sn-^{119}Sn couplings are considered together.

(i) Assume the natural abundance of spin ½ Sn(II) nuclei is P.
i.e., P = Abundance (^{117}Sn) + Abundance (^{119}Sn)

(ii) Abundance of other NMR inactive Sn(II) isotopes is (1-P).
Probability of each isotopomer of $Sn(II)_2$ is as follows.

	Isotopomer		Probability
(a)	None	$Sn(II)_2$	$(1-P)^2$
(b)	One	*Sn(II)Sn(II)	2P(1-P)
(c)	Two	$*Sn(II)_2$	P^2

(iii) The above combinations will exhibit the following spectral patterns and their relative intensities are given below.

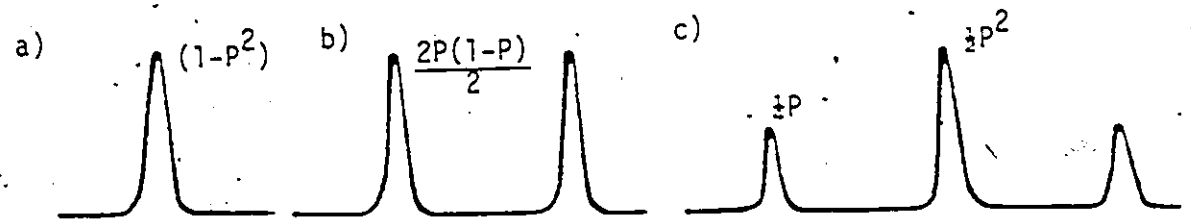

when a), b), and c) are superimposed and the relative intensities can be given below.

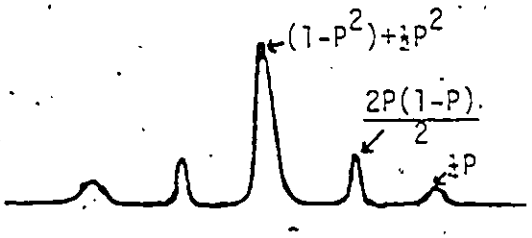

(iv) Therefore, the intensity ratio of the main signal to the satellites is equal to $\dfrac{P(1-P)}{\frac{P^2}{2}+(1-P^2)}$

(v) P = 0.076 + 0.086 (Natural abundance of ^{117}Sn = 7.6%, ^{119}Sn = 8.6%), substituting for P in the above equation,

Intensity Ratio = 0.19

This calculated ratio agrees well with the experimentally observed ratio (~ 0.23), confirming that each Sn(IV) is magnetically coupled to two Sn(II) nuclei and vice versa.

A crystal obtained from the reaction of SnF_2 with $Sn(CO_2CF_3)_4$ was used for X-ray diffraction studies and its structure was determined to be $Sn_4F_4(O_2CCF_3)_8 \cdot 2CF_3CO_2H$. The details of this structure are discussed in the next section. This structure consists of an eight membered ring with Sn(II)-F-Sn(IV) as repeating units (see Figures 5.11, 5.12). Both Sn(II) and Sn(IV) atoms are bonded to two fluorines and each tin atom is bridged to two other tin atoms by fluorine atoms. The low temperature ^{119}Sn NMR data of $SnF_2/Sn(CO_2R)_4$ (R = CF_3, C_3F_7) solutions are consistent with this structure provided that the fluorine atoms bonded to each tin atom are equivalent. In the crystal structure, the fluorines bonded to each tin atom are crystallographically different. In solutions however, they are not significantly different to be observed by NMR. Also, the ^{19}F NMR spectra of the $SnF_2/Sn(CO_2CF_3)_4$ solution exhibits only one signal corresponding to the fluorines of the ring structure.

Tin-119 NMR spectra recorded at ambient temperature do not show tin(II)-fluorine coupling, instead only a broad signal was observed. In the case of the $SnF_2/Sn(CO_2CHCl_2)_4$ solution, the tin(II) signal is so broad that it could not be detected at ambient temperature. The tin(IV)-fluorine coupling is however observed at ambient temperature and on cooling there is no significant change in its magnitude. The chemical shifts of the tin(IV) resonances change by only a few ppm with temperature. The variation in the line width of this signal as the temperature is lowered, depends on the carboxylate ligand and it was increased for the trifluoroacetate and decreased for the heptafluorobutyrate and dichloroacetate compared to their ambient temperature signals. The tin(II) signals showed large variations in their chemical shifts as well as

dramatic changes in their line widths. Since the tin(II) signal resolves into a triplet at lower temperatures, the variations in the $^{1}J_{Sn(II)-F}$ could not be monitored over a wide range of temperature. However, the $SnF_2/Sn(CO_2CF_3)_4$ in CF_3CO_2H/SO_2 solution shows an apparent increase of this coupling constant on cooling from -48°C to -53°C.

These observations show that the tin(II) environment undergoes drastic changes with changing temperature when compared to the tin(IV) resonance. The variation in the chemical shift and the line width of the tin(II) resonances with temperature indicates that an exchange process is occuring. In the case of $SnF_2/Sn(CO_2C_3F_7)_4$, a better quality ^{119}Sn NMR spectrum of the tin(IV) resonance was recorded at ambient temperature with good signal to noise ratio and relatively narrower line width (Figure 5.7). No satellite peaks associated with this signal were visible due to tin(II)-tin(IV) coupling. Therefore, there is no evidence to show the presence of a rigid Sn(IV)-F-Sn(II) unit at ambient temperature in solution. An exchange process involving the breaking and forming of Sn(II)-F bonds could wipe out the tin(II)-fluorine and tin(II)-tin(IV) coupling. Since the linewidth decreased by lowering the temperature, this indicates that this process is towards the slow exchange regime. A comparison of the bond lengths of the Sn(II)-F and Sn(IV)-F bonds in the structure $Sn_4F_4(O_2CCF_3)_8 \cdot 2CF_3CO_2H$ suggests that the Sn(II)-F bonds are weaker than the Sn(IV)-F bonds (Section 5.4). Hence the breaking and reforming of these bonds in this cyclic structure in solution is possible. During this process, the tin(II) atoms can adopt different coordination numbers and the NMR signal observed corresponds to the average tin(II) environment. Since the

tin(IV)-fluorine coupling constants do not change significantly with temperature, the coordination around tin(IV) presumably remains unchanged. However, the variation in the tin(IV) linewidth is due to the effect of the exchange process at tin(II). On cooling to low temperature, the exchange process slows down further and favours the formation of tin(II)-fluorine bonds. This enables one to observe tin(II)-fluorine and tin(II)-tin(IV) couplings at lower temperature.

Decomposition Process

On standing at room temperature, solutions of $SnF_2/Sn(CO_2R)_4$ (where $R = CF_3$, C_3F_7) undergo decomposition. The trifluoroacetate compound undergoes about 50% decomposition within a month to give a doublet in the tin(IV) region and a broad tin(II) signal. No splitting was observed on this tin(II) signal even on cooling. The heptafluorobutyrate showed only relatively small amounts of the doublet in the tin(IV) region even after about five months. The doublets in the tin(IV) region indicate that only one fluorine is attached to tin(IV). There is no evidence for the presence of any fluorines bonded to tin(II).

Fluorine-19 NMR spectra recorded on the $SnF_2/Sn(CO_2CF_3)_4$ solution showed two fluorine signals with their tin satellites (Figure 5.4). One signal corresponds to the initially formed species in which two fluorines are bonded to Sn(IV). The other fluorine signal is due to the decomposed species in which one fluorine is bonded to Sn(IV). One would expect another fluorine signal in the ^{19}F NMR spectrum as a result of the decomposition. When the high frequency region was scanned, a quartet was detected at +13.1 ppm with a coupling of 6 Hz. At this stage the region where $-CF_3$ groups appeared was looked at carefully. There are two

fluorine signals in this region. A broad signal due to the $-CF_3$ group of the CF_3CO_2H was observed at -77.8 ppm. Another relatively sharp signal at -78.2 ppm due to the $-CF_3$ group of $(CF_3CO_2)_2O$ was also observed. On this signal a shoulder was visible, this can be considered as one half of a doublet and the other half being underneath the main signal with a coupling of 6 Hz (see Figure 5.8).

The parameters of this quartet and doublet can be compared with that of trifluoroacetyl fluoride [CF_3-$\overset{O}{\overset{\|}{C}}$-F] in acetonitrile. This shows a doublet for the $-CF_3$ group (δ = -75.6 ppm; J = 6 Hz) and a quartet for the fluorine of the -COF group (δ = -15.0 ppm; J = 6 Hz). The difference in the chemical shifts between the two cases could very well be due to the different solvents employed. This clearly shows the presence of CF_3COF in the decomposed $SnF_2/Sn(CO_2CF_3)_4$ solution. Therefore, one can conclude from the NMR data that the cyclic structure breaks down leaving one fluorine with tin(IV) and the other fluorine goes into solution as fluoride ion. This fluoride ion attacks the carbonyl group of the trifluoroacetic anhydride which was present in solution to give trifluoroacetyl fluoride according to equation (5.1).

$$CF_3\text{-}\overset{O}{\overset{\|}{C}}\text{-}O\text{-}\overset{O}{\overset{\|}{C}}\text{-}CF_3 + F^- \longrightarrow CF_3\text{-}\overset{O}{\overset{\|}{C}}\text{-}F + CF_3\text{-}\overset{O}{\overset{\|}{C}}\text{-}O^- \qquad (5.1)$$

The driving force for the cleavage of the cyclic structure might be the abstraction of fluoride ion by the anhydride group. The tin(II) atom in acid solution would be coordinated by trifluoroacetate groups. However, the tin(II) signal on decomposition appears at -1351 ppm in the ^{119}Sn NMR spectrum which is at lower frequency compared to $Sn(CO_2CF_3)_2$

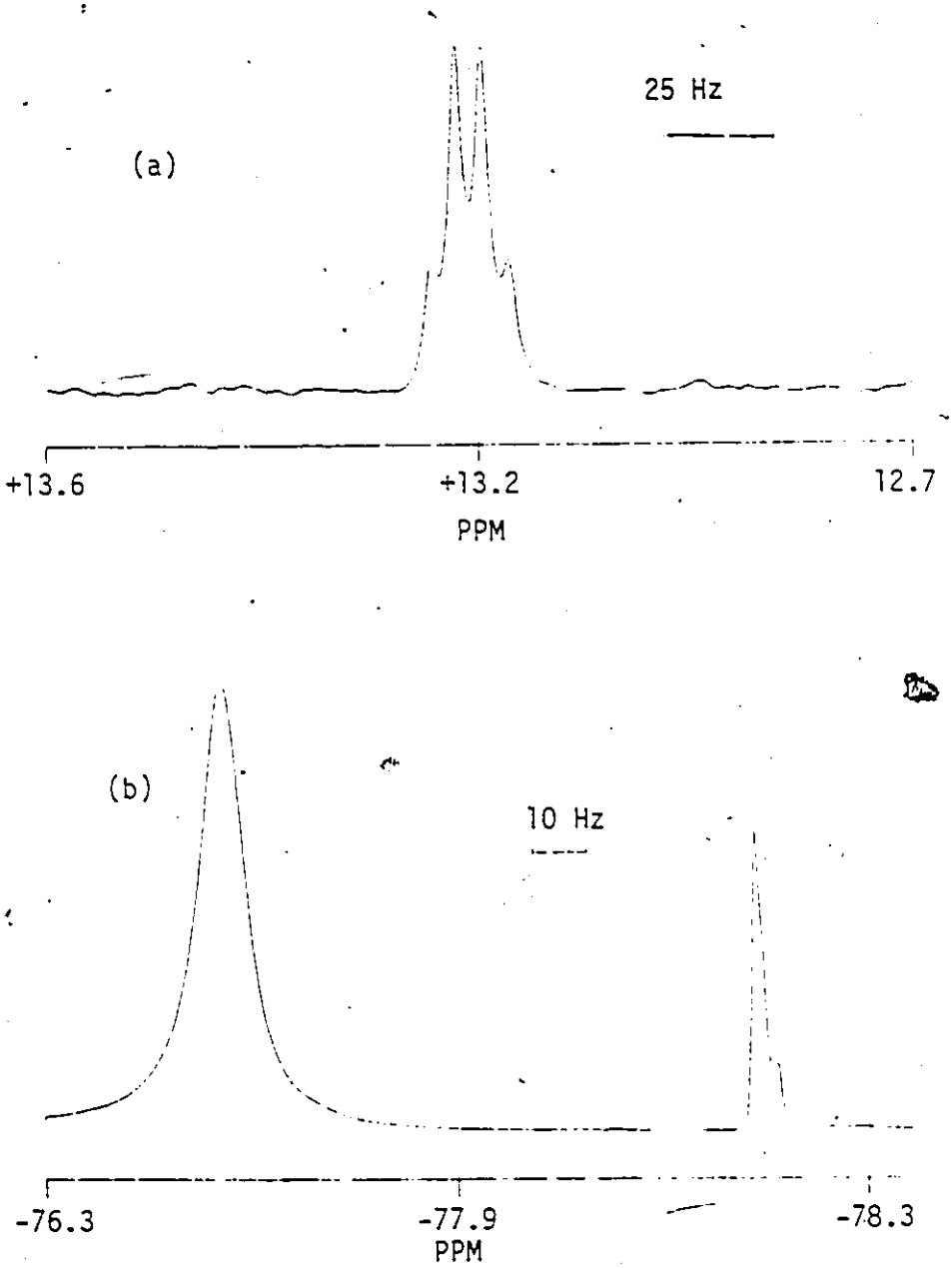

Figure 5.8: ^{19}F NMR spectra of $SnF_2/Sn(CO_2CF_3)_4$ mixture in CF_3CO_2H after 12 months at -23°C. The above spectra were recorded at two different chemical shift ranges (different region from Figure 5.4).

in CF_3CO_2H (-945 ppm). This indicates that the tin(II) in the decomposed species is more shielded than in $Sn(CO_2CF_3)_2$.

5.2.2 NMR Data of the $SnF_2/Sn(SO_3CF_3)_4$ Mixture .

Since the reaction between SnF_2 and tin tetracarboxylates results in a compound having a tetrameric structure with tin(II) and tin(IV) atoms bridged by fluorine, it was interesting to see whether similar structural species could be formed in the reaction between SnF_2 and the strong acid derivatives of tin(IV). Since $Sn(SO_3CF_3)_4$ can be conveniently prepared as a pure compound, the reaction between SnF_2 and $Sn(SO_3CF_3)_4$ was studied first. This was carried out by adding an equimolar amount of SnF_2 to a solution of $Sn(SO_3CF_3)_4$ dissolved in CF_3SO_3H. On stirring, some solid precipitated. The solution was filtered and its ^{119}Sn NMR spectrum was recorded. This exhibited a triplet and a doublet centred around -862 ppm and -855 ppm respectively (Table 5.2). The magnitude of the coupling constants indicated that they were due to direct tin(IV)-fluorine coupling. This showed the presence of two tin(IV) environments with one tin atom bonded to a single fluorine and the other bonded to two fluorines. In addition, in the lower frequency region, a broad signal was observed at -1625 ppm. On cooling this solution to lower temperatures the tin(II) signal broadened further but no tin(II)-fluorine or tin(II)-tin(IV) couplings were visible.

The reaction of $SnCl_2$ with CF_3SO_3H is known to form $Sn(SO_3CF_3)_2$ and HCl.[25] A similar reaction occured when SnF_2 was reacted with CF_3SO_3H; the presence of $Sn(SO_3CF_3)_2$ was confirmed by ^{119}Sn NMR spectroscopy. This reaction would result in the production of fluoride ions in solution which could then react with $Sn(SO_3CF_3)_4$. In order to verify this the ^{119}Sn

TABLE 5.2

NMR Data for Mixtures of SnF_2 and $Sn(SO_3CF_3)_4$

	Temp. (°C)	$\delta(^{119}Sn)$‡ ppm	$\Delta W_{\frac{1}{2}}$* Hz	$^1J_{(SnF)}$ Hz	Area Ratio‡
1. $SnF_2/Sn(SO_3CF_3)_4$ in CF_3SO_3H	Amb.	- 855(t) - 862(d)	55 65	1990(5) 2183(5)	$\frac{A(d)}{A(t)} = 2$
(a) After 10 days		-1625(b)	310		
(b) After 5 months	Amb.	- 863(d) - 871(s) -1580(b)	58 39 266	2155(8)	$\frac{A(d)}{A(s)} = 1.3$
(c) After 16 months	Amb.	- 861(d) - 879(s) ?	74 74	2159(8)	$\frac{A(d)}{A(s)} = 0.6$
	-35	-858(d) -873(s) ?	74 74	2152(8)	$\frac{A(d)}{A(s)} = 0.3$
2. $NaF/Sn(SO_3CF_3)_4$					
(a) After 1 day	Amb.	- 854(t) - 861(d)	47 47	1980(7) 2186(5)	$\frac{A(d)}{A(t)} = 3.0$
(b) After 2 months	Amb.	- 861(d) - 879(s)	34 51	2172(8)	$\frac{A(d)}{A(s)} = 2.5$
	-35	- 858(d) - 873(s)	51 68	2167(8)	$\frac{A(d)}{A(s)} = \sim 1.0$

* Width measured at half height of the signal recorded at a field strength of 5.872T.

‡ Abbreviations in parentheses: b = broad, d = doublet, s = singlet, t = triplet.

NMR spectrum of a solution of NaF in $Sn(SO_3CF_3)_4$ was recorded. This exhibited a doublet and a triplet in the tin(IV) region with the same parameters as that which resulted from the $SnF_2/Sn(SO_3CF_3)_4$ solution. This clearly shows that in both cases the changes around the tin(IV) environments are due to the attack of F^- ions on $Sn(SO_3CF_3)_4$. A ^{119}Sn NMR spectrum of the above two solutions were recorded after these solutions had stood for a few days at room temperature and both solutions then showed the presence of a doublet and a single line. On further standing at room temperature, the doublet intensity decreased and there was a corresponding increase in the singlet intensity (Table 5.2). The chemical shift of this single line agreed with the value for $Sn(SO_3CF_3)_4$ in CF_3SO_3H. The observation of a triplet in the Sn(IV) region and a broad signal in the Sn(II) region of the fresh $SnF_2/-$ $Sn(SO_3CF_3)_4$ solution at ambient temperature was similar to the signals exhibited by the $SnF_2/Sn(CO_2R)_4$ (where R = CF_3, C_3F_7, $CHCl_2$) solutions. Although this tends to suggest the presence of a tetrameric species in the trifluoromethylsulphonate solution similar to those in the carboxylates, there is no clear evidence for this interpretation.

5.3 Mössbauer Data of $SnF_2/Sn(CO_2R)_4$ Mixtures

Tin-119 Mössbauer data of the solids isolated from the reactions of SnF_2 with tin tetracarboxylates are summarized in Table 5.3. Among these, only the reaction of SnF_2 with $Sn(CO_2CF_3)_4$ gave a white crystalline material. Pure solids could not be isolated from the reactions of SnF_2 with the other two tin(IV) carboxylates. Since $Sn(CO_2C_3F_7)_4$ was not isolated as a pure compound its reaction with SnF_2 could not be

TABLE 5.3

Mössbauer Data of Solid Isolated from Mixtures of SnF_2 and $Sn(CO_2R)_4$

Compound	Temp	δ	Δ	Γ	δ	Δ	Γ	ASn(IV)/ASn(II)
		mm s^{-1}			mm s^{-1}			
1. $SnF_2/Sn(CO_2CF_3)_4$	77	-0.16	0.0	1.03	4.13	0.84	1.00	1.16
2. $SnF_2/Sn(CO_2C_3F_7)_4$	77	0.14	0.42	0.92	3.46	1.62	1.00	
					4.22	1.08	1.00	
3. $SnF_2/Sn(CO_2CHCl_2)_4$	77	0.02	0.48	0.96	3.02	1.86	0.96	
					4.16	1.32	0.96	

carried out stoichiometrically and this reaction yielded a dark red coloured material. In the reaction between equimolar amounts of SnF_2 and $Sn(CO_2CHCl_2)_4$ in dichloroacetic acid, some solid precipitated and the Mössbauer spectrum was recorded on the solid isolated upon filtering. Also it was observed that the initially precipitated solid was soluble when more acid was distilled onto it.

The Mössbauer spectrum of the solid obtained from the $SnF_2/Sn(CO_2CF_3)_4$ reaction is shown in Figure 5.9. The analysis of this spectrum in terms of peak positions and linewidths indicates the presence of a tin(IV) site in a near cubic environment and a tin(II) site in a distorted environment. Clearly the values of the parameters of the tin(II) and tin(IV) sites are different from those of the starting materials $Sn(CO_2CF_3)_4$ and SnF_2 respectively. This spectrum can be interpreted in terms of the structure which is discussed in detail in Section 5.4 of this thesis. The structure of $Sn_4F_4(CO_2CF_3)_8 \cdot 2CF_3CO_2H$ contains two slightly different nearly octahedral tin(IV) environments which is consistent with the single line observed in the Mössbauer spectrum. The two tin(IV) sites are so similar that they could not be differentiated by Mössbauer spectroscopy. Each tin(IV) atom is bonded to two fluorines and four oxygens. The absence of a quadrupole splitting is in agreement with the two fluorines being bonded to the tin in a cis arrangement to each other. If the fluorines had been trans, one would have expected a quadrupole splitting since trans ligands produce a larger electric field gradient when compared to a cis arrangement. It should be noted that the Mössbauer spectra of mixed halogenostannates $[SnX_4Y_2]^{2-}$ gave single lines with no quadrupole splitting.[159] In this case there exists a

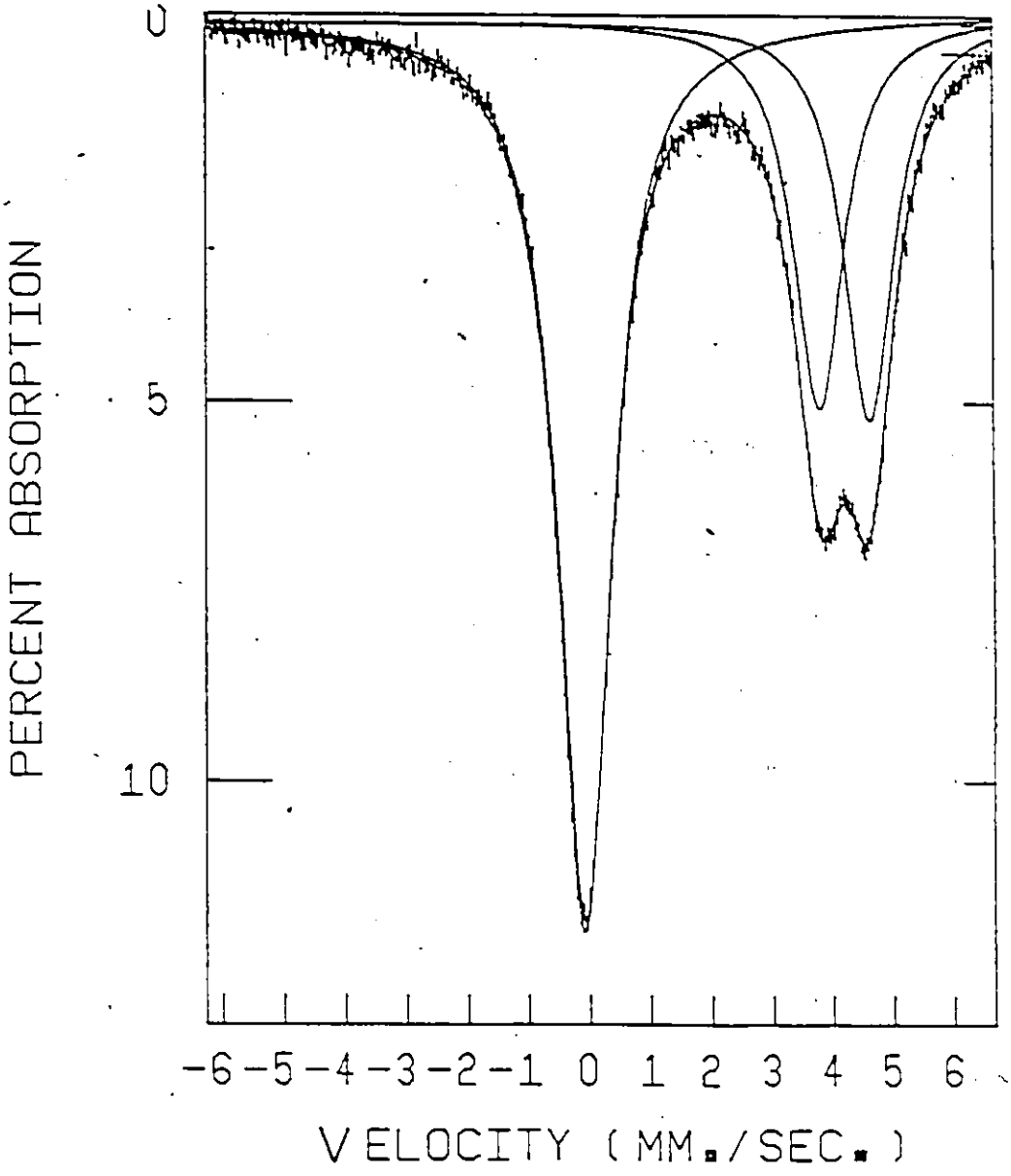

Figure 5.9: ^{119}Sn Mössbauer spectrum of the solid isolated from the reaction between SnF_2 and $Sn(CO_2CF_3)_4$ at 77 K.

linear relationship between the average electronegativity of the X and Y groups and the isomer shift.[160] The increase in the electronegativity causes a decrease in the isomer shift. The isomer shift of the tin(IV) resonance shown in Figure 5.9 (-0.16 mm/s) lies between those of $[SnCl_4F_2]^{2-}$ (+0.29) and $[SnF_6]^{2-}$ (-0.36). Since the tin(IV) resonance of the trifluoroacetate compound can be considered as arising from $[Sn(CO_2CF_3)_4)F_2]^{2-}$, the observed isomer shift is in agreement with the expected trend in electronegativity.

The values of the parameters of the tin(II) site show a higher isomer shift and smaller quadrupole splitting than those of the tin(II) carboxylate[94] and other tin(II) fluorine compounds.[27] The higher isomer shift (4.13 mm/s) indicates an increased s-electron density around tin and the smaller quadrupole splitting reflects less imbalance in the p-electron density at the tin atom. This means decreased p-electron density in the lone pair and more p-character in the tin-ligand bonds. This is reflected in the two tin(II) environments in this structure where the tin(II)-oxygen distances (2.25Å-3.20 Å) are longer than the average Sn(II)-O distances (2.14-2.19 Å) reported for tin(II) carboxylato complexes whose Mössbauer isomer shifts range from 2.90 to 3.15 mm/s.

Again the two tin(II) environments in this structure have essentially the same Mössbauer parameters even though the coordination around the two tin(II) atoms is somewhat different (Section 5.4). If inter atomic distances up to 3.00 Å around each tin(II) are considered, then one tin shows a coordination number of six whereas the other shows a coordination number of seven, including the lone pair in each case.

A comparison of the geometry around the two tin(II) atoms (Figure 5.13) shows that the additional interaction arises from a free acid molecule which is closer to one tin atom but this interaction appears to be not significant enough to change the Mössbauer parameters.

Tin-119 Mössbauer spectrum of the solid obtained from the reaction of SnF_2 with $Sn(CO_2CHCl_2)_4$ is shown in Figure 5.10. A similar spectrum was exhibited by the solid isolated from the reaction of SnF_2 with $Sn(CO_2C_3F_7)_4$. These show a tin(IV) resonance with a non-resolvable quadrupole splitting as was observed for the trifluoroacetate case. The tin(II) resonances could not be fitted to a simple doublet. The tin(II) absorptions were fitted to two overlapping doublets. The doublet with a higher isomer shift has parameters similar to those of the tin(II) site of the trifluoroacetate compound. The other doublet has a smaller isomer shift and a larger quadrupole splitting. It is possible that in these two cases the interaction between acid molecules and the tetrameric unit, "Sn_4F_4", might be strong enough to make the tin(II) sites different enough so that they are now detected by Mössbauer spectroscopy.

5.4 Crystal Structure of $[Sn(II)_2Sn(IV)_2F_4(CO_2CF_3)_8 \cdot 2CF_3CO_2H]$

The crystals obtained from the reaction of SnF_2 and $Sn(CO_2CF_3)_4$ described in the experimental section were used in the structure determination. The experimental data for the X-ray diffraction of this compound are summarized in Table 5.4. Initial precession photographs showed that the crystal decomposes in the X-ray beam over a period of one hour. Therefore the crystal was mounted on a $P2_1$ diffractometer and data

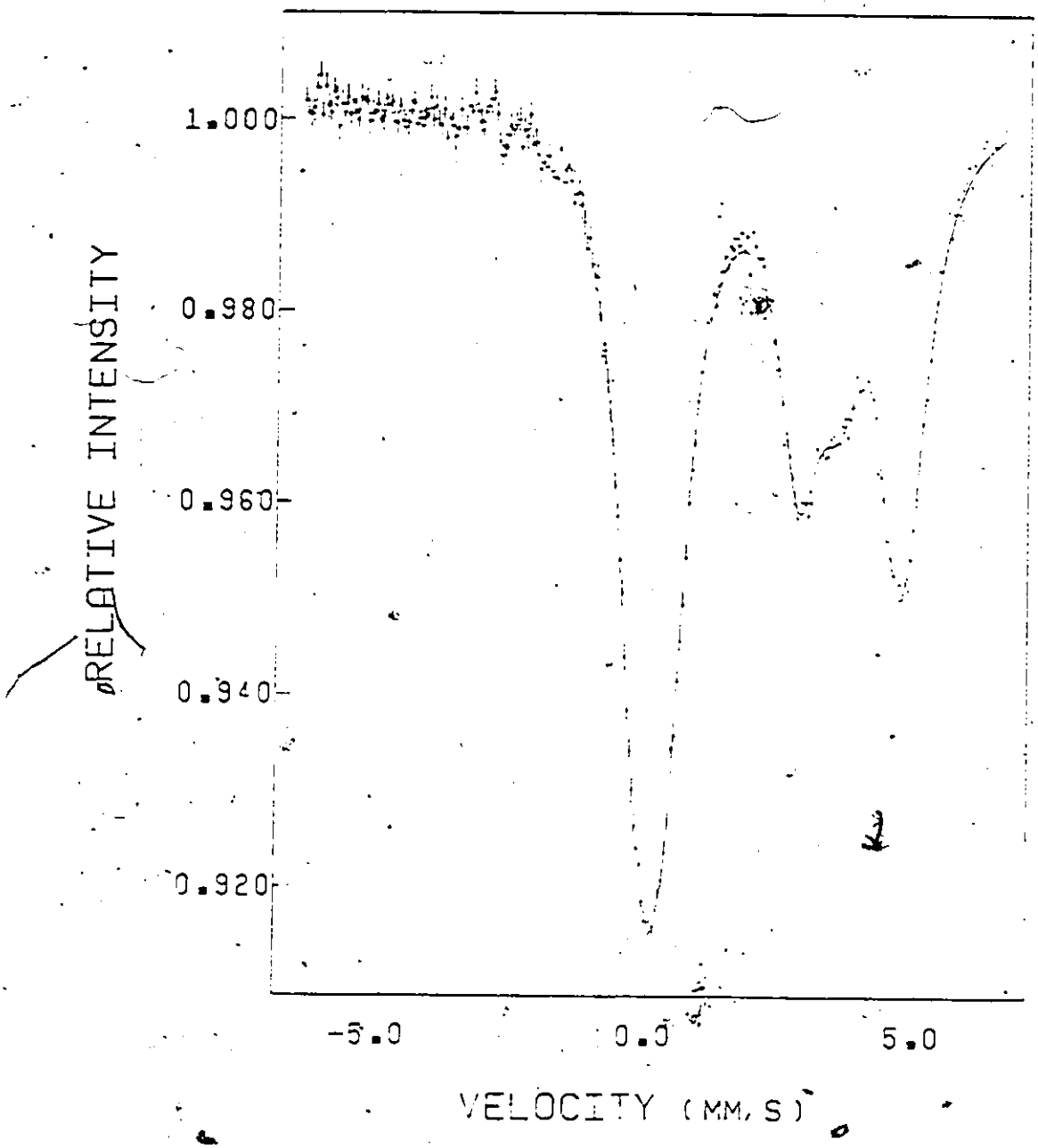

Figure 5.10: ^{119}Sn Mössbauer spectrum of the solid isolated from the reaction between SnF_2 and $Sn(CO_2CHCl_2)_4$ at 77 K.

TABLE 5.4

CRYSTAL DATA TABLE

Compound	$Sn_4F_4(O_2CCF_3)_8 \cdot 2CF_3CO_2H$
Formula weight	1682.9
Crystal shape and size (mm)	cylinder; r = 0.15, l = 0.37
Systematic absences	None
Space group	$P\bar{1}$
Unit cell parameters (°A) and (°)	a = 11.586(3) α = 110.44(1) b = 19.182(3) β = 119.50(2) c = 12.491(3) γ = 92.77(2)
Volume ($°A^3$)	2180.1(8)
Z	2
d_{calcd}, g cm^{-3}	2.56
Linear abosrbtion coefficient (cm^{-1})	25.13
Absorbtion correction limit	6.82% (minimum); 25.46% (maximum)
No. of reflections used to determine cell	15
Least square fit of χ, ϕ and 2θ(°)	$14.0 \leq 2\theta \leq 28.6$
Reflections measured	$0 \leq h \leq 13$; $+22 \leq k \leq -22$; $+14 \leq \ell \leq -14$
Maximum 2θ(°)	50

Continued.....

TABLE 5.4 (Continued)

Standard reflections (e.s.d.)	3 -2 2 (1.07%); 2 8 -3 (1.06%)
Temperature	-75°C
No. of reflections collected	8164
No. of independent reflections	7749
No. with $I > 0$	7091
No. with $I < 0$	658
Final R_1[a], R_2[b]	0.0708; 0.0514
Final shift/error max (av)	0.052 (0.011)
x (secondary extinction)	0.00016
Final difference map	
highest peak, e/Å^3; location	3.5; 0.12, 0.55, 0.40
lowest valley, e/Å^3; location	-1.5; 0.32, 0.02, 0.20
weighting scheme	$w = [\sigma(F_o)^2+\{0.0001(F_o)^2\}]^{-1}$
s[c]; error in an observation of unit weight	1.97
No. of varibles	350

a $$R_1 = \frac{\Sigma||F_o|-|F_c||}{\Sigma|F_o|}$$

b $$R_2 = \left[\frac{\Sigma w(|F_o|-|F_c|)^2}{\Sigma w|F_o|^2}\right]^{\frac{1}{2}}$$

where $w = \frac{1}{\sigma(F_o)^2+\{0.0001\sigma(F_o)^2\}}$, $\sigma(F_o)$ being the error derived from counting statistics.

Continued.....

TABLE 5.4 (Continued)

$$s^c = \left[\frac{\Sigma w(|F_o|-|F_c|)^2}{N_R - N_V} \right]^{\frac{1}{2}}$$

where N_R = number of reflections and N_V = number of parameters varied during the refinement.

collected at low temperature. The unit cell parameters were obtained by least squares refinement of fifteen accurately centred reflections. The cell found belonged to the triclinic system, and a Delauny reduction was carried out to look for any hidden symmetry. This procedure confirmed the triclinic cell and a full set of intensities was measured at -75°C. The structure was solved as described below. The crystal data are summarized in Table 5.4.

A total of 8164 reflections were measured. No absorption correction was used. Equivalent reflections were averaged to give 7749 unique reflections of which 658 (zero or negative intensity) reflections were rejected. The remaining 7091 reflections were used in the structure determination. The positions of four independent tin atom positions were obtained using the direct method programme MULTAN 80.[161] The positions of fluorine, oxygen and carbon were located from the difference Fourier synthesis. Least squares refinements were carried out using SHELX.[48] In the final stages, all atoms were refined with anisotropic temperature factors with a weighting scheme (see Table 5.4) and a correction for secondary extinction using SHELX. The refinement converged at R_1 = 0.0708 and R_2 = 0.0514. The final positional parameters and equivalent or isotropic temperature factors for the atoms are given in Table 5.5. Anisotropic temperature factors are given in Appendix I. Relevant bond lengths and bond angles are given in Table 5.6.

The structure consists of two independent centrosymmetric molecules (Figure 5.11 and 5.12). Each molecule consists of an eight membered ring with a Sn(II)-F-Sn(IV)-F arrangement. Similar Sn(II)-F-Sn(IV)-F bridging is observed in the mixed valence tin fluoride

TABLE 5.5

Atomic positional parameters (x 10^4) and equivalent temperature factors ($Å^2$ x 10^3) for $Sn(II)_2Sn(IV)_2F_4(O_2CCF_3)_8 \cdot 2CF_3CO_2H$. (Fluorine atoms F15, F16, F17 and F18, F19, F20 are disordered with site occupied by 60.0% and 40.0% of an atom respectively).

Atom	x	y	z	Ueq*
Sn1	2716(1)	596.3(3)	1809(1)	14.7(3)
Sn2	- 216(1)	1556.2(3)	160(1)	17.2(3)
Sn3	1271(1)	5541.6(3)	3990(1)	13.5(3)
Sn4	147(1)	3465.4(3)	3537(1)	16.7(3)
F1	905(5)	689(2)	480(5)	16(3)
F2	1696(5)	- 32(2)	1532(5)	16(3)
F3	3432(8)	- 290(4)	-1770(7)	49(5)
F4	4098(8)	- 1059(4)	- 858(8)	51(5)
F5	2158(8)	- 1445(5)	-2738(8)	71(6)
F6	6383(6)	313(4)	5450(6)	41(4)
F7	7311(7)	508(5)	4457(7)	53(5)
F8	6654(9)	- 640(5)	4134(9)	81(6)
F9	1062(8)	2383(4)	4869(6)	49(5)
F10	1023(8)	1222(4)	4561(7)	47(5)
F11	2962(9)	2072(4)	5867(6)	54(5)
F12	1080(10)	512(5)	-1839(8)	64(7)
F13	869(9)	438(4)	-3655(7)	54(5)
F14	2418(8)	1340(5)	-1782(9)	63(6)
F15	4102(13)	3156(8)	1369(14)	64(4)†
F16	5675(15)	2665(8)	2588(16)	75(4)†
F17	4644(15)	3309(8)	3358(14)	84(4)†
F18	5559(23)	2945(12)	3202(23)	85(6)†
F19	4097(19)	3345(11)	1898(20)	59(5)†
F20	4977(20)	2438(11)	1144(20)	75(5)†
F21	- 171(5)	5344(2)	6093(4)	15(2)
F22	- 1390(5)	3747(3)	4376(5)	18(3)
F23	2220(6)	3413(3)	8261(6)	31(4)
F24	3324(7)	4602(3)	9298(6)	41(4)
F25	3569(6)	3805(4)	7782(6)	40(4)
F26	5470(7)	2427(4)	5188(7)	52(5)
F27	6983(8)	1976(4)	6346(10)	62(7)
F28	6724(8)	3050(4)	7315(7)	56(5)
F29	398(11)	3160(4)	- 472(8)	71(7)
F30	- 1818(10)	5770(6)	9527(8)	96(8)
F31	- 235(10)	4128(5)	- 620(7)	69(6)
F32	4788(6)	5089(3)	7549(5)	34(4)
F33	- 5645(6)	5128(4)	6387(6)	37(4)

Continued.....

TABLE 5.5 (Continued)

Atom	x	y	z	Ueq*
F34	4861(7)	4044(3)	6245(7)	45(4)
F35	4662(7)	6466(4)	- 91(7)	43(4)
F36	3047(10)	6226(4)	187(8)	59(6)
F37	2597(7)	6163(4)	- 1720(6)	46(4)
O1	3022(6)	67(3)	291(6)	17(3)
O2	4548(6)	541(3)	3214(6)	19(3)
O3	2420(6)	1136(3)	- 3337(6)	21(3)
O4	3738(6)	1605(3)	2094(6)	21(3)
O5	- 1211(7)	1000(3)	1160(6)	23(4)
O6	- 416(7)	1505(4)	- 2007(7)	27(4)
O7	2132(7)	2073(4)	794(6)	24(4)
O8	4280(7)	- 716(4)	2093(7)	28(4)
O9	1473(7)	2071(3)	2858(6)	21(4)
O10	75(8)	1750(4)	- 3392(7)	30(5)
O11	596(6)	4322(3)	7291(6)	20(3)
O12	1149(6)	4814(3)	2270(6)	17(3)
O13	- 3027(6)	4679(3)	4738(6)	18(3)
O14	128(7)	3577(3)	1615(6)	27(4)
O15	1490(6)	4101(3)	6016(6)	19(3)
O16	2442(6)	4011(3)	4331(6)	20(3)
O17	2453(6)	6335(3)	3975(6)	18(3)
O18	- 1298(7)	2766(3)	6098(7)	26(4)
O19	- 2452(7)	2410(4)	623(7)	32(4)
O20	- 4479(7)	2170(4)	- 1278(7)	33(4)
C1	2304(9)	- 581(5)	- 754(9)	19(5)
C2	2966(12)	- 859(6)	- 1580(11)	35(7)
C3	4915(10)	- 98(6)	3054(10)	22(6)
C4	6328(12)	6(6)	4289(11)	32(7)
C5	1880(9)	1704(5)	3533(9)	19(5)
C6	1747(14)	1854(6)	4737(11)	34(7)
C7	170(10)	1426(5)	- 2601(9)	22(5)
C8	1153(14)	928(6)	- 2464(11)	35(8)
C9	3315(10)	2089(5)	1595(9)	21(5)
C10	4500(15)	2770(8)	2078(16)	56(10)
C11	636(10)	4093(5)	1483(9)	21(5)
C12	674(12)	3895(6)	206(10)	29(6)
C13	1474(9)	4147(5)	7014(9)	16(5)
C14	2688(10)	3998(5)	8121(9)	22(5)
C15	3215(9)	4660(5)	5181(8)	20(5)
C16	4661(10)	4732(6)	6369(10)	27(6)
C17	- 2227(10)	3022(5)	6103(9)	19(5)
C18	6717(11)	2608(6)	6241(11)	29(6)
C19	- 3390(10)	2599(5)	- 82(10)	23(6)
C20	- 3420(11)	3462(6)	398(10)	28(6)

* $Ueq = \frac{1}{3}(U_{11}+U_{22}+U_{33}+2U_{12}Cos\gamma+2U_{13}Cos\beta+2U_{23}Cos\alpha)$

+ U isotropic

TABLE 5.6

Selected Bond Distances (Å) and Bond Angles (°) for

$[Sn(II)_2Sn(IV)_2F_4(O_2CCF_3)_8 \cdot 2CF_3CO_2H]$

A. Tin Coordination

(i) Molecule I^+

Sn(1)-F(1)	2.000(5)	Sn(2)-F(1)	2.186(5)
Sn(1)-F(2)	1.975(5)	-F(2')	2.296(4)
Sn(1)-O(1)	2.027(8)	-O(5)	2.501(9)
Sn(1)-O(2)	2.020(6)	-O(6)	2.567(9)
Sn(1)-O(3)	2.033(8)	-O(7)	2.466(8)
Sn(1)-O(4)	2.038(7)	-O(9)	2.675(6)
		-O(19)	3.309(9)
F(1)-Sn(1)-F(2)	87.6(2)	F(1)-Sn(2)-F(2')	72.7(2)
F(1)-Sn(1)-O(1)	90.3(2)	-O(5)	78.9(2)
-O(2)	177.6(2)	-O(6)	100.4(2)
-O(3)	89.8(2)	-O(7)	72.3(2)
-O(4)	91.6(2)	-O(9)	73.9(2)
F(2)-Sn(1)-O(1)	94.3(3)	-O(19)	145.0(3)
-O(2)	93.3(2)	F(2')-Sn(2)-O(5)	73.8(2)
-O(3)	86.2(3)	-O(6)	74.6(2)
-O(4)	178.9(3)	-O(7)	126.3(2)
O(1)-Sn(1)-O(2)	91.9(3)	-O(9)	132.4(2)
-O(3)	179.5(2)	-O(19)	99.0(2)
-O(4)	86.5(3)	O(5)-Sn(2)-O(6)	147.1(2)
O(2)-Sn(1)-O(3)	88.0(3)	-O(7)	135.1(2)
-O(4)	87.6(3)	-O(9)	67.2(2)
O(3)-Sn(1)-O(4)	93.1(3)	-O(19)	66.2(2)
		O(6)-Sn(2)-O(7)	73.2(2)
		-O(9)	144.8(2)
		-O(19)	110.2(2)
		O(7)-Sn(2)-O(9)	72.1(3)
		-O(19)	132.1(2)
		O(9)-Sn(2)-O(19)	89.5(2)

Continued.....

TABLE 5.6 (Continued)

(ii) Molecule II‡

Sn(3)-F(21)	2.014(6)	Sn(4)-F(9)	3.014(8)
-F(22')	1.951(6)	Sn(4)-F(21)	2.162(5)
-O(11')	2.039(6)	-F(22)	2.469(7)
-O(12)	2.043(7)	-F(37')	3.164(7)
-O(13')	2.053(6)	-O(9)	3.214(7)
-O(17)	2.010(8)	-O(14)	2.473(9)
		-O(15)	2.435(6)
		-O(16)	2.357(7)
		-O(19)	3.144(5)

F(21)-Sn(3)-F(22')	91.0(2)	F(9)-Sn(4)-F(21)	144.6(2)
-O(11')	86.9(3)	-F(22)	90.9(3)
-O(12)	90.1(3)	-F(37')	139.5(2)
-O(13')	88.2(2)	-O(9)	50.3(2)
-O(17)	173.4(3)	-O(14)	132.8(3)
F(22')-Sn(3)-O(11')	93.4(3)	-O(15)	55.8(2)
-O(12)	178.9(3)	-O(16)	90.6(3)
-O(13')	87.1(2)	-O(19)	104.3(2)
-O(17)	94.7(3)	F(21)-Sn(4)-F(22)	75.6(2)
O(11')-Sn(3)-O(12)	86.1(3)	-F(37')	61.2(2)
-O(13')	175.0(3)	-O(9)	147.4(2)
-O(17)	96.2(3)	-O(14)	75.9(2)
O(12)-Sn(3)-O(13')	93.5(3)	-O(15)	78.8(2)
-O(17)	84.3(3)	-O(16)	78.1(2)
O(13')-Sn(3)-O(17)	88.7(3)	-O(19)	107.9(2)
		F(37')-Sn(4)-O(9)	132.3(1)
		-O(14)	69.9(3)
		-O(15)	122.9(2)
		-O16)	129.9(2)
		-O(19)	49.8(2)
		O(9)-Sn(4)-O(14)	82.5(2)
		-O(15)	103.5(2)
		-O(16)	72.3(2)
		-O(19)	83.6(2)
		O(14)-Sn(4)-O(15)	139.2(2)
		-O(16)	72.9(3)
		-O(19)	64.2(2)
		O(15)-Sn(4)-O(16)	70.9(3)
		-O(19)	155.7(3)
		O(16)-Sn(4)-O(19)	133.0(3)

Continued.....

TABLE 5.6 (Continued)

B. Fluorine Coordination

(i) Molecule I†

F(1)-F(1')	2.756(7)	Sn(1)-F(1)-Sn(2)	140.6(2)
-F(2)	2.751(8)	Sn(1)-F(2)-Sn(2')	141.0(3)
-F(2')	2.658(6)		

(ii) Molecule II‡

F(21)-F(21')	2.822(9)	Sn(3)-F(21)-Sn(4)	136.8(3)
-F(22')	2.827(6)	Sn(3')-F(22)-Sn(4)	138.0(2)
-F(22)	2.848(9)		

C. Trifluoroacetate Groups

(i) Bond Distances

C(1)-O(1)	1.279(8)	C(3)-O(2)	1.299(13)
-O(5)	1.221(13)	-O(8)	1.200(10)
-C(2)	1.54(2)	-C(4)	1.538(14)
C(5)-O(3)	1.293(12)	C(7)-O(6)	1.21(2)
-O(9)	1.217(13)	-O(10)	1.31(2)
-C(6)	1.52(2)	-C(8)	1.51(2)
C(9)-O(4)	1.280(13)		
-O(7)	1.227(11)		
-C(10)	1.55(2)		
C(11)-O(12)	1.276(9)	C(13)-O(11)	1.282(14)
-O(14)	1.228(15)	-O(15)	1.228(15)
-C(12)	1.53(2)	-C(14)	1.541(13)
C(15)-O(13)	1.274(12)	C(17)-O(17)	1.300(12)
-O(16)	1.230(9)	-O(18)	1.205(15)
-C(16)	1.553(12)	-C(18)	1.54(2)
C(19)-O(19)	1.186(13)		
-O(20)	1.298(9)		
-C(20)	1.561(14)		

(ii) Bond Angles

O(1)-C(1)-O(5)	129.7(12)	O(12)-C(11)-O(14)	129.3(12)
O(1)-C(1)-C(2)	113.2(4)	O(12)-C(11)-C(12)	114.4(11)
O(5)-C(1)-C(2)	117.1(8)	O(14)-C(11)-C(12)	119.2(8)
O(2)-C(3)-O(8)	127.3(9)	O(11)-C(13)-O(15)	128.3(8)
O(2)-C(3)-C(4)	112.0(7)	O(11)-C(13)-C(14)	113.3(10)
O(8)-C(3)-C(4)	120.8(10)	O(15)-C(13)-C(14)	118.3(10)
O(3)-C(5)-O(9)	127.7(11)	O(13)-C(15)-O(16)	129.9(8)
O(3)-C(5)-C(6)	110.2(10)	O(13)-C(15)-C(16)	111.6(6)
O(9)-C(5)-C(6)	122.1(10)	O(16)-C(15)-C(16)	118.6(9)

Continued.....

TABLE 5.6 (Continued)

O(6)-C(7)-O(10)	126.6(10)	O(17)-C(17)-O(18)	126.0(12)
O(6)-C(7)-C(8)	121.6(12)	O(17)-C(17)-C(18)	111.9(10)
O(10)-C(7)-C(8)	111.8(12)	O(18)-C(17)-C(18)	122.0(10)
O(4)-C(9)-O(7)	128.8(10)	O(19)-C(19)-O(20)	128.5(9)
O(4)-C(9)-C(10)	113.4(9)	O(19)-C(19)-C(20)	120.4(7)
O(7)-C(9)-C(10)	117.8(11)	O(20)-C(19)-C(20)	111.2(9)

† Primed (') atoms indicate the symmetry equivalent position (-x,-y,-z).

‡ Primed (') atoms indicate the symmetry equivalent position (-x,1-y,1-z).

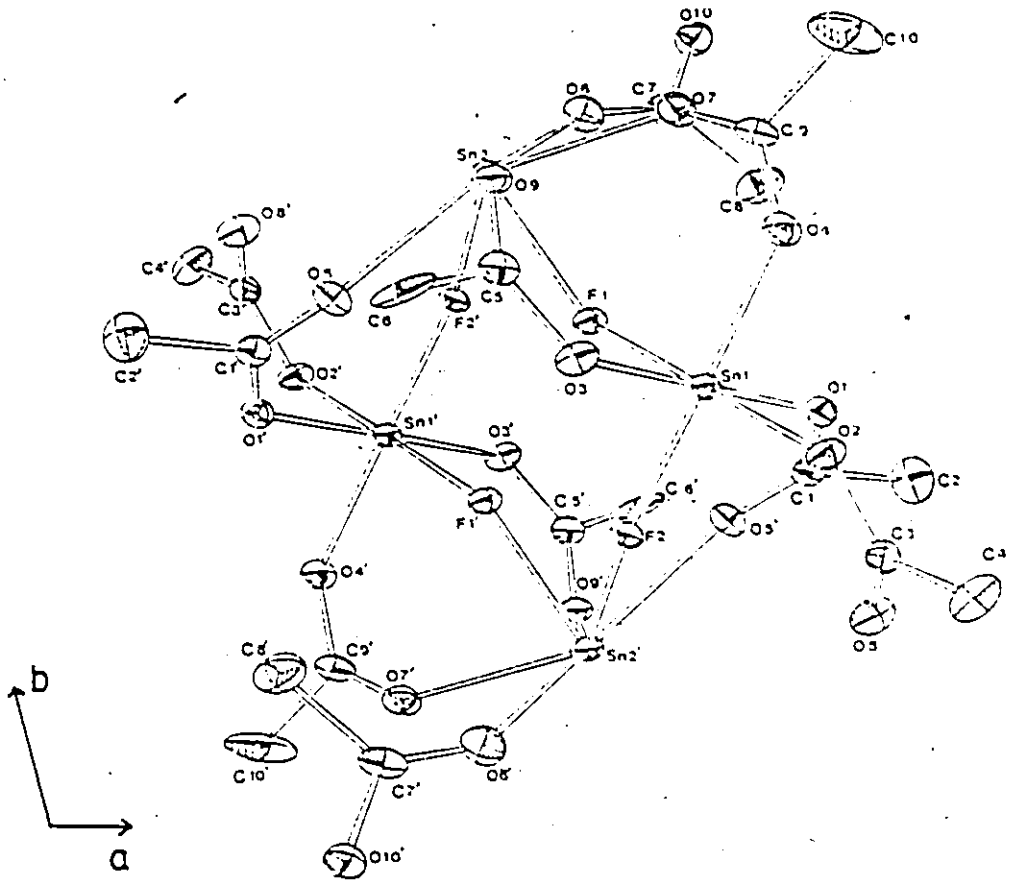

Figure 5.11: Molecular structure of cyclo-tetra-μ-fluoro-octakis-μ-(trifluoroacetato)-ditin(II)ditin(IV)-bis(trifluoroacetic acid). The molecule is viewed down the c axis. Fluorine atoms of the $-CF_3$ groups are omitted for clarity.

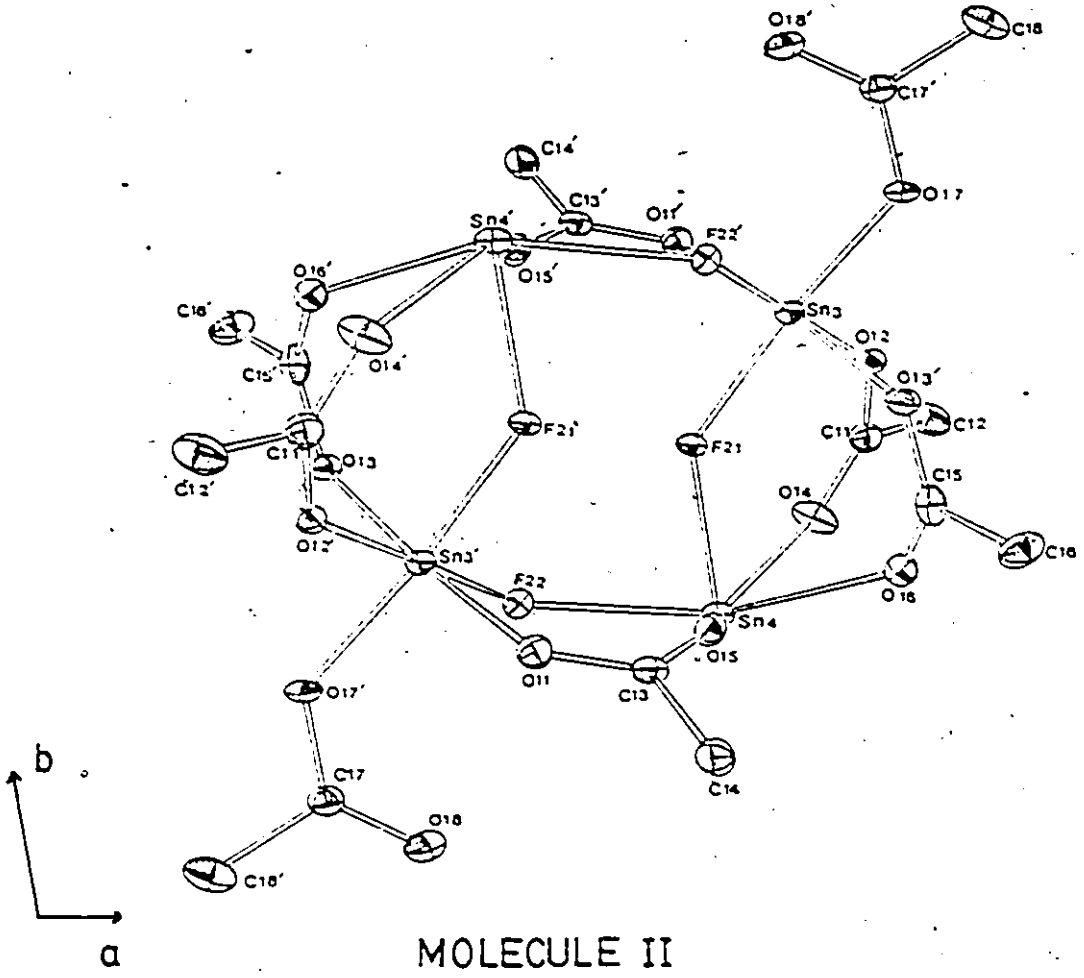

Figure 5.12: Molecular structure of cyclo-tetra-μ-fluoro-hexakis-μ-(trifluoroacetato)-bis(trifluoroacetato)-ditin(II)ditin(IV). The molecule is viewed down the c axis. Fluorine atoms of the $-CF_3$ groups are omitted for clarity.

Sn_3F_8,[23] and the structure of SnF_2[130] consists of cyclic tetramers, Sn_4F_8, held together by weaker Sn-F interactions. Adjacent Sn(II) and Sn(IV) atoms in Molecule I (Figure 5.11) and Molecule II (Figure 5.12) are also bridged by either one or two trifluoroacetate groups. There are also unidentate trifluoroacetate groups and free acid molecules present in this structure. There are eight trifluoroacetate groups associated with each tetramer. In addition, two trifluoroacetic acid molecules C(7)C(8)O(10)O(6) and C(7')C(8')O(10')O(6') are associated with Molecule I, which are coordinated to the two Sn(II) atoms, i.e., Sn(2) and Sn(2'), respectively. There are also two free acid molecules [C(19)C(20)O(19)O(20) and its symmetry related molecule] present in the unit cell which have only weak interactions with other atoms.

The Sn(IV)-F bond distances are similar to those found in other tin(IV) fluoride compounds. The observed Sn(II)-F bond distances tend more towards the longer side of the range usually exhibited by other tin(II) fluorides. For comparison, the Sn(II)-F distances and the Sn(IV)-F distances of related compounds are tabulated in Table 5.7. The Sn(IV) atoms in the two ring systems are in near octahedral environments. The two fluorine atoms coordinated to each tin(IV) which are part of the ring, form F-Sn(IV)-F angles of almost 90° in both molecules. The Sn(II)-F-Sn(IV) angles vary between 136.8° and 141.0° compared to the range of Sn(II)-F-Sn(II) (94-170.5°) angles in the SnF_2 tetramer.[130]

The coordination environment of the tin(II) atoms, namely Sn(2) and Sn(4) are quite irregular. Brown's bond valence approach provides a quantitative method for comparing the strength of these Sn-O and Sn-F bonds. The bond valencies are given in Figure 5.13 for the

TABLE 5.7

Tin(II)-fluorine and Tin(IV)-fluorine Bond Distances for Various Tin Fluorides

A. Compound	Sn(II)-F Bond Distances (°A)
SnF_2[130]	2.03 - 2.27
Sn_3F_8[23]	2.10 - 2.25
$Na_4Sn_3F_{10}$[166]	2.04 - 2.26
$NaSn_2F_5$[139]	2.07 - 2.22
$KSnF_3 \cdot \frac{1}{2}H_2O$[141]	2.01 - 2.27
NH_4SnF_3[142]	2.08
$(SnF)_3 \cdot 3AsF_6$[144]	2.097
$(Sn_2F_3) \cdot BF_4$[147]	
$(Sn_2F_3)Cl$[148]	2.11 - 2.20
$Sn_4F_4(O_2CCF_3)_8 \cdot 2CF_3CO_2H$ (This study)	2.162 2.469 2.186 2.296

B. Compound	Sn(IV)-F Bond Distances (°A)
SnF_4[162]	2.02 1.88
Li_2SnF_6[163]	1.962, 1.983
Na_2SnF_6[164]	1.83, 1.92, 1.96
$K_2SnF_6 \cdot KHF_2$[167]	1.91 - 2.05
Cs_2SnF_6[165]	1.952
Sn_3F_8[23]	1.96 - 1.98
$Sn_4F_4(O_2CCF_3)_8 \cdot 2CF_3O_2H$ (This study)	1.975 2.005 1.951 2.014

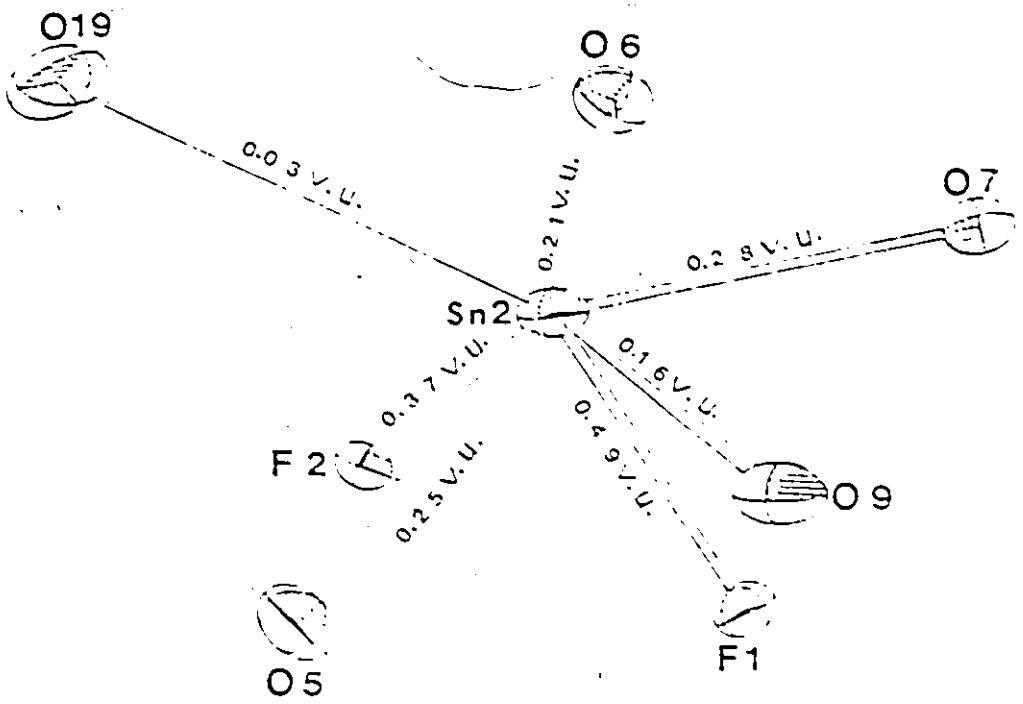

Figure 5.13(a): Geometry of Sn(2) atom. Bond valencies are given along the bonds in valence unit (v.u.).

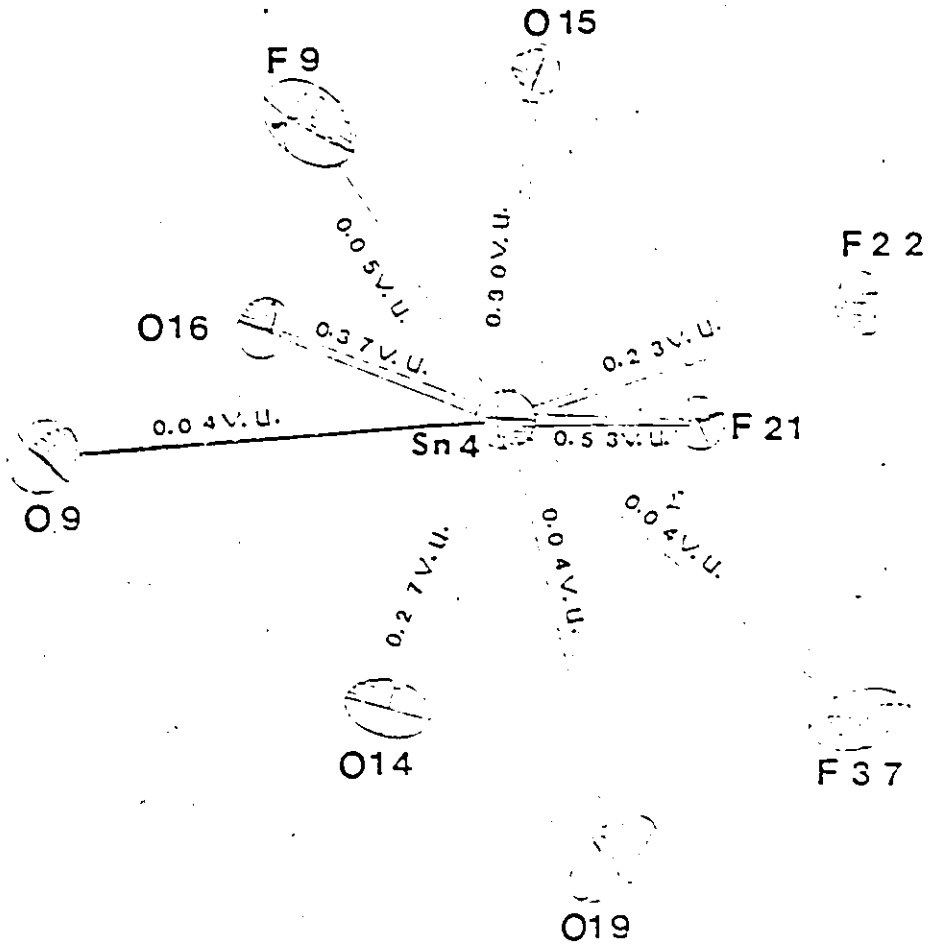

Figure 5.13(b): Geometry of Sn(4) atom. Bond valencies are given along the bonds in valence unit (v.u.).

Sn(2) and Sn(4) atoms. The bond valences around Sn(4) vary over a range from 0.53 v.u. to 0.04 v.u. for a total of 1.87 v.u.. The Sn(4)-F(21) bond can be considered to be strong, while the Sn(4)-O(14), Sn(4)-O(15), Sn(4)-O(16) and Sn(4)-F(22) bonds are of intermediate strength. In addition, there are four weak interactions between Sn(4) and O(9), F(9), O(19) and F(37). The environment of Sn(4) consists of one strong bond, four intermediate bonds and a vacant space presumably occupied by the lone pair. Therefore, this can be described as SnX_5E, where E represents the lone pair. This pseudo octahedral coordination is also exhibited by the tin(II) atoms in the structure discussed in Chapter 4. A few structures with this coordination have been reported.[18,130,131]

The environment of each of the Sn(2) atoms is seven coordinated. The strength of these bonds vary from 0.49 v.u. to 0.03 v.u.. These can be classified as one strong [Sn(2)-F(1)], five intermediate [Sn(2)-F(2), Sn(2)-O(5), Sn(2)-O(6), Sn(2)-O(7), Sn(2)-O(9)] and one weak bond [Sn(2)-O(19)]. When considering the five intermediate bonds, the angles between the adjacent bonds formed with Sn(2) vary in the range 67.2° to 78.9°. These values are close to 72° which is the ideal value for the five bonds to be in a regular pentagonal arrangement. The coordination of Sn(2) can be described as a pseudo pentagonal bipyramid with the strong bond Sn(2)-F(1) and the lone pair directed along the axial direction.

All of the bidentate trifluoroacetates which bridge between a tin(II) and a tin(IV) atom follow similar trends in their C-O bond distances. The C-O groups bonded to tin(II) are shorter than those bonded to tin(IV). This shortening is a consequence of a greater degree

of covalent character in the tin(IV)-oxygen bonds as compared to the tin(II)-oxygen bonds. The variations in the C-O distances indicate that the bonding in the bridging carboxylates are consistent with a Sn(IV)-O-C=O ⟶ Sn(II) arrangement. The asymmetry in the C-O bond distances of the monodentate trifluoroacetates, coordinated to Sn(IV), are greater than in those of the bidentate groups and is consistent with a Sn(IV)-O-C=O arrangement.

CHAPTER 6

CONCLUSION

6.1 Summary of Reactions

The reactions of the tin compounds studied in this work have been carried out in strongly acidic (HSO_3X; where X = F, OH, CH_3, C_2H_5 or CF_3) and in weakly acidic (RCOOH; where R = alkyl group) media. In this work, the tin compounds can be classified into five different categories and their reactions with acids are summarized in Table 6.1.

The alkyltin hydrides (type 1: Table 6.1) react with acids initially by the displacement of a hydrogen atom by an acid ligand and the evolution of one mole of hydrogen gas. The results discussed in Chapter 3 established the presence of solvated cationic species $(CH_3)_{3-n}SnH_n^+$ (n = 0→3). In fluorosulphuric acid solution, these species are solvated by fluorosulphate groups. Among these, SnH_3^+ undergoes rapid decomposition at -30°C, $(CH_3)SnH_2^+$ at -50°C and $(CH_3)_2SnH^+$ at -75°C while $(CH_3)_3Sn^+$ undergoes slow decomposition at -10°C. The instability of cationic species containing Sn-H bonds compared to $(CH_3)_3Sn^+$ is due to the weakness of the Sn-H bond relative to that of the Sn-C bond. The decreasing stability of the SnH_3^+, $(CH_3)SnH_2^+$ and $(CH_3)_2SnH^+$ species is opposite to the normally expected trend. In the carbocation series, there is stabilization of the cationic centre by the inductive effect of the methyl groups. This suggests that the fluorosulphate groups which are coordinated to the tin centre play an important part in stabilizing these tin cations. The observed trend suggests that the fluorosulphate

TABLE 6.1

Type of Compound	Acid	Representative Reaction Studied	Reference	Comments
1. Alkyltin hydrides $R_{4-n}SnH_n$ (n = 1-3)	i) RCO_2H	$Sn_2(n\text{-}Bu)_4H_2 + 4BuCO_2H \rightarrow 2Sn(n\text{-}Bu)_2(O_2CBu)_2 + 2H_2$	56	H is displaced by acid ligand. This indicates preferential cleavage of the Sn-H bond than the Sn-C bond.
	ii) HSO_3F	$Me_{4-n}SnH_n + HSO_3F \rightarrow Me_{4-n}SnH_{n-1}(SO_3F) + H_2$	This Work	
2. Tetraalkyltin Compounds R_4Sn	i) RCO_2H	$R_4Sn + nRCO_2H \rightarrow R_{4-n}Sn(O_2CR)_n + nRH$	11,13	Alkyl groups attached to tin are displaced with increasing difficulty.
	ii) HSO_3F	$(CH_3)_4Sn + HSO_3F \rightarrow (CH_3)_3Sn(SO_3F) + CH_4$ $(CH_3)_3Sn(SO_3F) + HSO_3F \rightarrow (CH_3)_2Sn(SO_3F)_2 + CH_4$	7,59	The first two alkyl groups are cleaved easily but there is no further cleavage.
3. Tetraphenyltin	i) RCO_2H	$(C_6H_5)_4Sn + nRCO_2H \rightarrow (C_6H_5)_{4-n}Sn(O_2CR)_n + nC_6H_6$ where R = CH_3, CH_2Cl, $CHCl_2$, CF_3, C_2F_5	11	All phenyl groups attached to tin are displaced by carboxylate groups.
	ii) HSO_3F	$(C_6H_5)_4Sn + HSO_3F \rightarrow$ [illegible] $+ C_6H_6$	13	Tin product not identified.
4. Hexaalkylditin Compound. $R_3Sn\text{-}SnR_3$	[illegible]	[illegible] Conditions	15	Two alkyl groups are displaced by carboxylate groups. No tin-tin bond cleavage.

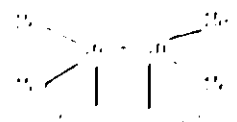

Continued.....

TABLE 6.1 (Continued)

Type of Compound	Acid	Representative Reaction Studied	Reference	Comments
		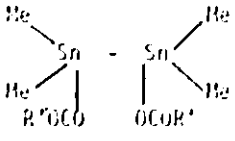 $+ O_2 \rightarrow \left\{[Me_2Sn(O_2CR')]_2O\right\}_2$ $R' = CF_3, CCl_3$	7	Oxygen inserts into the tin-tin bond.
	ii) HSO_3F	$Me_3Sn\text{-}SnMe_3 + HSO_3F \rightarrow Me_2Sn(SO_3F)_2 + 2CH_4 + H_2$	7	Two alkyl groups are displaced and symmetric cleavage of tin-tin bond occurs.
5. Hexaphenylditin	i) R'COOH	$(C_6H_5)_3Sn\text{-}Sn(C_6H_5)_3 + 6R'COOH \rightarrow$ $[Sn(II)Sn(IV)O(O_2CR)_4]_2O(OCR)_6 + 6C_6H_6$	1	All phenyl groups are cleaved and the tin-tin bond is asymmetrically cleaved.
	ii) $R'SO_3H$	$(C_6H_5)_3Sn\text{-}Sn(C_6H_5)_3 + R'SO_3H \rightarrow$ $[Sn(II)Sn(IV)(O_3SR')_6] + C_6H_6$ $R' = CH_3, C_2H_5, CF_3$	7	

a) F. Birchall, Unpublished results.

groups should be more strongly coordinated to tin in SnH_3^+ than they are in $(CH_3)_2SnH^+$. It is proposed that as a result of solvation, cations SnH_3^+, $(CH_3)SnH_2^+$ and $(CH_3)_2SnH^+$ have a trigonal bipyramidal arrangement about the tin atom. Mössbauer spectroscopic measurements of these species would provide additional evidence for the above coordination.

Since the reactions of methylstannanes with fluorosulphuric acid have established that there is initial cleavage of a Sn-H bond rather than a Sn-C bond, it would be of interest to extend this study to the reactions of phenyltin hydrides $[(C_6H_5)_{4-n}SnH_n$; n = 1-3] with this acid. Earlier reports on the reaction of triphenyltin hydride with hydrogen bromide indicated that there is initial cleavage of a Sn-C bond rather than a Sn-H bond and this reaction can be given by equation (6.1).[168]

$$(C_6H_5)_3SnH + HBr \longrightarrow (C_6H_5)_2SnHBr + C_6H_6 \qquad (6.1)$$

If similar reactions occur in fluorosulphuric acid solution, then one would expect species such as $(C_6H_5)_2SnH^+$ and $(C_6H_5)SnH_2^+$ to be produced. On the other hand, Sawyer and Kuvilia have studied the reaction of diphenyltin dihydridewith acetic acid and showed that the reaction product may be represented by equation (6.2).[56]

$$(C_6H_5)_2SnH_2 + 2\ CH_3COOH \longrightarrow (C_6H_5)_2Sn(O_2CCH_3)_2 + H_2 \qquad (6.2)$$

Spectroscopic analysis of the phenyltin hydride-fluorosulphuric acid system would provide information about the nature of species produced in these reactions.

A comparison of the reactions of tetraalkyltin (type 2; Table 6.1) and tetraphenyltin (type 3; Table 6.1) in acids indicates that phenyl groups are cleaved much more easily than alkyl groups. In tetraphenyltin, all of the phenyl groups bonded to tin are displaced by acid ligands whereas in the reaction of tetramethyltin with fluorosulphuric acid, only two methyl groups are substituted by fluorosulphate groups and no more methyl groups are displaced. All of these alkyltin compounds behave in a similar fashion with either strong or weak acids.

The reaction of alkyl substituted ditin compounds ($R_3Sn\text{-}SnR_3$, type 4; Table 6.1) and phenyl substituted ditin compounds (type 5: Table 6.1) depends on the acid. In the case of hexamethylditin with carboxylic acids, two alkyl groups are replaced by acid ligands and the tin-tin bond is not normally cleaved. In the reaction of hexamethylditin with fluorosulphuric acid, two methyl groups are again substituted but the tin-tin bond is cleaved symmetrically to give a tin(IV) compound. On the other hand, all of the phenyl groups in hexaphenylditin are substituted by acid ligands and the tin-tin bond is cleaved asymmetrically to give compounds containing tin(II) and tin(IV).[1] These observations suggest that in order to cleave a tin-tin bond asymmetrically, all Sn-C bonds have to be cleaved beforehand. This gives an insight into the reaction sequence for the acetolysis of hexaphenylditin (type 5; Table 6.1).

The reaction of hexaphenylditin (type 5; Table 6.1) with carboxylic acids results in the formation of mixed valence tin compounds with the empirical formula $Sn(OCOR)_3$. Based on spectroscopic data, they have been formulated as $[Sn(II)Sn(IV)O(OCOR)_4O(OCR)_2]_2$.[1] In an attempt to provide an alternate synthesis the reaction between $Sn(OCOCF_3)_2$ and

$Sn(OCOCF_3)_4$ produces a compound with the same empirical formula and the reaction is given by equation (6.3).

$$Sn(OCOCF_3)_2 + Sn(OCOCF_3)_4 \longrightarrow 2\ Sn(OCOCF_3)_3 \qquad (6.3)$$

Solution NMR data and solid state Mössbauer isomer shift and quadrupole splitting parameters suggest that the compound isolated from reaction (6.3) and the compound obtained from the reaction of hexaphenylditin with CF_3COOH (reaction type 5; Table 6.1) have similar local tin environments. However, comparison of the relative Mössbauer recoil free fractions of the Sn(II) and the Sn(IV) nuclei in these compounds, as well as infrared spectroscopic data, suggests that the two compounds may not have the same structure. An X-ray structural determination of the compound isolated from the reaction between $Sn(OCOCF_3)_2$ and $Sn(OCOCF_3)_4$ is necessary before this can be confirmed. There was no apparent reaction between stoichiometric mixtures of:

i) $Sn(OCOCH_3)_2$ and $Sn(OCOCH_3)_4$

ii) $Sn(SO_3CF_3)_2$ and $Sn(SO_3CF_3)_4$ or

iii) $Cs_2[Sn(SO_3F)_6]$ and $Sn(SO_3F)_2$.[169]

The mechanism of the solvolysis of hexaphenylditin by acids is not understood. Kinetic studies on this system should be carried out in order that a mechanism for this reaction may be proposed. Additionally, reactions of compounds $(C_6H_5)_3Si\text{-}Sn(C_6H_5)_3$, $(C_6H_5)_3Ge\text{-}Sn(C_6H_5)_3$ and $(C_6H_5)_3Pb\text{-}Sn(C_6H_5)_3$ with a variety of acids could be investigated. Earlier studies on the acetolysis of $(C_6H_5)_3Si\text{-}Sn(C_6H_5)_3$ and $(C_6H_5)_3Ge\text{-}Sn(C_6H_5)_3$ have shown that $(OCOCH_3)_3Si\text{-}Sn(OCOCH_3)_3$ and $(OCOCH_3)_3Ge\text{-}Sn(OCOCH_3)_3$ are produced.[170] This indicates that the

cleavage of Sn-C bonds is easier than the cleavage of the Sn-M (M - Si, Ge) bond. In the case of a tin-tin bond the reaction products indicate that there is asymmetric cleavage of this bond. In the case of the Sn-Pb bond, one might expect this to cleave forming a compound containing Sn(IV) and Pb(II) atoms since the more stable oxidation state of Pb is +2. Solvolysis of $(C_6H_5)_3Sn\text{-}M(C_6H_5)_3$ (where M = Si, Ge, Pb) in acids could be conveniently followed by ^{29}Si, ^{119}Sn and ^{207}Pb NMR spectroscopy. From metal-metal coupling constants, one could obtain information about the structure in solution.

Another successful route to the preparation of mixed valence tin compounds is given in equation (6.4).

$$SnF_2 + Sn(OCOR)_4 \longrightarrow [SnF_2 \cdot Sn(OCOR)_4] \qquad (6.4)$$

When R = CF_3, a crystalline material was isolated and its structure was shown by X-ray diffraction to be $[Sn(II)_2Sn(IV)_2F_4(OCOCF_3)_8 \cdot 2CF_3CO_2H]$ consisting of eight membered rings with Sn(II) and Sn(IV) atoms bridged by cis-fluorine atoms and trifluoroacetate groups. The above reaction opens up a new area of research. Reactions between different stoichiometric mixtures of SnF_2 and tin(IV) carboxylates could produce mixed valence tin compounds containing different ratios of Sn(II) and Sn(IV). This work could be extended further by studying the reactions between PbF_2 and tin(IV) carboxylates which are expected to form mixed valence compounds containing Pb(II) and Sn(IV) atoms probably bridged by fluorine.

6.2 Structures of Tin-Acid Complexes

The structures of only a few compounds of tin with carboxylic or fluorosulphuric acids are accurately known from X-ray studies, but in

other cases the structures have been inferred from spectroscopic data. This work is summarized in Table 6.2.

Dialkyltin(IV) and trialkyltin(IV) carboxylic and fluorosulphuric acid derivatives usually adopt octahedral and trigonal bipyramidal geometires, respectively. In the solid state, these coordination numbers are achieved through polymerization while in solution it is likely that an equilibrium exists between monomeric and polymeric units, but with an average tin environment similar to that of the solid presumably by addition of further molecules of solvation if necessary.

Tin(II) shows a variety of coordination numbers. Donaldson and Grimes have recently published a review on structures containing tin(II) atoms.[98] They consider that most tin(II) compounds adopt either a trigonal pyramidal or a distorted square pyramidal arrangement of ligands about the tin atom with a coordination number of four and five respectively, if the stereoactive lone pair is included in the coordination count. Other reviews on structural tin(II) chemistry cite examples where the coordination number of the tin atom is three, four, five and seven (including the lone pair).[102,103] Tin(II) atoms in mixed valence tin carboxylates exhibit coordination numbers of six and seven in all of the known cases (Table 6.2). There are three crystallographically distinct tin(II) atoms described in this thesis which contain trifluoroacetate groups in their coordination spheres.

When tin(II) is coordinated by trifluoroacetate ions the arrangement can be analysed using bond valences.[122] The bonds between tin(II) and the trifluoroacetate ion can be considered as being the result of an acid (Sn^{2+}) and a base ($CF_3CO_2^-$) interaction. This acid-base bond

TABLE 6.2

Compound	Solid Structure; Tin Coordination Number	Probable Solution Structure; Tin Coordination Number
I Tin(IV)		
(a) R_3SnA, A=$R'COO^-$ or SO_3F^-	Polymeric; 5	Monomer ⇌ polymer equilibrium; 5
		Monomeric unit $[R_2SnA_2]^-$ where A = SO_3F^-
$(CH_3)_{3-n}SnX_nA$; A = SO_3F^-		Monomeric unit $[Me_{3-n}SnX_nA_2]^-$; 5
(b) R_2SnA_2; A=$R'COO^-$ or SO_3F^-	Polymeric; 6	Monomer ⇌ polymer eqm; 6
		Monomeric unit $[R_2SnA_4]^{2-}$; 6 A = SO_3F^-
(c) SnA_4; A = CH_3COO^- [93]	Monomeric; 6	Unknown
A = $CF_3SO_3^-$ [25]	Monomeric; 6 or 4	
A = FSO_3^-	?	
II Tin(II)		
(a) $Sn(O_2CH)_2$ [101]	Polymeric; 6 (SnX_5E)	Unknown
(b) $Sn(O_2CR_3)$ [96-97]	Monomeric; 4 (SnX_3E)	
(c) $Sn(O_2C_2)^{2-}$ [100]	Monomeric; 5 (SnX_4E)	

III Mixed valence tin(II),tin(IV) carboxylates

Compound	Solid State Structure-Monomer: Tin(II) Coordination Number	Tin(IV) Coordination Number
1. $[Sn(II)Sn(IV)(O_2C{\cdot}C_6H_4NO_2)_4O(THF)]_2$ [26]	7	6
2. $[Sn(II)Sn(IV)O(O_2CCF_3)_4]_2C_6H_6$ [18]	6-(SnX_5E)	6
3. $[Sn(II)_4Sn(IV)O_2(O_2CCF_3)_8]$	6-(SnX_5E)	6
4. $[Sn(II)_2Sn(IV)_2F_4(O_2CCF_3)_8{\cdot}2CF_3CO_2H]_2$ i)	7	6
ii)	6 (SnX_5E)	6

will normally be formed only when the Lewis acid strength of the electron acceptor (Sn^{2+}) is close to that of the Lewis base strength of electron donor ($CF_3CO_2^-$).[171]

The coordination of tin(II) atoms in a number of complexes formed to oxygen and fluorine-containing ligands has been considered to be derived from an octahedral arrangement.[126] The possible environments are given below.

(i) 3 coordinated, based on a tetrahedron (SnX_3E)

(ii) 4 coordinated, based on a trigonal bipyramid (SnX_4E)

(iii) 5 coordinated, based on an octahedron (SnX_5E).

The possible assignment of bond valencies around the tin in the above three cases are shown below.

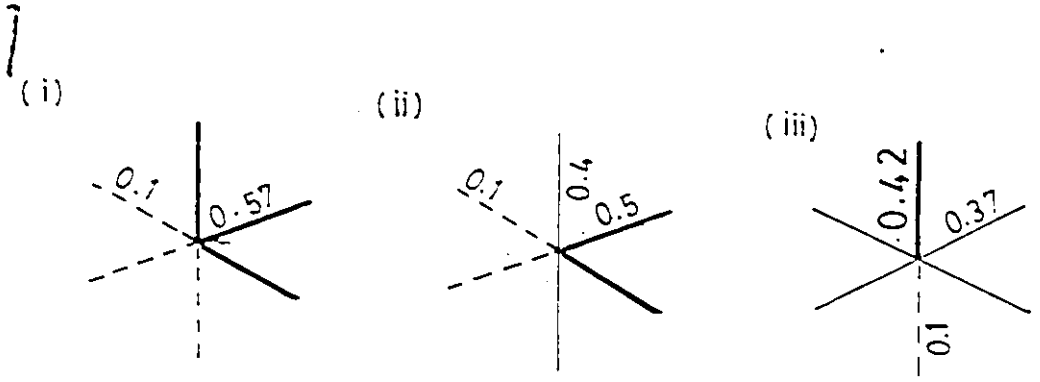

In all cases there are also a number of longer bonds arranged about the lone pair direction, these are indicated by dashed lines. Also each octahedron has been distorted so that the weak bonds occur opposite the strong bonds, and bonds of intermediate strength occur opposite to each other. Initially the valence of each long bond is assumed to be 0.1 v.u. (valence unit) and then the rest of the valencies are distributed between strong and intermediate bonds such that the total valence around tin is 2.

Firstly, in order to form coordination of type (i), the base strength of one oxygen atom of the trifluoroacetate ion has to be 0.57 v.u.. Such a strength is unusually high[171] and in addition it would cause the trifluoroacetate ion to be asymmetric. Its bond valencies would be represented as below.

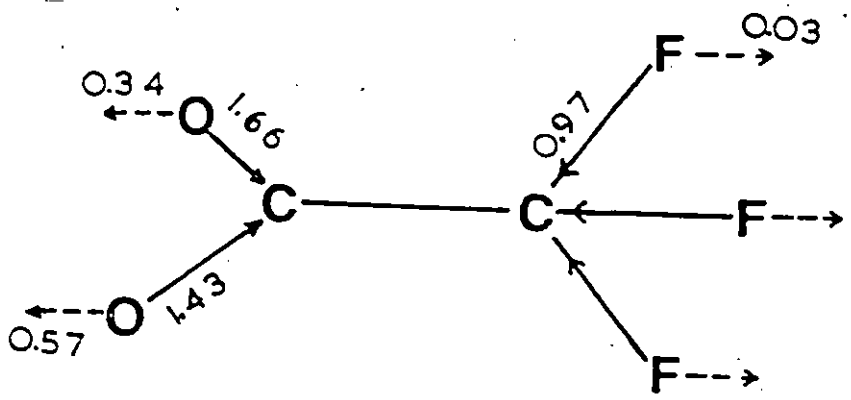

An arrow placed on the bond indicates the direction of net electron flow into the bond when isolated ions are brought together or when an electron donor forms a bond with an electron acceptor. Each fluorine atom of the $-CF_3$ group acts as an electron donor to other atoms usually with an acid strength of 0.03 v.u.. The combined acid strength of the three fluorines is 0.09 (3x0.03)v.u., leaving an acid strength of 0.91 (1-0.09) v.u. to be distributed between the two oxygens. If the base strength of one of the oxygens of the trifluoroacetate ion is 0.57 v.u. then, the other oxygen would be 0.34 v.u.. This implies that Sn-O bonds having valencies 0.57 v.u. and 0.34 v.u. would be formed. This is in disagreement with type (i) coordination where only three strong Sn-O bonds of valence

0.57 are allowed. Therefore this is unlikely to occur.

For type (ii), the basicity of one of the trifluoroacetate oxygens would be 0.50 v.u. and this would cause less asymmetry than in the previous case. The bond valencies can be represented as shown below.

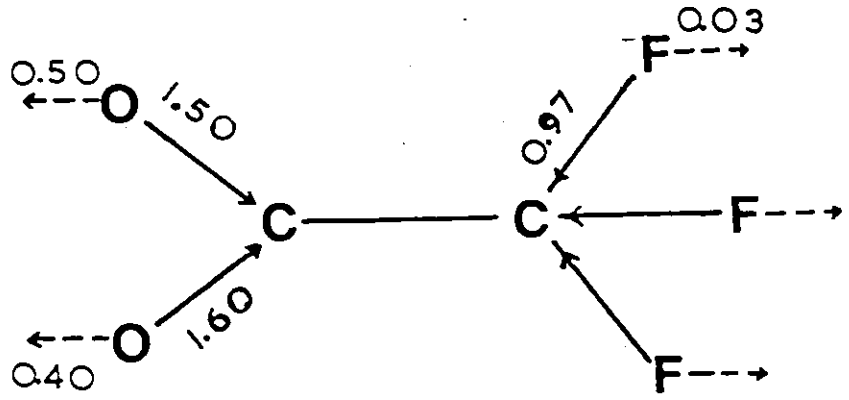

This ion would form Sn-O bonds of strength 0.50 v.u. and 0.40 v.u., hence coordination of type (ii) is more reasonable.

In type (iii), the strong bond of valency 0.42 v.u. would cause the trifluoroacetate ion to be less asymmetric than in the above two cases and can be represented as shown below.

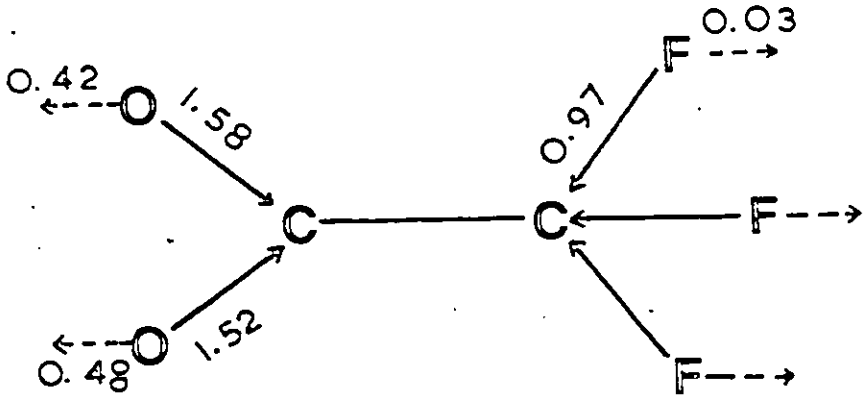

The base strength of the oxygens of this trifluoroacetate ion (0.42, 0.48 v.u.) can vary in order to form bonds of valency 0.42 and 0.37 v.u. but some adjustment would be required in its internal structure.

The tin(II) coordination in the mixed valence tin compound, discussed in Section 4.5 of this thesis, can also be described as SnX_4E if the weaker interaction is ignored. The Mössbauer parameters of this tin(II) atom and that of $Sn(OCOCF_3)_2$ are similar. This supports the inference that the geometry about the tin in $Sn(OCOCF_3)_2$ is best represented by SnX_4E. Based on the above arguments, one can propose a polymeric structure for $Sn(OCOCF_3)_2$ which is shown in Figure 6.1. The tin coordination in this structure is similar to that of $Sn(O_2CH)_2$ yet, different from the generally assumed trigonal pyramidal coordination for tin(II)carboxylates.[98]

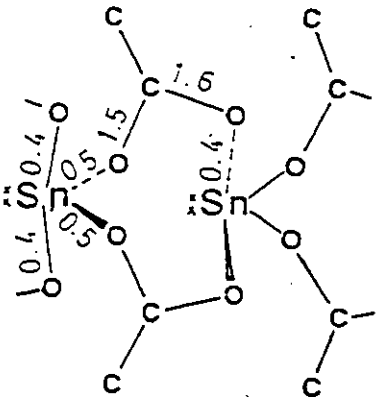

Figure 6.1 Proposed structure of $Sn(CO_2CF_3)_2$. The bond valencies are given along the bonds in valence unit (v.u.).

6.3 Analysis of Trifluoroacetate Ions Using the Bond Valence Model

The geometry of the solid state acetates and trifluoroacetates have been analysed by Brown based on the bond valence model.[171] He has considered a large number of structures containing these ions and has studied the variations in their internal geometry. Since the crystal structures described in this thesis contains a variety of trifluoroacetate groups, it was decided to examine their geometry based on the trends observed in Brown's work.[171]

The geometry of the CO_2 group can be analysed and Figure 6.2 shows the O-C-O and C-C-O angles (θ) plotted against the average bond valence <s> of the C-O and C-C bonds that define them. The set of angles obtained from other structures reported in the literature have been well described by equation (6.5).[171]

$$\theta = 71 + 36.7 \langle s \rangle^{\circ} \qquad (6.5)$$

The correlation corresponding to this equation is shown as a dashed line in Figure 6.2. It can be seen that a least square fitted line ($r = 0.98$), to the data reported in this thesis, can be drawn which is represented by equation (6.6). This is shown as the solid line in Figure 6.2.

$$\theta = 50.7 + 53.2 \langle s \rangle^{\circ} \qquad (6.6)$$

Equation (6.5) is derived from a large data set which describes both the acetate and the trifluoroacetate ions whereas, equation (6.6) is obtained only for the trifluoroacetate ions discussed in this thesis. This probably accounts for the difference between equations (6.5) and (6.6).

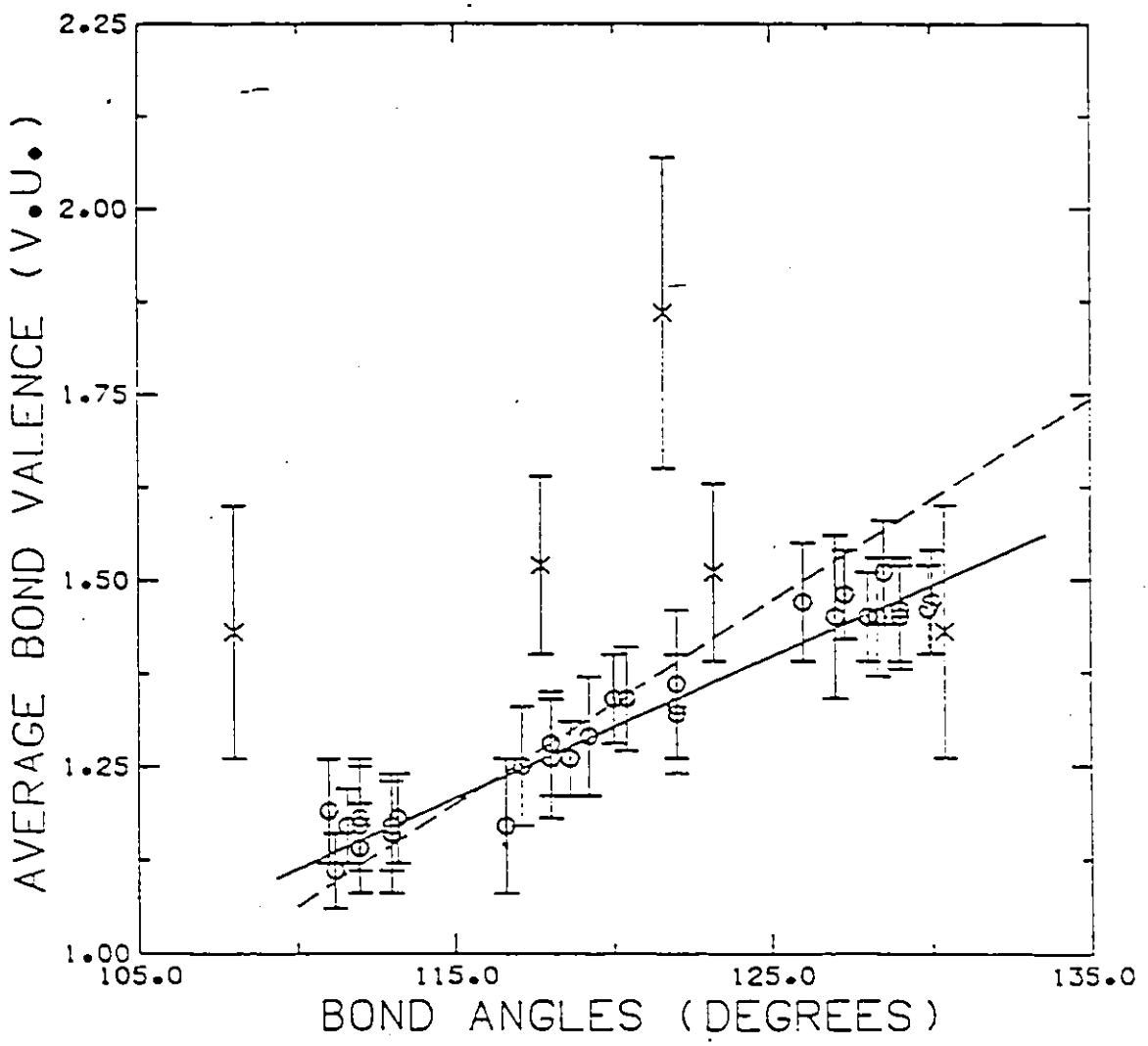

Figure 6.2: Plot of bond angles against average bond valencies of trifluoroacetate ions. The solid line represents the best fitted line through the points. Points denoted by (X) are excluded from the fit. These points arise from the structure discussed in Section 4.5. The dashed line is drawn according to the equation derived by Brown.[171]

REFERENCES

1. T. Birchall and J. P. Johnson, Inorg. Chem., 21, 3724, (1982).
2. T. Birchall, P.K.H. Chan and A. Pereira, J. Chem. Soc. Dalton Trans., 2157, (1974).
3. M. Yasuda and R. S. Tobias, Inorg. Chem., 2, 207, (1963).
4. H. N. Farrer, M. M. McGrady and R. S. Tobias, J. Am. Chem. Soc., 87, 5019, (1965).
5. R. S. Tobias and C. E. Freidline, Inorg. Chem., 4, 215, (1965).
6. M. M. McGrady and R. S. Tobias, Inorg. Chem., 3, 1157, (1964).
7. J. P. Johnson, Ph.D. Thesis, McMaster University, (1983).
8. J. R. Webster and W. L. Jolly, Inorg. Chem., 10, 877, (1971).
9. F. Paneth and K. Fürth, Ber., 52, 2020, (1919).
10. G. A. Olah, Top. Curr. Chem., 80, 19, (1979).

11a) R. Sasin and G. S. Sasin, J. Org. Chem., 20, 770 (1955).

b) G. S. Sasin, A. L. Borror and R. Sasin, J. Org. Chem., 23, 1366, (1958).

12. A. Henderson and A. K. Holliday, J. Organomet. Chem., 4, 377, (1965).
13. R. K. Ingham, S. D. Rosenberg and H. Gilman, Chem. Rev., 60, 459, (1960).
14. A. K. Sawyer and C. Frey, Synth. React. Inorg. Met.-Org. Chem., 13, 259, (1983).
15. T. Birchall and J. P. Johnson, Can. J. Chem., 57, 160, (1979).
16. V. G. Kumar Das and P. R. Wells, J. Organomet. Chem., 23, 143, (1970).
17. J. D. Donaldson and A. Jelen, J. Chem. Soc. (A), 2244, (1968).
18. T. Birchall and J. P. Johnson, J. Chem. Soc. Dalton Trans., 69, (1981).

19. K. Hasselbach, G. Murken and M. Trömel, Z. Anorg. Allg. Chem., 397, 127, (1973).

20. D. Mootz and H. Puhl, Acta. Crystallogr., 23, 471, (1967).

21. M. Nardelli, C. Pelizzi and G. Pelizzi, J. Organomet. Chem., 85, C43, (1975).

22. E. J. Bulten and H. A. Budding, J. Organomet. Chem., 157, C3, (1978).

23. M. F. A. Dove, R. King and T. J. King, J. Chem. Soc. Chem. Commun., 944, (1973).

24. R. Sabatier, A.-M. Hebrard and J.-C. Cousseins, Compt. rend. Acad. Sci. Paris, Series C, 1121, (1974).

25. R. J. Batchelor, J. N. Ruddick, J. R. Sams and F. Aubke, Inorg. Chem., 16, 1414, (1977).

26. P. F. R. Ewings, P. G. Harrison, A. Morris and T. J. King, J. Chem. Soc. Dalton Trans., 1602, (1976).

27. T. Birchall, P. A. W. Dean and R. J. Gillespie, J. Chem. Soc. (A), 1777, (1971).

28. J. D. Donaldon and J. D. O'Donoghue, J. Chem. Soc., 271, (1964).

29. R. C. Poller, "The Chemistry of Organotin Compounds", Logos, London, (1970).

30. V. S. Petrosyan, Prog. Nucl. Magn. Reson. Spectrosc., 11, 115, (1977).

31. T. N. Mitchell, J. Organomet. Chem., 59, 189, (1973).

32. P. A. W. Dean, R. J. Gillespie and P. K, Ummat, Inorg. Synth., 15, 213, (1974).

33. A. D. Norman, J. R. Webster and W. L. Jolly, Inorg. Synth., 11, 170, (1968).

34. N. Flitcroft and H. D. Kaesz, J. Am. Chem. Soc., 85, 1377, (1963).

35. A. E. Finholt, A. C. Bond, Jr., K. E. Wilzback and H. I. Schlesinger, J. Am. Chem. Soc., 69, 2692, (1947).

36. J. D. Donaldson, W. Moser and W. B. Simpson, J. Chem. Soc., 5942, (1964).

37. R. J. Gillespie, J. V. Oubridge and C. Solomons, J. Chem. Soc., 1804, (1957).

38. J. Barr, R. J. Gillespie and R. C. Thompson, Inorg. Chem., 3, 1149, (1964).

39. D. Shaw in "NMR and the Periodic Table", Edited by R. K. Harris and B. E. Mann, Academic Press, New York, Chapter 2, p. 21, (1978).

40. N. R. Draper and H. Smith, "Applied Regression Analysis", 2nd Edition, Wiley, New York, Chapter 10, (1981).

41. G. M. Bancroft, W. K. Ong, A. F. Maddock, R. K. Prince and A. J. Stone, J. Chem. Soc., (A), 1966, (1967).

42. K. Ruebenbauer and T. Birchall, Hyperfine Interactions, 7, 125, (1979).

43. R. Faggiani, D.K. Kennepohl, C.J.L. Lock and G.J. Schrobilgen, Inorg. Chem., 25, 563, (1986).

44. J. F. Britten, Ph.D. Thesis, McMaster University, (1984).

45. J. M. Stewart, The X-Ray 76 System, Technical Report TR-446; Computer Science Centre, University of Maryland; College Park, MD, (1976).

46. D. T. Crommer and J. T. Waber, "International Tables for X-ray Crystallography", J. A. Ibers, W. L. Hamilton, Eds. Kynoch Press, Birmingham, England, (1974); Vol. IV, Table 2.2B, p. 99-101.

47. D. T. Crommer, Reference (45), Vol. IV, Table 2.3.1, p. 119-150.

48. G. M. Sheldrick, SHELX program for Crystal Structure Determination, University of Cambridge, (1976).

49. C. K. Johnson, ORTEP II, Report ORLN-5138, Oak Ridge National Laboratory;

Oak Ridge, TN, (1976).

50. R. Okawara and E. G. Rochow, J. Am. Chem. Soc., 82, 3285, (1960).

51. M. L. Maddox, N. Flitcroft and H. D. Kaesz, J. Organomet. Chem., 4, 50, (1965).

52. R. H. Herber and G. I. Parisi, Inorg. Chem., 5, 769, (1966).

53. L. May, J. J. Spijkerman, J. Chem. Phys., 46, 3272, (1967).

54. C. D. Schaeffer, S. E. Ulrich and J. J. Zuckerman, Inorg. Nucl. Chem. Lett., 14, 55, (1978).

55. A. K. Sawyer and H. G. Kuivila, J. Org. Chem., 27, 837, (1962).

56. A. K. Sawyer and H. G. Kuivila, J. Org. Chem., 27, 610, (1962).

57. A. K. Sawyer, J. E. Brown and E. L. Hanson, J. Organomet. Chem., 3, 464, (1965).

58. A. K. Sawyer and H. G. Kuivila, Chem. Ind. (London), 260, (1961).

59. P. A. Yeats, J. R. Sams and F. Aubke, Inorg. Chem., 10, 1877, (1971).

60. R. J. Gillespie, A. Netzer and G. J. Schrobilgen, Inorg. Chem., 13, 1455, (1974).

61a) P. Pregosin and E. W. Randall, in "Determination of Organic Structures by Physical Methods", Eds. F. C. Nachod and J. J. Zuckerman, N.Y. 4, 263, (1971).

b) R. Lichter, ibid, 4, 195, (1971).

62. B. K. Hunter and L. W. Reeves, Can. J. Chem., 46, 1399, (1968).

63. S. L. Manatt, G. L. Juvinall, R. I. Wagner and D. D. Elleman, J. Am. Chem. Soc., 88, 2689, (1966).

64. P. G. Harrison, S. E. Ulrich and J. J. Zuckerman, J. Am. Chem. Soc., 93, 5398, (1971).

65. R. K. Harris, "Nuclear Magnetic Resonance Spectroscopy", Pitman Books Ltd., London, p. 211, (1983).

66. H. C. Clark, R. J. O'Brien and J. Trotter, Proc. Chem. Soc., 85, (1963).

67. P. A. Yeats, B. F. E. Ford, J. R. Sams and F. Aubke, J. Chem. Soc. Chem. Commun., 791, (1969).

68. F. H. Allen, J. A. Lerbscher and J. Trotter, J. Chem. Soc. (A), 2507, (1971).

69. P. J. Smith and A. P. Tupčiauskas, Annu. Rep. NMR Spectrosc. , 8, 291, (1978).

70. B. Wrackmeyer, Annu. Rep. NMR Spectrosc. , 16, 73, (1985).

71. J. D. Kennedy and W. McFarlane, J. Chem.Soc. Chem. Commun., 983, (1974).

72. W. McFarlane, J. Chem. Soc. (A), 528, (1967).

73. Y. C. Puskar, T. A. Saluvere, E. T. Lippmaa, A. B. Permin and V. S. Petrosyan, Dokl. Akad. Nauk SSSR, 220, 112, (1975).

74. C. R. Lassigne and E. J. Wells, J. Magn. Reson., 26, 55, (1977).

75. R. R. Sharp and J. W. Tolan, J. Chem. Phys., 65, 522, (1976).

76. S. J. Blunden, A. Frangou and D. G. Gillies, Org. Magn. Reson., 20, 170, (1982).

77. G. A. Webb, in Reference (39), Chapter 3, p. 49.

78. J. H. Noggle, R. E. Schirmer, "The Nuclear Overhauser Effect", Academic Press , New York, (1971).

79. D. Wallach, J. Chem. Phys., 47, 5258, (1967).

80. L. Werbelow, J. Magn. Reson., 57, 136, (1984).

81. J.-Y. Lallemand, J. Soulié and J-C. Chottard, J. Chem. Soc. Chem. Commun., 436, (1980).

82. R. E. Wasylishen, R. E. Lenkinski and C. Rodger , Can. J. Chem., 60, 2113, (1982).

83. F. Brady, R. W. Matthew, M. J. Foster and G. D. Gillies, Inorg. Nucl. Chem. Lett., 17, 155, (1981).

84. G. R. Hays, D. G. Gillies, L. P. Blaauw and A. D. H. Clague, J. Magn. Reson., 45, 102 (1981).

85. S. C. F. Au-Yeung and D. R. Eaton, J. Magn. Reson., 52, 366, (1983).

86. R. Okawara and M. Ohara, in "Organotin Compounds", Ed. A. K. Sawyer, Dekker, New York, Vol. 2, p. 253, (1971).

87. W. McFarlane and R. J. Wood, J. Organomet. Chem., 40, C17, (1972).

88. P. J. Smith, Organomet. Chem. Rev. (A), 5, 373, (1970).

89. J. N. R. Ruddick, Rev. Silicon, Germanium, Tin Lead Compd., 2, 115, (1976).

90. Y. Maeda and R. Okawara, J. Organomet. Chem., 10, 247, (1967).

91. W. F. Howard, R. W. Crecely and W. H. Nelson, Inorg. Chem., 24, 2204, (1985).

92. H. H. Anderson, Inorg. Chem., 3, 912, (1964).

93. N. W. Alcock and V. L. Tracy, Acta Crystallogr., B35, 80, (1979).

94. J. D. Donaldson and A. Jelen, J. Chem. Soc. (A), 1448, (1968).

95. A. Jelen and O. Linquist, Acta. Chem. Scand., 23, 3071, (1969).

96. J. C. Dewan, J. Silver , J. D. Donaldson and M. J. K. Thoman, J. Chem. Soc. Dalton Trans., 2319, (1977).

97. S. J. Clark, J. D. Donaldson, J. C. Dewan and J. Silver, Acta Crystallogr., B35, 2550, (1979).

98. J. D. Donaldson and S. M. Grimes, Rev. Silicon, Germanium, Tin, Lead Compd., 8, 1, (1984).

99. Z. Arifin, E. J. Filmore, J. D. Donaldson and S. M. Grimes, J. Chem. Soc. Dalton Trans., 1965, (1984).

100. J. D. Donaldson, M. T. Donoghue and C. H. Smith, Acta, Crystallogr., B32, 2098, (1976).

101. P. G. Harrison and E. W. Thornton, J. Chem. Soc. Dalton Trans., 1274, (1978).

102. Y. K. Ho and J. J. Zuckerman, J. Organomet. Chem., 49, 1, (1973).

103. P. G. Harrison, Cord. Chem. Rev., 20, 1, (1976).

104. J. Holeček, K. Handlíř, M. Nádvorník and A. Lyčka, J. Organomet. Chem., 258, 147, (1983).

105. A. G. Davies, P. G. Harrison, J. D. Kennedy, T. N. Mitchell, R. J. Puddephatt and W. McFarlane, J. Chem. Soc. (C), 1136, (1969).

106. A. P. Tupčiauskas, N. M. Sergeyev, Yu. A. Ustynyuk, Org. Magn. Reson., 3, 655, (1971).

107. Ho-M. M. Yeh and R. A. Geanangel, Inorg. Chim. Acta, 52, 113, (1981).

108. P. A. W. Dean. D. D. Phillips and L. Polensek, Can. J. Chem., 59, 50, (1981).

109. J. J. I. Arsenault and P. A. W. Dean, Can. J. Chem., 61, 1516, (1983).

110. B. Wrackmeyer, J. Magn. Reson., 61, 536, (1985).

111. A. Bonny, A. D. McMaster and S. R. Stobart, Inorg. Chem., 17, 935, (1978).

112. T. Birchall, R. J. Batchelor and J. P. Johnson, Unpublished results.

113. N. W. G. Debye, D. E. Fenton and J. J. Zuckerman, J. Inorg. Nucl. Chem., 34, 352, (1972).

114. E. N. Vasantha, G. Srivastava and R. C. Mehrotra, Inorg. Chim. Acta, 26, 47, (1978).

115. A. Lyčka and J. Holeček, J. Organomet. Chem., 294, 179, (1985).

116. C. D. Garner, D. Sutton and S. C. Wallwork, J. Chem. Soc. (A), 1949, (1967).

117. T. Yano, K. Nakashima, J. Otera and R. Okawara, Organometallics, 4, 1501, (1985).

118. F. W. B. Einstein, C. H. W. Jones, T. Jones and R. D. Sharma, Can. J. Chem., 61, 2611, (1983).

119. P. G. Harrison, M. J. Begley and K. C. Molloy, J .Organomet. Chem, 186, 213, (1980).

120. R. Okawara, Proc. Chem. Soc., 383, (1961).

121. R. Faggiani, J. P. Johnson, I. D. Brown and T. Birchall, Acta Crystallogr., B34, 3743, (1978).

122. I. D. Brown, Chem. Soc. Rev., 7, 359, (1978).

123. I. D. Brown and R. D. Shannon, Acta Crystallogr., A29, 266, (1973).

124. I. D. Brown and D. Altermatt, Acta Crystallogr., B41, 244, (1985).

125. I. D. Brown, personal communication.

126. I. D. Brown, J. Solid State Chem., 11, 214, (1974).

127. R. J. Gillespie, "Molecular Geometry", Van Nostrand Reinhold Company, London, (1972).

128. J. Gally, G. Meunier, S. Anderson and A. Aström, J. Solid State Chem., 13, 142, (1975).

129. G. Dénès, J. Pannetier, J. Lucas and J. Y. Le Marouille, J. Solid State Chem., 30, 335, (1979).

130. R. C. McDonald, H. Ho_Kuen Hau and K. Eriks, Inorg. Chem., 15, 762, (1976).

131. J. Pannetier and T. Birchall, Unpublished results.

132. R. Faggiani, J. P. Johnson, I. D. Brown and T. Birchall, Acta Crystallogr., (a) B34, 3743, (1978). (b) ibid B35, 1227, (1979).

133. R. H. Herber, "Chemical Mössbauer Spectroscopy", Ed. R. H. Herber, Chapter VII, p. 199, (1984).

134. R. H. Herber, A. Shanzer and J. Libman, Organometallics 3, 586, (1984).

135. P. G. Harrison, R. C. Philips and E. W. Thornton, J. Chem. Soc. Chem. Commun., 603, (1977).

136. A. B. Deacon and R. J. Philips, Coord. Chem. Rev., 33, 227, (1980).

137. T. Birchall, G. Dénès, K. Rubenbauer and J. Pannetier, J. Chem. Soc. Dalton Trans., 1831, (1981).

138. G. Dénès, J. Pannetier and J. Lucas, J. Solid State Chem., 33, 1, (1980).

139. R. R. McDonald, A. C. Larson and D. T. Cromer, Acta Crystallogr., 17, 1104, (1964).

140. J. D. Donaldson and B. J. Senior, J. Chem. Soc. (A), 1821, (1967).

141. G. Bergerhoff, L. Goost and E. Schultze-Rhonhof, Acta Crystallogr., B24, 803, (1968).

142. G. Bergerhoff and H. Namgung, Acta Crystallogr., B34, 699 (1978).

143. T. Birchall and G. Dénès, Can. J. Chem., 62, 591, (1984).

144. L. Golič, and I. Leban, Acta Crystallogr., B33, 232, (1977).

145. A. J. Edwards and K. I. Khallow, J. Chem. Soc. Chem. Comm., 50, (1984).

146. B. Frlec, D. Gantar and J. H. Holloway, J. Fluorine Chem., 20, 385, (1982).

147. J. Von Bönisch and G. Bergerhoff, Z. Anorg. Allg. Chem., 473, 35, (1981).

148. J. D. Donaldson, D. R. Laughlin and D. C. Puxley, J. Chem. Soc. Dalton Trans., 865, (1971).

149. P. A. W. Dean and D. F. Evans, J. Chem. Soc. (A), 1154, (1968).

150. P. A. W. Dean, Can. J. Chem., 51, 4024, (1973).

151. R. Colton, D. Dakternieks and C. A. Harvey, Inorg. Chim. Acta, 61, 1, (1982).

152. K. B. Dilon and M. Andrew, J. Chem. Soc. Dalton Trans., 1245, (1984).

153. T. N. Mitchell and G. Walter, J. Chem. Soc. Perkin Trans., 1842, (1977).

154. B. Mathiasch and T. N. Mitchell, J. Organomet. Chem., 185, 351, (1980).

155. T. N. Mitchell and M. El-Behairy, J. Organomet. Chem., 172, 293, (1979).

156. A. Blecher, B. Mathiasch and T. N. Mitchell, J. Organomet. Chem., 184, 175, (1980).

157. T. P. Lockhart, W. F. Manders and F. Brinckman, J. Organomet. Chem., 286, 153, (1985).

158. M. E. Redwood and C. J. Willis, Can. J. Chem., 45, 389, (1967).

159. A. G. Davis, L. Smith and P. J. Smith, J. Organomet. Chem., 23, 135, (1970).

160. C. A. Clausen and M. L. Good, Inorg. Chem., 9, 817, (1970).

161. P. Main, S. J. Fiske, S. E. Hull, L. Lessinger, G. Germain, J.-P. Declercq and M. M. Woolfson, (1980). MULTAN80. A System of Computer Programs for the Automatic Solution of Crystal Structures from X-ray Diffraction Data. Univs. of York, England, and Louvain, Belgium.

162. R. Hoppe and W. Dähne, Naturwissenschaften, 49, 254, (1962).

163. E. A. Marseglia and I. D. Brown, Acta. Crystallogr., B29, 1352, (1973).

164. C. Hebecker, H. G. Von Schnering and R. Hoppe, Naturwissenschaften, 53, 154, (1966).

165. M. J. Durand, J. L. Galigne and A. Lari-Lavassani, J. Solid State Chem., 16, 157, (1976).

166. G. Bergerhoff and L. Goost, Acta. Crystallogr., B26, 19, (1970).

167. R. Weiss, B. Chevrier and J. Fischer, Compt. Rend., 260, 3664, (1965).

168. V. G. Fritz and H. Scheer, (a) Z. Naturforsch., 19B, 537 (1964); (b) Z. Anorg. Allg. Chem., 338, 1, (1965).

169. S. P. Mallela, K. C. Lee and F. Aubke, Inorg. Chem., 23, 653, (1984).

170. E. Wiberg, E. Amberger and H. Cambensi, Z. Anorg. Allg. Chem., 351, 164, (1967).

171. I. D. Brown, J. Chem. Soc. Dalton Trans., 1118, (1980).

APPENDIX I - ANISOTROPIC TEMPERATURE FACTORS ($Å^2 \times 10^3$) FOR $[Sn(II)_2Sn(IV)_2F_4(O_2CCF_3)_8 \cdot 2CF_3CO_2H]$

APPENDIX I

Anisotropic Temperature Factors ($°A^2 \times 10^3$) for

$Sn(II)_2Sn(IV)_2F_4(O_2CCF_3)_8 \cdot 2CF_3CO_2H$

Atom	U_{11}	U_{22}	U_{33}	U_{12}	U_{13}	U_{23}
Sn1	20.2(3)	18.0(3)	23.7(3)	5.8(2)	9.6(3)	11.1(2)
Sn2	30.1(4)	19.2(3)	29.4(3)	10.2(3)	16.5(3)	14.3(3)
Sn3	21.3(3)	16.8(3)	22.9(3)	7.1(2)	12.2(3)	11.3(2)
Sn4	29.1(4)	16.8(3)	26.7(3)	7.0(3)	14.6(3)	10.8(3)
F1	21(3)	18(2)	25(3)	5(2)	7(2)	9(2)
F2	25(3)	20(2)	28(3)	5(2)	14(2)	14(2)
F3	98(6)	73(5)	80(5)	21(4)	72(5)	40(4)
F4	73(5)	84(5)	98(6)	43(5)	66(5)	44(5)
F5	82(6)	114(7)	60(5)	- 14(5)	55(5)	- 19(5)
F6	40(4)	89(5)	44(4)	17(4)	18(3)	41(4)
F7	32(4)	114(6)	62(5)	9(4)	19(4)	42(4)
F8	103(7)	76(6)	100(6)	69(5)	6(6)	33(5)
F9	134(7)	64(4)	64(4)	79(5)	74(5)	49(4)
F10	123(7)	55(4)	90(5)	45(4)	88(5)	50(4)
F11	112(7)	61(4)	30(4)	38(4)	26(4)	16(3)
F12	152(8)	99(6)	97(6)	92(6)	88(6)	85(5)
F13	122(7)	66(5)	58(4)	67(5)	55(5)	28(4)
F14	52(5)	92(6)	118(7)	37(5)	39(5)	40(5)
F21	27(3)	16(2)	28(3)	8(2)	17(2)	13(2)
F22	27(3)	25(3)	31(3)	11(2)	19(2)	14(2)
F23	47(4)	50(3)	61(4)	27(3)	30(3)	45(3)
F24	52(4)	48(4)	33(3)	14(3)	- 2(3)	12(3)
F25	42(4)	97(5)	62(4)	44(4)	34(4)	60(4)
F26	50(5)	83(5)	74(5)	- 11(4)	21(4)	41(4)
F27	96(6)	63(5)	201(9)	43(5)	102(7)	99(6)
F28	107(6)	70(5)	73(5)	- 7(4)	68(5)	21(4)
F29	240(11)	36(4)	86(6)	48(5)	123(7)	30(4)
F30	108(8)	167(9)	72(6)	- 37(7)	74(6)	- 15(6)
F31	155(9)	100(6)	52(5)	69(6)	57(6)	51(5)
F32	45(4)	60(4)	29(3)	14(3)	11(3)	25(3)
F33	31(4)	77(5)	57(4)	14(3)	26(3)	36(4)
F34	58(4)	45(4)	65(5)	36(3)	12(4)	24(3)
F35	51(4)	56(4)	71(5)	32(4)	26(4)	26(4)
F36	168(9)	35(4)	110(6)	29(5)	107(7)	36(4)
F37	58(5)	55(4)	32(4)	16(3)	2(3)	3(3)
O1	24(3)	23(3)	28(3)	4(3)	13(3)	11(3)
O2	23(3)	21(3)	28(3)	8(3)	6(3)	9(3)
O3	36(4)	26(3)	26(3)	13(3)	14(3)	13(3)

APPENDIX 1 (Continued)

Atom	U_{11}	U_{22}	U_{33}	U_{12}	U_{13}	U_{23}
O4	21(3)	27(3)	34(4)	3(3)	9(3)	15(3)
O5	31(4)	32(4)	36(4)	2(3)	19(3)	16(3)
O6	43(4)	37(4)	32(4)	7(3)	19(4)	15(3)
O7	30(4)	39(4)	41(4)	12(3)	16(3)	29(3)
O8	43(4)	32(4)	43(4)	17(3)	20(4)	17(4)
O9	37(4)	24(3)	37(4)	12(3)	20(3)	19(3)
O10	61(5)	49(4)	59(5)	31(4)	46(4)	42(4)
O11	26(4)	33(3)	32(4)	12(3)	15(3)	19(3)
O12	37(4)	15(3)	31(3)	9(3)	25(3)	9(3)
O13	23(3)	18(3)	32(3)	4(3)	10(3)	12(3)
O14	54(5)	27(3)	29(4)	-3(3)	21(4)	10(3)
O15	25(3)	33(4)	32(4)	14(3)	17(3)	18(3)
O16	27(4)	27(3)	34(4)	8(3)	16(3)	14(3)
O17	34(4)	14(3)	39(4)	9(3)	21(3)	15(3)
O18	51(5)	25(3)	55(5)	20(3)	36(4)	22(3)
O19	31(4)	41(4)	54(5)	13(3)	7(4)	30(4)
O20	40(4)	39(4)	35(4)	10(4)	2(4)	13(3)
C1	30(5)	34(5)	24(5)	15(5)	14(4)	21(4)
C2	53(8)	46(7)	39(7)	8(6)	28(6)	5(6)
C3	33(6)	37(6)	42(6)	17(5)	25(5)	28(5)
C4	48(7)	47(7)	43(7)	29(6)	23(6)	21(6)
C5	24(5)	25(5)	25(5)	3(4)	7(4)	12(4)
C6	92(10)	27(5)	39(6)	42(6)	40(7)	18(5)
C7	36(6)	22(5)	25(5)	0(4)	10(5)	11(4)
C8	75(9)	48(7)	42(7)	33(7)	38(7)	28(6)
C9	40(6)	18(4)	32(5)	1(4)	18(5)	11(4)
C10	67(9)	63(8)	86(11)	-1(7)	3(8)	62(9)
C11	30(5)	33(5)	33(5)	13(4)	17(5)	20(5)
C12	53(7)	37(6)	35(6)	8(5)	23(6)	20(5)
C13	23(5)	20(4)	25(5)	5(4)	9(4)	13(4)
C14	30(5)	35(5)	30(5)	10(5)	16(5)	18(5)
C15	22(5)	37(6)	18(5)	5(4)	11(4)	8(4)
C16	34(6)	38(6)	39(6)	18(5)	10(5)	22(5)
C17	37(6)	21(5)	31(5)	11(4)	22(5)	12(4)
C18	43(7)	31(5)	41(6)	-3(5)	15(6)	18(5)
C19	36(6)	25(5)	41(6)	10(5)	20(5)	14(5)
C20	48(7)	34(5)	35(6)	20(5)	24(6)	16(5)

APPENDIX II(a)

MODULI OF THE OBSERVED AND CALCULATED STRUCTURE FACTORS AND STANDARD DEVIATIONS FOR $[Sn(II)_4Sn(IV)O_2(CO_2CF_3)_8]$. F(000) ON THE SAME SCALE IS 28400.

OBSERVED AND CALCULATED STRUCTURE FACTORS FOR SNBO2(OCOCF3)4 PAGE 1 OF 14

(UNOBSERVED REFLECTIONS ARE MARKED *)

OBSERVED AND CALCULATED STRUCTURE FACTORS FOR SN502(02CCF3) PAGE 2 OF 14

(UNOBSERVED REFLECTIONS ARE MARKED *)

OBSERVED AND CALCULATED STRUCTURE FACTORS FOR SN502(OCOOF)4 PAGE 3 OF 14

(UNOBSERVED REFLECTIONS ARE MARKED *)

OBSERVED AND CALCULATED STRUCTURE FACTORS FOR SN502(OZOOF)4 PAGE 4 OF 16

(UNOBSERVED REFLECTIONS ARE MARKED *)

H	K	L	FO	FC	SIG	H	K	L	FO	FC	SIG	H	K	L	FO	FC	SIG

OBSERVED AND CALCULATED STRUCTURE FACTORS FOR SN502(C2CCF3)2 PAGE 5 OF14

(UNOBSERVED REFLECTIONS ARE MARKED *)

OBSERVED AND CALCULATED STRUCTURE FACTORS FOR SN502(OCOCF3)4 PAGE 6 OF 14

(UNOBSERVED REFLECTIONS ARE MARKED *)

H	K	L	FO	FC	SIG	H	K	L	FO	FC	SIG	H	K	L	FO	FC	SIG

OBSERVED AND CALCULATED STRUCTURE FACTORS FOR [illegible]

(UNOBSERVED REFLECTIONS ARE MARKED *)

H	K	L	FO	FC	SIG
H	K	L	FO	FC	SIG
H	K	L	FO	FC	SIG
H	K	L	FO	FC	SIG
H	K	L	FO	FC	SIG

OBSERVED AND CALCULATED STRUCTURE FACTORS FOR SN502(OSCOPY)4 PAGE 9 OF 14

(UNOBSERVED REFLECTIONS ARE MARKED *)

OBSERVED AND CALCULATED STRUCTURE FACTORS FOR SMSO2(OCOOF)2

(UNOBSERVED REFLECTIONS ARE MARKED *)

OBSERVED AND CALCULATED STRUCTURE FACTORS FOR SN502(OZCOCF3)2

(UNOBSERVED REFLECTIONS ARE MARKED *)

OBSERVED AND CALCULATED STRUCTURE FACTORS FOR SMB02(C22OOF)4 PAGE12 OF14

(UNOBSERVED REFLECTIONS ARE MARKED *)

H	K	L	FO	FC	SIG	H	K	L	FO	FC	SIG	H	K	L	FO	FC	SIG

OBSERVED AND CALCULATED STRUCTURE FACTORS FOR SMGOZ(OZCOCF3)4

(UNOBSERVED REFLECTIONS ARE MARKED *)

OBSERVED AND CALCULATED STRUCTURE FACTORS FOR SNBO3(OZOOF3)4

(UNOBSERVED REFLECTIONS ARE MARKED *)

H	K	L	FO	FC	SIG	H	K	L	FC	FC	SIG	H	K	L	FO	FC	SIG

APPENDIX II(b)

MODULI OF THE OBSERVED AND CALCULATED STRUCTURE FACTORS AND STANDARD DEVIATIONS FOR $[Sn(II)_2Sn(IV)_2F_4(CO_2CF_3)_8 \cdot 2CF_3CO_2H]$. F(000) ON THE SAME SCALE IS 15720.

OBSERVED AND CALCULATED STRUCTURE FACTORS FOR SNAFM(OCOOF)2:6.6CF3COOH

(UNOBSERVED REFLECTIONS ARE MARKED *)

OBSERVED AND CALCULATED STRUCTURE FACTORS FOR SN8FB(O2CDFT)16.4DF3CO2H

(UNOBSERVED REFLECTIONS ARE MARKED *)

OBSERVED AND CALCULATED STRUCTURE FACTORS FOR SN8F8(C2COF3)16.6CF3CO2H
PAGE 3 OF 37

(UNOBSERVED REFLECTIONS ARE MARKED *)

H	K	L	FO	FC	SIG	H	K	L	FO	FC	SIG	H	K	L	FO	FC	SIG

OBSERVED AND CALCULATED STRUCTURE FACTORS FOR SN9F8(O2CCF3)16.4CFJCO2H
(UNOBSERVED REFLECTIONS ARE MARKED *)

OBSERVED AND CALCULATED STRUCTURE FACTORS FOR SN8F9(02CCF3)16.4CF3C024 PAGE 5 OF 37

(UNOBSERVED REFLECTIONS ARE MARKED *)

H	K	L	FO	FC	SIG	H	K	L	FO	FC	SIG	H	K	L	FO	FC	SIG

OBSERVED AND CALCULATED STRUCTURE FACTORS FOR SN8F8(C2CCF)116.4CF3CO2H

(UNOBSERVED REFLECTIONS ARE MARKED *)

OBSERVED AND CALCULATED STRUCTURE FACTORS FOR SNAFB(02CCFT):6.4CF30024
(UNOBSERVED REFLECTIONS ARE MARKED *)

OBSERVED AND CALCULATED STRUCTURE FACTORS FOR SN8F8(O2CCF3)16.4CF3CO2H

(UNOBSERVED REFLECTIONS ARE MARKED *)

H	K	L	FO	FC	SIG	H	K	L	FO	FC	SIG	H	K	L	FO	FC	SIG
8	-5	2	991	951	18	-10	-2	2	696	686	21	-12	2	2	371	346	31
9	-5	2	387	363	28	-12	-1	2	603	539	22	-11	2	2	833	877	19
10	-5	2	284	294	68	-11	-1	2	234	248	45	-10	2	2	782	744	33
11	-5	2	287	312	39	-10	-1	2	510	492	22	-9	2	2	231	262	33
10	-4	2	448	425	26	-9	-1	2	1212	1165	21	-8	2	2	509	685	19
9	-4	2	459	441	23	-8	-1	2	1052	1028	18	-7	2	2	339	320	23
8	-4	2	375	347	27	-7	-1	2	460	448	19	-6	2	2	279	260	25
7	-4	2	867	835	27	-6	-1	2	443	458	17	-5	2	2	522	517	24
6	-4	2	973	945	18	-5	-1	2	472	455	15	-4	2	2	1817	1721	24
5	-4	2	969	931	17	-4	-1	2	297	212	20	-3	2	2	2339	2296	27
4	-4	2	54	23	64	-3	-1	2	375	335	16	-2	2	2	722	661	13
3	-4	2	841	769	16	-2	-1	2	131	121	23	-1	2	2	250	229	16
2	-4	2	3113	2946	33	-1	-1	2	1731	1730	20	0	2	2	1098	1119	14
1	-4	2	574	506	13	0	-1	2	382	399	8	1	2	2	752	778	15
0	-4	2	717	668	11	1	-1	2	2120	2217	24	2	2	2	942	953	16
1	-4	2	2659	2482	29	2	-1	2	104	50	44	3	2	2	1060	1025	17
2	-4	2	1611	1552	23	3	-1	2	2731	2633	21	4	2	2	1616	1590	24
3	-4	2	2906	2668	32	4	-1	2	1107	1065	18	5	2	2	344	337	25
4	-4	2	253	270	25	5	-1	2	754	742	17	6	2	2	0	71	37
5	-4	2	1259	1198	20	6	-1	2	328	298	27	7	2	2	410	409	25
6	-4	2	896	850	18	7	-1	2	50	155	96	8	2	2	234	156	38
7	-4	2	229	258	39	8	-1	2	698	690	19	9	2	2	424	421	27
8	-4	2	507	458	22	9	-1	2	804	789	19	-12	3	2	0	19	1
9	-4	2	443	478	26	10	-1	2	314	276	36	-11	3	2	328	369	34
10	-4	2	222	223	46	-12	0	2	0	112	151	-10	3	2	174	140	51
11	-4	2	1046	1077	83	-11	0	2	759	722	20	-9	3	2	458	441	23
12	-4	2	0	57	156	-10	0	2	994	1010	19	-8	3	2	834	785	18
11	-3	2	614	391	26	-9	0	2	335	291	30	-7	3	2	1329	1314	20
10	-3	2	0	146	141	-8	0	2	99	157	68	-6	3	2	538	565	15
9	-3	2	971	957	19	-7	0	2	144	168	47	-5	3	2	359	327	16
8	-3	2	897	878	18	-6	0	2	482	490	16	-4	3	2	652	619	14
7	-3	2	1945	1871	26	-5	0	2	221	241	25	-3	3	2	209	176	24
6	-3	2	1476	1426	22	-4	0	2	350	329	19	-2	3	2	97	137	41
5	-3	2	1086	1020	17	-3	0	2	138	114	34	-1	3	2	1355	1399	20
4	-3	2	1413	1370	21	-2	0	2	601	593	12	0	3	2	1553	1634	19
3	-3	2	122	80	31	-1	0	2	317	315	11	1	3	2	597	600	14
2	-3	2	1085	1029	16	0	0	2	427	423	8	2	3	2	472	458	14
1	-3	2	82	89	26	1	0	2	1584	1651	21	3	3	2	487	492	15
0	-3	2	1946	1885	23	2	0	2	1114	1166	19	4	3	2	213	338	27
1	-3	2	1388	1314	21	3	0	2	946	957	16	5	3	2	900	873	18
2	-3	2	1525	1498	21	4	0	2	340	351	21	6	3	2	343	273	28
3	-3	2	1581	1535	23	5	0	2	221	248	34	7	3	2	533	644	19
4	-3	2	1134	1139	20	6	0	2	623	597	18	8	3	2	279	299	18
5	-3	2	351	266	25	7	0	2	146	95	56	9	3	2	337	310	33
6	-3	2	415	454	24	8	0	2	197	94	46	-12	4	2	131	86	53
7	-3	2	315	344	32	9	0	2	861	849	19	-11	4	2	116	4	70
8	-3	2	519	508	23	10	0	2	871	855	20	-10	4	2	645	626	13
9	-3	2	132	43	69	-12	1	2	316	331	36	-9	4	2	913	895	18
10	-3	2	621	578	23	-11	1	2	154	130	58	-8	4	2	810	735	17
11	-3	2	322	251	55	-10	1	2	128	155	64	-7	4	2	536	566	17
12	-3	2	146	95	58	-9	1	2	19	123	123	-6	4	2	1442	1354	14
11	-2	2	621	440	25	-8	1	2	79	80	76	-5	4	2	727	675	14
10	-2	2	984	983	19	-7	1	2	1085	1031	18	-4	4	2	79	93	50
9	-2	2	610	566	17	-6	1	2	1197	1158	31	-3	4	2	349	322	16
8	-2	2	1186	1151	19	-5	1	2	1353	1307	20	-2	4	2	331	364	15
7	-2	2	1941	1868	26	-4	1	2	959	978	17	-1	4	2	838	817	15
6	-2	2	1434	1371	26	-3	1	2	155	42	28	0	4	2	601	580	14
5	-2	2	1256	1215	20	-2	1	2	2830	2711	30	1	4	2	749	781	14
4	-2	2	0	64	84	-1	1	2	1538	1555	19	2	4	2	136	99	38
3	-2	2	746	717	33	0	1	2	1376	1358	16	3	4	2	644	710	16
2	-2	2	270	291	9	1	1	2	218	244	25	4	4	2	714	727	16
1	-2	2	265	226	18	2	1	2	1419	1389	20	5	4	2	111	36	63
0	-2	2	136	89	37	3	1	2	1086	1089	17	6	4	2	0	50	40
1	-2	2	3610	3474	33	4	1	2	296	284	24	7	4	2	219	146	42
2	-2	2	380	381	18	5	1	2	1268	1254	21	8	4	2	0	100	147
3	-2	2	439	439	19	6	1	2	1041	1045	19	9	4	2	170	252	58
4	-2	2	0	71	132	7	1	2	339	355	30	-12	5	2	231	153	41
5	-2	2	137	50	58	8	1	2	154	142	56	-11	5	2	407	386	28
6	-2	2	617	595	19	9	1	2	335	365	34	-10	5	2	739	737	15
9	-2	2	199	6	48	10	1	2	91	220	87	-9	5	2	119	111	64

OBSERVED AND CALCULATED STRUCTURE FACTORS FOR SN4F8(O2CO2F3)2.6.4CF3CO2H
PAGE 3 OF37

(UNOBSERVED REFLECTIONS ARE MARKED *)

OBSERVED AND CALCULATED STRUCTURE FACTORS FOR SNAF8(O2CCF3)16.4CF3CO2H

(UNOBSERVED REFLECTIONS ARE MARKED +)

H	K	L	FO	FC	SIG
-6	16	2	114	72	71
-5	16	2	660	716	20
-4	16	2	0+	125	144
-3	16	2	563	513	19
-2	16	2	445	488	26
-1	16	2	0+	17	142
0	16	2	524	477	15
1	16	2	402	386	26
2	16	2	133	113	60
3	16	2	0+	162	142
-9	17	2	420	364	31
-8	17	2	0+	80	155
-7	17	2	535	565	23
-6	17	2	755	658	20
-5	17	2	475	439	26
-4	17	2	505	616	22
-3	17	2	303	316	38
-2	17	2	117	117	57
-1	17	2	337	126	34
0	17	2	310	507	17
1	17	2	735	684	19
2	17	2	153	281	58
-8	18	2	392	350	32
-7	18	2	324	339	27
-6	18	2	639	731	22
-5	18	2	505	844	21
-4	18	2	495	431	26
-3	18	2	353	245	31
-2	18	2	143	257	65
-1	18	2	530	566	22
0	18	2	121	192	49
1	18	2	533	507	22
-7	19	2	293	195	40
-6	19	2	0+	119	159
-5	19	2	395	360	32
-4	19	2	373	342	31
-3	19	2	505	499	25
-2	19	2	539	653	22
-1	19	2	422	314	18
-5	20	2	184	92	64
-4	20	2	532	461	27
-3	20	2	573	376	15
0	-22	3	156	27	63
1	-22	3	701	634	21
2	-22	3	442	499	23
3	-22	3	565	524	23
4	-22	3	399	388	20
-2	-21	3	0+	14	142
-1	-21	3	0+	59	142
0	-21	3	255	230	28
1	-21	3	381	410	30
2	-21	3	565	485	24
3	-21	3	722	753	20
4	-21	3	240	203	47
5	-21	3	0+	160	154
-4	-20	3	204	236	52
-3	-20	3	168	126	54
-2	-20	3	782	774	19
-1	-20	3	1022	994	18
0	-20	3	550	590	15
1	-20	3	332	225	31
2	-20	3	533	504	21
3	-20	3	143	163	65
4	-20	3	132	268	69
5	-20	3	100	62	80
6	-20	3	645	627	22
-5	-19	3	363	330	32
-4	-19	3	171	134	56
-3	-19	3	610	631	21
-2	-19	3	351	334	30

H	K	L	FO	FC	SIG
-1	-19	3	353	372	29
0	-19	3	358	372	25
1	-19	3	0+	12	138
2	-19	3	583	549	20
3	-19	3	288	331	35
4	-19	3	0+	98	145
5	-19	3	114	21	75
6	-19	3	146	44	62
7	-19	3	461	467	29
-5	-18	3	330	255	34
-4	-18	3	382	415	30
-3	-18	3	174	42	50
-2	-18	3	971	902	17
-1	-18	3	620	580	19
0	-18	3	209	155	29
1	-18	3	73	49	79
2	-18	3	0+	17	138
3	-18	3	0+	27	138
4	-18	3	252	257	38
5	-18	3	782	767	19
6	-18	3	1172	1190	21
7	-18	3	504	574	25
8	-18	3	361	261	33
-6	-17	3	577	584	22
-5	-17	3	364	354	31
-4	-17	3	576	513	21
-3	-17	3	638	625	19
-2	-17	3	290	244	32
-1	-17	3	672	611	18
0	-17	3	317	310	20
1	-17	3	112	212	65
2	-17	3	565	539	19
3	-17	3	182	260	47
4	-17	3	554	503	20
5	-17	3	0+	93	140
6	-17	3	0+	51	146
7	-17	3	459	500	26
8	-17	3	96	158	87
-7	-16	3	650	644	22
-6	-16	3	491	491	24
-5	-16	3	676	641	20
-4	-16	3	685	633	19
-3	-16	3	0+	48	135
-2	-16	3	185	210	46
-1	-16	3	751	713	17
0	-16	3	1230	1181	17
1	-16	3	1176	1141	20
2	-16	3	924	904	18
3	-16	3	1030	1039	18
4	-16	3	513	506	21
5	-16	3	0+	191	138
6	-16	3	185	251	49
7	-16	3	1028	1024	19
8	-16	3	611	581	22
9	-16	3	220	213	52
-8	-15	3	0+	10	153
-7	-15	3	373	398	30
-6	-15	3	1016	993	18
-5	-15	3	130	229	63
-4	-15	3	448	417	23
-3	-15	3	238	191	36
-2	-15	3	720	658	17
-1	-15	3	161	55	47
0	-15	3	285	282	21
1	-15	3	1223	1156	20
2	-15	3	653	632	17
3	-15	3	124	201	61
4	-15	3	463	429	22
5	-15	3	370	326	25
6	-15	3	81	153	81

H	K	L	FO	FC	SIG
7	-15	3	153	178	59
8	-15	3	255	305	41
9	-15	3	499	497	25
-8	-14	3	230	147	50
-7	-14	3	422	411	29
-6	-14	3	776	779	19
-5	-14	3	297	259	32
-4	-14	3	262	249	35
-3	-14	3	1245	1192	21
-2	-14	3	1123	1048	19
-1	-14	3	341	268	24
0	-14	3	295	249	20
1	-14	3	478	430	22
2	-14	3	168	7	44
3	-14	3	524	511	19
4	-14	3	329	364	29
5	-14	3	241	117	37
6	-14	3	136	153	46
7	-14	3	450	447	25
8	-14	3	250	247	39
9	-14	3	434	467	28
-9	-13	3	113	152	80
-8	-13	3	0+	101	149
-7	-13	3	132	153	64
-6	-13	3	148	153	56
-5	-13	3	575	553	19
-4	-13	3	734	702	18
-3	-13	3	35	66	68
-2	-13	3	134	70	52
-1	-13	3	443	407	19
0	-13	3	535	558	13
1	-13	3	1529	1437	23
2	-13	3	613	595	16
3	-13	3	748	769	17
4	-13	3	144	17	52
5	-13	3	30	55	74
6	-13	3	337	325	29
7	-13	3	359	370	28
8	-13	3	550	624	20
9	-13	3	379	370	31
-9	-12	3	627	648	22
-8	-12	3	599	676	13
-7	-12	3	275	310	35
-6	-12	3	254	211	35
-5	-12	3	122	113	62
-4	-12	3	452	435	21
-3	-12	3	1257	1168	19
-2	-12	3	312	310	25
-1	-12	3	538	480	17
0	-12	3	557	535	11
1	-12	3	1175	1049	18
2	-12	3	923	908	17
3	-12	3	737	692	16
4	-12	3	1644	1671	24
5	-12	3	940	832	18
6	-12	3	1049	1073	13
7	-12	3	35	88	95
8	-12	3	543	590	21
9	-12	3	401	402	30
10	-12	3	376	335	33
-10	-11	3	254	252	44
-9	-11	3	0+	131	150
-8	-11	3	116	177	70
-7	-11	3	331	356	23
-6	-11	3	535	474	21
-5	-11	3	345	366	13
-4	-11	3	435	355	22
-3	-11	3	318	298	23
-2	-11	3	346	341	22
-1	-11	3	518	441	16

OBSERVED AND CALCULATED STRUCTURE FACTORS FOR SN6F9(02CCF3)2(6.4CF3CO2H
PAGE 21 OF 37

(UNOBSERVED REFLECTIONS ARE MARKED *)

OBSERVED AND CALCULATED STRUCTURE FACTORS FOR SN8F8(O2CCF3)16.4CF3CO2H
PAGE12 OF37
(UNOBSERVED REFLECTIONS ARE MARKED *)

OBSERVED AND CALCULATED STRUCTURE FACTORS FOR SNAP3(02CCF3)16.4CF3CO2H
PAGE13 OF37

(UNOBSERVED REFLECTIONS ARE MARKED *)

H	K	L	FO	FC	SIG	H	K	L	FO	FC	SIG	H	K	L	FO	FC	SIG

OBSERVED AND CALCULATED STRUCTURE FACTORS FOR SN8F8(02CDF3)16.4DF3CD2H
PAGE14 OF37

(UNOBSERVED REFLECTIONS ARE MARKED *)

H	K	L	FO	FC	SIG	H	K	L	FO	FC	SIG	H	K	L	FO	FC	SIG

OBSERVED AND CALCULATED STRUCTURE FACTORS FOR SN8F9(C2OOF3)16.4OF3OO2H
PAGE 15 OF 37

(UNOBSERVED REFLECTIONS ARE MARKED *)

H	K	L	FO	FC	SIG	H	K	L	FO	FC	SIG	H	K	L	FO	FC	SIG

OBSERVED AND CALCULATED STRUCTURE FACTORS FOR SNBF3(O2CCF3)2.6CF3CO2H
PAGE16 OF37

(UNOBSERVED REFLECTIONS ARE MARKED *)

H	K	L	FO	FC	SIG	H	K	L	FO	FC	SIG	H	K	L	FO	FC	SIG
1	1	1	377	374	29	1	1	1	139	124	24	1	1	1	377	374	29
1	1	2	631	660	25	1	1	2	276	224	22	1	1	2	631	660	25
1	1	3	333	298	21	1	1	3	337	346	21	1	1	3	333	298	21
1	1	4	0 *	102	156	1	1	4	328	412	20	1	1	4	0 *	102	156
1	1	5	0 *	104	155	1	1	5	0 *	0	0	1	1	5	0 *	104	155
1	1	6	737	801	9	1	1	6	867	880	9	1	1	6	737	801	9
1	1	7	514	777	8	1	1	7	777	777	8	1	1	7	514	777	8
1	1	8	349	339	22	1	1	8	333	352	22	1	1	8	349	339	22
1	1	9	0 *	70	22	1	1	9	0 *	0	0	1	1	9	0 *	70	22
1	1	10	304	289	7	1	1	10	279	279	7	1	1	10	304	289	7
1	1	11	607	607	7	1	1	11	559	555	7	1	1	11	607	607	7
1	1	12	151	210	8	1	1	12	0 *	0	0	1	1	12	151	210	8
1	1	13	356	327	7	1	1	13	333	333	7	1	1	13	356	327	7
1	1	14	0 *	0	0	1	1	14	0 *	0	0	1	1	14	0 *	0	0
1	1	15	0 *	28	0	1	1	15	0 *	0	0	1	1	15	0 *	28	0
1	1	16	780	780	7	1	1	16	0 *	0	0	1	1	16	780	780	7
1	1	17	0 *	0	0	1	1	17	0 *	0	0	1	1	17	0 *	0	0
1	1	18	0 *	0	0	1	1	18	0 *	0	0	1	1	18	0 *	0	0
1	1	19	0 *	0	0	1	1	19	0 *	0	0	1	1	19	0 *	0	0
1	1	20	0 *	0	0	1	1	20	0 *	0	0	1	1	20	0 *	0	0
1	1	21	0 *	0	0	1	1	21	0 *	0	0	1	1	21	0 *	0	0
1	1	22	0 *	0	0	1	1	22	0 *	0	0	1	1	22	0 *	0	0
1	1	23	0 *	0	0	1	1	23	0 *	0	0	1	1	23	0 *	0	0
1	1	24	0 *	0	0	1	1	24	0 *	0	0	1	1	24	0 *	0	0
1	1	25	0 *	0	0	1	1	25	0 *	0	0	1	1	25	0 *	0	0
1	1	26	0 *	0	0	1	1	26	0 *	0	0	1	1	26	0 *	0	0
1	1	27	0 *	0	0	1	1	27	0 *	0	0	1	1	27	0 *	0	0
1	1	28	0 *	0	0	1	1	28	0 *	0	0	1	1	28	0 *	0	0
1	1	29	0 *	0	0	1	1	29	0 *	0	0	1	1	29	0 *	0	0
1	1	30	0 *	0	0	1	1	30	0 *	0	0	1	1	30	0 *	0	0
1	1	31	0 *	0	0	1	1	31	0 *	0	0	1	1	31	0 *	0	0
1	1	32	0 *	0	0	1	1	32	0 *	0	0	1	1	32	0 *	0	0
1	1	33	0 *	0	0	1	1	33	0 *	0	0	1	1	33	0 *	0	0
1	1	34	0 *	0	0	1	1	34	0 *	0	0	1	1	34	0 *	0	0
1	1	35	0 *	0	0	1	1	35	0 *	0	0	1	1	35	0 *	0	0
1	1	36	0 *	0	0	1	1	36	0 *	0	0	1	1	36	0 *	0	0
1	1	37	0 *	0	0	1	1	37	0 *	0	0	1	1	37	0 *	0	0
1	1	38	0 *	0	0	1	1	38	0 *	0	0	1	1	38	0 *	0	0
1	1	39	0 *	0	0	1	1	39	0 *	0	0	1	1	39	0 *	0	0
1	1	40	0 *	0	0	1	1	40	0 *	0	0	1	1	40	0 *	0	0
1	1	41	0 *	0	0	1	1	41	0 *	0	0	1	1	41	0 *	0	0
1	1	42	0 *	0	0	1	1	42	0 *	0	0	1	1	42	0 *	0	0
1	1	43	0 *	0	0	1	1	43	0 *	0	0	1	1	43	0 *	0	0
1	1	44	0 *	0	0	1	1	44	0 *	0	0	1	1	44	0 *	0	0
1	1	45	0 *	0	0	1	1	45	0 *	0	0	1	1	45	0 *	0	0
1	1	46	0 *	0	0	1	1	46	0 *	0	0	1	1	46	0 *	0	0
1	1	47	0 *	0	0	1	1	47	0 *	0	0	1	1	47	0 *	0	0
1	1	48	0 *	0	0	1	1	48	0 *	0	0	1	1	48	0 *	0	0
1	1	49	0 *	0	0	1	1	49	0 *	0	0	1	1	49	0 *	0	0
1	1	50	0 *	0	0	1	1	50	0 *	0	0	1	1	50	0 *	0	0
1	1	51	0 *	0	0	1	1	51	0 *	0	0	1	1	51	0 *	0	0
1	1	52	0 *	0	0	1	1	52	0 *	0	0	1	1	52	0 *	0	0
1	1	53	0 *	0	0	1	1	53	0 *	0	0	1	1	53	0 *	0	0
1	1	54	0 *	0	0	1	1	54	0 *	0	0	1	1	54	0 *	0	0
1	1	55	0 *	0	0	1	1	55	0 *	0	0	1	1	55	0 *	0	0
1	1	56	0 *	0	0	1	1	56	0 *	0	0	1	1	56	0 *	0	0
1	1	57	0 *	0	0	1	1	57	0 *	0	0	1	1	57	0 *	0	0
1	1	58	0 *	0	0	1	1	58	0 *	0	0	1	1	58	0 *	0	0
1	1	59	0 *	0	0	1	1	59	0 *	0	0	1	1	59	0 *	0	0
1	1	60	0 *	0	0	1	1	60	0 *	0	0	1	1	60	0 *	0	0
1	1	61	0 *	0	0	1	1	61	0 *	0	0	1	1	61	0 *	0	0
1	1	62	0 *	0	0	1	1	62	0 *	0	0	1	1	62	0 *	0	0
1	1	63	0 *	0	0	1	1	63	0 *	0	0	1	1	63	0 *	0	0
1	1	64	0 *	0	0	1	1	64	0 *	0	0	1	1	64	0 *	0	0
1	1	65	0 *	0	0	1	1	65	0 *	0	0	1	1	65	0 *	0	0
1	1	66	0 *	0	0	1	1	66	0 *	0	0	1	1	66	0 *	0	0
1	1	67	0 *	0	0	1	1	67	0 *	0	0	1	1	67	0 *	0	0
1	1	68	0 *	0	0	1	1	68	0 *	0	0	1	1	68	0 *	0	0
1	1	69	0 *	0	0	1	1	69	0 *	0	0	1	1	69	0 *	0	0
1	1	70	0 *	0	0	1	1	70	0 *	0	0	1	1	70	0 *	0	0
1	1	71	0 *	0	0	1	1	71	0 *	0	0	1	1	71	0 *	0	0
1	1	72	0 *	0	0	1	1	72	0 *	0	0	1	1	72	0 *	0	0
1	1	73	0 *	0	0	1	1	73	0 *	0	0	1	1	73	0 *	0	0
1	1	74	0 *	0	0	1	1	74	0 *	0	0	1	1	74	0 *	0	0
1	1	75	0 *	0	0	1	1	75	0 *	0	0	1	1	75	0 *	0	0
1	1	76	0 *	0	0	1	1	76	0 *	0	0	1	1	76	0 *	0	0
1	1	77	0 *	0	0	1	1	77	0 *	0	0	1	1	77	0 *	0	0
1	1	78	0 *	0	0	1	1	78	0 *	0	0	1	1	78	0 *	0	0
1	1	79	0 *	0	0	1	1	79	0 *	0	0	1	1	79	0 *	0	0
1	1	80	0 *	0	0	1	1	80	0 *	0	0	1	1	80	0 *	0	0
1	1	81	0 *	0	0	1	1	81	0 *	0	0	1	1	81	0 *	0	0
1	1	82	0 *	0	0	1	1	82	0 *	0	0	1	1	82	0 *	0	0
1	1	83	0 *	0	0	1	1	83	0 *	0	0	1	1	83	0 *	0	0
1	1	84	0 *	0	0	1	1	84	0 *	0	0	1	1	84	0 *	0	0
1	1	85	0 *	0	0	1	1	85	0 *	0	0	1	1	85	0 *	0	0
1	1	86	0 *	0	0	1	1	86	0 *	0	0	1	1	86	0 *	0	0
1	1	87	0 *	0	0	1	1	87	0 *	0	0	1	1	87	0 *	0	0
1	1	88	0 *	0	0	1	1	88	0 *	0	0	1	1	88	0 *	0	0
1	1	89	0 *	0	0	1	1	89	0 *	0	0	1	1	89	0 *	0	0
1	1	90	0 *	0	0	1	1	90	0 *	0	0	1	1	90	0 *	0	0
1	1	91	0 *	0	0	1	1	91	0 *	0	0	1	1	91	0 *	0	0
1	1	92	0 *	0	0	1	1	92	0 *	0	0	1	1	92	0 *	0	0
1	1	93	0 *	0	0	1	1	93	0 *	0	0	1	1	93	0 *	0	0
1	1	94	0 *	0	0	1	1	94	0 *	0	0	1	1	94	0 *	0	0
1	1	95	0 *	0	0	1	1	95	0 *	0	0	1	1	95	0 *	0	0
1	1	96	0 *	0	0	1	1	96	0 *	0	0	1	1	96	0 *	0	0
1	1	97	0 *	0	0	1	1	97	0 *	0	0	1	1	97	0 *	0	0
1	1	98	0 *	0	0	1	1	98	0 *	0	0	1	1	98	0 *	0	0
1	1	99	0 *	0	0	1	1	99	0 *	0	0	1	1	99	0 *	0	0
1	1	100	0 *	0	0	1	1	100	0 *	0	0	1	1	100	0 *	0	0

OBSERVED AND CALCULATED STRUCTURE FACTORS FOR SN8F8(02CDF3)16.6DF3002H
(UNOBSERVED REFLECTIONS ARE MARKED *)

OBSERVED AND CALCULATED STRUCTURE FACTORS FOR SN8F8(O2CCF3)16.4CF3CO2H
(UNOBSERVED REFLECTIONS ARE MARKED *)

H	K	L	FO	FC	SIG	H	K	L	FO	FC	SIG	H	K	L	FO	FC	SIG

OBSERVED AND CALCULATED STRUCTURE FACTORS FOR SN8F8(D2CCF3)16.+CF3CO2H
(UNOBSERVED REFLECTIONS ARE MARKED *)

OBSERVED AND CALCULATED STRUCTURE FACTORS FOR SN8F8(O2CCF3)16.4CF3CO2H
PAGE 20 OF 37

(UNOBSERVED REFLECTIONS ARE MARKED *)

OBSERVED AND CALCULATED STRUCTURE FACTORS FOR SN8F8(OCOOF8)16.6OF3OO2H
PAGE21 OF37
(UNOBSERVED REFLECTIONS ARE MARKED *)

H	K	L	FO	FC	SIG	H	K	L	FO	FC	SIG	H	K	L	FO	FC	SIG

OBSERVED AND CALCULATED STRUCTURE FACTORS FOR SN8F8(O2CCF3)16.4CF3CO2H
PAGE22 OF37
(UNOBSERVED REFLECTIONS ARE MARKED *)

OBSERVED AND CALCULATED STRUCTURE FACTORS FOR SNAF9(C2CCF3) 16-OCT-2002
PAGE23 OF37

(UNOBSERVED REFLECTIONS ARE MARKED *)

H	K	L	FO	FC	SIG

OBSERVED AND CALCULATED STRUCTURE FACTORS FOR SNRF3(O2CCF3)2.6CF3CO2H
(UNOBSERVED REFLECTIONS ARE MARKED *)

OBSERVED AND CALCULATED STRUCTURE FACTORS FOR SN8F4(C2CCF3)2;6.4CF3CO2H
(UNOBSERVED REFLECTIONS ARE MARKED *)

OBSERVED AND CALCULATED STRUCTURE FACTORS FOR SNBF8(O2CCF3)16.4CF3CO2H PAGE26 OF37
(UNOBSERVED REFLECTIONS ARE MARKED +)

H	K	L	FO	FC	SIG	H	K	L	FO	FC	SIG	H	K	L	FO	FC	SIG
0	6	7	217	241	27	-9	11	7	0+	21	169	2	-19	8	517	511	24
1	6	7	273	237	34	-8	11	7	374	793	19	3	-19	8	737	677	20
2	6	7	0+	62	142	-7	11	7	982	955	20	4	-19	8	135	37	71
3	6	7	432	433	24	-6	11	7	536	564	23	-7	-18	8	1044	1062	20
4	6	7	275	225	39	-5	11	7	61	120	98	-6	-18	8	957	997	19
-13	7	7	133	10	54	-4	11	7	0+	222	151	-5	-18	8	557	543	23
-12	7	7	133	209	43	-3	11	7	355	125	31	-4	-18	8	913	794	19
-11	7	7	433	401	29	-2	11	7	348	55	32	-3	-18	8	527	585	19
-10	7	7	33	127	31	-1	11	7	0+	65	150	-2	-18	8	155	222	54
-9	7	7	378	358	28	0	11	7	436	443	19	-1	-18	8	212	135	42
-8	7	7	534	472	21	-11	12	7	447	419	30	0	-18	8	714	695	14
-7	7	7	242	242	38	-10	12	7	89	47	91	1	-18	8	726	693	19
-6	7	7	477	427	22	-9	12	7	403	483	35	2	-18	8	330	340	24
-5	7	7	331	349	29	-8	12	7	316	353	40	3	-18	8	345	340	28
-4	7	7	102	9	67	-7	12	7	458	355	27	4	-18	8	563	559	23
-3	7	7	0+	40	118	-6	12	7	607	583	24	-9	-17	8	112	101	73
-2	7	7	204	224	42	-5	12	7	346	213	37	-7	-17	8	179	35	64
-1	7	7	230	185	33	-4	12	7	621	552	22	-6	-17	8	524	627	21
0	7	7	153	185	40	-3	12	7	558	537	24	-5	-17	8	317	312	19
1	7	7	473	437	18	-2	12	7	40	72	113	-4	-17	8	51	34	94
2	7	7	314	700	20	-1	12	7	142	140	66	-3	-17	8	350	303	19
3	7	7	433	407	20	0	12	7	0+	17	104	-2	-17	8	339	319	32
-13	8	7	43	136	122	-10	13	7	255	162	47	-1	-17	8	326	334	30
-12	8	7	344	335	34	-9	13	7	0+	17	161	0	-17	8	454	434	17
-11	8	7	411	411	21	-8	13	7	588	551	24	1	-17	8	243	233	39
-10	8	7	934	967	19	-7	13	7	421	434	32	2	-17	8	352	826	18
-9	8	7	130	207	43	-6	13	7	0+	80	156	3	-17	8	223	217	44
-8	8	7	435	433	22	-5	13	7	0+	76	154	4	-17	8	510	577	24
-7	8	7	0+	135	140	-4	13	7	253	356	45	5	-17	8	355	229	32
-6	8	7	354	345	23	-3	13	7	208	165	51	-9	-16	8	430	522	27
-5	8	7	603	533	19	-2	13	7	91	135	88	-8	-16	8	159	217	60
-4	8	7	225	213	19	-9	14	7	677	619	24	-7	-16	8	515	584	20
-3	8	7	432	518	22	-8	14	7	253	245	48	-6	-16	8	155	31	62
-2	8	7	252	224	35	-7	14	7	0+	139	161	-5	-16	8	143	76	49
-1	8	7	247	304	39	-6	14	7	155	135	67	-4	-16	8	133	204	35
0	8	7	143	92	48	-5	14	7	0+	85	180	-3	-16	8	0+	46	138
1	8	7	151	20	54	-4	14	7	474	432	28	-2	-16	8	75	52	33
2	8	7	541	508	23	-3	14	7	305	53	39	-1	-16	8	0+	5	136
3	8	7	433	514	25	-7	15	7	465	414	30	0	-16	8	728	704	13
-12	9	7	265	409	50	-6	15	7	391	887	21	1	-16	8	1010	981	18
-11	9	7	143	143	71	-5	15	7	566	557	26	2	-16	8	576	544	20
-10	9	7	359	272	33	-2	-22	8	264	223	39	3	-16	8	459	477	25
-9	9	7	315	354	19	-1	-22	8	504	522	25	4	-16	8	741	579	13
-8	9	7	675	613	19	0	-22	8	554	530	17	5	-16	8	148	139	64
-7	9	7	308	284	33	-4	-21	8	343	366	34	-9	-15	8	275	142	33
-6	9	7	0+	7	1[illegible]	-3	-21	8	103	159	77	-8	-15	8	133	121	55
-5	9	7	733	730	18	-2	-21	8	430	467	28	-7	-15	8	0+	154	143
-4	9	7	764	736	18	-1	-21	8	119	158	71	-6	-15	8	838	853	18
-3	9	7	497	900	19	0	-21	8	196	191	36	-5	-15	8	130	46	55
-2	9	7	894	822	17	1	-21	8	462	466	26	-4	-15	8	723	720	13
-1	9	7	1277	1200	21	2	-21	8	252	37	40	-3	-15	8	249	263	37
0	9	7	277	179	26	-6	-20	8	53	15	103	-2	-15	8	0+	40	137
1	9	7	134	91	60	-5	-20	8	176	165	55	-1	-15	8	212	176	42
2	9	7	205	194	48	-4	-20	8	240	210	43	0	-15	8	347	373	20
-12	10	7	683	27	41	-3	-20	8	237	213	42	1	-15	8	377	365	27
-11	10	7	725	670	22	-2	-20	8	954	912	18	2	-15	8	332	390	25
-10	10	7	730	710	21	-1	-20	8	1511	1507	23	3	-15	8	249	246	74
-9	10	7	210	153	53	0	-20	8	865	847	14	4	-15	8	745	699	19
-8	10	7	0+	129	143	1	-20	8	368	294	30	5	-15	8	139	236	51
-7	10	7	301	257	34	2	-20	8	563	574	23	-10	-14	8	451	467	28
-6	10	7	255	254	39	3	-20	8	394	361	29	-9	-14	8	426	430	29
-5	10	7	515	537	23	-7	-19	8	0+	67	153	-8	-14	8	141	157	63
-4	10	7	486	485	23	-6	-19	8	181	155	54	-7	-14	8	135	70	62
-3	10	7	305	857	20	-5	-19	8	773	725	20	-6	-14	8	735	705	19
-2	10	7	0+	230	149	-4	-19	8	339	399	33	-5	-14	8	431	821	19
-1	10	7	303	160	34	-3	-19	8	111	144	70	-4	-14	8	944	955	19
0	10	7	210	355	23	-2	-19	8	400	274	27	-3	-14	8	1212	1200	20
1	10	7	0+	38	145	-1	-19	8	122	146	65	-2	-14	8	1335	1332	22
-11	11	7	401	459	24	0	-19	8	251	223	23	-1	-14	8	131	73	53
-10	11	7	0+	268	165	1	-19	8	0+	143	145	0	-14	8	139	197	36

OBSERVED AND CALCULATED STRUCTURE FACTORS FOR SN8F8(D2DCF3)16.4CF3CO2H
(UNOBSERVED REFLECTIONS ARE MARKED *)

OBSERVED AND CALCULATED STRUCTURE FACTORS FOR SNBF8(O2CCF3)16.4CF3CO24
(UNOBSERVED REFLECTIONS ARE MARKED *)

OBSERVED AND CALCULATED STRUCTURE FACTORS FOR SN8F8(C2CCF3)16.6CF3CO2H
(UNOBSERVED REFLECTIONS ARE MARKED *)

OBSERVED AND CALCULATED STRUCTURE FACTORS FOR SN8F8(OZCOCF3)16.4CF3CO2H
(UNOBSERVED REFLECTIONS ARE MARKED *)

OBSERVED AND CALCULATED STRUCTURE FACTORS FOR SN8FA(O2OOF3)16.6CF30024
(UNOBSERVED REFLECTIONS ARE MARKED *)

H	K	L	FO	FC	SIG	H	K	L	FO	FC	SIG	H	K	L	FO	FC	SIG	H	K	L	FO	FC	SIG

OBSERVED AND CALCULATED STRUCTURE FACTORS FOR SN3F8(O2CDF3)2.6H2O(F3002H
(UNOBSERVED REFLECTIONS ARE MARKED *)

OBSERVED AND CALCULATED STRUCTURE FACTORS FOR SNAFU(C2CDF2)

(UNOBSERVED REFLECTIONS ARE MARKED *)

OBSERVED AND CALCULATED STRUCTURE FACTORS FOR SNAFAYCOOOF-SI 16.6CF30024
PAGE 36 OF 37

(UNOBSERVED REFLECTIONS ARE MARKED *)

H	K	L	FO	FC	SIG	H	K	L	FO	FC	SIG	H	K	L	FO	FC	SIG

OBSERVED AND CALCULATED STRUCTURE FACTORS FOR SNAFR(C2CCF3)2(C6F5)2M
PAGE35 OF37
(UNOBSERVED REFLECTIONS ARE MARKED *)

H	K	L	FO	FC	SIG	H	K	L	FO	FC	SIG	H	K	L	FO	FC	SIG

OBSERVED AND CALCULATED STRUCTURAL FACTORS FOR SNAFU(C2CCF3)2(C6.4CF3CO2H
PAGE36 OF37

(UNOBSERVED REFLECTIONS ARE MARKED *)

H	K	L	FO	FC	SIG	H	K	L	FO	FC	SIG	H	K	L	FO	FC	SIG	H	K	L	FO	FC	SIG

OBSERVED AND CALCULATED STRUCTURE FACTORS FOR SN5P3(O2COF2)2:S+6CF3CO2H

(UNOBSERVED REFLECTIONS ARE MARKED *)

H	K	L	FO	FC	SIG	H	K	L	FO	FC	SIG	H	K	L	FO	FC	SIG